

Copyright Warning & Restrictions

The copyright law of the United States (Title 17, United States Code) governs the making of photocopies or other reproductions of copyrighted material.

Under certain conditions specified in the law, libraries and archives are authorized to furnish a photocopy or other reproduction. One of these specified conditions is that the photocopy or reproduction is not to be “used for any purpose other than private study, scholarship, or research.” If a user makes a request for, or later uses, a photocopy or reproduction for purposes in excess of “fair use” that user may be liable for copyright infringement,

This institution reserves the right to refuse to accept a copying order if, in its judgment, fulfillment of the order would involve violation of copyright law.

Please Note: The author retains the copyright while the New Jersey Institute of Technology reserves the right to distribute this thesis or dissertation

Printing note: If you do not wish to print this page, then select “Pages from: first page # to: last page #” on the print dialog screen

The Van Houten library has removed some of the personal information and all signatures from the approval page and biographical sketches of theses and dissertations in order to protect the identity of NJIT graduates and faculty.

ABSTRACT

Title of Thesis: Thermal Decomposition of Chlorobenzene
Reaction With Hydrogen and Oxygen Mixture
In An Atmosphere

Chun-Chen Yang, Master of Science in Chemical Engineering,
1989

Thesis Directed by Dr. Joseph. W. Bozzelli and Dr. E. R.
Ritter.

The thermal reactions of chlorobenzene in hydrogen and oxygen mixtures were studied in tubular flow reactors at 1 atmosphere total pressure. Experiments were carried out in flow reactors of varied diameter for determining effects of different surface to volume ratios. Residence times ranged from 0.03 to 2.5 seconds and temperature was varied over a range of 560 - 660 °C. The O₂/H₂ ratios ranged from 1% to 5%.

It was found that the conversion of chlorobenzene in hydrogen and oxygen mixtures increased with both temperature and residence time. The oxidation of chlorobenzene also occurred more rapidly when oxygen concentration was increased. A small amount of oxygen exhibited a significant effect on the decomposition of chlorobenzene, because equivalent decomposition without O₂ (H₂ only) required temperatures over 900 °C for 2 seconds residence times. Complete decay

(99%) for the chlorobenzene at 1 second residence time occurs at about 660 °C for all the O₂/H₂ ratios studied.

The major products were benzene, CH₄, C₂H₆, and HCl. The minor products were toluene, cyclopentadiene, C₂H₂, C₂H₄, CO and CO₂. The hydrocarbon products increased approximately linearly with temperature. An increase in surface to volume ratio of the reactor was observed to slow the chlorobenzene decomposition in mixtures of hydrogen and oxygen, but it had no effect on the relative distribution of major products. The oxygen concentration did, however, have significant effect on product distribution.

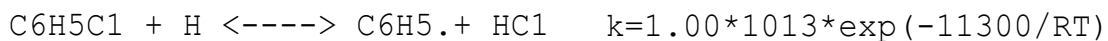
The pseudo first order plug flow model was utilized to analyze the global experimental data. This study demonstrates that small amounts of oxygen (1% to 5%) in excess H₂ is a practical route to detoxification of chlorinated aromatics. Expressions for the pseudo-first order rate constant were obtained as follows:

For 16 mm ID reactor

$$\begin{aligned}k_{exp} &= 6.9 * 10^{11} e^{(-48900/RT)} && (O_2/H_2: 1\%) \\k_{exp} &= 1.5 * 10^{13} e^{(-53700/RT)} && (O_2/H_2: 2\%) \\k_{exp} &= 7.0 * 10^{14} e^{(-60000/RT)} && (O_2/H_2: 3\%) \end{aligned}$$

A detailed kinetic reaction mechanism was developed and used to model the experimental data. The detailed kinetic reaction mechanism includes 84 elementary reactions involving

stable compounds and free radical species. The addition, beta scission and recombination type reactions were all analyzed by QRRK theory and sensitivity analysis on the model was performed to show the most important reactions in the mechanism. The three most important reactions were found to be:



THERMAL DECOMPOSITION OF CHLOROBENZENE REACTION
WITH HYDROGEN AND OXYGEN MIXTURE IN AN ATMOSPHERE

BY

CHUN-CHEN YANG

Thesis submitted to the faculty of the Graduate School of
the New Jersey Institute of Technology in partial
fulfillment of the requirements for the degree of
Master of Science in Chemical Engineering

1989

APPROVAL SHEET

Title of Thesis: Thermal Decomposition of Chlorobenzene
Reaction With Hydrogen and Oxygen
Mixture in an Atmosphere

Name of Candidate: Chun-Chen Yang

Master of Science in Chemical
Engineering, 1989

Thesis and Abstract Approved:

Joseph W. Bozzelli

Dept. Chemical Engineering,
Chemistry and Environmental
Science

Piero Armenante
Assistant Professor
Dept. Chemical Engineering,
Chemistry and Environmental
Science

Dr. Edward Ritter
Research Associate
Dept. Chemical Engineering,
Chemistry and Environmental
Science

VITA

Name: Chun-Chen Yang

Permanent Address:

Degree and Date to be conferred: Master of Science in
Chemical Engineering 1989

Date of Birth:

Place of Birth:

Collegiate Institutions attended	Dates	Degree	Date
Ming-Chi Institute of Technology	74-79	Diploma	June 79.
National Taiwan Institute of Technology	83-85	B.S.	June 85.

Major: Chemical Engineering

New Jersey institute of Technology 87-89 M.S. Sept. 89

Major: Chemical Engineering

Acknowledgement

I wish to express appreciation to Dr. Joseph W. Bozzelli for his advice and encouragement. I am deeply indebted to him for the opportunities which he made available to me. I acknowledge the helpful corrections and comments by Dr. Edward Ritter and Dr. P. Armenante. I spent lots of time on experiment, but I really got good experience at real work.

I feel grateful to my parents for their love and inspiration. It is my pleasure to thank my colleagues at Kinetics Research Laboratory of the New Jersey Institute of Technology: Mr. Yang Soo Won, Greg Wu, and Dustin Ho for their help and guidance.

CONTENTS

	page
I. Introduction	1
II. Previous Studies	6
III. Theory	11
A. Tubular Flow Reactor Theory	11
B. Decoupling of the Wall and Bulk Reaction Rate Constants	13
C. Rate of Reaction Predicted by the Theories	14
D. Prediction of Rate Constants for Radical Addition and Combination Reactions by Bimolecular QRRK Theory	20
IV. Experimental Method	30
A. Temperature Measurement and Control	31
B. Quantitative Analysis by Gas Chromatograph	33
C. Quantitative Analysis of HCl	37
D. Quantitative Analysis of CO and CO ₂ by TCD	41
E. Mechanism Modeling by CHEMKIN Program	42
V. Results and Discussion	46
A. Reaction of Chlorobenzene with H ₂ /O ₂ Mixtures	47
B. Reagent Conversion and Product Distribution	93
C. Effect of the Amount of Oxygen	120
D. Comparison of Chlorobenzene Reaction of Previous Studies	131
E. Kinetic Model and Calculations	132
VI. Conclusion	160
VII. References	162
Appendices	166

LIST OF TABLES

4.1	Relative Response Factors for FID (Capillary Column)	38
4.2	Relative Response Factors for FID (Carbosieve S.S. Column)	38
5.1	Carbon Material Balance (Rt = 1 sec, O ₂ /H ₂ : 1%)	94
5.2	Carbon Material Balance (Rt = 1 sec, O ₂ /H ₂ : 2%)	94
5.3	Carbon Material Balance (Rt = 1 sec, O ₂ /H ₂ : 3%)	95
5.4	Carbon Material Balance (Rt = 1 sec, O ₂ /H ₂ : 4%)	95
5.5	Carbon Material Balance (Rt = 1 sec, O ₂ /H ₂ : 5%)	96
5.6	Carbon Material Balance (Rt = 2 sec, O ₂ /H ₂ : 1%)	96
5.7	Carbon Material Balance (Rt = 2 sec, O ₂ /H ₂ : 2%)	97
5.8	Carbon Material Balance (Rt = 2 sec, O ₂ /H ₂ : 3%)	97
5.9	Carbon Material Balance (Rt = 2 sec, O ₂ /H ₂ : 4%)	98
5.10	Carbon Material Balance (Rt = 2 sec, O ₂ /H ₂ : 5%)	98
5.11	Carbon Material Balance (Rt = 1 sec, O ₂ /H ₂ : 1%)	99
5.12	Carbon Material Balance (Rt = 1 sec, O ₂ /H ₂ : 2%)	99
5.13	Carbon Material Balance (Rt = 1 sec, O ₂ /H ₂ : 3%)	100
5.14	Carbon Material Balance (Rt = 1 sec, O ₂ /H ₂ : 4%)	100
5.15	Carbon Material Balance (ID = 4 mm, Temp. = 640 °C)	101
5.16	Carbon Material Balance (ID = 4 mm, Temp. = 650 °C)	101
5.17	Carbon Material Balance (ID = 4 mm, Temp. = 650 °C)	102
5.18	Carbon Material Balance (ID = 4 mm, Temp. = 650 °C)	102
5.19	Carbon Material Balance (ID = 4 mm, Temp. = 650 °C)	103
5.20	Carbon Material Balance (ID = 4 mm, Temp. = 650 °C)	103
5.21	Reaction Mechanism of C ₆ H ₅ Cl + O ₂ + H ₂	149
5.22	Sensitivity Analysis Summary	159

LIST OF FIGURES

3.1 Energy Diagram for Pressure-dependent Reaction	24
4.1 Experimental Set Up	32
4.2 Reactor Temperature Profile (axial)	34
4.3 Auto-Sampler Diagram	36
4.4 Sample Chromatogram of C ₆ H ₅ Cl + O ₂ + H ₂ Decomposition(Capillary Column with FID)	39
4.5 Sample Chromatogram of C ₆ H ₅ Cl + O ₂ + H ₂ Decomposition(Cabosieve S.S. Column with FID)	40
4.6 Sample Chromatogram of C ₆ H ₅ Cl + O ₂ + H ₂ Decomposition(Carbosphere S.S. Column with TCD)	43
4.7 Structure of the CHEMKIN package	44
5.1 Decay Curve of C ₆ H ₅ Cl vs Time(ID= 16mm,O ₂ /H ₂ : 1%)	48
5.2 Decay Curve of C ₆ H ₅ Cl vs Time(ID= 16mm,O ₂ /H ₂ : 2%)	49
5.3 Decay Curve of C ₆ H ₅ Cl vs Time(ID= 16mm,O ₂ /H ₂ : 3%)	50
5.4 Decay Curve of C ₆ H ₅ Cl vs Time(ID=10.5mm,O ₂ /H ₂ : 1%)	51
5.5 Decay Curve of C ₆ H ₅ Cl vs Time(ID=10.5mm,O ₂ /H ₂ : 2%)	52
5.6 Decay Curve of C ₆ H ₅ Cl vs Time(ID=10.5mm,O ₂ /H ₂ : 2%)	53
5.7 Decay Curve of C ₆ H ₅ Cl vs Time(ID= 4mm,O ₂ /H ₂ : 1%)	54
5.8 Decay Curve of C ₆ H ₅ Cl vs Time(ID= 4mm,O ₂ /H ₂ : 2%)	55
5.9 Decay Curve of C ₆ H ₅ Cl vs Time(ID= 4mm,O ₂ /H ₂ : 3%)	56
5.10 Decay Curve of C ₆ H ₅ Cl vs Time(ID= 4mm,O ₂ /H ₂ : 4%)	57
5.11 Decay Curve of C ₆ H ₅ Cl vs Time(ID= 4mm,O ₂ /H ₂ : 5%)	58
5.12 Decay Curve of C ₆ H ₅ Cl vs Temp(ID= 16mm, O ₂ /H ₂ : 1%, Rt= 1 sec)	59
5.13 Decay Curve of C ₆ H ₅ Cl vs Temp(ID= 16mm, O ₂ /H ₂ : 2%, Rt= 1 sec)	60
5.14 Decay Curve of C ₆ H ₅ Cl vs Temp(ID= 16mm, O ₂ /H ₂ :	61

	3%, Rt= 1 sec)	
5.15	Decay Curve of C6H5Cl vs Temp(ID = 16mm, O2/H2: 1%, Rt= 2 sec)	62
5.16	Decay Curve of C6H5Cl vs Temp(ID = 16mm, O2/H2: 2%, Rt= 2 sec)	63
5.17	Decay Curve of C6H5Cl vs Temp(ID = 16mm, O2/H2: 3%, Rt= 2 sec)	64
5.18	Decay Curve of C6H5Cl vs Temp(ID = 16mm, O2/H2: 4%, Rt= 2 sec)	65
5.19	Decay Curve of C6H5Cl vs Temp(ID = 16mm, O2/H2: 5%, Rt= 2 sec)	66
5.20	Decay Curve of C6H5Cl vs Temp(ID = 10.5mm, O2/H2: 1%, Rt= 1 sec)	67
5.21	Decay Curve of C6H5Cl vs Temp(ID = 10.5mm, O2/H2: 2%, Rt= 1 sec)	68
5.22	Decay Curve of C6H5Cl vs Temp(ID = 10.5mm, O2/H2: 4%, Rt= 1 sec)	69
5.23	2nd Order Kinetics Fit of C6H5Cl Decomposition (ID = 10.5 mm, O2/H2: 2%)	71
5.24	2nd Order Kinetics Fit of C6H5Cl Decomposition (ID = 16 mm, O2/H2: 1%)	72
5.25	2nd Order Kinetics Fit of C6H5Cl Decomposition (ID = 16 mm, O2/H2: 2%)	73
5.26	2nd Order Kinetics Fit of C6H5Cl Decomposition (ID = 16 mm, O2/H2: 3%)	74
5.27	1st Order Kinetics Fit of C6H5Cl Decomposition (ID = 10.5 mm, O2/H2: 1%)	76
5.28	1st Order Kinetics Fit of C6H5Cl Decomposition (ID = 10.5 mm, O2/H2: 2%)	77
5.29	1st Order Kinetics Fit of C6H5Cl Decomposition (ID = 10.5 mm, O2/H2: 4%)	78
5.30	1st Order Kinetics Fit of C6H5Cl Decomposition (ID = 16 mm, O2/H2: 1%)	79
5.31	1st Order Kinetics Fit of C6H5Cl Decomposition	80

(ID = 16 mm, O2/H2: 2%)	
5.32 1st Order Kinetics Fit of C6H5Cl Decomposition (ID = 16 mm, O2/H2: 3%)	81
5.33 1st Order Kinetics Fit of C6H5Cl Decomposition (ID = 4 mm, O2/H2: 1%)	82
5.34 1st Order Kinetics Fit of C6H5Cl Decomposition (ID = 4 mm, O2/H2: 2%)	83
5.35 1st Order Kinetics Fit of C6H5Cl Decomposition (ID = 4 mm, O2/H2: 3%)	84
5.36 Arrhenius Behavior of k_{exp} for C6H5Cl 1st Order(ID =16 mm)	85
5.37 Arrhenius Behavior of k_{exp} for C6H5Cl 1st Order(ID = 4 mm)	86
5.38 The Influence of Surface to Volume (S/V) on the Decay of C6H5Cl(O2/H2: 2%, Temp= 590 C)	87
5.39 The Influence of Surface to Volume (S/V) on the Decay of C6H5Cl(O2/H2: 2%, Temp= 620'C)	89
5.40 The Influence of Surface to Volume (S/V) on the Decay of C6H5Cl(O2/H2: 2%, Temp= 640'C)	90
5.41 Decoupling k_b and k_w : Plug Flow Model	92
5.42 Benzene Product Distribution (ID= 16 mm, O2/H2: 1%)	104
5.43 Benzene Product Distribution (ID = 16 mm, O2/H2 : 2%)	105
5.44 Benzene Product Distribution (ID = 16 mm, O2/H2: 3%)	107
5.45 Benzene Product Distribution (ID = 10.5 mm, O2/H2 : 2%)	108
5.46 CH4 Product Distribution(ID = 16mm, O2/H2: 5%, Rt = 2 sec)	109
5.47 Light Hydrocarbon Product Distribution(ID = 16 mm O2/H2: 1%- 4%, Rt = 2 sec)	110
5.48 Product Dist.(ID = 16 mm, O2/H2: 1%, Rt= 1 sec)	112

5.49	Product Dist.(ID = 16 mm, O ₂ /H ₂ : 2%, Rt= 1 sec)	113
5.50	Product Dist.(ID = 16 mm, O ₂ /H ₂ : 3%, Rt= 1 sec)	114
5.51	Product Dist.(ID = 16 mm, O ₂ /H ₂ : 1%, Rt= 2 sec)	115
5.52	Product Dist.(ID = 16 mm, O ₂ /H ₂ : 2%, Rt= 2 sec)	116
5.53	Product Dist.(ID = 16 mm, O ₂ /H ₂ : 3%, Rt= 2 sec)	117
5.54	Product Dist.(ID = 16 mm, O ₂ /H ₂ : 4%, Rt= 2 sec)	118
5.55	The Influence of Oxygen on C ₆ H ₅ Cl Decomposition (ID = 4 mm, Temp.= 660 C, O ₂ /H ₂ : 1% - 5%)	121
5.56	The Influence of Oxygen on C ₆ H ₅ Cl Decomposition (ID = 4 mm, Temp.= 650 C, O ₂ /H ₂ : 1% - 5%)	122
5.57	The Influence of Oxygen on C ₆ H ₅ Cl Decomposition (ID = 16 mm, Temp.= 590 C, O ₂ /H ₂ : 1% - 5%)	123
5.58	The Influence of Oxygen on C ₆ H ₅ Cl Decomposition (ID = 16 mm, Temp.= 610°C, O ₂ /H ₂ : 1% - 5%)	124
5.59	The Influence of Oxygen on C ₆ H ₅ Cl Decomposition (ID = 16 mm, Temp.= 620 C, O ₂ /H ₂ : 1% - 4%)	125
5.60	The Influence of Oxygen on C ₆ H ₅ Cl Decomposition (ID = 16 mm, Temp.= 640 C, O ₂ /H ₂ : 1% - 3%)	126
5.61	Formation Of CH ₄ vs Diff. O ₂ /H ₂ Ratios	127
5.62	Formation Of C ₂ H ₆ vs Diff. O ₂ /H ₂ Ratios	128
5.63	The Influence of Oxygen on Benzene Production (ID = 10.5 mm, Temp.= 625 C, O ₂ /H ₂ : 1% - 6%)	129
5.64	The Influence of Oxygen on Benzene Production (ID = 10.5 mm, Temp.= 615 C, O ₂ /H ₂ : 1% - 6%)	130
5.65	Potential Energy Diagram for C ₆ H ₅ Cl + H Addition	134
5.66	Potential Energy Diagram for C ₆ H ₆ + H Addition(a)	136
5.67	Potential Energy Diagram for C ₆ H ₆ + H Addition(b)	137
5.68	(a) Potential Energy Diagram for CH ₃ + C ₆ H ₆ Addition to form Toluene + H	139
	(b) Potential Energy Diagram for CH ₃ + C ₆ H ₅ Cl Addition to form Toluene + Cl	

5.69	Decay of C ₆ H ₅ Cl Model Prediction and Expt. Point vs Time (O ₂ /H ₂ : 1% -3%, Temp:620 C)	141
5.70	Decay of C ₆ H ₅ Cl Model Prediction and Expt. Point vs Temp. (O ₂ /H ₂ : 1% - 2%)	142
5.71	Decay of C ₆ H ₅ Cl Model Prediction and Expt. Point vs Time (O ₂ /H ₂ : 1%, Temp.:560 - 640 C)	143
5.72	Benzene Product Distribution Model and Expt. Point vs Temp. (O ₂ /H ₂ : 1%, Rt= 1 sec)	144
5.73	Benzene Product Distribution Model and Expt. Point vs Temp. (O ₂ /H ₂ : 2%, Rt= 1 sec)	145
5.74	HCl Product Distribution Model and Expt. Point vs Temp. (O ₂ /H ₂ : 1%, Rt= 1 sec)	146
5.75	HCl Product Distribution Model and Expt. Point vs Temp. (O ₂ /H ₂ : 2%, Rt= 1 sec)	147

I. INTRODUCTION

Chlorinated organic chemicals are manufactured and used on large scale in a significant number of chemical industries. These industries include those which produce polychlorinated vinyls, waxes, resins, cleaning solvents, lacquers and varnishes. The chlorocarbon used range from solvents and monomers, such as trichloroethylene and vinyl chloride, to polychlorinated benzenes and polychlorinated biphenyls (PCB) which have been used as insulators in transformers^{<1>}. Disposal of these wastes has become an issue of significant environmental concern due mainly to their toxicity and their stability.

Polychlorobiphenyls (PCBs), chlorinated dioxins and furans are often observed in the effluent streams from the oxidation or incineration of chlorinated aromatics such as chlorobenzene, biphenyls etc^{<4,28,29>}. Because these chlorinated compounds are thought to be highly toxic and as a consequence they are highly undesirable products of incomplete combustion. Local residents (communities) are therefore usually strongly opposed to local refuse to energy plants, which otherwise appear to present a viable solution to urban refuse disposal problems.

It would be very valuable to understand the fundamental reaction mechanisms by which these species are produced

during incineration or oxidation processes. It is hoped that we could initiate development of a detailed mechanism or model for chlorobenzene incineration processes. The model could then be utilized for prediction of desired end products and for optimization of combustion process efficiency to minimize or completely eliminate undesirable species.

Many researchers have tried to develop technologies for effective and safe destruction of chlorocarbons. Non-thermal methods such as biodegradation^{<30>}, Na-based dechlorination^{<2>} are costly, incomplete and often difficult to apply. Thermal methods such as incineration (combustion), hydrodechlorination are also being developed to disposal of these toxic waste compounds. It is reported that combustion of chlorinated hydrocarbons under severe conditions of 537 °c at 2 seconds converts all carbon to CO₂^{<3>}. High-temperature incineration has been identified as a desirable method for treatment of hazardous organic waste^{<31>}. Commercialized incinerators at high temperature with excess oxygen have been installed at a number of sites around the country; but, high temperature oxygen-rich incineration seem to produce trace amount of several undesirable and thermally stable combustion products, such as PCBs, polychlorinated dibenzo dioxins (PCDDs) <4,28,29>.

If we operate the oxidation at temperatures below 700°C, with the addition of a limited amount of oxygen, we may avoid producing some toxic compounds, such as PCBs and dioxins, because oxygen rich conditions are a source of producing dioxins^{<42>}. Louw, et. al.^{<5>}, have noted the drastic operating conditions needed in order to avoid emission of intolerable quantities of PCDDs.

Graham et. al.^{<6>} have investigated the oxidation of a mixture of five organic hazardous compounds in a flow reactor at temperature 600°C - 1000°C. These toxic compounds were composed of 2.5% carbon tetrachloride, 2.5% trichloroethylene, 2.5% monochlorobenzene, 2.5% 1,1,2-trichloro-1,2,2-trifluoroethane 90% toluene by weight. Results from their studies under pyrolytic conditions and at equivalence ratios of 0.06 and 1, showed that more than 50 stable products were observed under each condition. Out of these products, more than 27 were halogenated compounds such as chlorinated furans, phenols, and polycyclic aromatic hydrocarbons (PAHs). This study was showed incomplete oxidation in incinerators can create environmental problems resulting from the release of carcinogenic polycyclic aromatic hydrocarbons (PAHs) into the atmosphere.

Ruby, et. al.^{<7>}, have studied the oxidation of a mixture of PCBs over temperature ranges of 500°C - 1000°C

using a 1 mm ID flow reactor with 2 second residence times. They found that polychlorinated dibenzofuran (PCDBF) and polychlorinated polyaromatic hydrocarbons (PCPAHs) were produced as a result of the PCB oxidation. Moreover, they found that at any given temperature in the range that was studied, an increase in the oxygen available for oxidation resulted in an increase in the amount of PCDBF produced. Gochfeld, et. al.⁵, have reported that dioxin exposure to humans is a serious health problem. Public attention has focused on the incinerator as a source of dioxin fallout.

The end products for chlorine is HCl, which can be easily neutralized and the limited oxygen reduced products like dioxin and dibenzofuran formation.

Pyrolysis studies of chlorobenzene (Hydrodechlorination) have been performed by R. Louw, H. Dijks, and P. Mulder⁵ and by E. Ritter⁹ in hydrogen atmospheres with reaction temperatures 800 - 1010 °C. Ritter found significant quantities of soot formation and incomplete mass balance for Cl (as HCl). However, the addition of small amount of oxygen to the excess H₂ in reactions with chlorobenzene may lower the pyrolysis temperature and possibly reduce high molecular weight compounds and improve Cl conversion to HCl.

Because chlorobenzene is the least chlorinated aromatic we selected it in this study to help us understand the

complex reactions of chloro aromatic oxidation and conversion.

II. PREVIOUS STUDIES

Few studies have been performed on oxidation of chlorobenzene. I first list thermal reactions of chlorobenzene in non-oxidizing atmospheres and will later present oxidation studies. The thermal decomposition of chlorobenzene was earlier studied by Cullis and Priddy^{<10>}. This initial study was limited to a static (batch) reactor. Cullis and Manton^{<11>} later extended this work to a flow system which was operated at a low pressure in a flow tank reactor at the temperature range 770 °C to 890 °C. They found that addition of hydrogen gas to the system accelerated the decomposition of chlorobenzene. Small questions remained, however, about the design of their " tank flow reactor " and non-ideal residence time distribution which was neglected in their analysis.

In 1973, Louw, Dijks and Mulder^{<12>} published a study on the reaction of chlorobenzene with chlorine and hydrogen atoms at 500 °C in a low pressure reactor. The residence time within their reactor system averaged two minutes. Reactant and product information is available and a part of a mechanistic model was proposed.

Recently, Louw , et al.^{<15>} published a second study on the decomposition of chlorobenzene by using a tank flow reactor in hydrogen bath gas at 1 atm pressure. The resi-

deuce time ranged from 5 - 10 seconds and the temperatures were 500°C - 1000°C. A reaction mechanistic scheme for the formation of methane through a methyl - cyclopentadiene intermediate was proposed. In the study, they also observed C2 hydrocarbons such as C2H2, C2H4 and C2H6. CH4 is about 0.5 percent of initial reagent at 750°C. C2H4 and C2H6 rise to much smaller amounts (ratio ca 2:3, about 10 per cent of CH4). C2H2 is produced in trace amounts only. Biaryls arise in 1-2 mole percent proportions on HCl, together with trace amounts of naphthalene and biphenylene. They also indicated that pyrolysis in excess H2 would be a promising method for dechlorination of organic chlorine compounds.

Manion, Mulder, and Louw^{<1>} examined the hydrodechlorination of a mixture of polychlorobiphenyls (PCB's) using a spiralized quartz reactor, which was 3.5 meters long and of 4 mm ID. The temperature ranged from 700°C to 925°C with residence time ranging from 5 to 15 seconds. Their results showed that the hydrodechlorination of PCB yields polychlorinated benzenes such as: chlorobenzene, di-chlorobenzene, and tri-chlorobenzene, and non-chlorinated organic products, mainly benzene. They pointed out that the dechlorination of aliphatic and olefinic chlorides reacted much faster than chlorobenzenes in an excess of H2.

More recently, Y. D. Yang^{<13>} studied the hydrode-

chlorination of chlorobenzene over a palladium catalyst at atmosphere pressure in the temperature range from 35 °C to 85 °C. The conversions of 45 - 60 % were reported, but deactivation of the catalyst was considered to be a problem. The major products of this reaction were benzene and carbon.

In 1986, E. Ritter^{<9>} studied the thermal decomposition of chlorobenzene in a tubular flow reactor system at one atmosphere pressure and average residence times of 0.02 to 2.5 seconds. Experiments carried out in 3 different diameter quartz reactor tubes, to examine the wall reactions in these reactors by the application of pseudo first order reaction kinetics and assumption of plug flow reactor. The major products he reported were benzene, HCl, and a small amount of polycyclic aromatic hydrocarbons (PAHs). But, he did not look for any specific light hydrocarbons such as CH₄, C₂H₂, and C₂H₄. This lack of light hydrocarbon detection was due to the limited GC analysis method for light hydrocarbons. His study also found minor products such as cyclopentadiene, toluene, biphenyl, chlorobiphenyl, terphenyl, triphenylene, and naphthalene. He also studied the pyrolysis of chlorobenzene in a helium atmosphere.

Mingta Hung^{<15>} studied the high temperature pyrolysis of dichlorobenzene in a plug flow reactor, where reaction temperature ranged from 800 °C to 1000 °C at one atmosphere pressure of hydrogen bath gas. This study found the major

products: chlorobenzene, benzene, HCl and C(s). The carbon formation was significant and sometimes amounting to 50% the reacted dichlorobenzene. However, he also did not report any data about light hydrocarbons analysis.

Larry Zhu¹⁵, further studied the kinetic of thermal decomposition of chlorobenzene and dichlorobenzene in a hydrogen and helium atmospheres. He examined formation of light hydrocarbons and soot. The experiments were performed at atmosphere pressure with residence times ranging from 0.2 to 1.2 seconds, and temperature ranged from 850 °C to 925 °C. Light hydrocarbon products were identified as CH₄, C₂H₂, C₂H₄, and C₂H₆. Under a hydrogen atmosphere, C₂H₄ was formed but no C₂H₂, where in a helium atmosphere C₂H₂ was produced as a higher concentration end product. All light hydrocarbons from the pyrolysis of chlorobenzene in this study of Zhu were less than 5% of the initial reactant chlorobenzene or dichlorobenzene concentration.

Although a number of studies on pyrolysis of chlorobenzene have been completed, some of disadvantages existed, such as high reaction temperature, large amount of carbon.

The current study focuses on addition of small percentages of oxygen (1% - 5%) in the pyrolysis of dilute chlorobenzene in H₂. We investigated reaction products to initiate development of a mechanistic model. By addition of

oxygen, the reaction temperatures of chlorobenzene were significantly reduced and ranged only from 560 °C to 660 °C much lower than the 900 °C required for the non oxygen atmospheres. In addition, the study also examined all light hydrocarbons products plus CO and CO₂ (note CO and CO₂ were not expected in the non-oxygen containing atmospheres). **By** collecting and then analyzing the products distribution data vs time and temperature, we have tried to develop an initial combustion reaction model. We realize that there are a significant numbers of studies on benzene oxidation in the literature such as those of Tsang^{<43>}, Felder^{<44>} et al, and Brezinsky^{<45>} et al; we focus here on chlorobenzene only. We have not found any studies in the literature on oxidation of chlorobenzene. This model can be utilized to scale up incineration processes with specific mixtures of chlorinated aromatic compounds. At present we realize that there are reactions of cyclopentadiene a key intermediate, which we do not fully account for.

III. THEORY

A. Tubular Flow Reactor Theory

A comparison of the kinetic values found by plug flow analysis with values obtained by applying both the numerical and analytical solution of the continuity equation for first order kinetics with laminar flow was presented by Chang and Bozzelli^{<34>}. This study showed that the plug flow assumption for our experimental system is accurate to within 5% to 7% for all temperatures ranges (560 - 660 °C), residence time from 0.03 second to 2.5 seconds, and three different quartz reactors of 4 mm, 10.5 mm, and 16 mm ID.

The idealized model of the plug flow reactor assumes that an entering fluid element moves as a plug of material that completely fills the cross section. While, we will limit our analysis to the simplest possible model: the plug flow model, when we attempt to compare the results predicted by the model with what we observe in the real world, we should discuss the deviations from ideal behavior in three categories^{<35>} below:

1. There will be velocity gradients in the radial direction so all fluid elements may not have the same residence time in the reactor.
2. There will be an interchange of material between fluid elements at different axial positions by virtue of ordinary molecular diffusion and eddy diffusion processes arising from turbulence and/or the influence of any packing in the bed.

3. There may be radial temperature gradients in the reactor that arise from the interaction between the energy released by reaction and convective transport of energy.

To estimate the deviation of a tubular flow reactor with axial diffusion from the plug flow assumption, Reman^{<36>} has used Danckwerts solution of a differential equation which describes a plug flow reactor following first-order kinetics. He found that for $D/vl < 0.1$ the reactor follows the plug flow assumption, and for $D/vl > 2.0$ the reactor behaves like a well-mixed one^{<37>}. Here D is diffusion coefficient, v is mean velocity, l is reactor length. In addition, the ratio of actual reactor volume to plug flow reactor volume should approach 1.

$$\frac{V_{act}}{V_{pf}} = 1 + kt \frac{D}{vl}$$

Here k is rate constant, t is residence time. For our reactor, D/vl is always below 0.1 (from max. $1.669E-3$ to min $3.126E-5$) and the highest value of the ratio V_{act}/V_{pf} was 1.01. This would be sufficient for the plug flow assumption to hold true if the Reynolds number were in the upper range of laminar flow when molecular diffusion effects in dispersion are negligible compared to the effect of the velocity^{<38>}. This is, however, not true for our experiments (We are in the lower laminar flow range).

A more rigorous analysis that is applicable to our system is given in the paper by Poirier and Carr³⁹. They solved the continuity equations for a tubular flow reactor with radial diffusion first-order kinetics. They propose that if D/kR^2 (where D is diffusion coefficient, R is the radius of reactor, k is the homogeneous rate constant) is equal to or greater than 0.5, the plug flow approximation is satisfied ($D/kR^2 \geq 0.54$).

B. Decoupling of the wall and Bulk Reaction Rate Constants

The decomposition of chlorinated hydrocarbons is not only a function of temperature and residence time but also of the radius of the reactor. This means that, the reaction at the wall in addition to the bulk reaction needs to be evaluated if one is occurring.

In order to simplify the formulation of governing equations for a reactor system in which both bulk and wall reactions are present, it is usually assumed that the two reactions are parallel and independent¹⁷. Hence, for the first order reaction of species A one can write:



$$\begin{aligned} \text{Rate} &= - \frac{d[A]}{dt} = k_b * [A] + k_w * [A] * [A_w] \\ &= (k_b + k_w * [A_w]) * [A] \end{aligned} \quad (1)$$

$$k_{exp} = k_b + k_w * [A_w] \quad (2)$$

Assuming a rapid radical diffusion, A_w can be written as^{<36>}:

$$A_w = (S/V) \quad (3)$$

where:

A_w = wall concentration

S/V = surface to volume ratio

= $2/R$ for a cylindrical reactor

From (2) and (3) one obtains:

$$K_{exp} = K_b + K_w * (2/R) \quad (4)$$

In this equation k_b is the first order reaction rate constant for the bulk or homogeneous reaction and k_w is the rate constant for the wall or heterogeneous reaction. If we use several reactors of different radius this equation allows k_b and k_w to be evaluated. The Arrhenius behavior of each rate constant can then be determined.

C. Rate of Reaction Predicted by the Theories

Experimental values for rates of reaction are generally either in the order of magnitude of, or are below, those

predicted by **collision theory**. Thus collision theory may be used to estimate the upper bound to the expected rate of reaction. Once in a while a reaction is encountered with much higher rates than predicted. This suggests a complex reaction, frequently catalytic. Occasionally, for the elementary reaction between simpler molecules, enough information is available to allow prediction of the rates from **transition-state theory**. When available, these predictions usually agree more closely with the experiment than do the predictions of collision theory where references to this are presented by Levenspiel <17>.

[1]. **Transiton-State Theory**

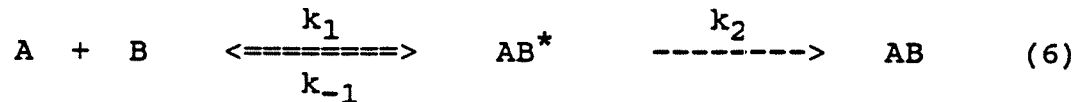
For many reactions, particularly elementary, the rate expression can be written as a product of a temperature dependent term and a composition term.

A more detailed explanation for the transformation of reactants into products is given by the transition-state theory. The reactants combine to form unstable intermediates called activated complexes which then decompose spontaneously into products or back to reactants. It assumes that an equilibrium exists between the concentration of reactants and activated complex at all times. Further, it assumes the rate of decomposition of

complex is the same for all reactions which is given by kT/h where k is the Boltzmann constant and h is the Planck constant. For the forward elementary reaction of a reversible reaction.



we have the following conceptual elementary scheme:



$$K^* = \frac{k_1}{k_{-1}} = \frac{[AB^*]}{[A][B]}$$

$$k_2 = \frac{kT}{h}$$

The observed rate of the forward reaction is then

$$\begin{aligned} r_{AB, \text{forward}} &= (\text{conc. of activated complex}) \times (\text{rate of decomposition activated complex}) \\ &= \frac{kT}{h} [AB^*] \\ &= \frac{kT}{h} K^* C_A C_B \end{aligned} \quad (7)$$

By expressing the equilibrium constant of activated complex

in terms of the standard free energy,

$$\begin{aligned}
 \text{LIG}^* &= \text{LIB}^* - \text{TLIS}^* = -RT \ln K^* & (8) \\
 K^* &= \text{EXP}(-\text{LIG}^*/RT) = \text{EXP}(-\text{LIH}^*/RT + \text{LIS}^*/R)
 \end{aligned}$$

the rate becomes

$$r_{AB, \text{forward}} = \frac{kT}{\text{EXP}(\text{LIS}^*/R) \text{EXP}(-\text{LIH}^*/RT)} C_A C_B \quad (9)$$

Theoretically both LS^* and LIB^* vary slowly with temperature. Hence, of the three terms that make up the rate constant in Eq. 9, the middle one, $\text{EXP}(\text{LIS}^*/R)$, is much less temperature-sensitive than the other two. We may take it to be constant. For the forward reaction, and the reverse reaction of Eq. 5, we have approximately

$$\begin{aligned}
 k_f &= T \text{EXP}(-\text{LIH}_f^*/RT) & (10) \\
 k_r &= T \text{EXP}(-\text{LIH}_r^*/RT)
 \end{aligned}$$

where $\text{LIH}_f^* - \text{LIH}_r^* = \Delta H_{RXN}$

[2]. Collision Theory

The collision rate of molecules in a gas can be found from the kinetic theory of gases. For the bimolecular collisions of like molecules A we have

$$Z_{AA} = d_A^2 n_A^2 \left[\frac{4 kT}{M_A} \right]^{1/2} = d_A^2 \frac{N^2}{10^6} \left[\frac{4 kT}{M_A} \right]^{1/2} C_A^2$$

where d = diameter of molecule, cm

M = mass of molecule, gm

N = Avogadro's number

C_A = concentration of A, mol/liter

n_A = number of molecules of A/cm³

k = Boltzmann constant

For bimolecular collisions of unlike molecules in a mixture of A and B, the kinetic theory gives

$$Z_{AB} = \left(\frac{d_A + d_B}{2} \right)^2 \frac{N^2}{10^6} \left[8 kT \left(\frac{1}{M_A} + \frac{1}{M_B} \right) \right]^{1/2} C_A C_B$$

If every collision between reactant molecules results in the conversion of reactants into product, these expressions give the rate of bimolecular reaction. The actual rate is usually much lower than that predicted, and this indicates that only a small fraction of all collisions result in reaction. Suggesting that only more energetic and violent collisions, those involving energies in excess of a given minimum energy E , lead to a reaction. From the Maxwell Boltzmann distribution law of molecular energies the fraction of all bimolecular collisions that involve energies in excess of this minimum energy is given approximately by $\exp(-E/RT)$, where E is usually much greater than RT . Since we are only considering energetic collisions, this assumption is reasonable. Thus the rate of reaction is given by

$$\begin{aligned}
 -r_A &= k C_A C_B = \left[\text{collision rate} \right] * \left[\text{fraction of collisions involving energies in excess of } E \right] \\
 &= Z_{AB} \frac{10^3}{N} e^{-E/RT} \\
 &= \left(\frac{d_A + d_B}{2} \right)^2 \frac{N}{10^3} \left[8 kT \left(\frac{1}{M_A} + \frac{1}{M_B} \right) \right]^{1/2} e^{-E/RT} C_A C_B
 \end{aligned}$$

A similar expression can be found for the bimolecular collisions between like molecules. For both, in fact for all bimolecular reactions, the above equation shows that the temperature dependency of the rate constant is given by

$$k = T^{1/2} e^{-E/RT}$$

[3]. Comparison of Two Theories

It is interesting to note the difference in approach between the **transition-state** and **collision** theories. Consider A and B colliding and forming an unstable intermediate which then decomposes into product, or



collision theory views the rate to be governed by the number of energetic collisions between reactants. What happens to

the unstable intermediate is of no concern. The theory assumes that this intermediate breaks down rapidly enough into products so as not to influence the rate of the overall process. Transition-state theory, on the other hand, views the reaction rate to be governed by the rate of decomposition of intermediate. The rate of formation of intermediate is assumed to be governed by collisions plus thermodynamics. It is dependent on equilibrium concentrations at all times. Thus collision theory views the first step to be slow and rate-controlling, whereas transition-state theory views the second step combined with the determination of complex concentration to be the rate controlling factors.

D. Prediction of Rate Constants for Radical Addition and Recombination Reactions by Bimolecular QRRK Theory

The significant aspects of this thesis are the experimental results and the detailed chemical kinetic model, both of which are presented later on. The **QRRK** theory described below is very important to our model development research. A brief description of this theory from the article by Westmoreland and Dean^{<22>} is therefore treated as a quote.

Bimolecular QRRK (**Quantum Rice Ramsperger Kassel**)^{<40>}

analysis is a simple method for calculating rate constants of addition and recombination reactions, based on unimolecular quantum RRK theory. Input parameters are readily derived, and rate constants and reaction branching can be predicted with remarkable accuracy. Such predictive power makes the method especially useful in developing mechanisms of elementary reactions²⁰.

"Predictions by this method can be made quickly, in part because the input data are few and frequently are easy to obtain:

1. Preexponential factors and activation energies in the high pressure limit, A_i and E_{act} .
2. The number of vibrational degrees of freedom for the adduct, s .
3. The geometric mean of the adduct's vibrational frequencies, $\langle \nu \rangle$, calculated from them.
4. Lennard Jones transport properties, σ and ϵ/k , for the adduct and for the third body gas.
5. The average energy transferred per collision with the third body gas, $\langle E_{coll} \rangle$, which has been experimentally evaluated for a variety of gases.

Obtaining A_i and E_{act} may be the most difficult task. These parameters can come from literature data, from estimates by the methods of Benson (1976,1983), from the generic rate constants of Dean ^{<20>} (1985), or from the equilibrium constant and the reverse rate constant (high pressure limit). References are in the Dean's paper^{<20>}."

[1]. Unimolecular QRRK Equation

"Dean^{<20>} (1985) has presented equations for bimolecular rate constants based on the Quantum-RRK or QRRK unimolecular reaction theory of Kassel (1928), which treats the storage of excess energy (relative to the ground state) as quantized vibrational energy.

In the simplest form of the theory, the assumption is made that the vibrations of the decomposing molecule can be represented by a single frequency ν , usually a geometric mean $\langle \nu \rangle$ of the molecule's frequencies. Using a single geometric mean $\langle \nu \rangle$ to present all the ν 's in a molecule is one approximation, and use of the arithmetic mean has been suggested by Thiele et.al.,1980. For the total energy variable E , the symbol n is used. For the number of quanta to the energy barrier to reaction E_0 , the quantized energy

is m quanta. The quantum level and the rate processes are illustrated in Figure 11-

The apparent k_{uni} :

$$k_{uni} = \frac{1}{[A]} \frac{d [\text{Products}]}{dt} \quad (11)$$

then is evaluated by a sum over all energies, assuming pseudo-steady state for each energy level of A^* and collisional excitation or deexcitation with rate constants k_{exc} and k_{deexc} :

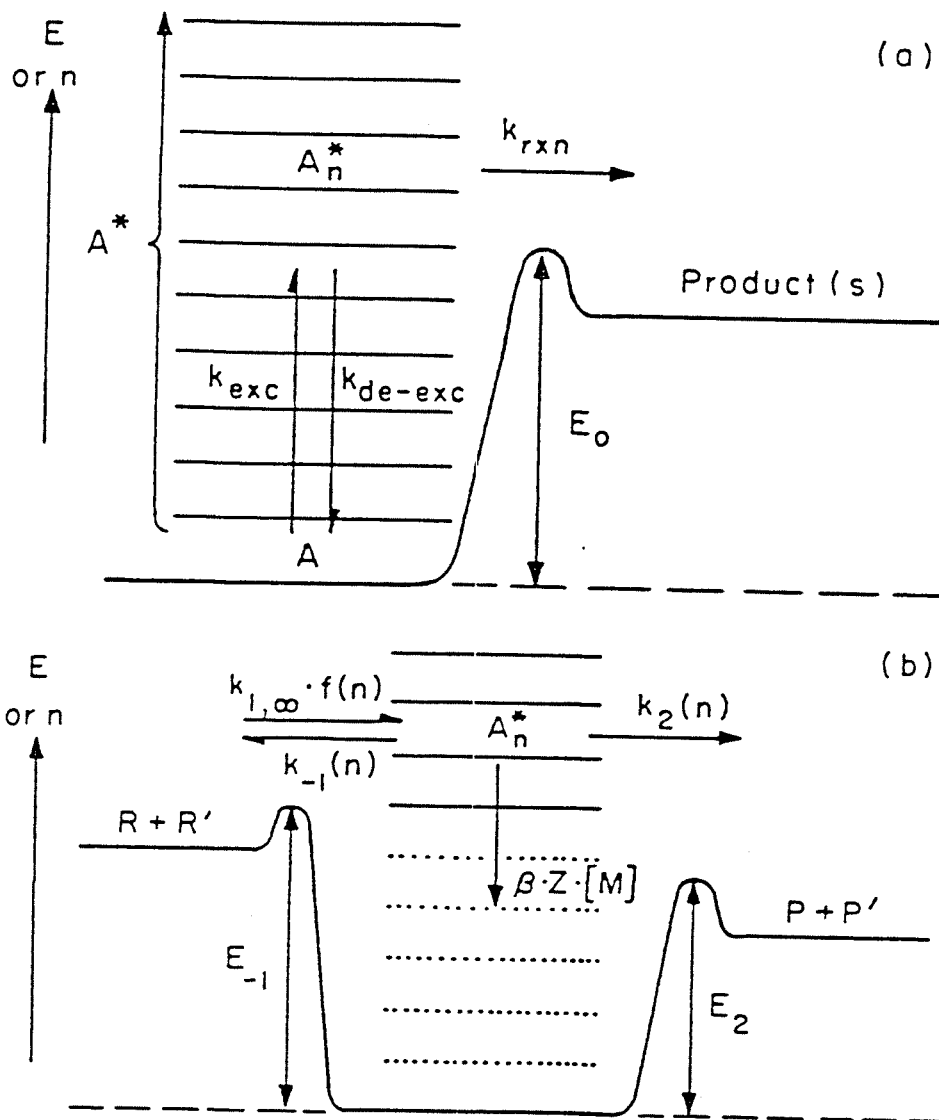
$$\begin{aligned} k_{uni} &= \frac{1}{[A]} \sum k_{rxn}(E) [A^*(E)] \\ &= \sum k_{rxn}(E) \frac{k_{deexc}[M] K(E,T)}{k_{deexc}[M] + k_{rxn}(E)} \end{aligned} \quad (12)$$

where $K(E,T)$ is the thermal-energy distribution function (k_{exc}/k_{deexc}). Kassel assumed that if a molecule were excited to an energy E , then $k_{rxn}(E)$ would be proportional to the probability that one of the s oscillators could have energy E_0 or greater (sufficient energy to cause reaction); that is, m or more of the n total quanta.

The energy-dependent rate constant can be written as:

$$k_{rxn}(E) = A_i \frac{n! (n-m_i+s-1)!}{(n-m_i)! (n+s-1)!} \quad (13)$$

where A_i is the high pressure Arrhenius preexponential



Energy diagrams for pressure-dependent reactions.

- a. Unimolecular reaction
- b. Bimolecular reaction with chemically activated pathway

Figure 3.1

(Reprinted from Dean paper^{<20>})

factor for reaction i , and m_i is the number of quanta ($E_i/h\nu$) corresponding to the energy threshold for the reaction i . Likewise, he derived the quantized thermal energy distribution $K(E,T)$ to be:

$$K(E,T) = a^n (1-a)^s \frac{(n+s-1)!}{n! (s-1)!} \quad (14)$$

where $a = e(-h\langle v \rangle/kT)$.

In the present development, we have modified the theory to utilize the Gamma function in place of factorials. A collisional efficiency β has been applied to modify the traditional but incorrect strong-collision assumption that $k_{deexc} = Z_{[M]}$, where Z is the collision frequency rate constant. The strong-collision assumption implies that any collision between A^+ and M would have to remove all the excess energy from A^+ . Note that any species included as M would have to accommodate this energy content, regardless of its capacity for accepting the energy. Analyzing collisional energy transfer for master-equation methods, Troe (1977) fit most of the temperature dependence of β with the equation:

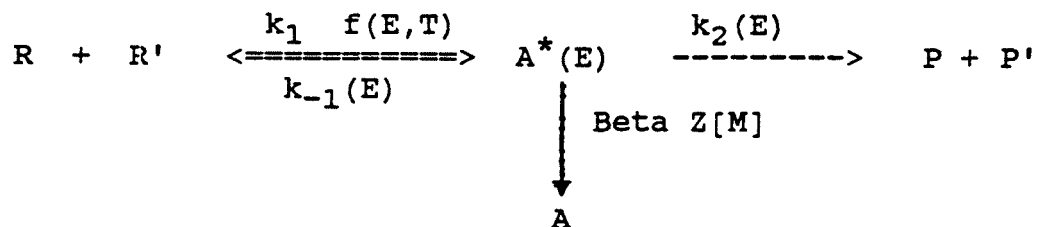
$$\frac{\beta}{1-(\beta)^{1/2}} = \frac{-\langle \Delta E_{coll} \rangle}{F(E) k T} \quad (15)$$

where $\langle E_{coll} \rangle$ is the average amount of energy transferred

per collision and $F(E)$ is a factor, weakly dependent on energy, that is related to the number of excited states. Over the temperature range of 300-2500 °K for a series of reactions (Troe, 1977); $F(E) = 1.15$ was observed as a median value. The value of Beta depends on the specific third-body molecule M through the value of $\langle AE_{coll} \rangle^*$

[2]. Bimolecular QRRK Equations

The bimolecular QRRK equations follow (Dean, 1985) from unimolecular QRRK and the definition of the chemical activation distribution function. Consider recombination or addition to occur via the sequence:



Here, k_1 is the high-pressure-limit rate constant for forming adduct and $f(E,T)$ is the energy distribution for chemical activation:

$$f(E,T) = \frac{k_{-1}(E) K(E,T)}{\int_{E=E_{-1}}^{\infty} k_{-1}(E) K(E,T) dE} \quad (16)$$

where $K(E,T)$ is the QRRK thermal distribution from Eq. 14. Rate constants $k_1(E)$ and $k_2(E)$ are calculated from the QRRK equation for $k_{rxn}(E)$ (Eq. 13) using $m_1(E_i/h\langle v \rangle)$ and $m_2(E_2/h\langle v \rangle)$, respectively. A typical energy diagram for these reactions is shown in Figure 1-b.

To obtain the bimolecular rate constant for a particular product channel, a pseudo steady-state analysis is made as before. The rate constant for forming the addition/stabilization product $A^*(E)$ from $R + R'$ is:

$$k_{a/s} = \sum_{\substack{E=E_{-1} \\ (n=m_{-1})}}^{\infty} \text{Beta } Z[M] \frac{k_{1,\infty} f(E,T)}{\text{Beta } Z[M] + k_{-1}(E) + k_2(E)} \quad (17)$$

and, for forming the addition/decomposition product $P + P'$:

$$k_{a/d} = \sum_{\substack{E=E_{-1} \\ (n=m_{-1})}}^{\infty} k_2(E) \frac{k_{1,\infty} f(E,T)}{\text{Beta } Z[M] + k_{-1}(E) + k_2(E)} \quad (18)$$

If more decomposition channels are available, the $k_{rxn}(E)$ for each channel is added in the denominator of Eqs. 17 and 18, and an equation in the form of Eq.18 is written for each additional channel, substituting the respective $k_{rxn}(E)$ for $k_2(E)$ as the multiplier term.

[3]. Low and High-Pressure Limits

The low-pressure and high-pressure limits for these channels may be derived from Eqs. 17 and 18. As pressure changes, the rate constants change because of the relative magnitudes of terms in the denominator, $\text{Beta} \cdot Z[M]$ vs. $k_1(E)$ and $k_2(E)$.

The low-pressure limit for addition/stabilization (or recombination) is derived from Eq. 17 to be

$$\lim_{[M] \rightarrow 0} k_{a/s} = [M] \sum_{\substack{E=E_{-1} \\ (n=m-1)}}^{\infty} \text{Beta} Z \frac{k_{1,\infty} f(E,T)}{k_{-1}(E) + k_2(E)} \quad (19)$$

sometimes written as $[M] \cdot k_0$ (as a termolecular reaction), and the high-pressure limit reduces properly to k_1 . At a given temperature, the falloff curve for stabilization can be plotted as $\log(k_{a/s})$ vs. $\log(P)$ or $\log(M)$.

Note the presence of $k_2(E)$ in Eq. 19. If chemically activated conversion of $A^*(E)$ is more rapid than decomposition to reactants [$k_2(E) \gg k_{-1}(E)$], then Eq. 19 shows that $k_{a/s}$ will be divided by $k_2(E)$ rather than by $k_{-1}(E)$. Thus, ignoring the chemically activated pathway could give incorrect rate constants for "simple" addition.

Similar analysis of Eq. 18 implies that chemically

activated decomposition has a falloff curve that is the opposite of addition/stabilization, with a rate constant that is pressure-independent at low pressure and inversely proportional to pressure at high pressure. From Eq. 18, the low-pressure limit for the chemically activated pathway to P and P' will be

$$\lim_{[M] \rightarrow 0} k_{a/d} = k_{1,\infty} \sum_{\substack{E=E_{-1} \\ (n=m_{-1})}}^{\infty} \frac{k_2(E) f(E,T)}{k_{-1}(E) + k_2(E)} \quad (20)$$

and the high-pressure limit will be

$$\lim_{[M] \rightarrow \infty} k_{a/d} = \frac{1}{[M]} \frac{k_{1,\infty}}{\text{Beta } Z} \sum_{\substack{E=E_{-1} \\ (n=m_{-1})}}^{\infty} k_2(E) f(E,T) \quad (21)$$

with an inverse pressure dependence. While this result goes against past intuition about low- and high- pressure limits, it is a natural consequence of physics when chemically activated reaction are recognized as possibilities. One consequence is that a reaction of the form $A + B \rightarrow C + D$ with a rate constant measured to be pressure-independent may be proceeding via addition."

IV. EXPERIMENTAL METHOD

The reactions of chlorobenzene in hydrogen and oxygen mixtures were studied in three different tubular flow quartz reactors of 4 mm, 10.5 mm, and 16 mm ID. The reactor system was operated isobarically and isothermally at one atmosphere pressure and temperature ranging from 833K to 933K (560 °C-660 °C).

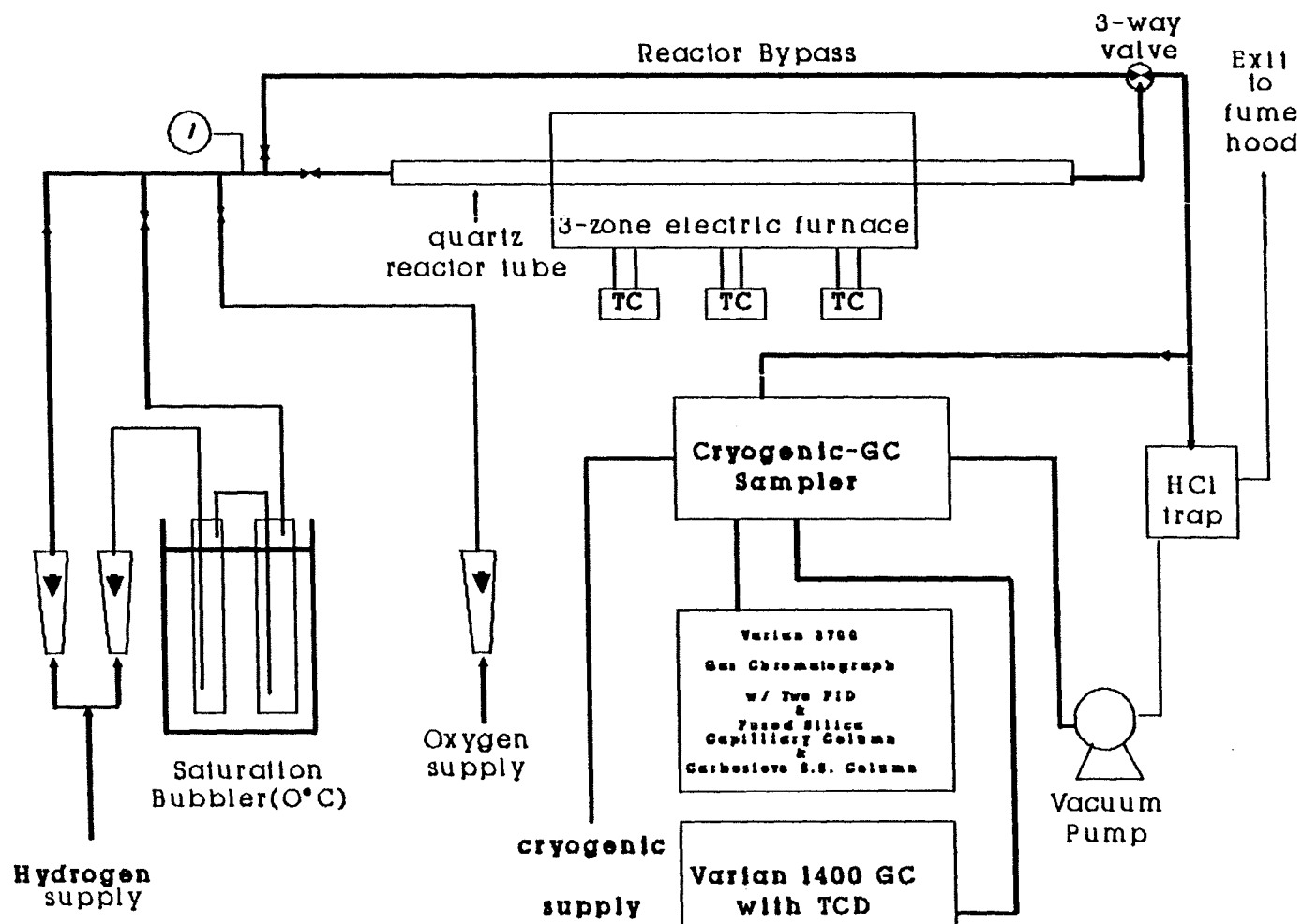
Hydrogen gas was bubbled through four bubblers all in series to insure the gas was completely saturated with the chlorobenzene. All four bubblers were set at 0 °C (So the initial C₆H₅Cl mole fraction was 0.0037) for all reaction conditions. Hydrogen gas saturated with the chlorobenzene was then mixed with 1% to 5% oxygen gas. The mixture was preheated to nearly 573K (300 °C) before entering the furnace by heating tape to prevent adsorption and help achieve uniform temperature in the reactor. The hydrogen carrier gas flow ranged from 50 cm³/min to 3000 cm³/min and was controlled by two parallel needle valves. The oxygen gas flow ranged from 1 to 150 cm³/min.

The quartz reactor tube was heated with a three zone (3 - 12 - 3 inch Clamshell segments) Thermcraft. The furnace had an over-all length of 18 inches and 1.25 inches I.D. Upon exiting the furnace the effluent passed through a

heated transfer line before either being sampled by an on-line GC (Gas Chromatography) or being exhausted to the fume hood. All transfer lines, including the reactor bypass, were heated. (300°C) to prevent adsorption or condensation of reagent or products. A small fraction of the reactor gas effluent was collected in the GC sample valve loop (0.25 ml). Gas was drawn through a heated Pyrex line to the valve by means of vacuum pump. A glass wool filter was set before GC in order to prevent contamination of the GC sampling valve with solid carbon. The bulk of the effluent was exhausted to a fume hood after the HCl was neutralized. The combustion reactor flow systems are illustrated in Figure 4.1.

[A]. **Temperature Measurement and Control**

The temperature profile within the reactor was maintained isothermal at the desired temperature using a three zone furnace which was equipped with three independent Omega CN 300 PI digital temperature controllers. Continuous feedback control helped keep the reactor at the desired reaction temperature. The furnace also contained a separate quartz tube 4 mm ID (not a reactor tube) which housed three K type thermocouples to measure the temperature in each zone. The actual temperature profile in and throughout the tubular reactor was obtained by using an additional K type



Figur€431 Experimental systerr

thermocouple which could be moved axially inside reactor over the entire length. Helium gas was allowed to pass through the reactor while this measurement was taken, which reduced radiation error and helped produce flow conditions similar to those obtained during the experimental runs. The probe was removed from the reactor once temperature measurements were finished.

The temperature profiles were isothermal to within $\pm 5^{\circ}\text{C}$ over 90 % of the reaction zone (center of reactor). Figure 4.2 shows the temperature profiles in this system. The thermocouple calibration was necessary to accurately measure the actual temperature profile of the gas in the reaction zone.

[B].Quantitative Analysis By Gas Chromatography

Quantitative analysis of the products was performed using a Varian 3700 Gas Chromatograph equipped with two Flame Ionization Detectors (**FID**). One is to analyze heavy hydrocarbons ($\text{C}_4\text{-C}_{18}$), and the second is to analyze light hydrocarbon products ($\text{C}_1\text{-C}_3$). A Chrompack fused silica capillary column, 25 meters in length and 0.32 mm ID, was used to analyze heavier hydrocarbon reagent and products. The capillary column had a bonded stationary phase of methyl silicone (CPSil 5). Helium was supplied to the column inlet

TEMPERATURE PROFILE OF CLBZ + H₂ + O₂ IN 10.5 mm REACTOR

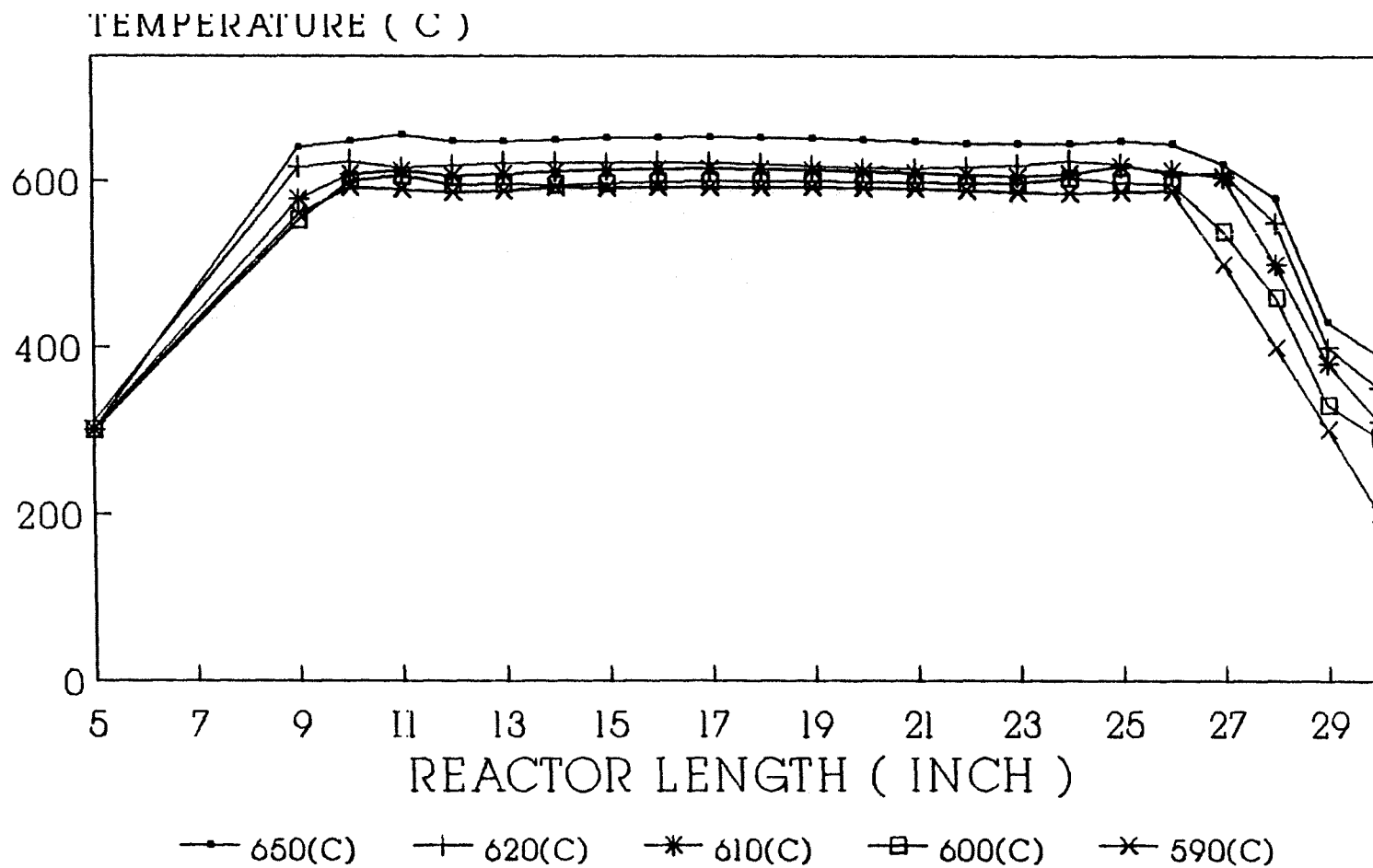


Figure 4.2

at a pressure of 10 psig. The GC gas samples of 0.25 ml volume were maintained at 150 °C and 1 ATM. The samples were injected with the use of a 6 port Valco gas sampling valve. The sampling system structure is shown in Figure 4.3. Reproducibility (95%) of the injection volume and conditions was maintained by use of fixed volume sample loop together with a six port gas sampling valve. After injection, the sample was cryogenically focused (concentrated) at the head of the column. Focussing was achieved by keeping the capillary column immersed in a bath of liquid O₂/N₂. The liquid O₂ was generated by passing dry air through a heat exchanger which was submerged in liquid N₂. Cryogenic focussing was carried out for a period of 1 min. At the end of the cryo-focussing cycle, the sample was reinjected into the helium carrier gas by rapidly heating it to 200 °C. This was accomplished by passing pulses of 6 - 10 VAC through a short piece of thin walled 1/16" S.S. tube which reached 200 °C. The time required to heat the sample from -150 °C to 200 °C was approximately 1 min. The heating element rise time was found to be an important factor in determining the peak resolution and selectivity of the chromatogram. The GC column oven was constantly maintained at 70 °C.

In order to separate light hydrocarbon, a Carboseive G 60-80 mesh packed column tubing size 1/8" * 5 ft length was employed as column B. The oven temperature for column B

AUTO-SAMPLER DIAGRAM

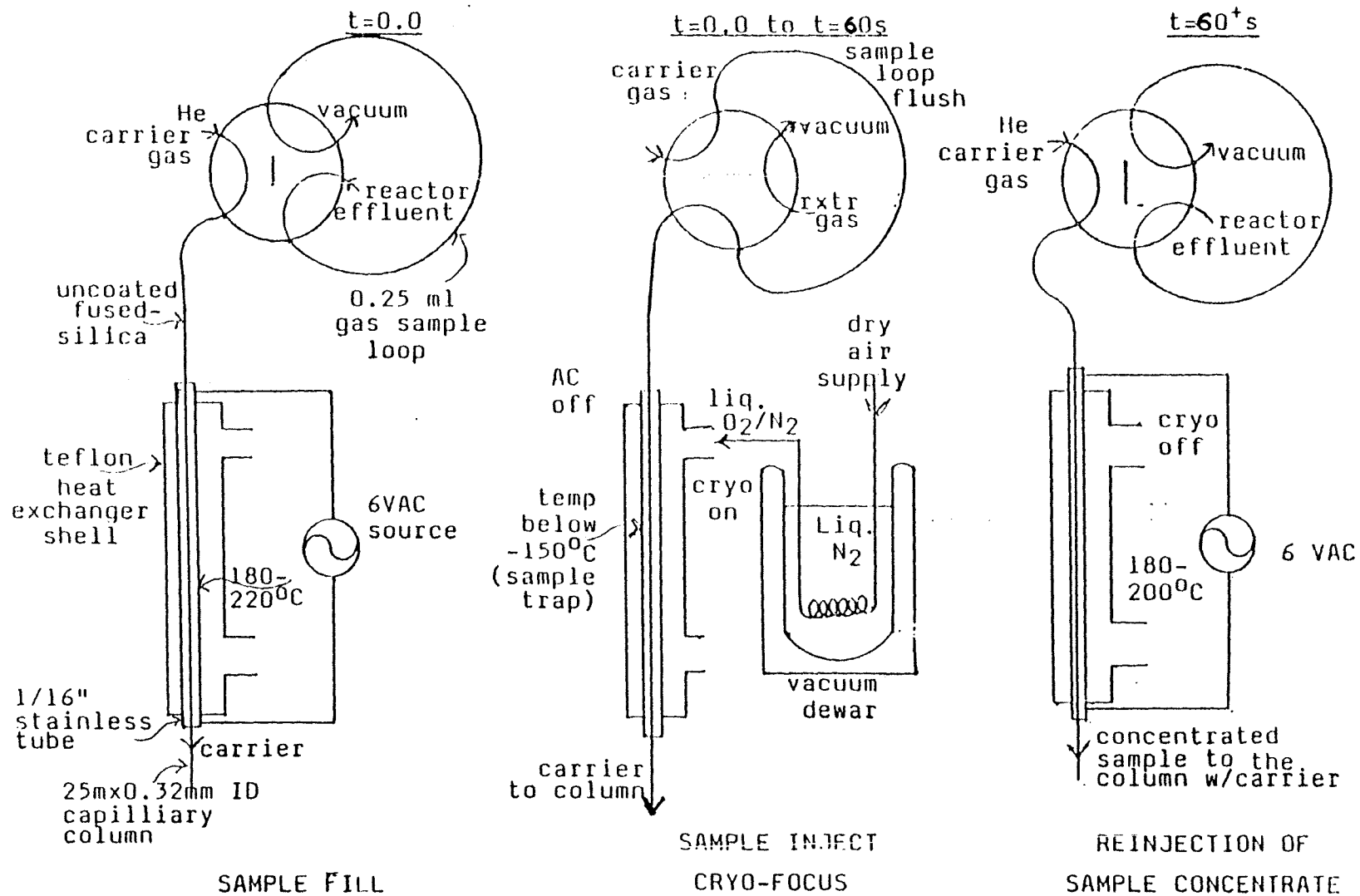


Figure 4.3

(Permitted by J. W. Bozzelli and Ritter^{<9>})

analysis was ramped from 145°C to 185°C at a rate of 20 °C/min and held for 4 min. The flow rate of the carrier gas, nitrogen, was 50 cm³/min (no cryofocusing was utilized here).

The two FID's were set at 280°C. The FID for channel A (capillary column) was supplied with nitrogen make-up gas at a rate of 35 ml/ min. Hydrogen and air were supplied to the detector at the rate of 30 cm³/min and 250 cm³/min respectively. The signal amplification sensitivity was set to 10E-11 amp/mv for both channel A and channel B. Integration was performed with a Spectra Physics SP 4270 integrator/plotter using an attenuation of 512 and a chart speed of 1 in/min.

The response factors (Channel A) had been previously determined for this GC/FID at similar operating conditions^{<9>}. These response factors are listed in Table (I). ,The response factor (Channel B) are listed in Table (II)^{<16>}. Integrator chromatograms are shown in Figure 4.4 and Figure 4.5, respectively.

[C].Quantitative Analysis of HCl

Quantitative analysis of HCl was performed using the 16 mm and 10.5 mm diameter reactor and a residence time of 1 second. In this analysis, the effluent was diverted through

TABLE 4.1 RESPONSE FACTORS FOR CHANNEL A

COMPOUND	RELATIVE RESPONSE FACTOR (RRF)
C6H5CL	1.0
C6H6	1.2
C6H5CH3 (toluene)	1.4
C5H6 (cyclopentadiene)	1.0

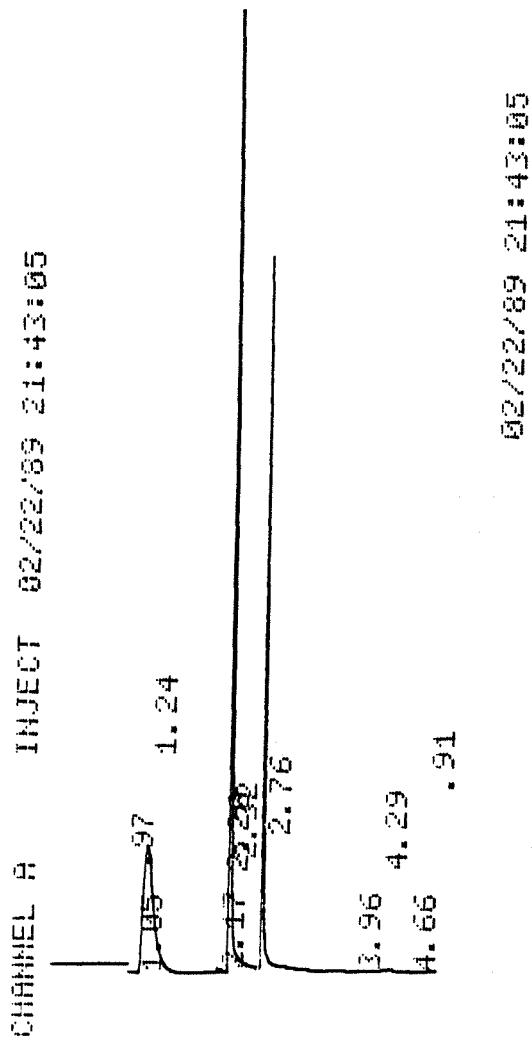
*corrected area = measured area * RRF

TABLE 4.2 RESPONSE FACTORS FOR CHANNEL B

COMPOUND	RELATIVE RESPONSE FACTOR (RRF)
CH4	1.0
C2H2	1.45
C2H4	1.81
C2H6	2.0
C3H4	2.47
C3H6	2.8
C3H8	3.2

*corrected area = measured area * RRF

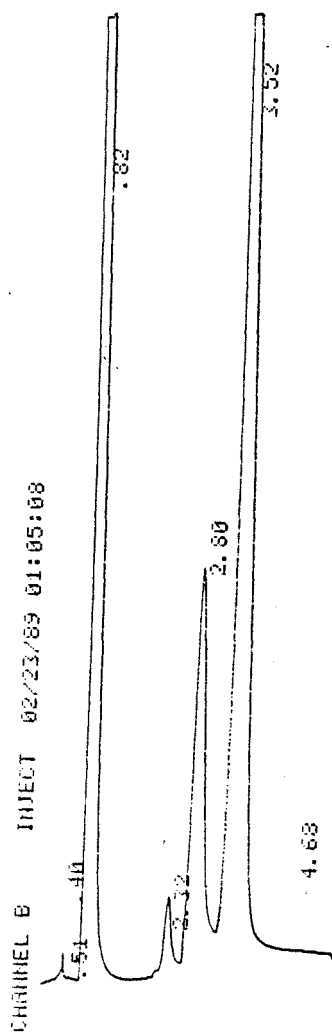
Figure 4.4
Channel A Sample Chromatogram



PEAK #	COMPOUND	RETENTION TIME (MIN)
1	C2s	1.02
2	CYCLOPENTADIENE	2.0
3	BENZENE	2.2
4	TOLUENE	2.3
5	CHLOROBENZENE	2.7

Column: 25m * 0.32 mm ID CP Sil 5 (methyl silicone)
 Detector: flame ionization detector (FID) at 270 C
 Temperature : at constant temperature of 70 C
 Carrier gas : Helium supplied at 10 psig

Figure 4.5
Channel B Sample Chromatogram



PEAK #	COMPOUND	RETENTION TIME (MIN)
1	CH ₄	0.8
2	C ₂ H ₂	2.3
3	C ₂ H ₄	2.8
4	C ₂ H ₆	3.5

Column: 5ft * 1/8"ss ID Carbosieve G
 Detector: flame ignition detector (FID) at 270 °C
 Temperature : 145 C to 195 C
 programmed at rate 20 °C/min, hold 4 min
 Carrier gas : Nitrogen supplied at 10 psig, 50 cm³/min

a two stage bubbler before being exhausted to the hood. Each of two stages contained 15 ml of 0.01 N NaOH. The gas was passed through the two bubblers until the first one reached its phenolphthalein end point. The NaOH solution also collected CO₂ produced from reaction ($\text{CO}_2 + \text{H}_2\text{O} \rightarrow \text{H}_2\text{CO}_3$). H₂CO₃ will dissociate to form H⁺ and HCO₃⁻. The H⁺ ion will affect HCl titration. Because only a few percent CO₂ (less than 2%) formation, we can omit this titration error. The time required for this to occur was recorded. At this point bubbling was stopped, the aliquots combined, and titrated to their phenolphthalein end point with 0.01 N HCl. The HCl produced by reaction was then calculated.

[D]. Quantitative Analysis of CO and CO₂ by TCD

Quantitative analysis of CO and CO₂ was performed using the 1/8" * 5 ft stainless steel column packing with Carbo-sphere(80-100 mesh). Thermal Conductivity Detector (TCD attenuation =16) was maintained at a temperature of 40 °C and was supplied with helium gas at a rate of 20 ml/min. A fraction of reactor effluent was passed through a six port gas sampling valve which collected a 1 ml sample volume. Analysis was performed using a Varian 1400 GC oven at constant temperature of 40 °C. Integration was performed with a Spectra Physics SP 4290 Integrator/ Plotter using a chart speed of 0.25 in/min. The analysis integration chart is

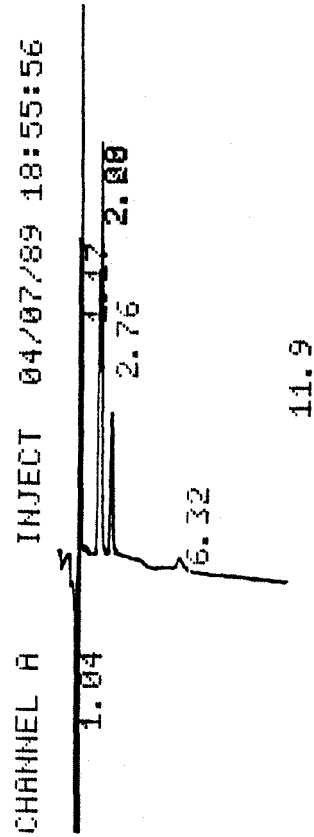
shown in Figure 4.6.

E. Mechanism Modeling by CHEMKIN Program

The **CHEMKIN** computer package is used for interpreting and integrating the detailed reaction mechanism (model) of the systems which were studied. The **CHEMKIN** program^{<27>}, Figure 44, reads the user's symbolic description of the reaction mechanism. The thermodynamic database has the appropriate thermodynamic information, mass and elemental composition for all species present in mechanism, and is in a format similar to the one used by the NASA chemical equilibrium code^{<27>}. The **CHEMKIN** gas phase subroutines, which can be called to return information on the elements, species, reactions, equation of state, specific thermodynamic properties, chemical production rates, and derivatives of thermodynamic properties relative to any time in the integration are all included in the **CHEMKIN** package. Generally, in addition to the mechanism, the input to these subroutines are the state variables of gas pressure or density, temperature and species composition. All routines can be called with the species composition defined in terms of mass fractions or molar concentrations. Numerical calculations were carried out using the **CHEMKIN** computer code.

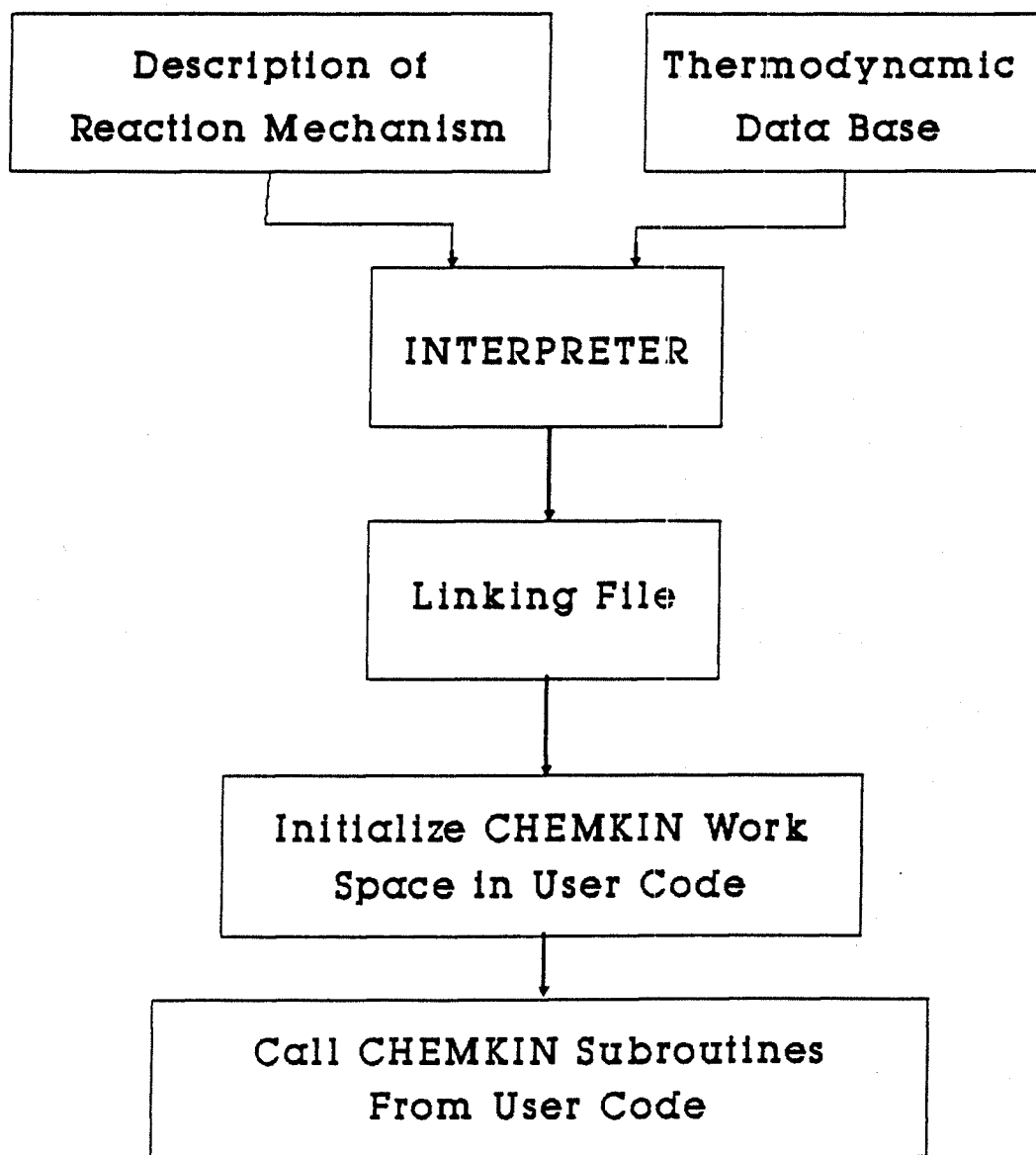
The input data requirement to run **CHEMKIN** program
Include:

Figure 4.6
Channel C Sample Chromatogram



PEAK #	COMPOUND	RETENTION TIME (MIN)
1	H2	1.01
2	O2	2.0
3	N2	2.2
4	CO	2.8
5	CH4	6.5

Column: 5.* 1/8" SS ID packed with Carbosphere
 Detector: Thermal Conductivity detector (TCD) at 40 °C
 Temperature : at constant temperature of 40 C
 Carrier gas : Helium supplied at 10 psig



Structure of the CHEMKIN Package

Figure 4.7

- [1] Detailed reaction mechanism
- [2] Mole fraction of all gases present in the reaction system
- [3] Pressure and temperature at which the reaction system being studied
- [4] Time increment at which the concentration of species present in the system be reported
- [5] Thermo database for all elements & species in mechanism

A thermodynamic database for species with C/H/O/Cl elements is developed at NJIT and used for modeling of the kinetic scheme of reaction system investigated. Heats of formation (H_f) entropies (S), and heat capacities (C_p) were calculated by using THERM program which is developed by E. Ritter and Bozzelli³³ to calculate thermodynamic data when not available in literature.

This computer work was executed on Digital VAX/VMS 11/785 computer of NJIT.

V.RESULTS and DISCUSSION

The experimental conditions of combustion of chlorobenzene reaction with dilute mixtures of oxygen in hydrogen are listed below:

[1]Reactants Ratio (ClBZ : O₂ : H₂):

From 1% of O₂ (ClBZ:O₂:H₂ = 1: 3.05 : 301) to 5% of O₂ (ClBZ:O₂:H₂ = 1 :15.3 :289). Initial C₆H₅Cl concentration is always at mole fraction of **0.0037**.

[2]Reactor Temperatures (°C):

560 , 580 , 590 , 600 , 610 , 620 , 640 , 650 , 660

[3]Effective Reactor Length: 40.6 cm

[4]Reactor Diameter (mm): 4.0, 10.5, 16.0

[5]Residence Time Range:

I.D. = 4.0 mm , RT = 0.03 - 0.4 (sec)

I.D. = 10.5 mm , RT = 0.3 - 2.0 (sec)

I.D. = 16.0 mm , RT = 0.7 - 2.5 (sec)

[6]Operating Pressure: 1 atm.

Seven temperatures ranging from 590 to 640 °C were studied within the 10.5 mm ID reactor. For each temperature 6 residence times were investigated 0.3 to 2.0 seconds.

When using the 4.0 mm and 16 mm ID reactors, five temperatures ranging from 560 to 660 °C were studied. Average residence times within 4 mm ID ranged from 0.05 second to 0.4 second, and within the 16 mm ID reactor from 0.8 second to 2.5 seconds.

A. Reaction of Chlorobenzene with Hydrogen and Oxygen

Mixtures

Experimental results on decomposition of chlorobenzene are shown in Figures 5.1 through 5.11. The normalized concentration (C/C_0) of chlorobenzene reagent as a function of the residence time for several temperatures was studied in different ratios of oxygen in H₂ bath gas for each reactor size.

The concentration of chlorobenzene consistently decreased with increasing residence time for all temperatures shown; and for a constant residence time increases in temperature result in lower reactant concentrations - higher conversion. Figures 5.12 through 5.22 show the loss of chlorobenzene along with the production of benzene, CH₄ and C₂ hydrocarbons at 1 second and 2 seconds residence time in

CLBZ + H₂ + O₂ AT 1 ATM ,O₂/H₂: 1%,
L SIZE (D = 16 mm), DIFF. TEMP.

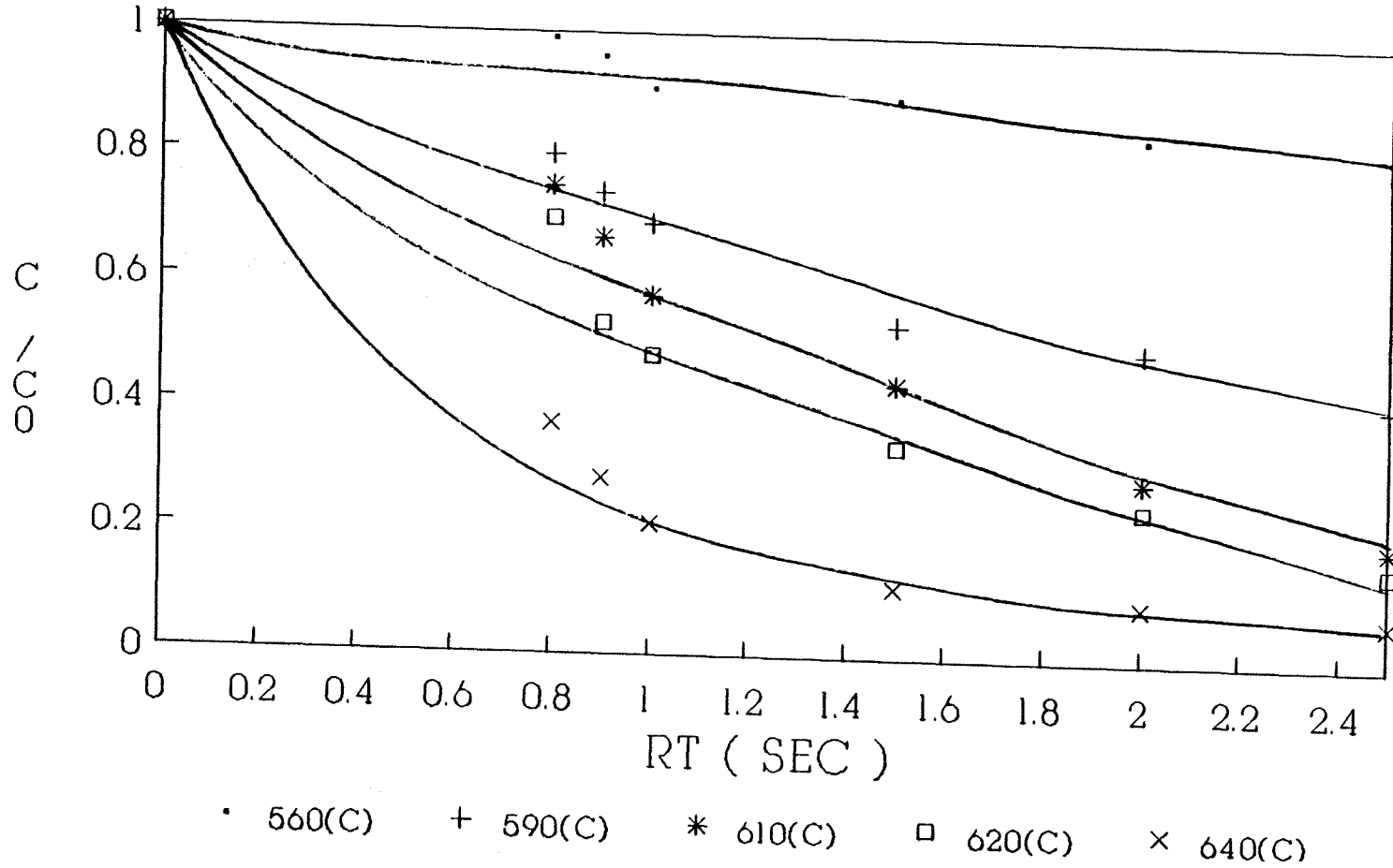


Figure 5.1

CLBZ + H₂ + O₂ AT 1 ATM ,O₂/H₂: 2%,
 L SIZE (D = 16 mm), DIFF. TEMP.

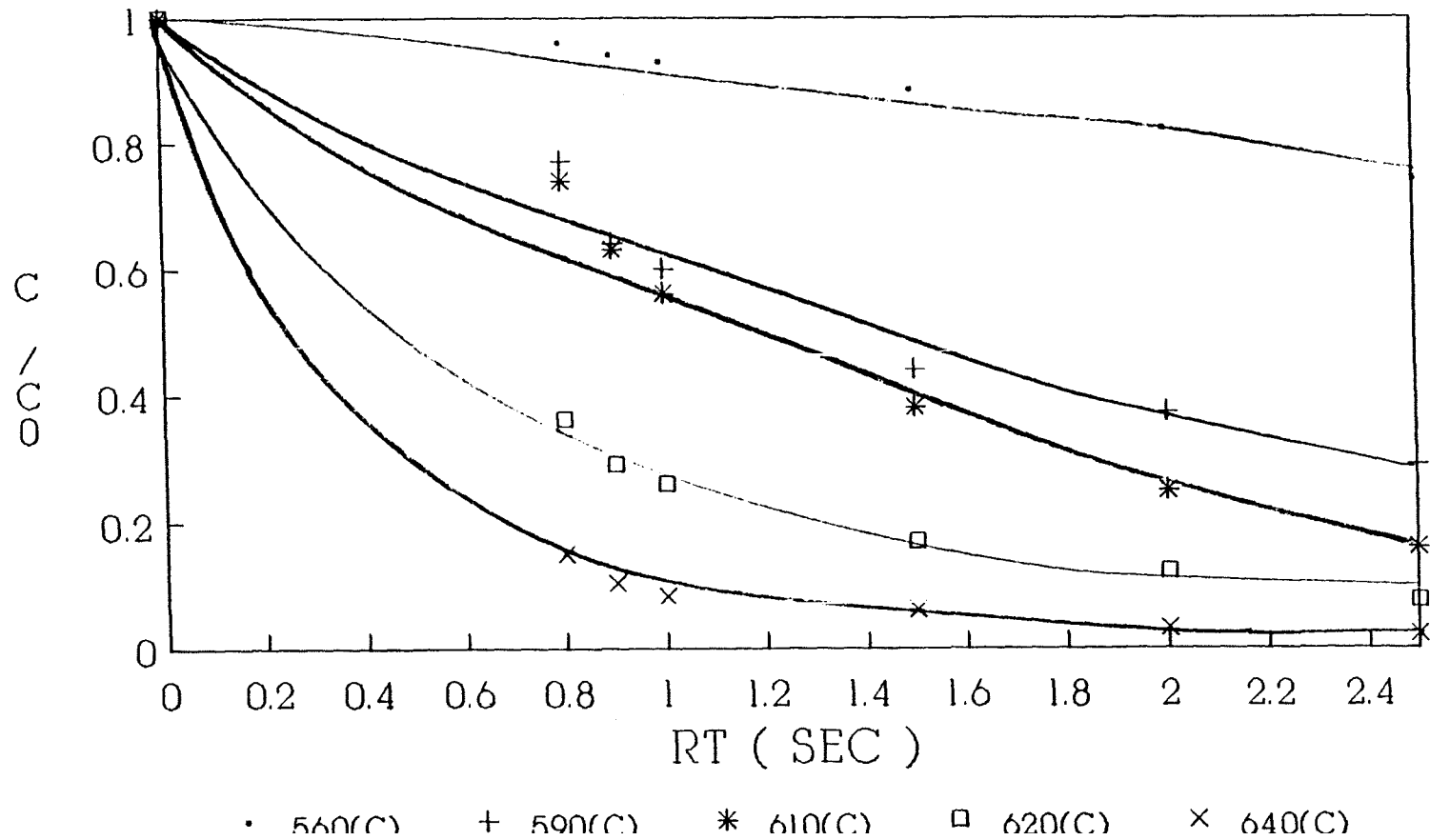


Figure 5.2

CLBZ + H2 + O2 AT 1 ATM ,O2/H2: 3%,
 L SIZE (D a: 16 mm), RIFF. TEMP.

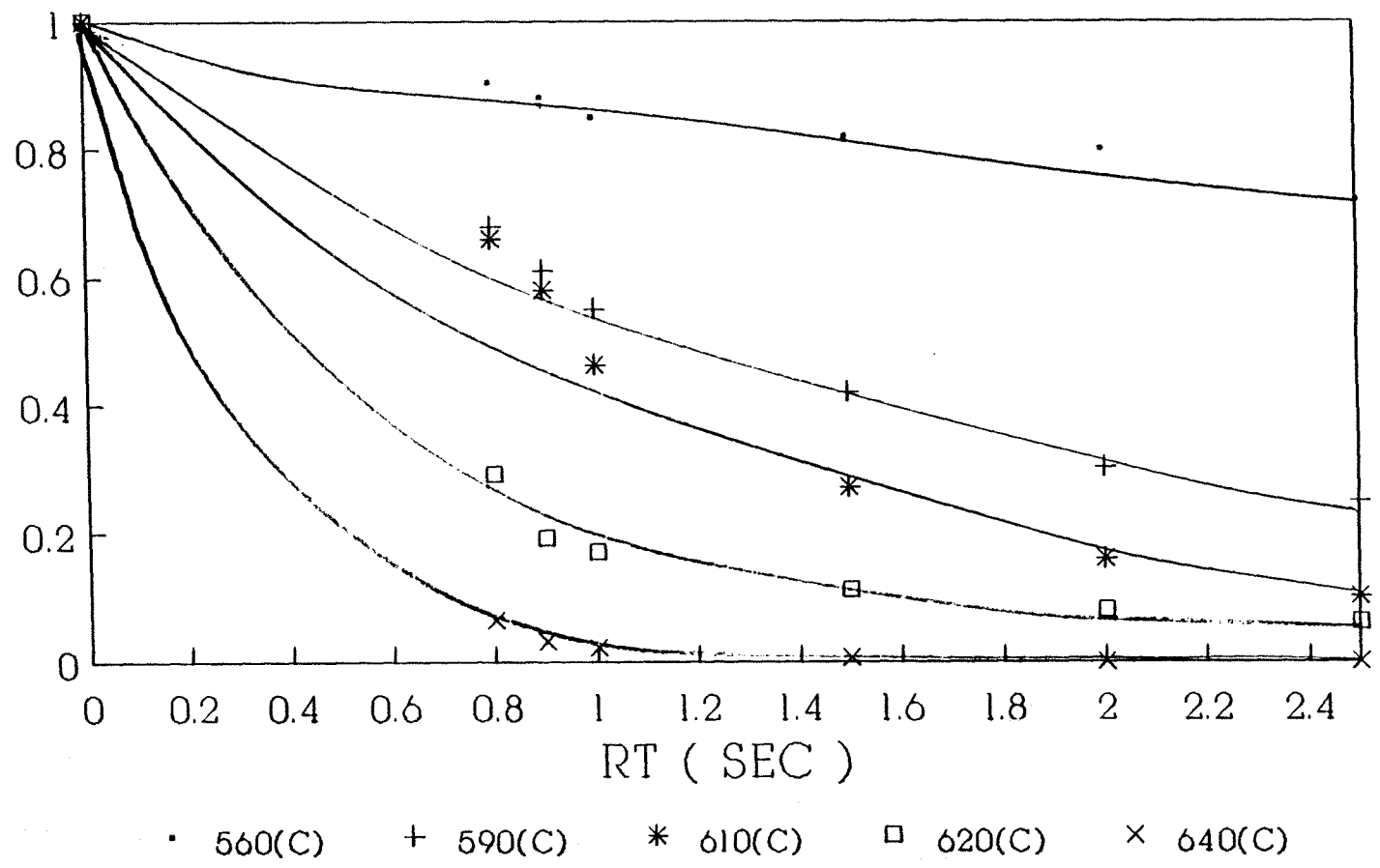


Figure 5.3

REACTION OF CLBZ + H₂ + O₂/H₂: 1% M SIZE (IDa 10.5 mm), RIFF. TEMP.

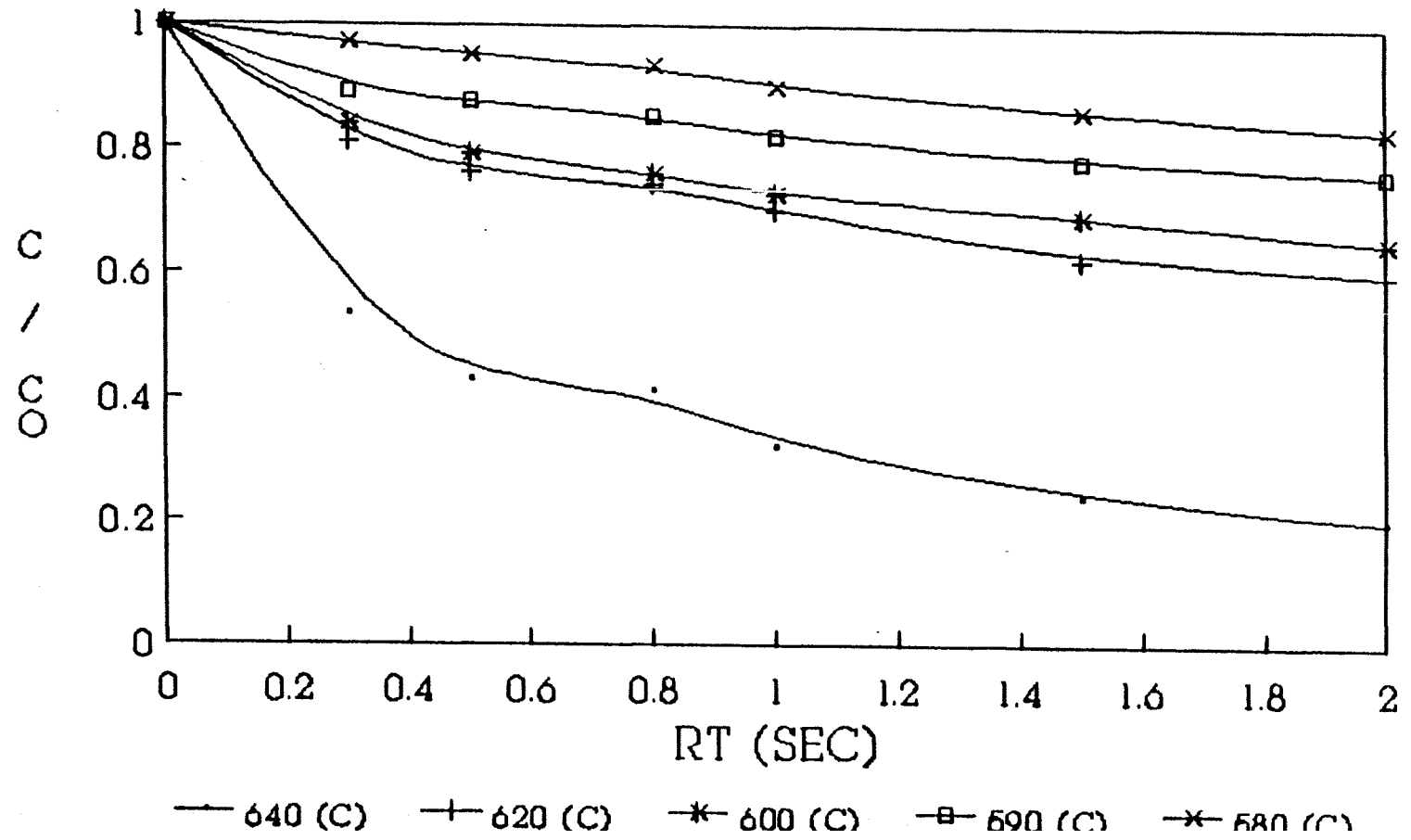


Figure 5.4

REACTION OF CLBZ + H₂ + O₂, O₂/H₂: 2% M SIZE (IDE 10.5 mm), RIFF. TEMP.

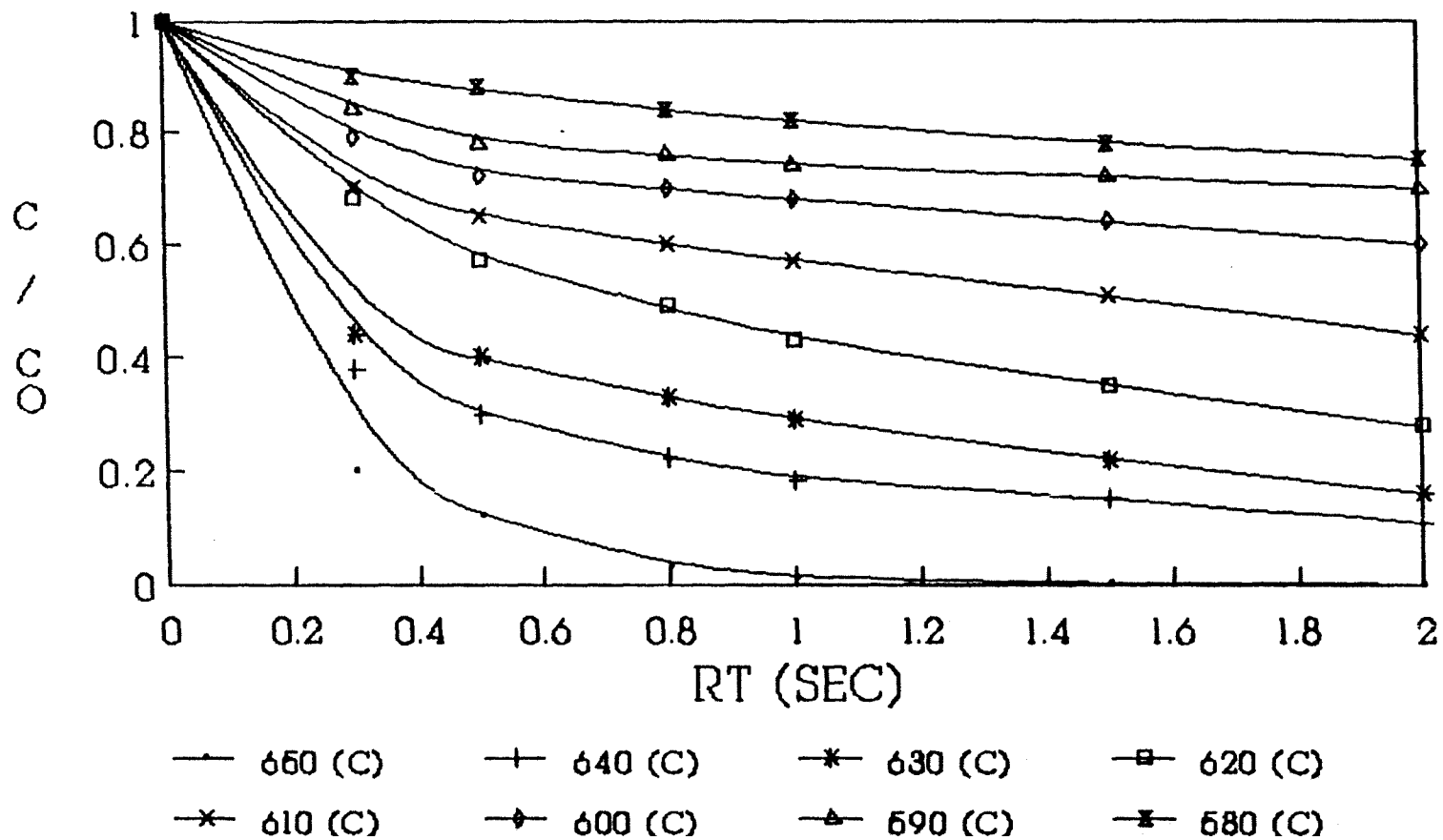


Figure 5!5

**REACTION OF CLBZ + H₂ + O₂: 4%
M SIZE (ID 10.5 mm), RIFF, TEMP,**

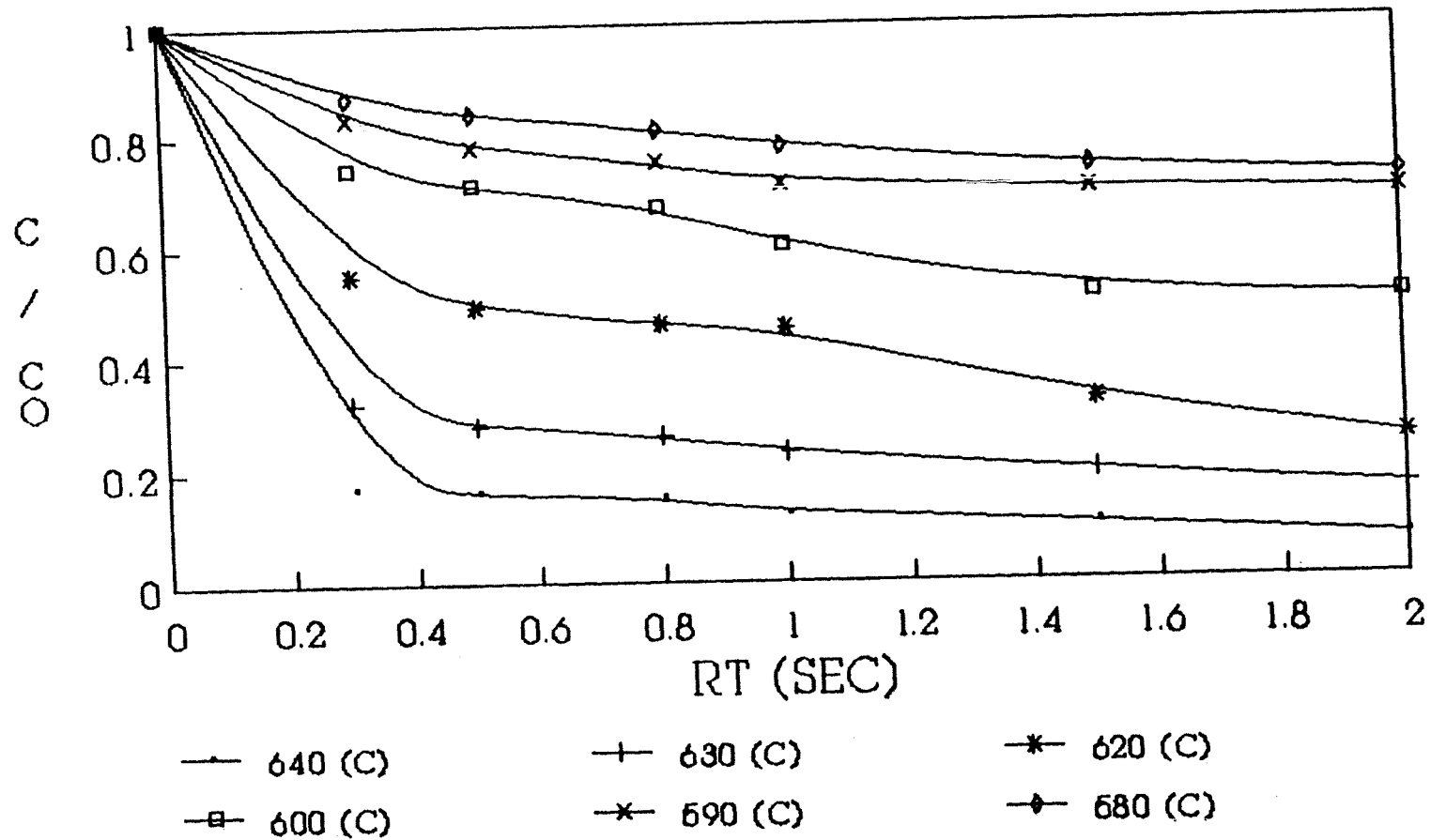


Figure 5.6

REACTION OF CLBZ + H₂ + O₂ 1 O₂/H₂ : 1%
 S SIZE (ID = 4 mm),DIFF. TEMP.

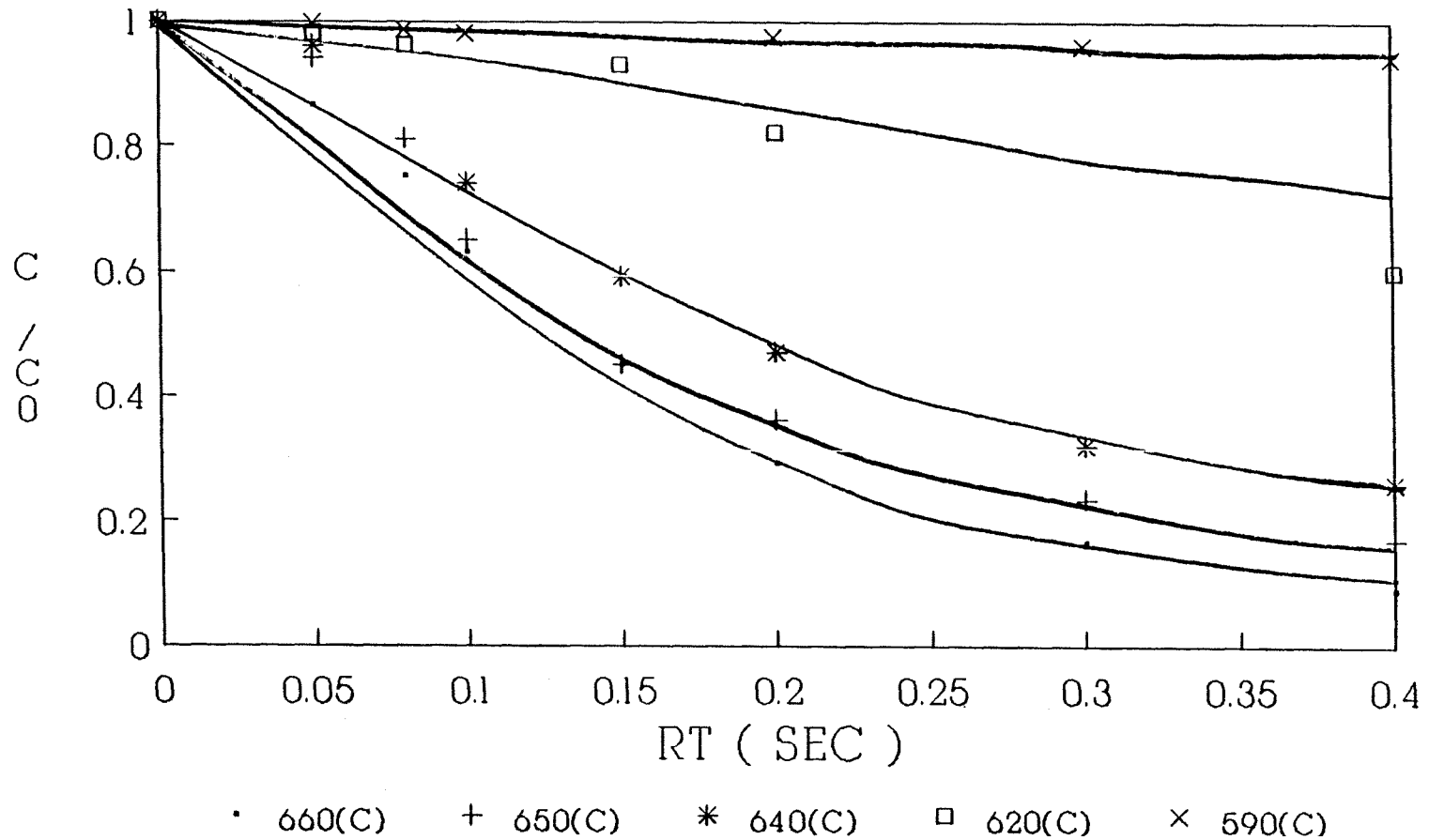


Figure 5.7

REACTION OF CLBZ + H₂ + O₂ O₂/H₂ : 2%
 S SIZE (ID = 4 mm) TEMP.

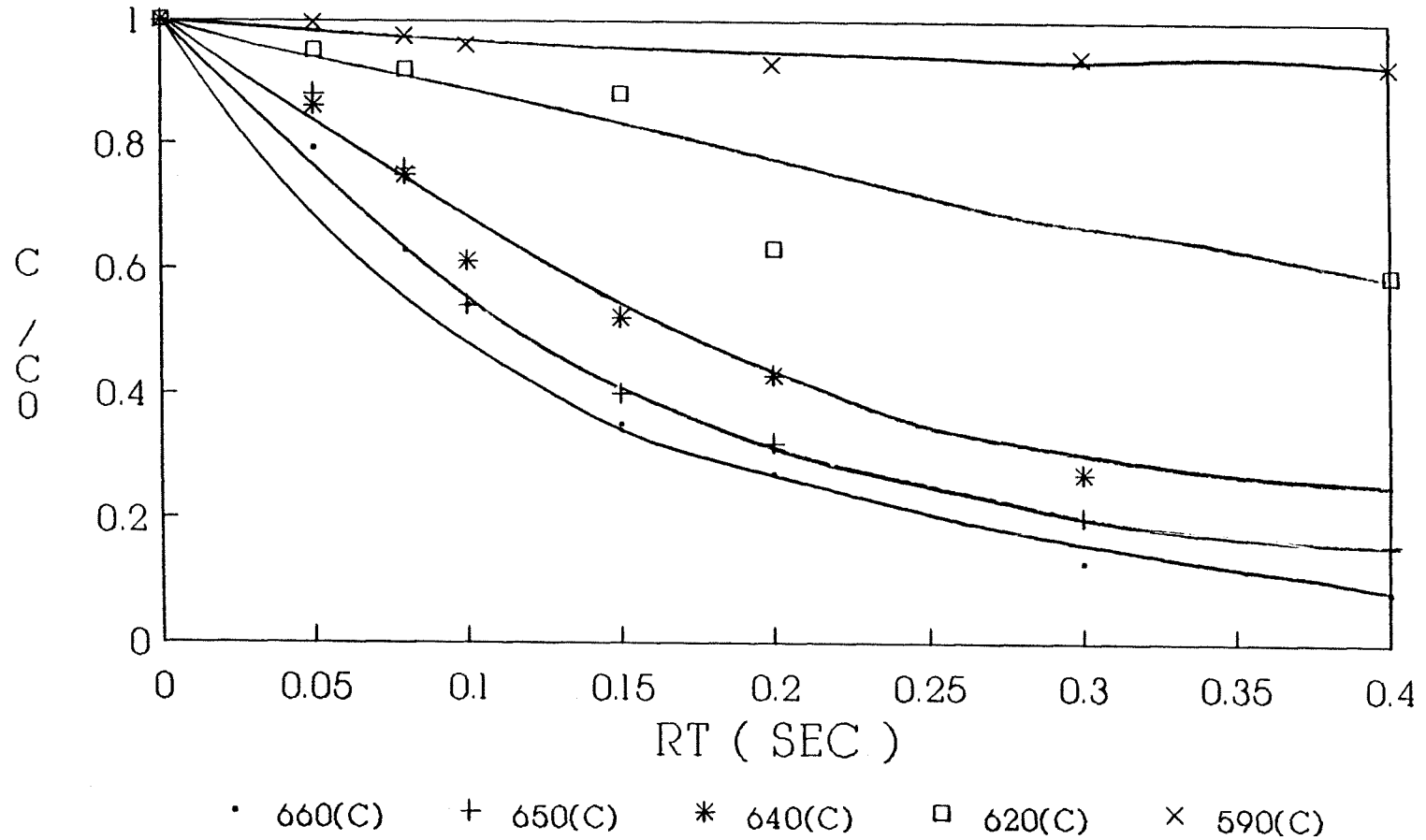
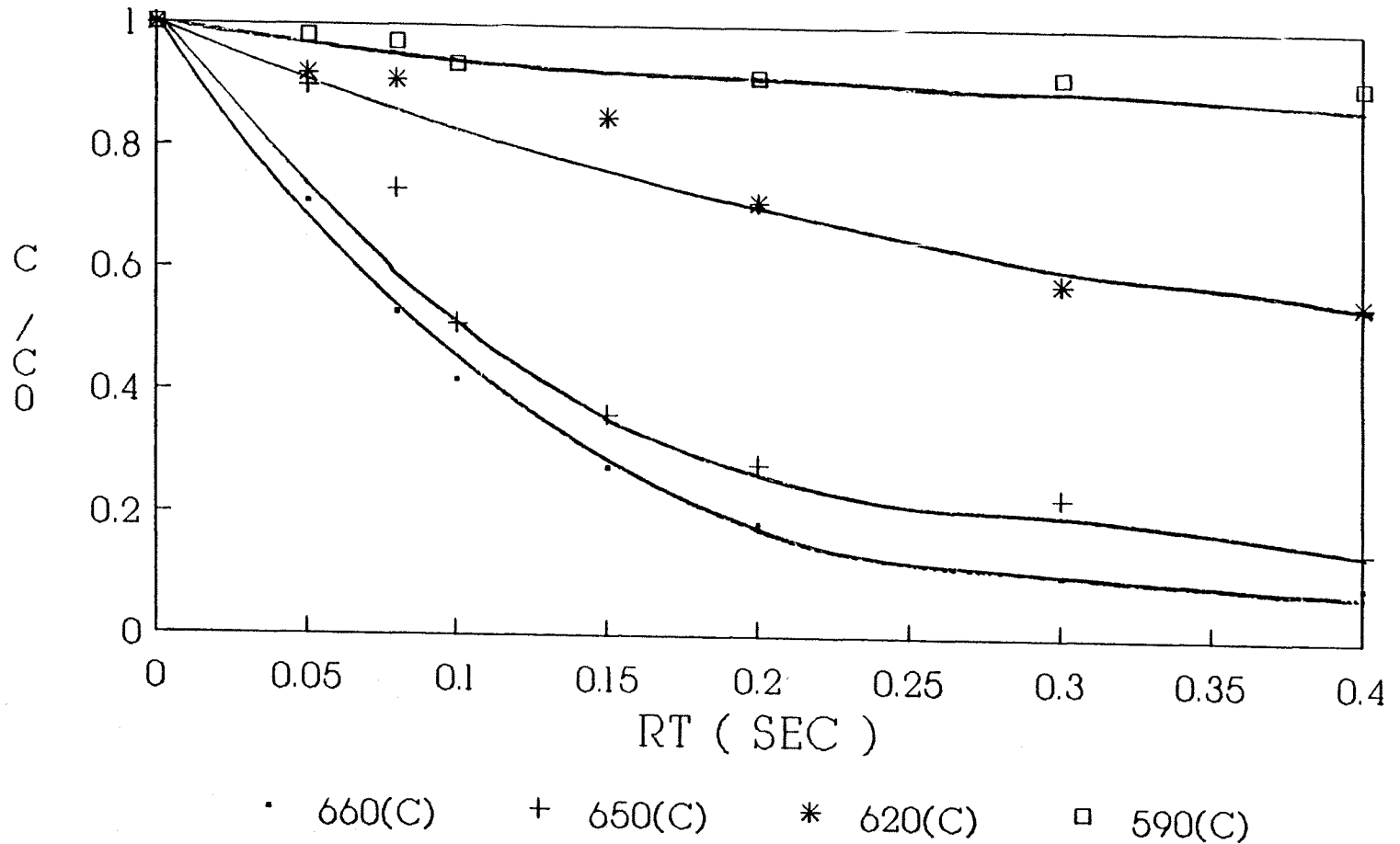


Figure 578

**REACTION OF CLBZ + 1-12 + 02 02/H2: 3%
S SIZE (ID al 4 mm),DIFF. TEMP.**



Fi re .9

REACTION OF CLBZ + H₂ + O₂ / O₂/112 : 4%
S SIZE (ID = 4 mm), RIFF. TEMP.

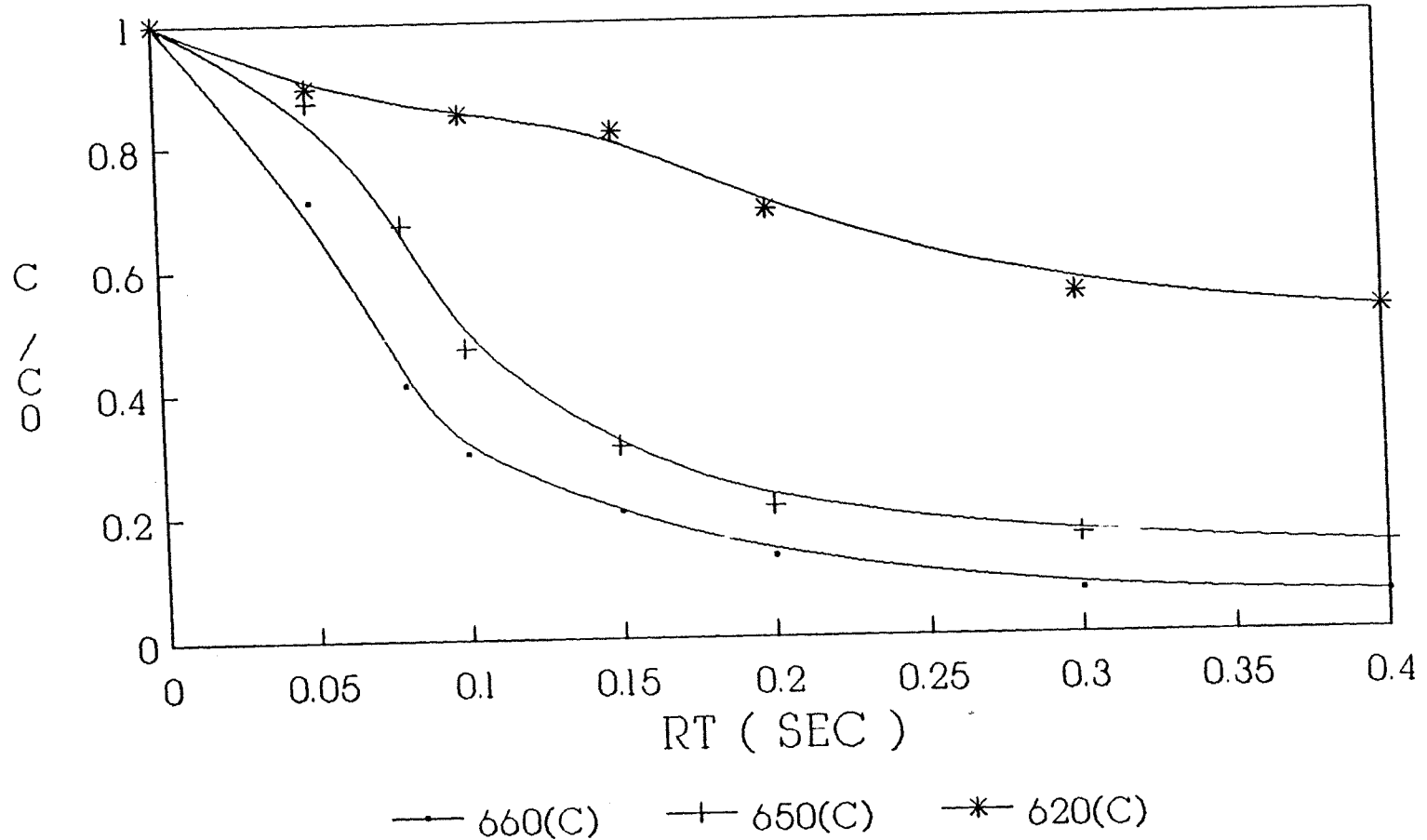


Figure 5.10

REACTION OF CLBZ + 112 + 02 02/112: 5%
S SIZE (ID = 4 mm),RIFF. TEMP.

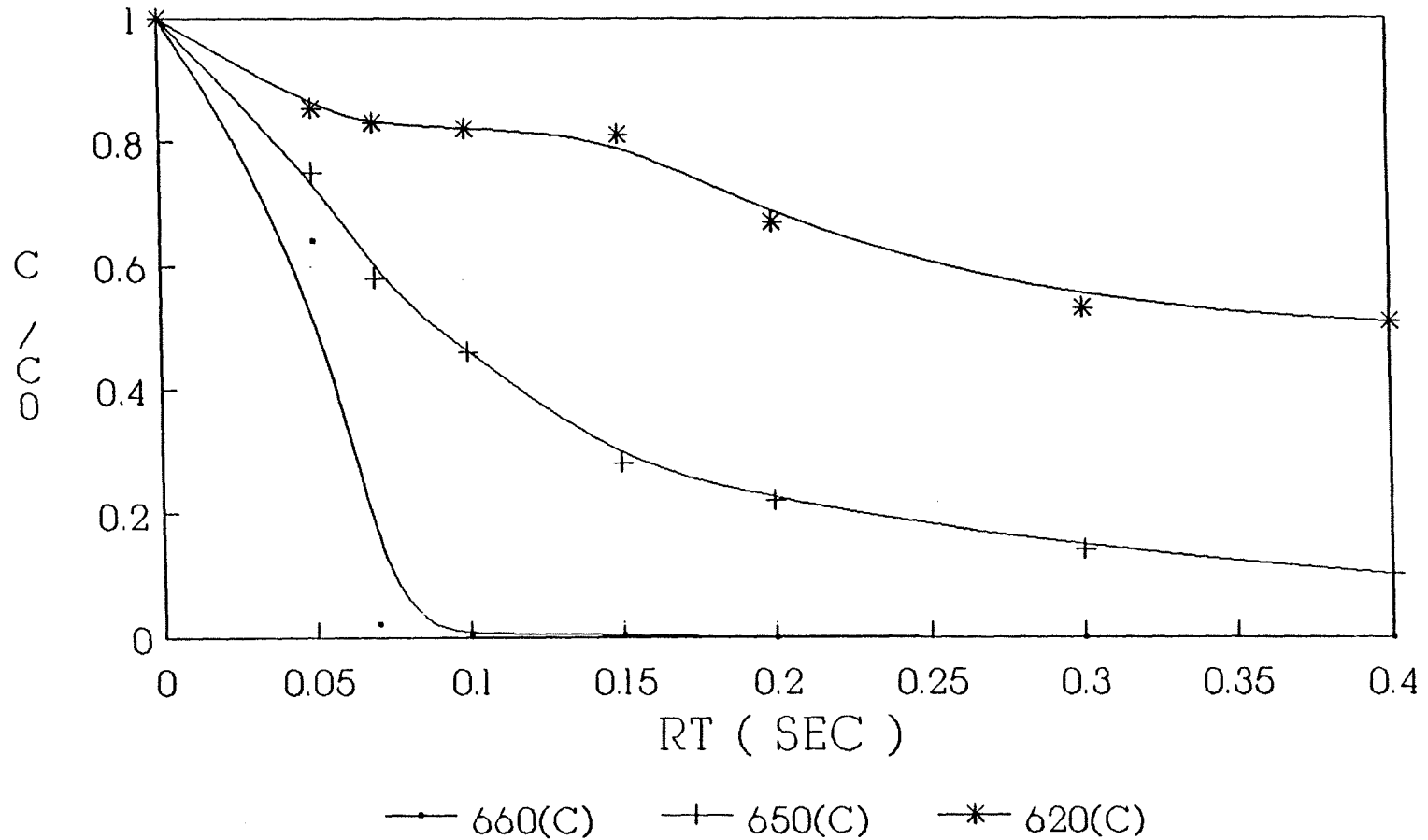
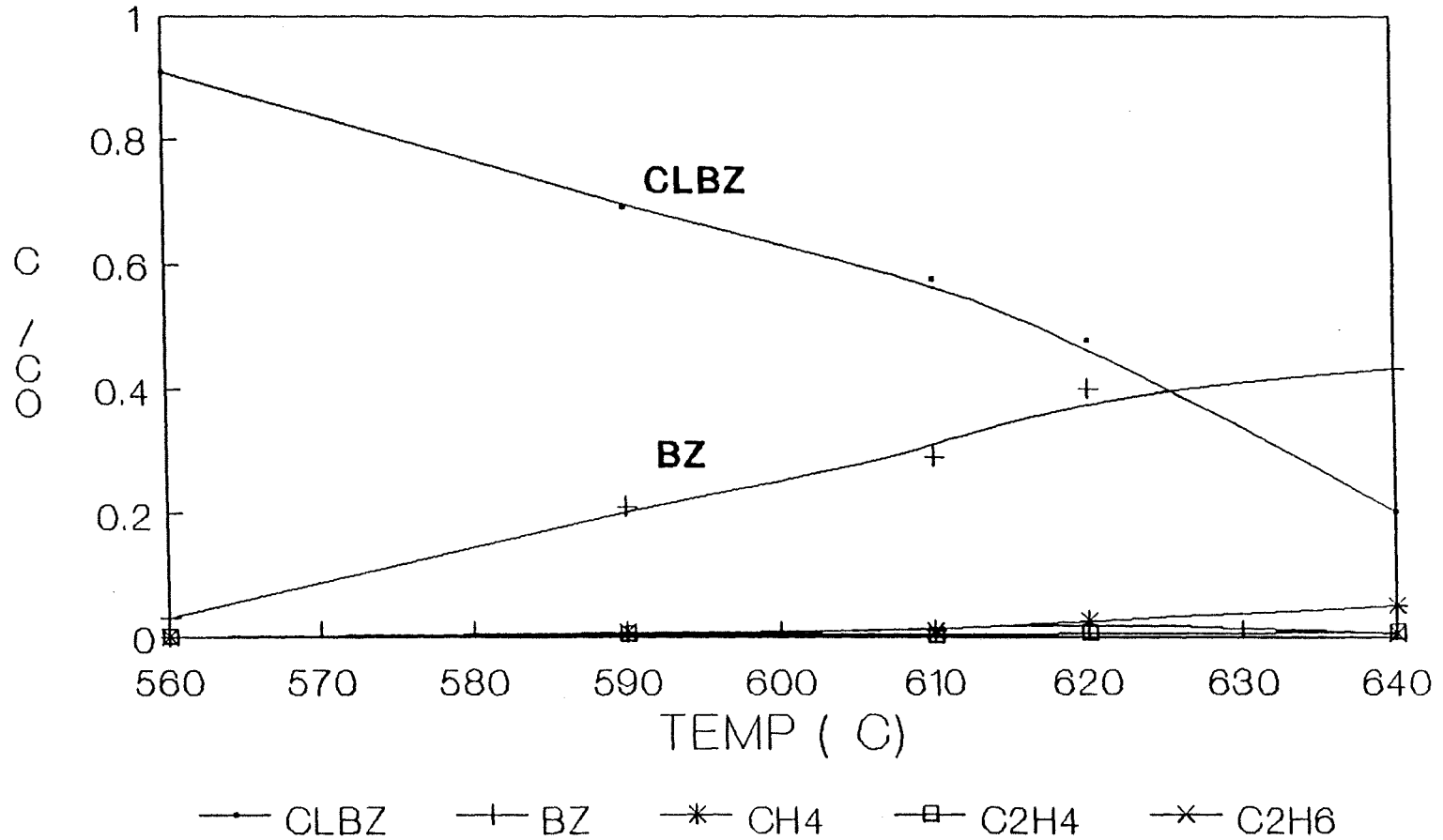


Figure 5.11

**REACTION OF CLBZ + H₂ + O₂ , 1 ATM
RT 1 (SEC), O₂/H₂ : 1% , ID 16 mm**



Fi.gue 5.12

**REACTION OF CLBZ + H₂ + O₂ 1 ATM
 RT 1 (SEC) O₂ / H₂ : 2° / 0 ID 74 16 mm**

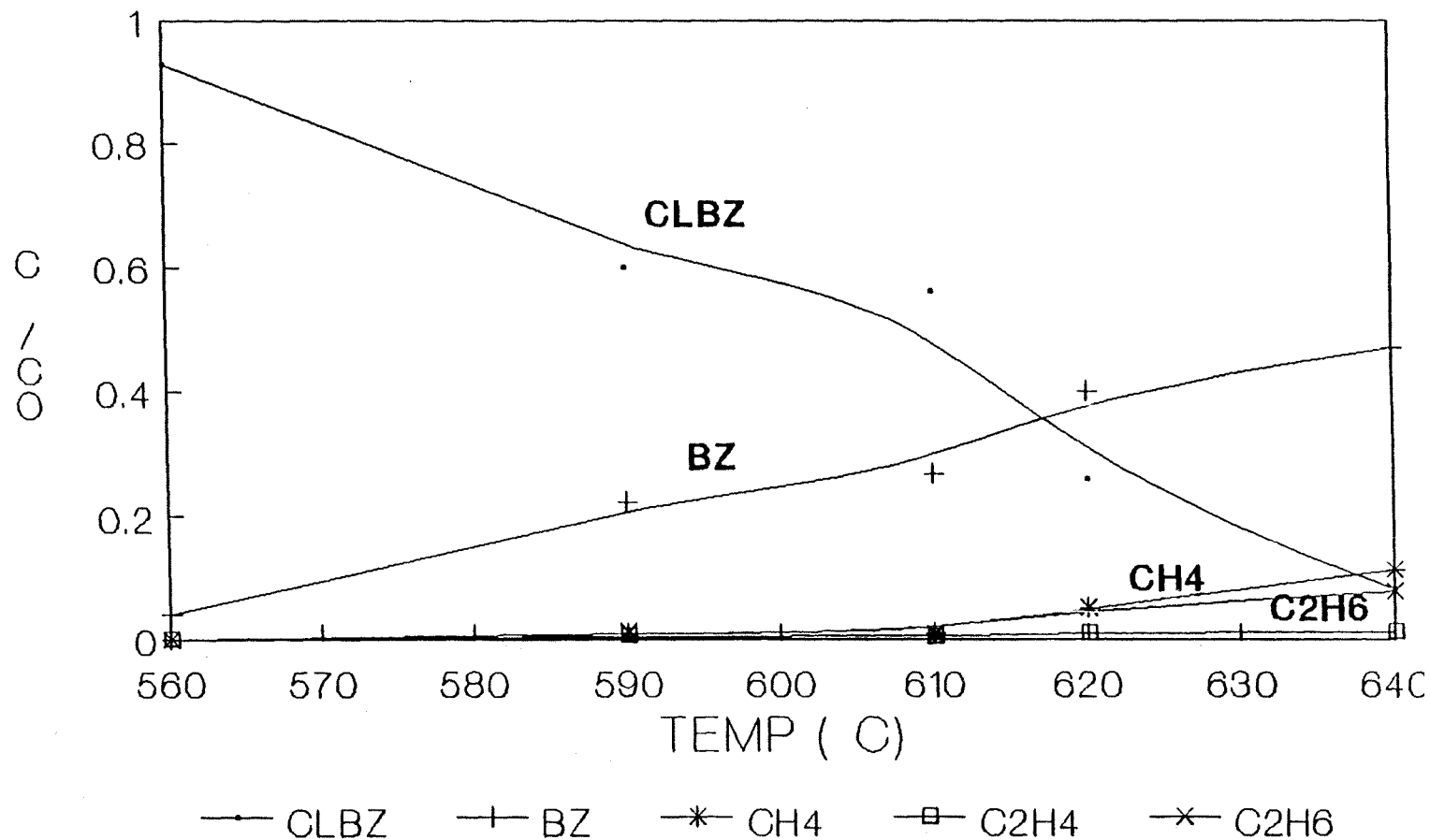


Figure 5.13

**REACTION OF CLBZ + H₂ + O₂ , 1 ATM
 RT = 1 (SEC , O₂/H₂ : 3°/0 , ID = 16 mm**

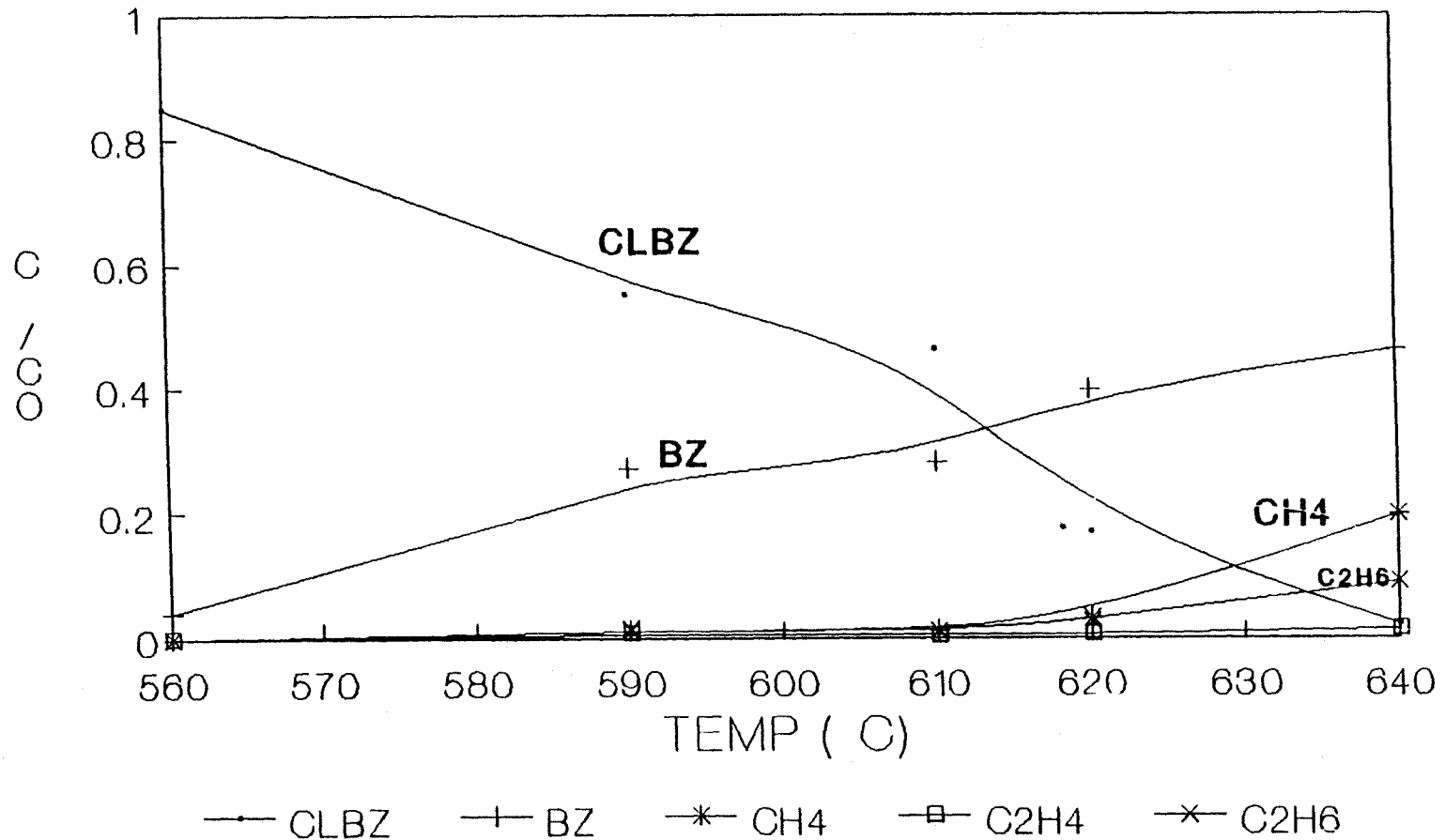


Figure 5.14

**REACTION OF CLBZ + H₂ + O₂ , 1ATM
RT a 2 (SEC) , O₂/H₂: 1% , ID = 16 mm**

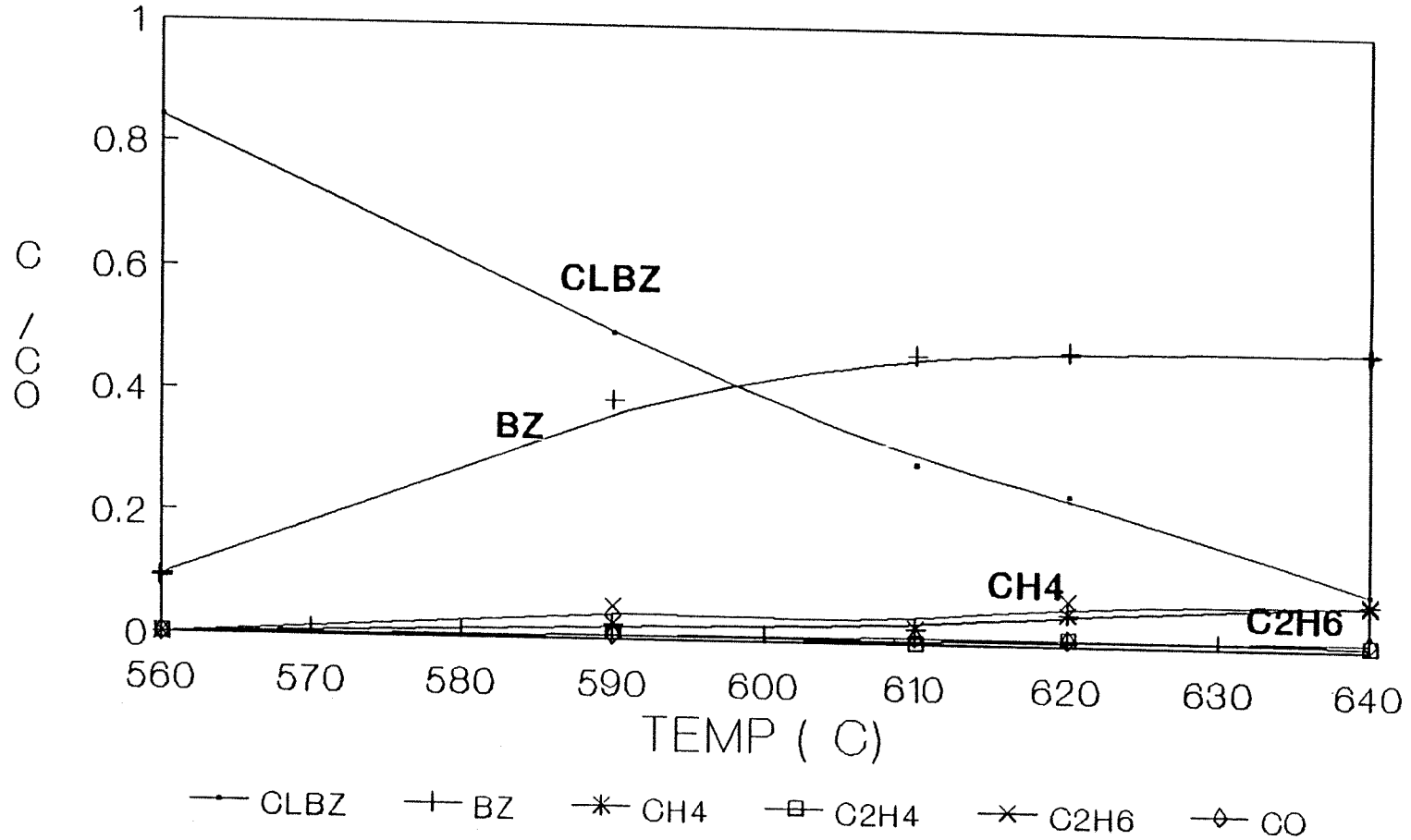


Figure 5.15

**REACTION OF CLBZ + H₂ + O₂ , 1 ATM
 RT = 2 (SEC) , O₂/H₂: 2% , ID = 16 mm**

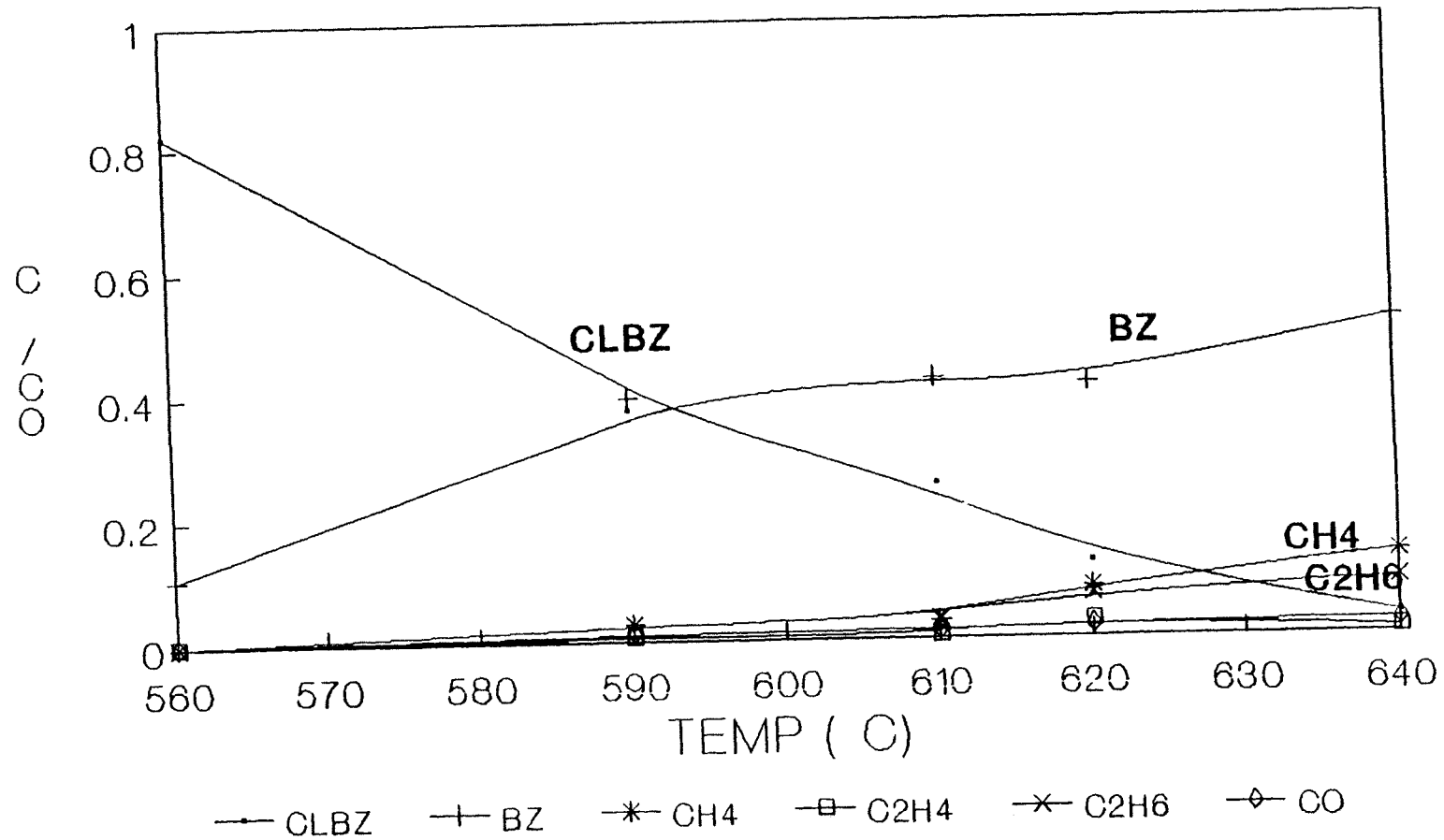


Figure 5.16

**REACTION OF CLBZ + H₂ + O₂, 1 ATM
 RT = 2 (SEC) , O₂/H₂: 3% , ID = 16 WI**

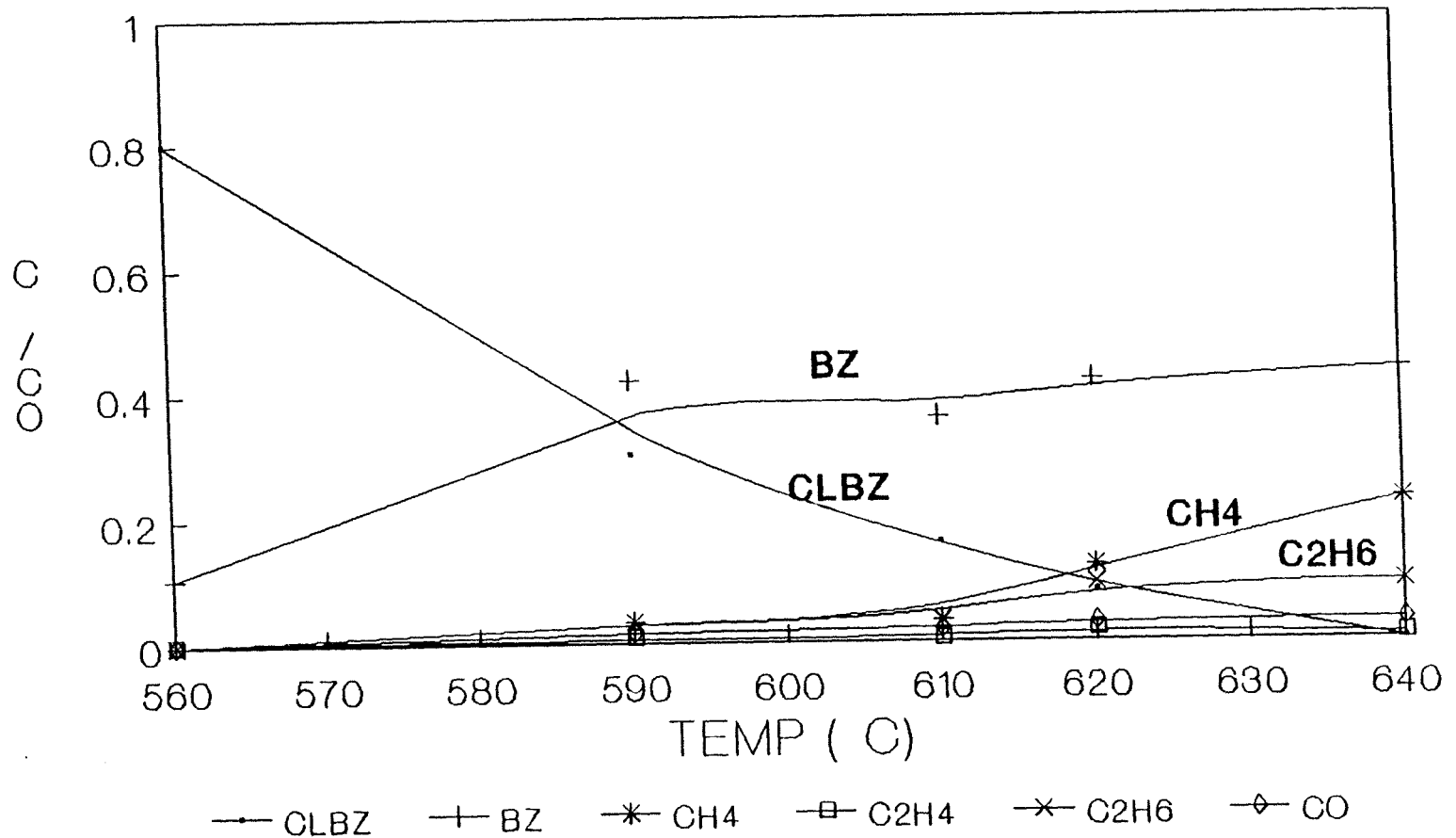


Figure 5.17

**REACTION OF CLBZ + H₂ + O₂ , 1 ATM
 RT = 2 (SEC) , O₂/H₂: 4% , ID = 16 mm**

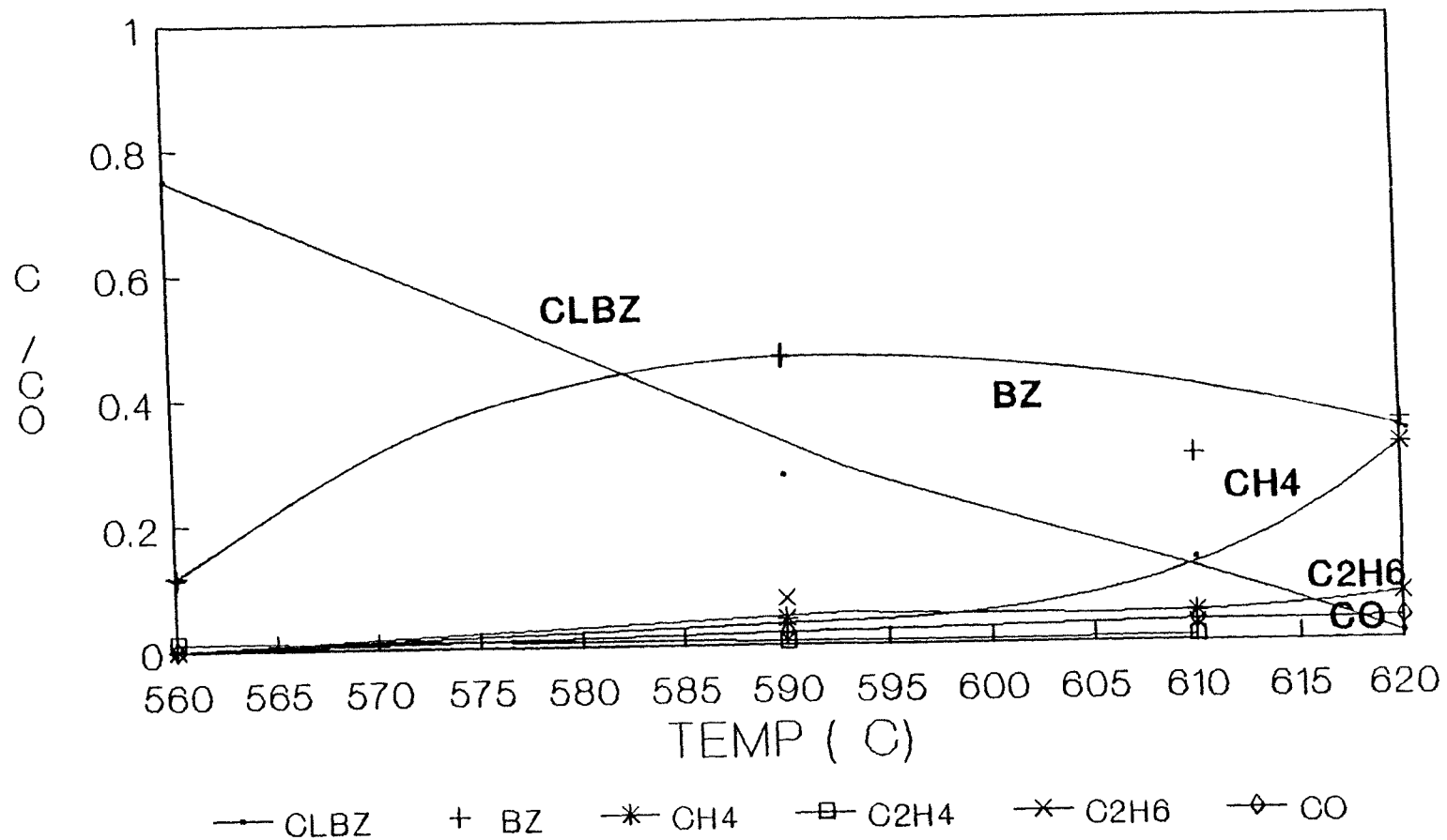


Figure 5.18

**REACTION OF CLBZ + H₂ + O₂ , 1 ATM
 RT = 2 (SEC) , O₂/H₂: 5% , ID = 16 mm**

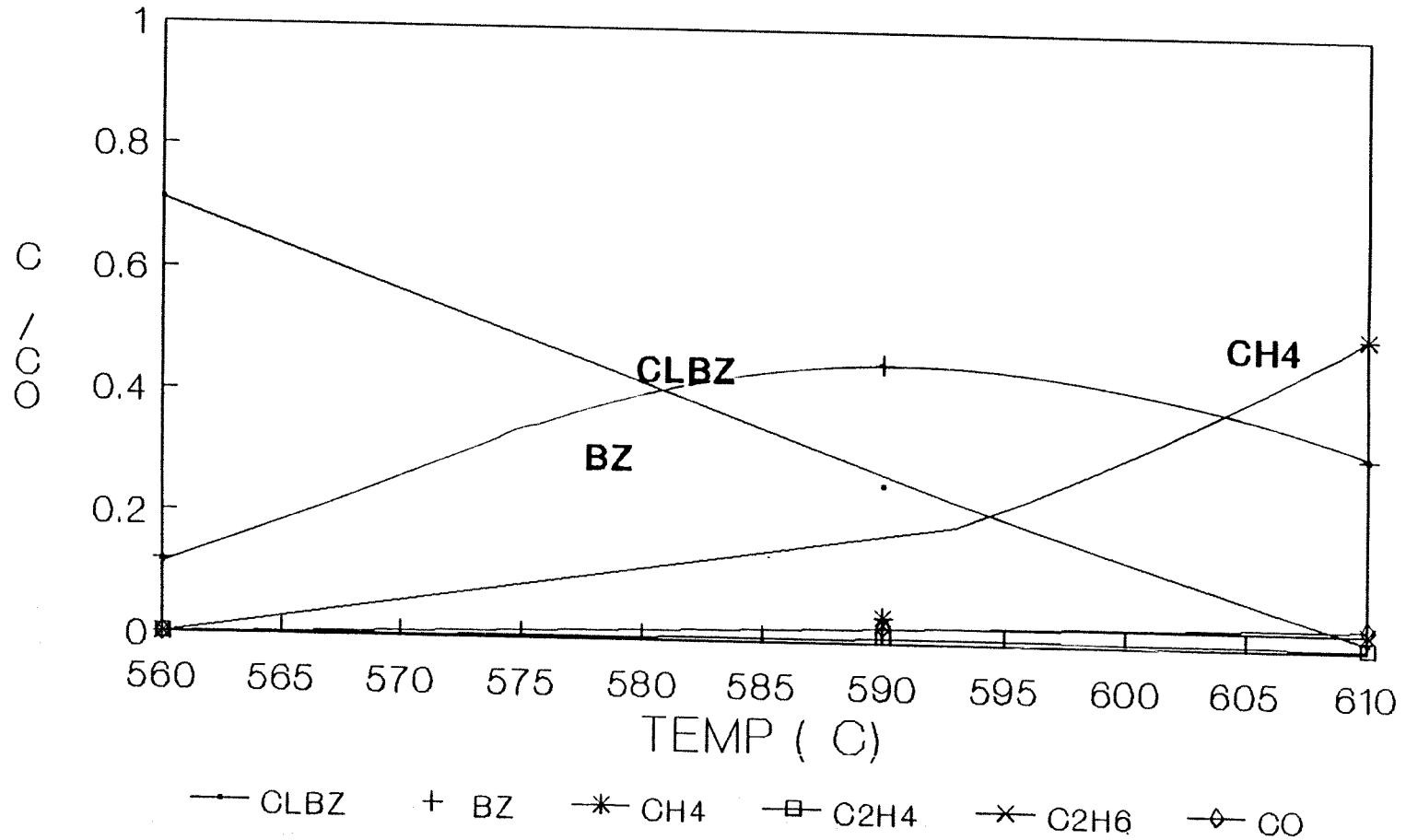
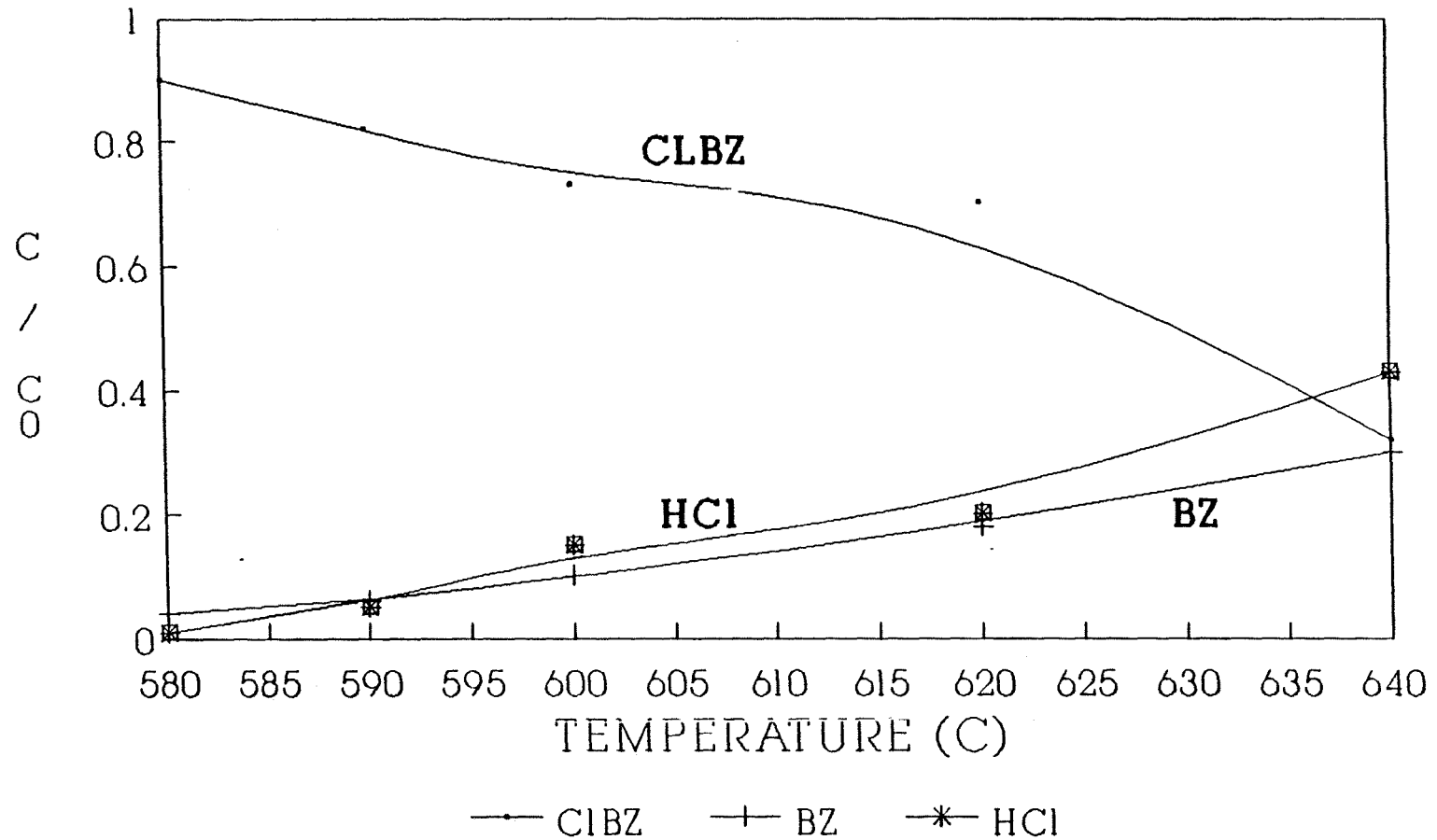


Figure 5.19

REACTION OF CLBZ + 112 + O₂, 1 ATM
 RT = 1 (SEC), O₂/1-12: 1%, ID=10.5 mm



Fjqqre 5,20

**REACTION OF CLBZ + H₂ + O₂, 1 ATM
RT = 1 (SEC), O₂/H₂: 2%, ID=10.5 rnm**

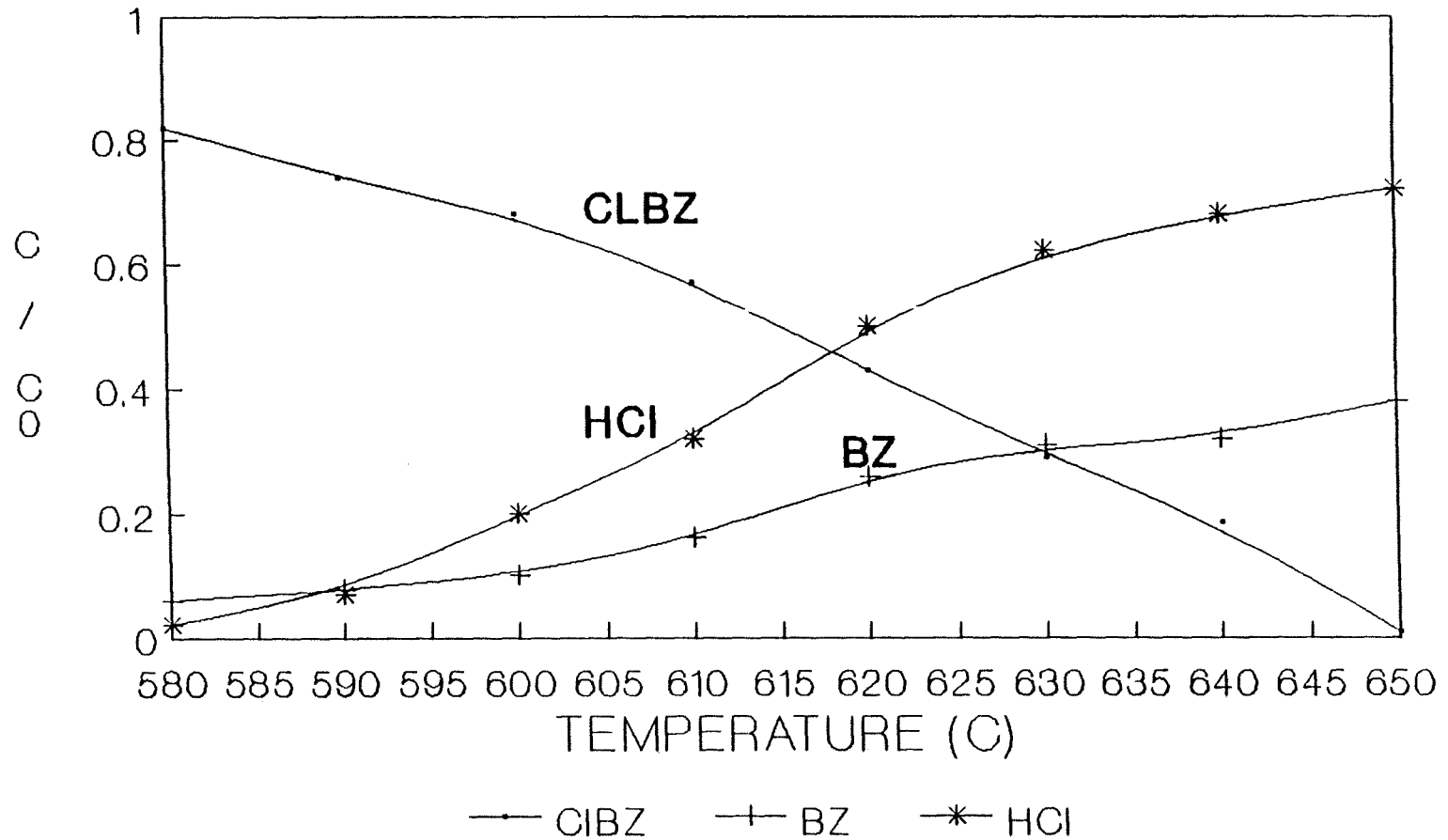


Figure 5.21

REACTION OF CLBZ + H₂ + O₂, 1 ATM
RT = 1 (SEC), O₂/H₂: 4%, ID=10.5 mm

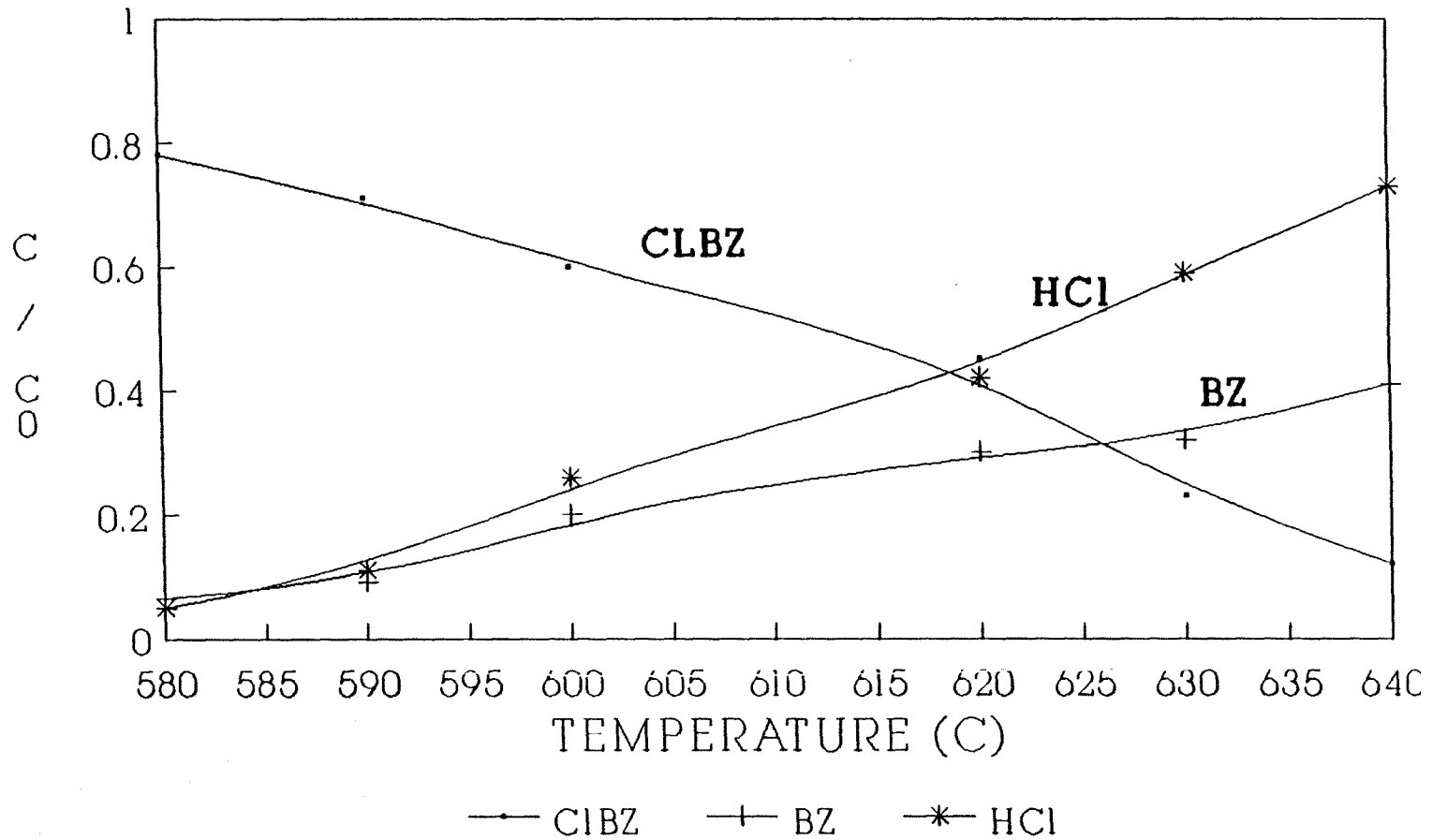


Figure 5.22

10.5 mm and 16 mm ID reactors. Higher O₂ concentration resulted in lower observed concentration of chlorobenzene.

The initiation reaction is not dissociation of the chlorobenzene to Cl + phenyl radical but the bimolecular reaction of O₂ + H₂ → HO₂ + H. The activation energy for dissociation of chlorobenzene is 97 kcal/mole at these temperatures^{<23>}, but E_a for O₂ + H₂ chain branching reaction is only 55.5 kcal/mole. The reaction with both oxygen and hydrogen present should show faster chlorobenzene decomposition rates than the pyrolysis of chlorobenzene in excess of H₂ only; where initiation must be unimolecular decomposition of chlorobenzene. This is because the H atom produced rapidly reaction with C₆H₅Cl via a displacement path. Further evidence is illustrated by all of the experimental pyrolysis temperatures for reaction of chlorobenzene in the 1 - 2 second residence time are above 900°C^{<9, 12>}. Observed reactions on the time scale of seconds in this study found the reaction temperatures below 700°C, clearly demonstrating reaction H₂ + O₂ to HO₂ + H, to be the initiation step. Because the addition of oxygen is observed to accelerate the decomposition of chlorobenzene, we conclude oxygen initiates the reaction via the chain branching reaction H₂ + O₂ to HO₂ + H.

Figures 5.23 through 5.26 illustrate second order reaction plot in 10.5 mm and 16 mm ID reactors. It is shown

CLBZ REACTION AT 1 AM ,2%,M SIZE

2ND ORDER APPROX. , DIFF TEMP

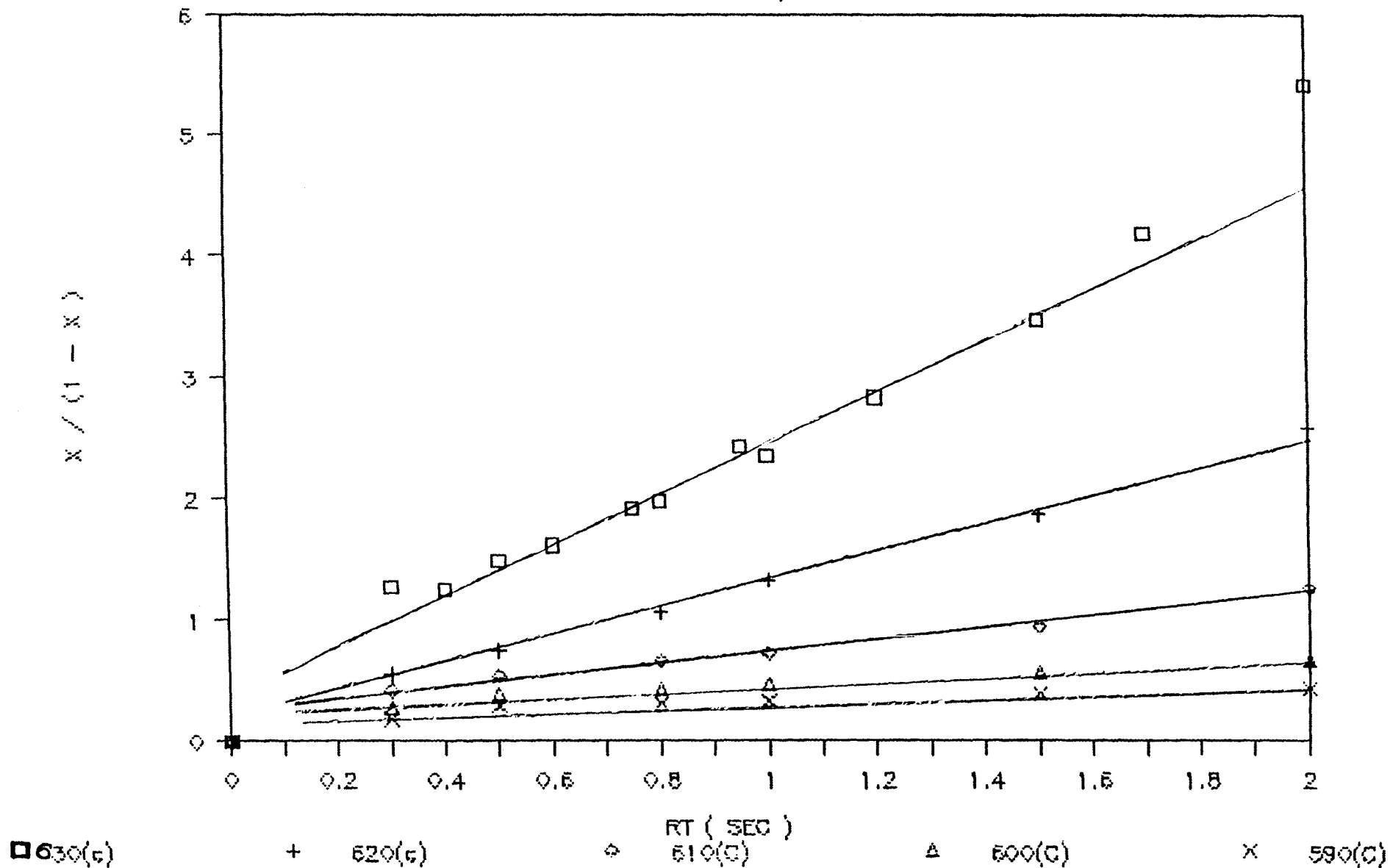


Figure 5.23

CLBZ REACTION AT 1 ATM 1% ID = 16 mm SECOND ORDER APPROX. DIFF. TEMP.

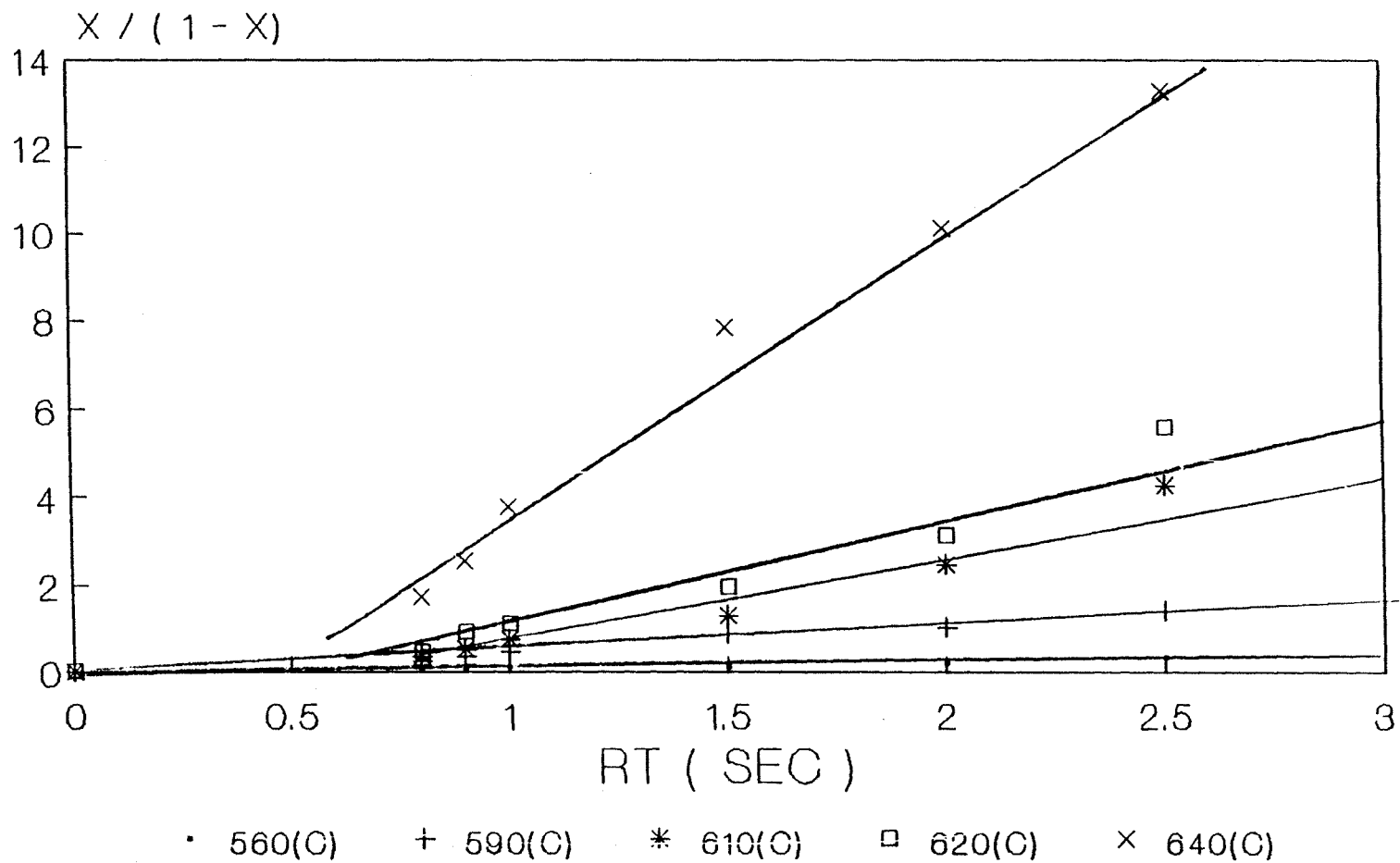


Figure 5.24

CLBZ REACTION AT 1 ATM 2% , ID = 16 mm SECOND ORDER APPROX. , DIFF. TEMP.

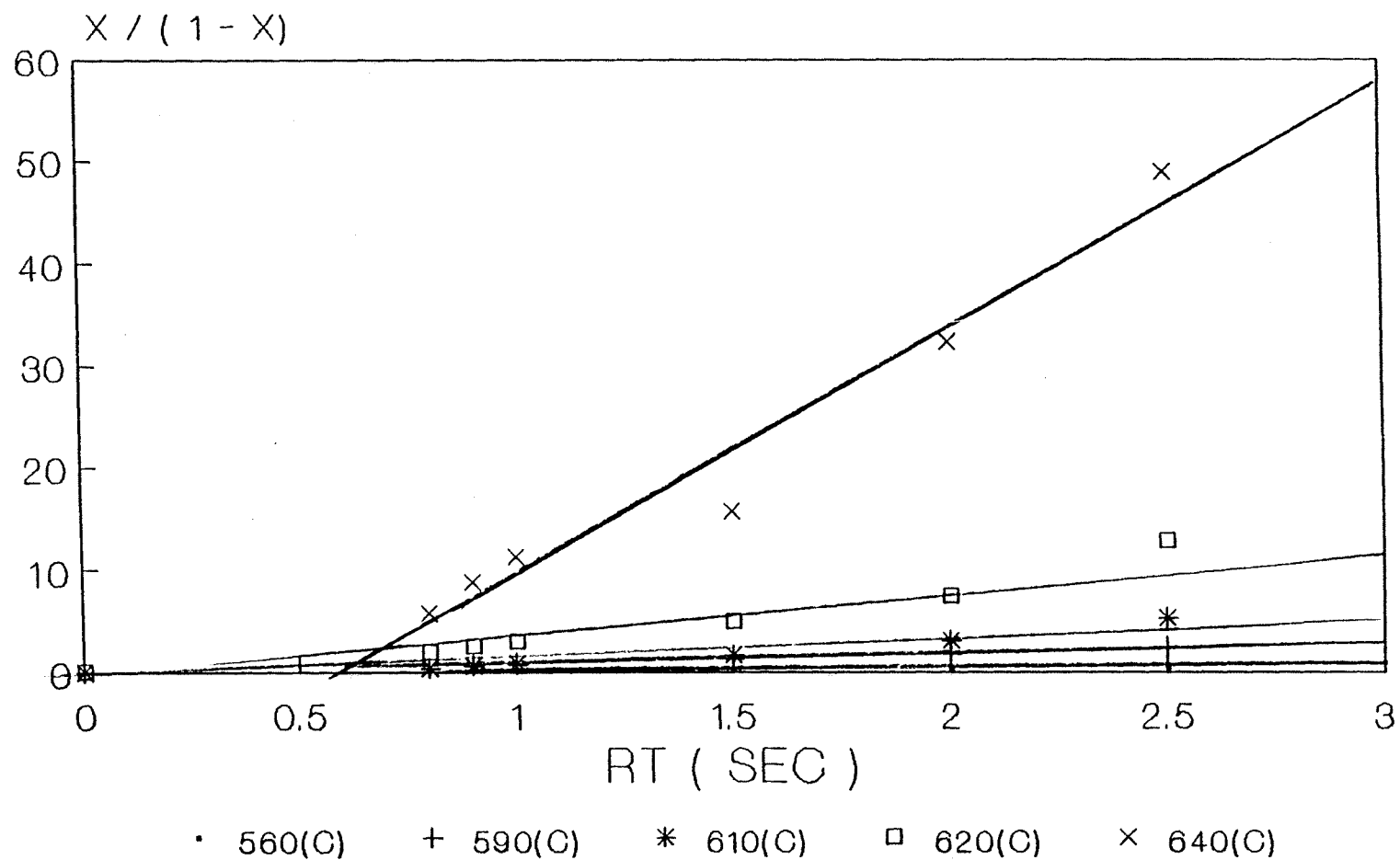


Figure 5.25

CLBZ REACTION AT 1 ATM , 3% , ID re 16 mm SECOND ORDER APPROX., RIFF. TEMP.

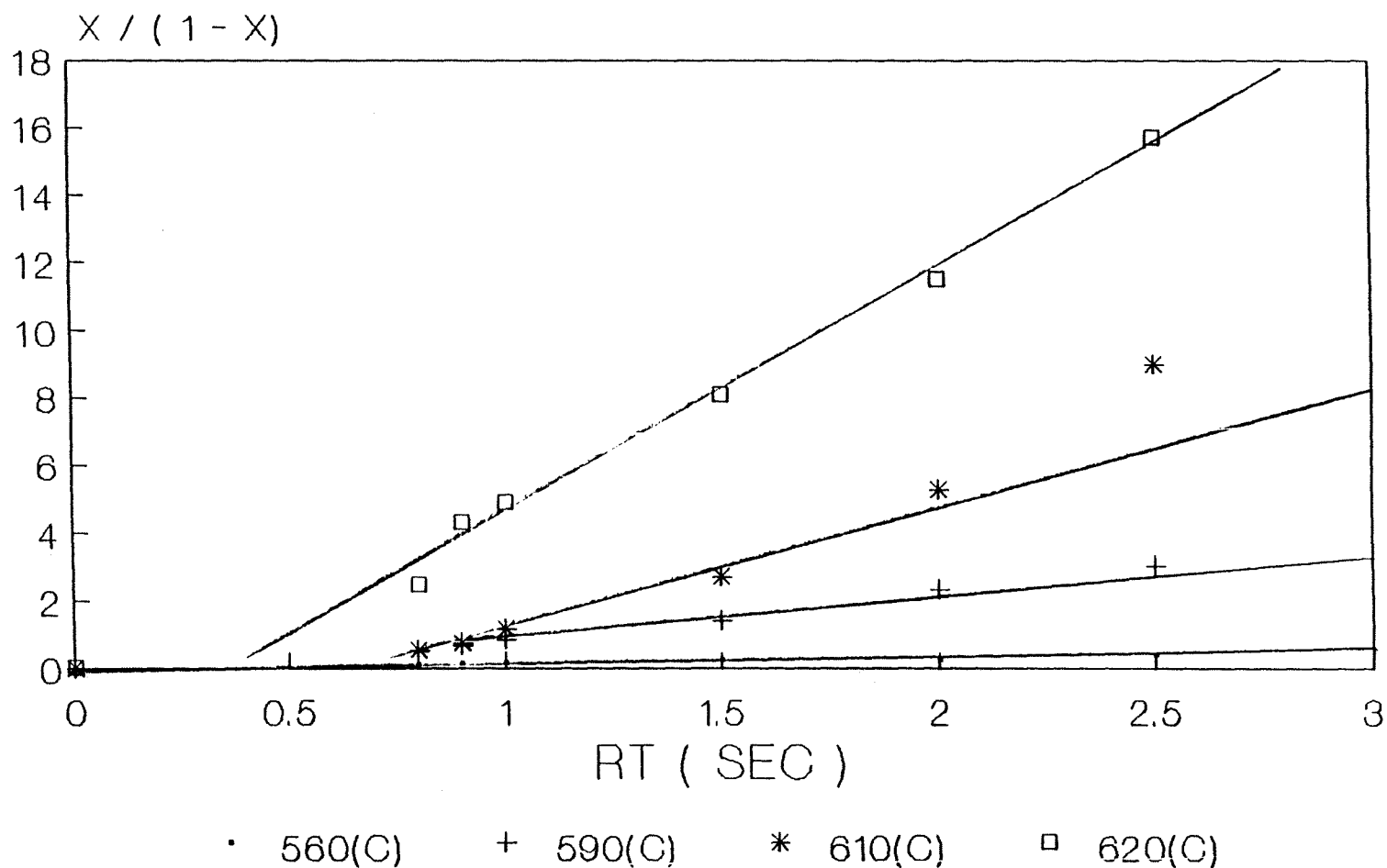


Figure 5.26

that these plot can **be** fit to straight line, but these lines do not pass through the origin. Separate analysis for pseudo first order decay of chlorobenzene in figures from 5.27 to 5.29 show that the data in the 10.5 mm ID reactor do not fit an over first order decay rate equation very well the other reactors (16 mm and 4 mm) do however show better fits to a first order rate expression. Clearly the data using first order approximation is better than second order for the 16 mm and 4 mm ID reactors. We concluded, however, that upon close examination some curvature exists on these plots as well and the overall reaction is not elementary. The data in the 10.5 mm ID reactor needs to be reexamined.

The data in 16 mm and 4 mm ID reactors fit pseudo-first order kinetics reasonably well for all experiments. And we feel a global analysis of the data will be worthwhile. Application of the first order rate expression to these data yields a linear relationship for each temperature studied. Figures 5.30 through 5.35 illustrate the pseudo-first order kinetics obtained for several temperatures using the 16.0 mm and 4.0 mm ID reactor data. The experimental rate constant (k_{exp}) is taken as the slope of these lines and has units of reciprocal seconds. The dependence of the experimental first order rate constant (k_{exp}) upon temperature was obtained by fitting k_{exp} to the Arrhenius law. Figures 5.36 and 5.37 show data from these two reactors size

1ST ORDER OF CLBZ + H2 + O2, O2/H2: 1%

M SIZE (ID= 10.5 mm), DIFF. TEMP.

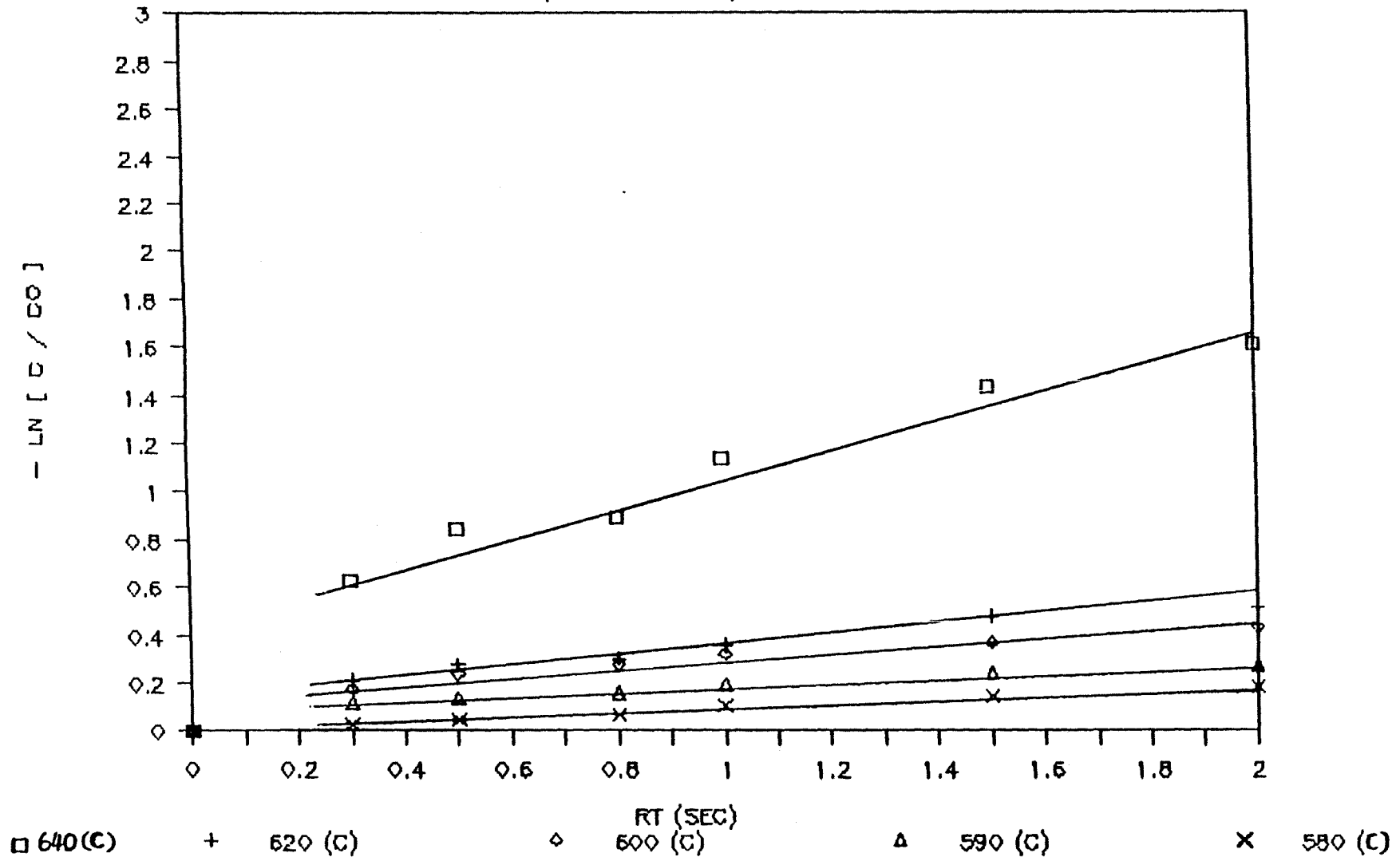


Figure 5.27:

1ST ORDER OF CLBZ + H2 + O2, O2/112. 2%

M SIZE (ID= 10.5 mm), DIFF. TEMP.

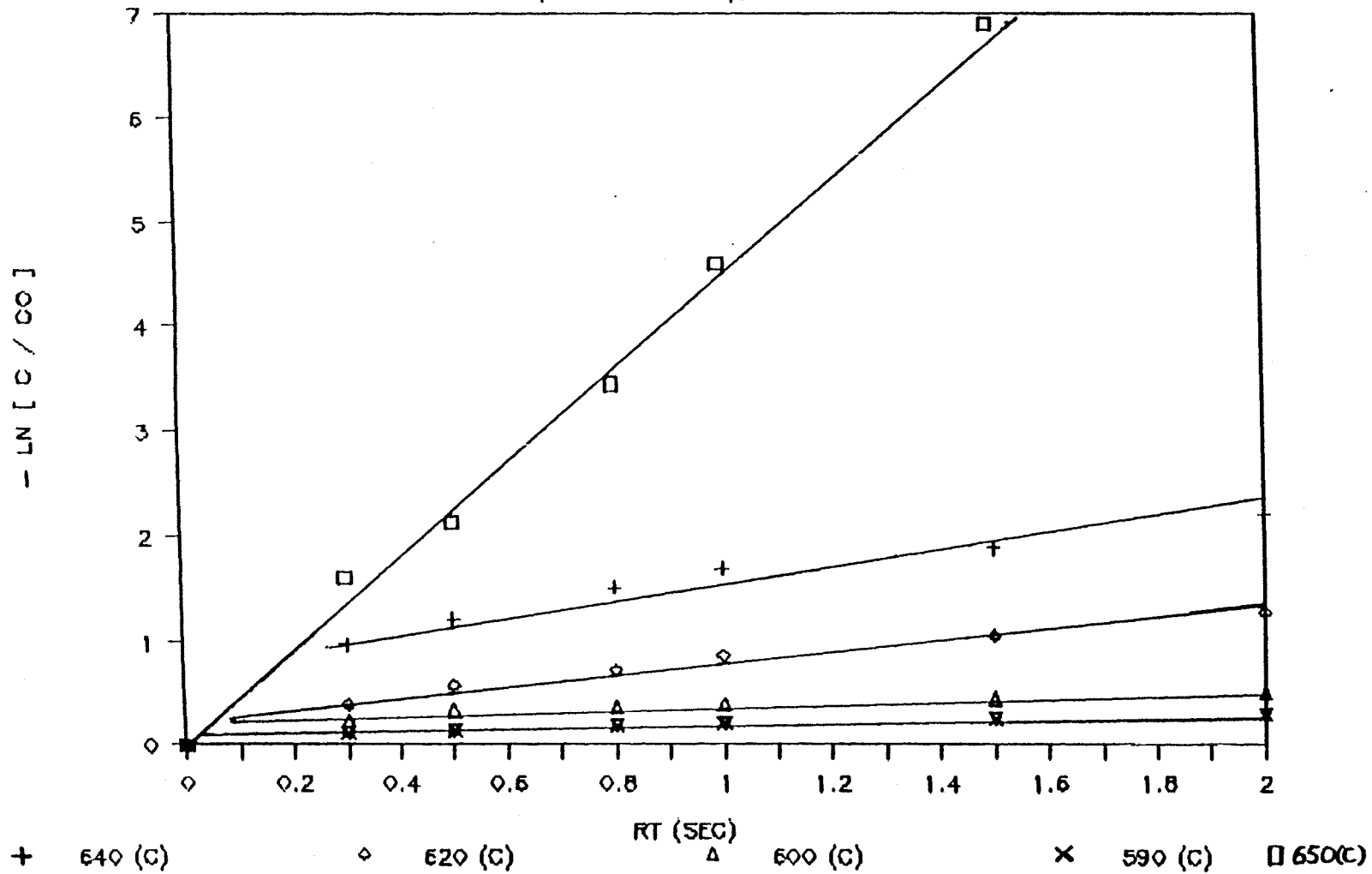


Figure 5.28

1ST ORDER OF CLBZ + H2 + O2, O2/H2: 4%

M SIZE (ID= 10.5 mm), DIFF. TEMP.

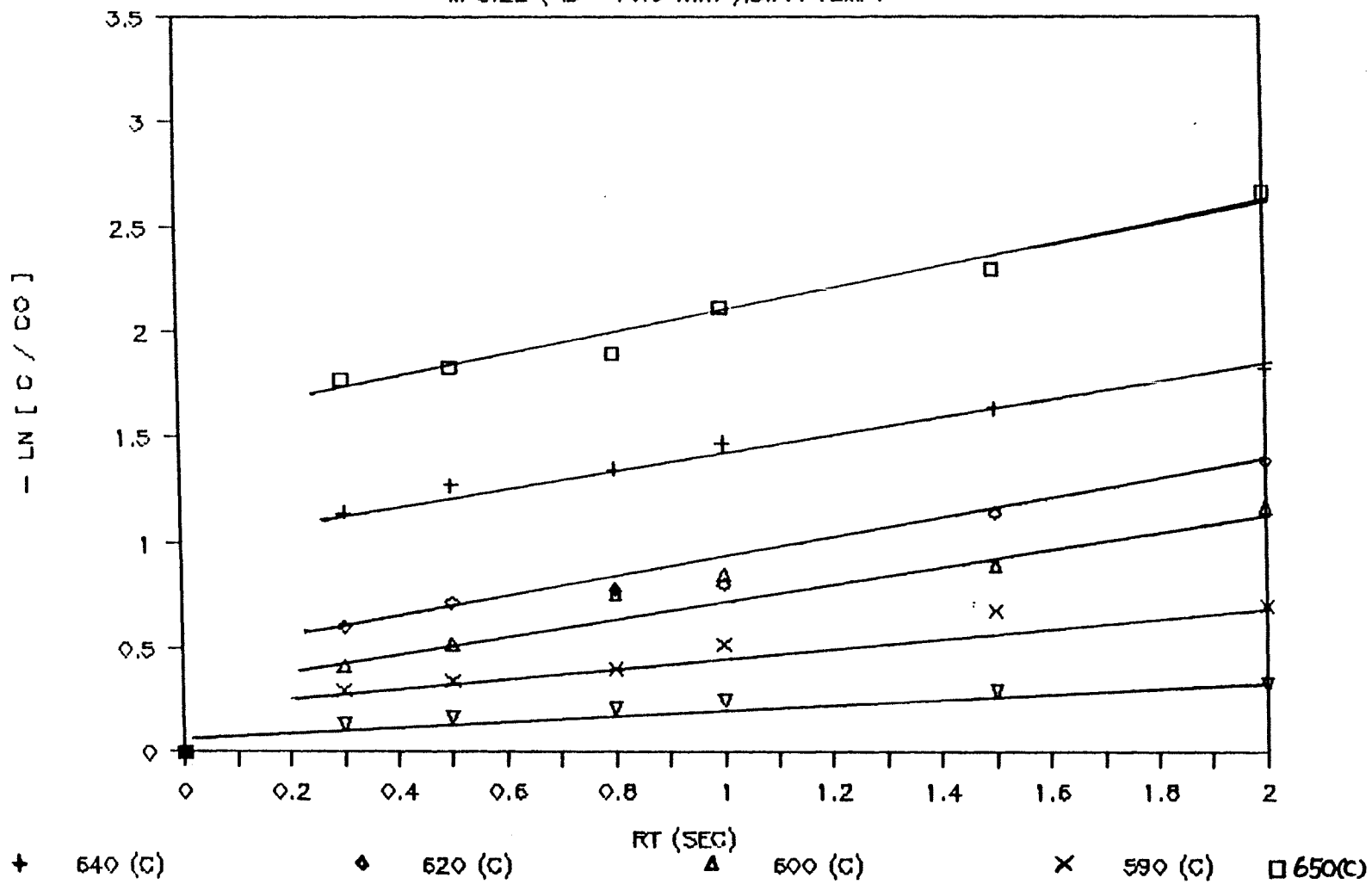


Figure 5.29

1 ST ORDER OF CLBZ + H2 + O2, O2/H2: 1%,
L SIZE (D = 16 mm), RIFF. TEMP.

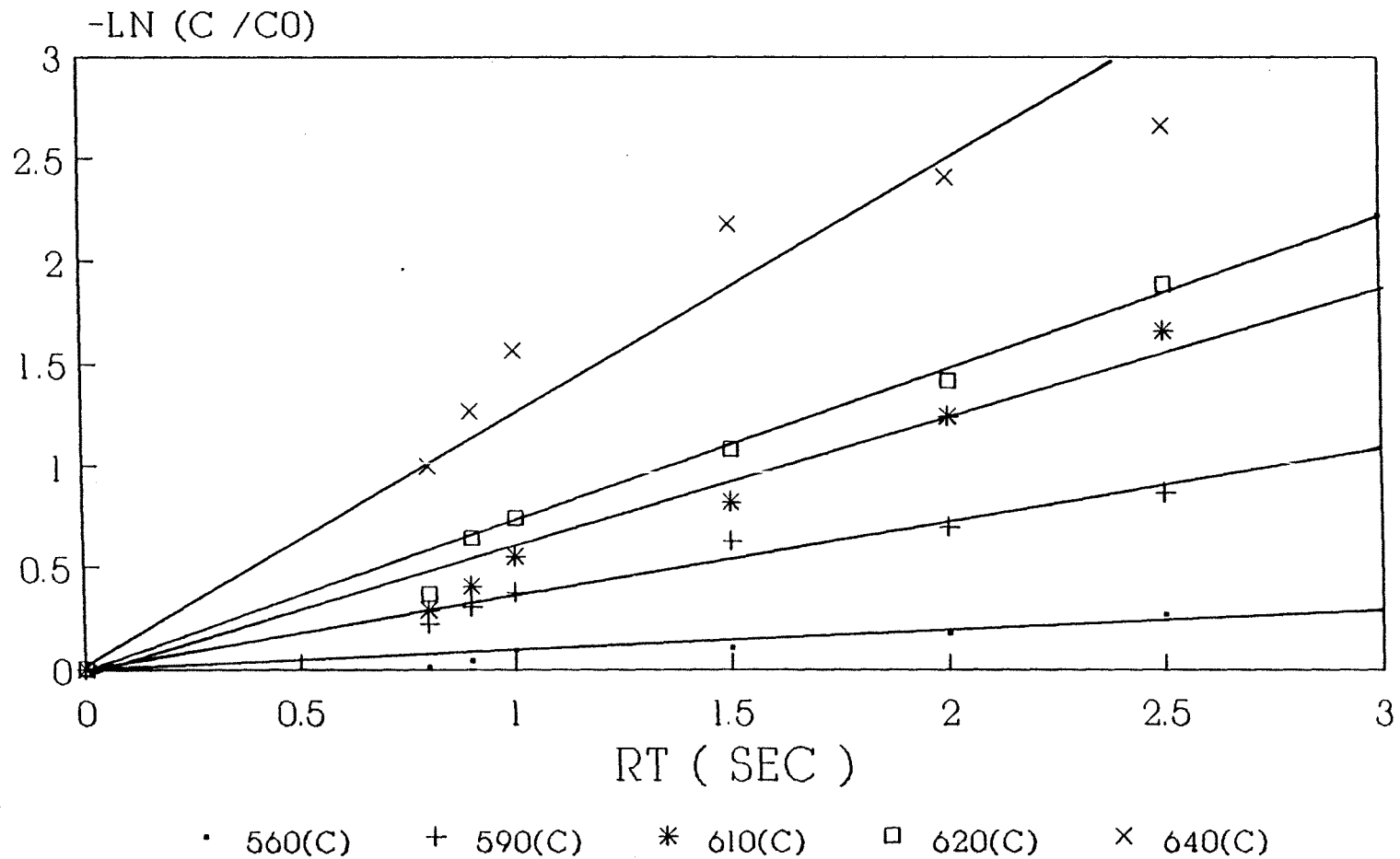


Figure 5.30

1 ST ORDER OF CLBZ + H2 + O2, O2/H2: 2%,
L SIZE (D = 16 mm), DIFF. TEMP.

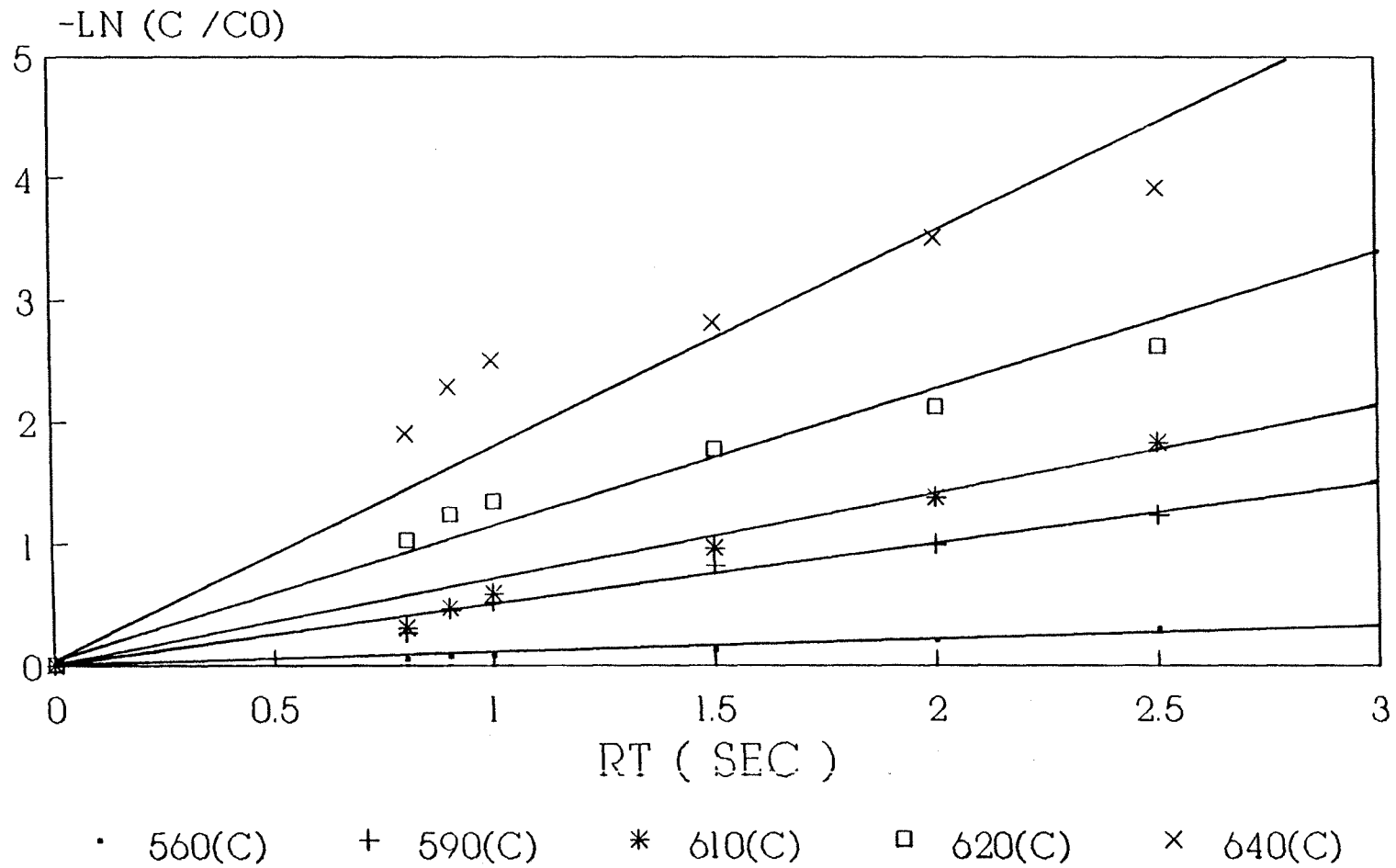


Figure 5.31

1 ST ORDER OF CLBZ + H2 + O2, O2/H2: 3%
 L SIZE (D = 16 mm), DIFF. TEMP,

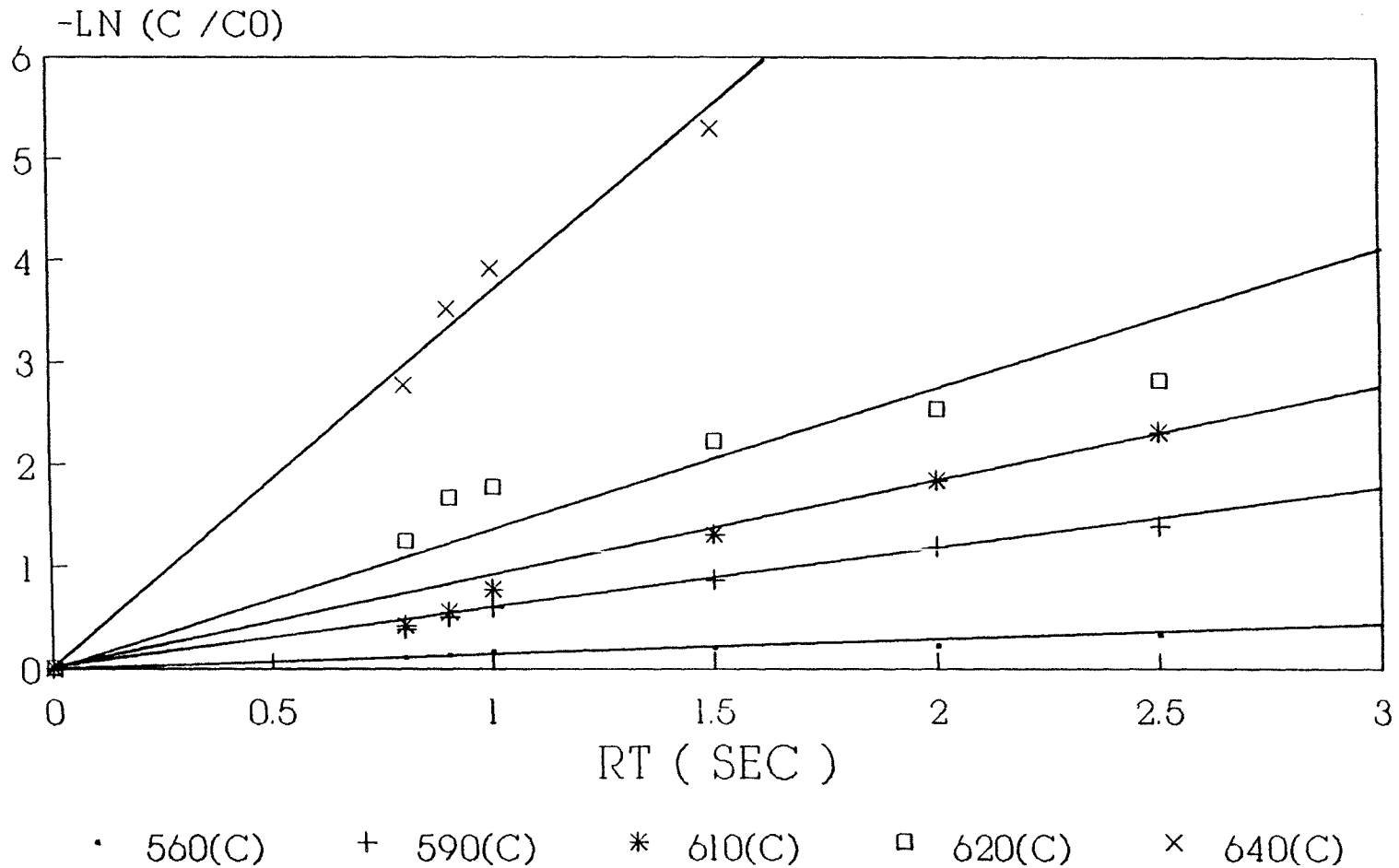


Figure 5.32

1 ST ORDER OF CLBZ + H2 + O2, O2 /H2: 1%
 S SIZE (D = 4 mm),DIFF. TEMP.

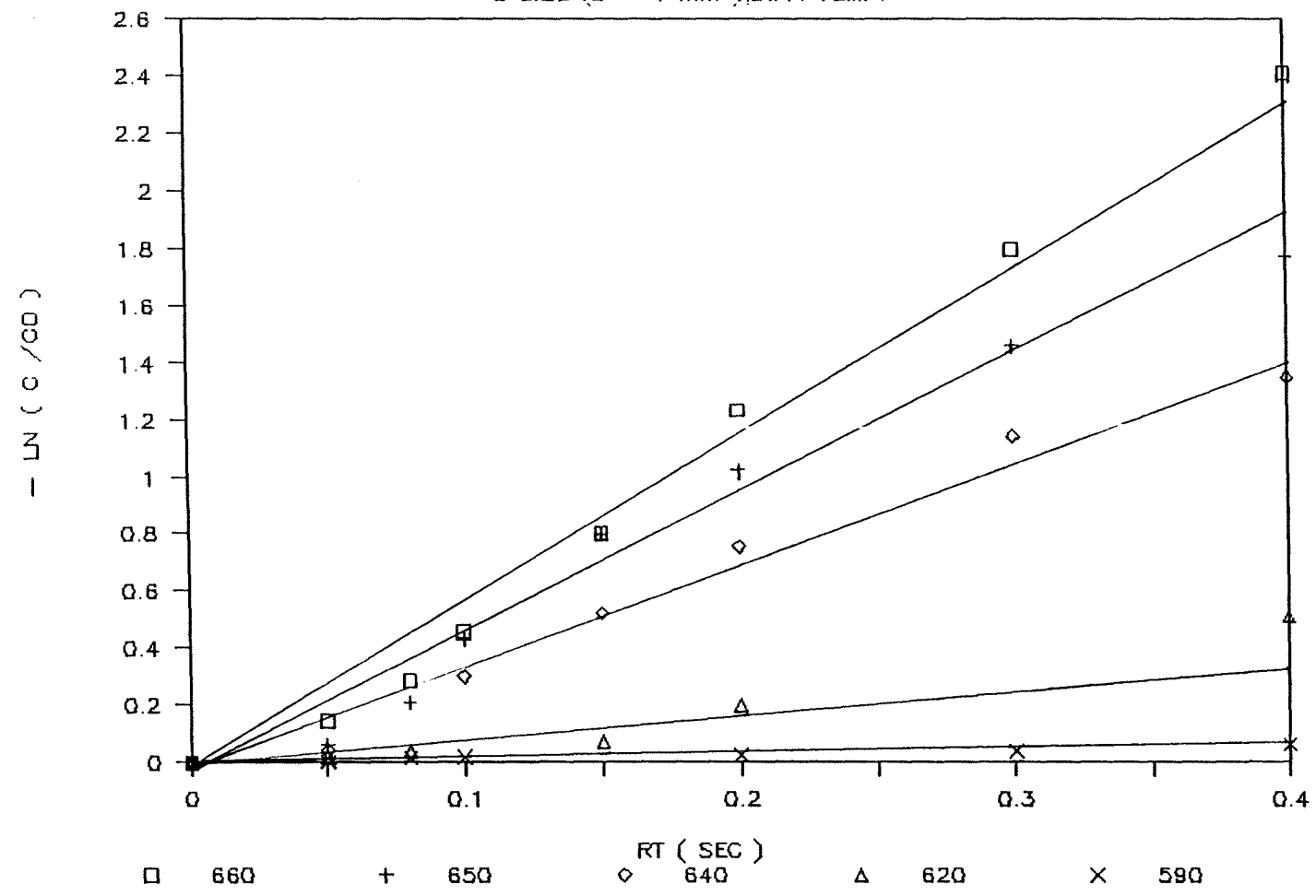


Figure 5.33

1ST ORDER OF CLBZ + H2 + O2, O2 / H2: 2%
 S SIZE (D = 4 mm), DIFF. TEMP.

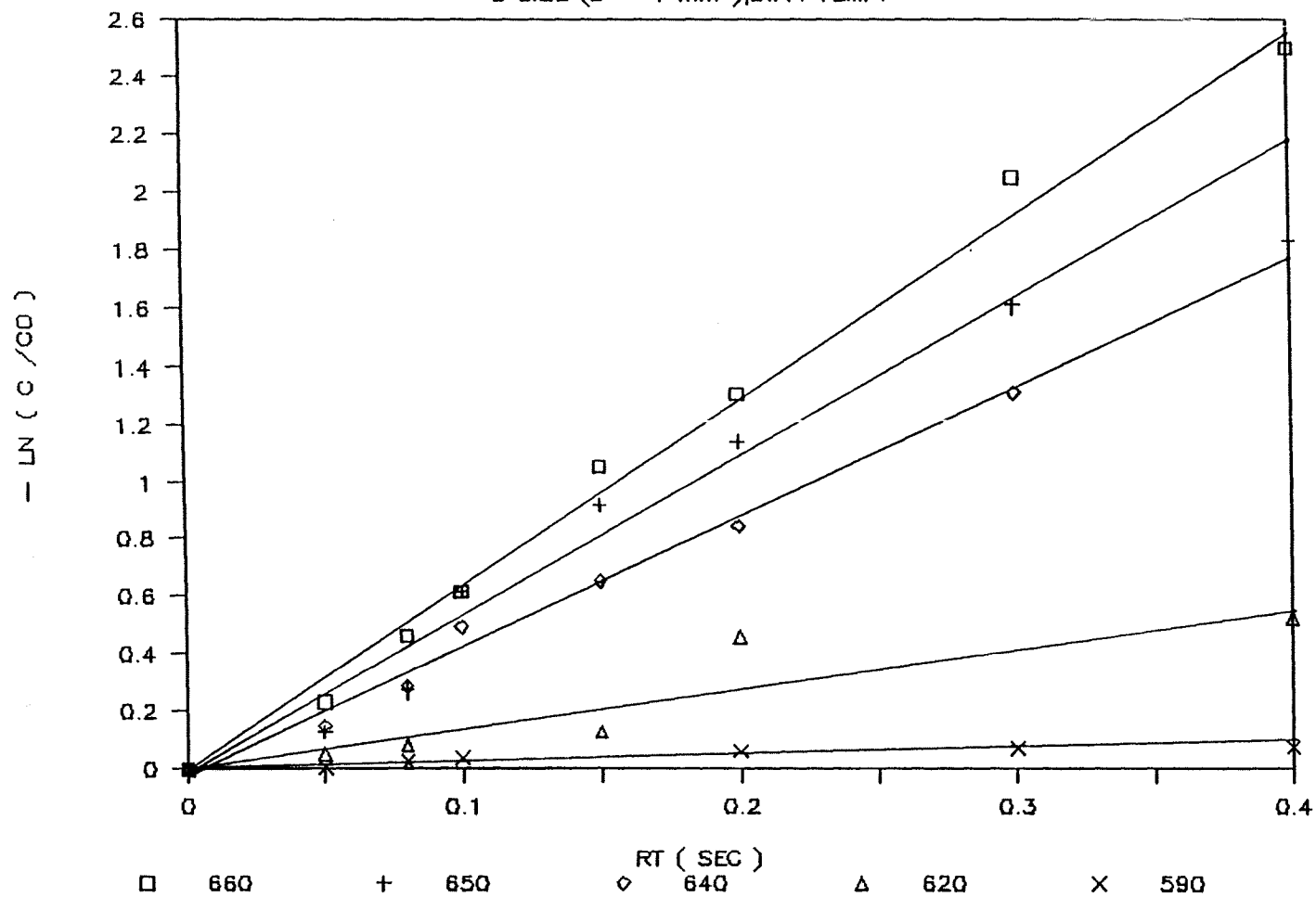


Figure 5.34

1 ST ORDER OF CLBZ + H.2 + O2, O2 A12: 30

S SIZE (D = 4 mm),DIFF. TEMP.

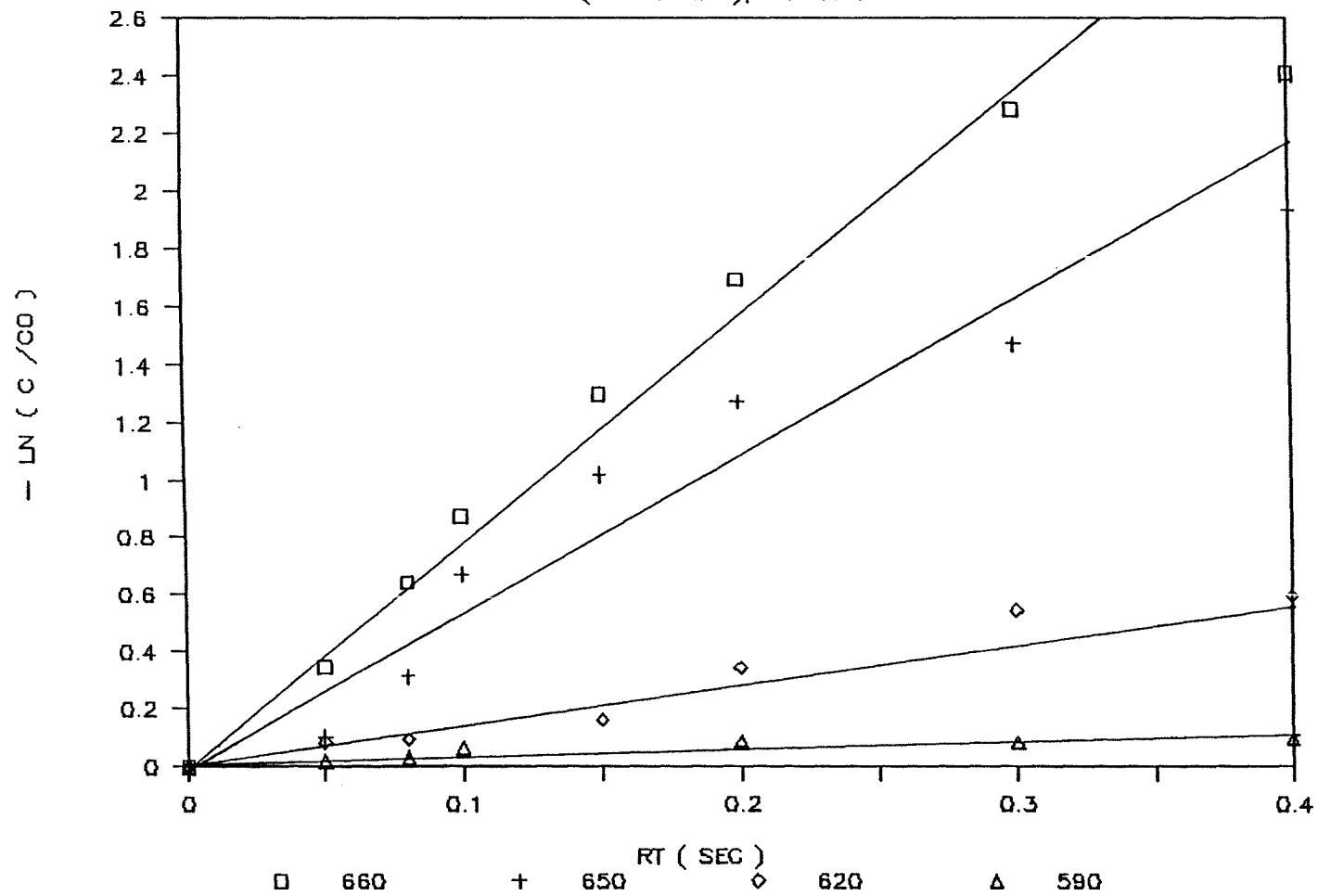


Figure 5.35

ARRHENIUS BEHAVIOR OF CLBZ + H2 + O2 L SIZE (D = 16 mm)

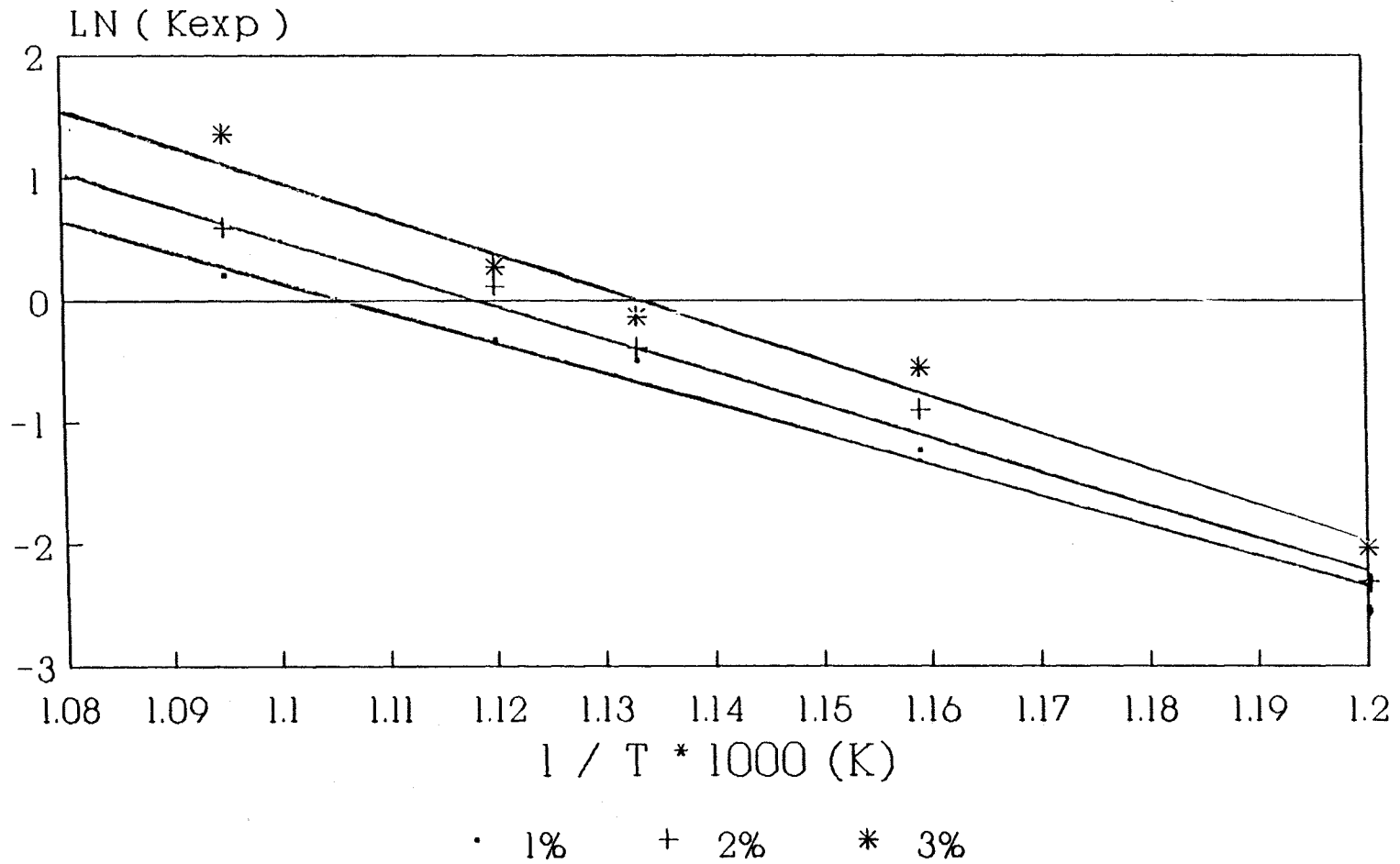


Figure 5.36

ARRHENIUS BEHAVIOR OF CLBZ + H2 + O2 S SIZE (ID ; -4 mm)

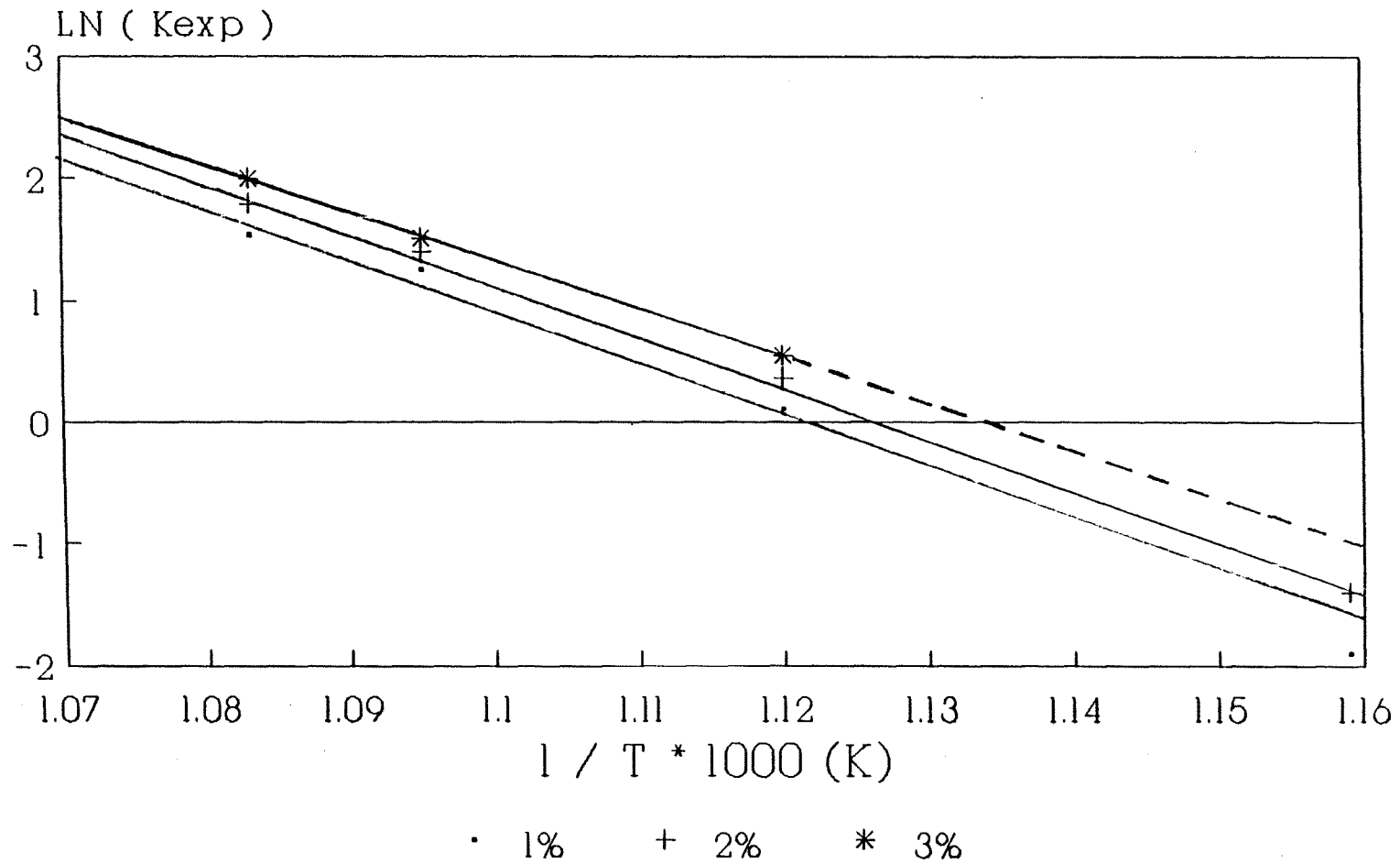


Figure 5.37

with 1% to 3% oxygen ratios. Here, the natural log (ln) of k_{exp} is plotted as a function of reciprocal temperature in degrees Kelvin. As expected, a linear relationship is obtained over the temperature range studied. The global activation energy (E_a) and Arrhenius pre-exponential factor (A) can be determined for the decomposition of chlorobenzene by equation (A).

$$\ln(k_{exp}) = \ln (A) - E_a / R T \quad (A)$$

For 16 mm ID reactor,

$$k_{exp} = 6.9 \cdot 10^{11} e^{(-48800/RT)} \quad (O_2/H_2 \text{ .1\%})$$

$$k_{exp} = 1.5 \cdot 10^{13} e^{(-53700/RT)} \quad (O_2/H_2 \text{ .2\%})$$

$$k_{exp} = 6.9 \cdot 10^{14} e^{(-59900/RT)} \quad (O_2/H_2 \text{ .3\%})$$

Decomposition was most rapid with the 16 mm ID and slowest with the 4 mm ID reactor. This trend is different from the Ritter study results^{<9>} but similar to that of Hung. We consider two reaction paths, which are the homogeneous reaction and heterogeneous reaction, both contributing in our reaction system. The homogeneous reaction occurs in the bulk of the gas mixture and a heterogeneous reaction occurs on the surface of the flow tube wall. Clearly the relative importance of the bulk reaction is greater when the surface to volume (S/V) ratio (relative extent of the wall surface) is less.

Figures 5.38 through 5.40 demonstrate the influence of

REACTION OF CLBZ + H₂ + O₂ • 590 (C)
O₂/H₂ : 2 % ,COMPARE RIFF. REACTOR SIZE

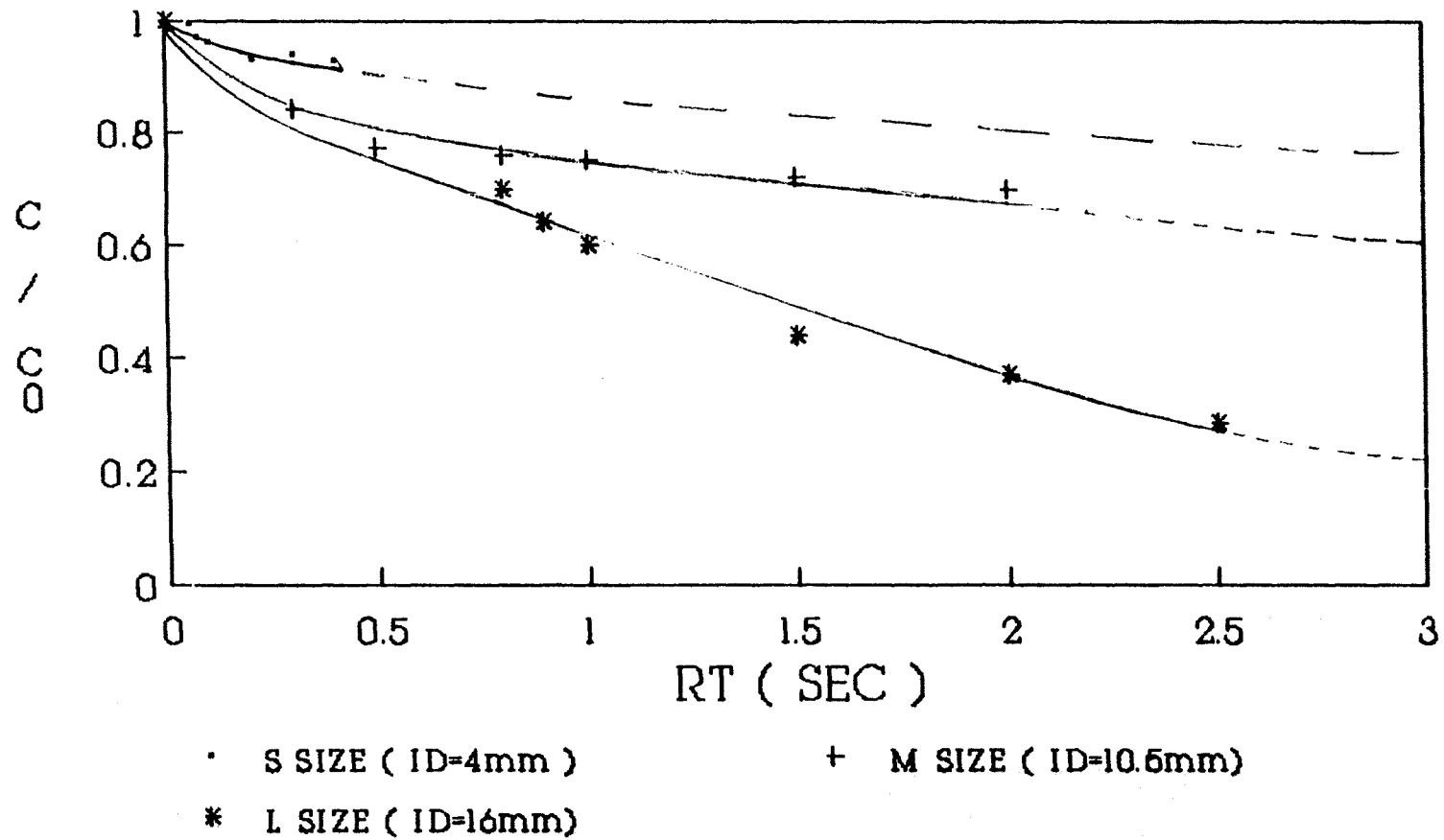


Figure 5.38

REACTION OF CLBZ + H₂ + O₂ , 0 640 (C) O₂/H₂ : 2 % /COMPARE RIFF. REACTOR SIZE

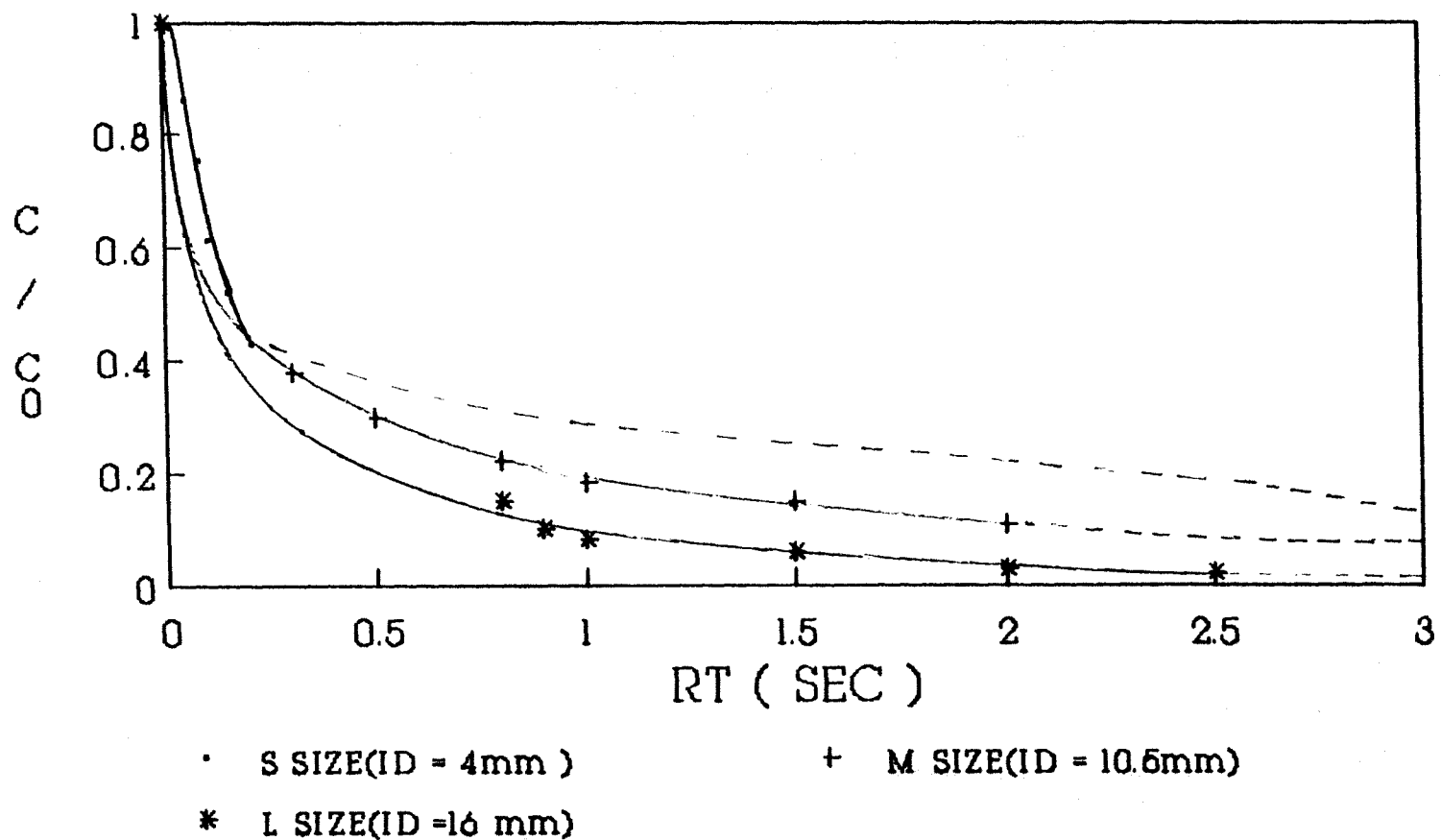


Figure 5.40

S/V ratio on the decay of chlorobenzene. The larger S/V (small reactor diameter) is observed to lower chlorobenzene conversion, while the small S/V (large reactor diameter) has higher chlorobenzene conversion. It is seen that while the decomposition of chlorobenzene is complex, the bulk (homogeneous) reaction dominates. The larger ID reactor consistently shows more reaction and the small reactor has lower overall reaction for all cases.

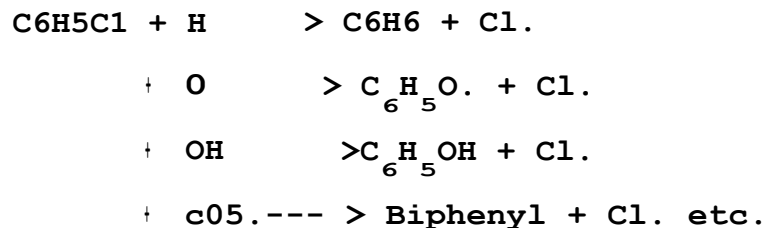
This is seen by plotting k_{exp} against $2/R$ (S/V), where R is the radius of reactor in centimeters. The slope is k_w and the intercept is k_b , from equation (B).

$$k_{exp} = k_b + k_w * (2/R) \quad (B)$$

As can be seen in Figure 5.41, it is somewhat unclear how to determine a relationship for bulk and wall reaction rate constants. This is probably due to a combination of different effects, which include:

[1] Atom and radical loss on the wall.

[2] Complex reactions via varied multiple reactions leading to loss of chlorobenzene.



VARIATION OF K_{exp} VS REACTOR (S/V DECOUPLING K_b and K_w O₂/H₂ 2%

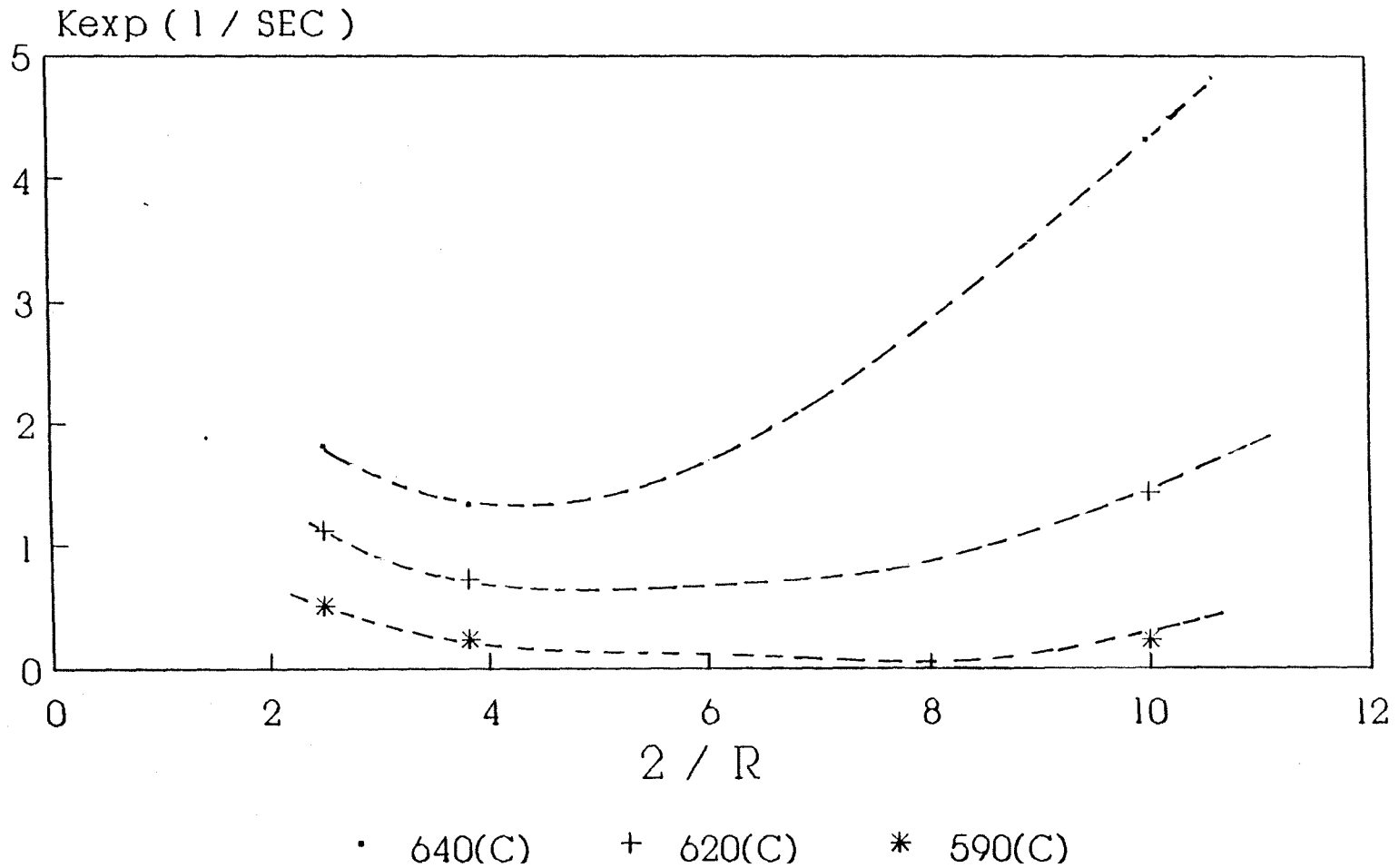


Figure 5.41

B. Reagent Conversion and Products Distribution

The products of chlorobenzene reaction were described by Ritter^{<9>}, but he did not measure C1 to C2 products from pyrolysis of chlorobenzene in excess hydrogen. Zhu however did quantitatively examine formation of light hydrocarbons from C₆H₅Cl + H₂ reaction. His study relative to initial C₆H₅Cl concentration showed a few percent of CH₄, C₂H₂, C₂H₄ and C₂H₆. In our study, major products from oxidation of chlorobenzene were benzene, HCl, CH₄, and C₂H₆. Minor products observed were cyclopentadiene, toluene, ethylene, acetylene, and CO and CO₂. Nearly 20% to 30% of the C₆H₅Cl initially present was lost to solid carbon (soot.) formation in the oxidation of chlorobenzene. The propensity of chlorobenzene to form soot was published by Frenklach et. al.^{<21>}. Solid carbon formation inside the reactor as obtained in this study, amounts to as much as 25% of the chlorobenzene. Tables 5.1 through 5.20 is shown normalized concentration of C₆H₅Cl material balance.

This study did not examine the formation of light **hydrocarbon** in 10.5 mm ID reactor but did in the 16.0 mm and the 4.0 mm ID reactor. All of the chlorobenzene was destroyed at 650 °C, 2 seconds residence time, and 2% of oxygen in the 10.5 mm ID reactor; but in 16 mm ID reactor, all the chlorobenzene totally reacted around 640 °C, 2.0

TABLE (5.1) Normalized Concentration (C/Co) of C6H5C1
 C6H5C1 + H2 + O2 in 16.0 mm ID REACTOR AT 1.0 SEC Rt
 O2/H2: 1%

TEMP (C)	560	590	610	620	640
C6H5C1	0.959	0.69	0.576	0.477	0.208
C6H6	0.022	0.211	0.299	0.404	0.432
CH4	*	0.009	0.0082	0.024	0.045
C2H2	*	/	/	/	0.001
C2H4	*	0.0035	0.002	0.005	0.0076
C2H6	*	0.0062	0.008	0.025	0.04
CO	*	0.003	0.0044	0.0051	0.007

Seqnnt. n n7 n n77 n in/ n nA n 7RO

/ : trace amount, & : by difference,
 * : No analysis

TABLE (5.2) Normalized Concentration (C/Co) of C6H5C1
 C6H5C1 + H2 + O2 in 16.0 mm ID REACTOR AT 1.0 SEC Rt
 O2 / R2 : 2%

TEMP (C)	560	590	610	620	640
C6H5C1	0.931	0.603	0.558	0.261	0.082
C6H6	0.037	0.223	0.267	0.40	0.470
CPD	/	/	/	/	0.0215
CH4	*	0.010	0.008	0.046	0.113
C2H2	*	0.0006	0.0007	0.0015	0.0011
C2H4	*	0.0051	0.0025	0.010	0.011
C2H6	*	0.0127	0.0062	0.051	0.077
CO	*	0.005	0.0053	0.0124	0.018
Soot	0.032	0.141	0.152	0.218	0.230

/ : trace amount, & : by difference,
 * : No analysis, CPD:cyclopentadiene

TABLE (5.3) Normalized Concentration (C/Co) of C6H5C1
 C6H5C1 + H2 + O2 in 16.0 mm ID REACTOR AT 1.0 SEC Rt
 O2 / H2 : 3%

TEMP (C)	560	590	610	620	640
C6H5C1	0.853	0.55	0.462	0.170	0.02
C6H6	0.04	0.272	0.28	0.395	0.46
CPD'	/	/	/	/	0.03
CH4	*	0.0115	0.012	0.084	0.196
C2H2	*	0.002	0.0008	0.002	/
C2H4	*	0.0065	0.004	0.011	0.0125
C2H6	*	0.0143	0.0091	0.0632	0.089
CO	*	0.0091	0.0119	0.023	0.027
Soot	0.107	0.135	0.22	0.251	0.166

/ : trace amount, & : by difference
 * : No analysis, CPD: cyclopentadiene

TABLE (5.4) Normalized Concentration (C/Co) of C6H5C1
 C6H5C1 + H2 + O2 in 16.0 mm ID REACTOR AT 1.0 SEC Rt
 O2 / H2 : 4%

TEMP (C)	560	1590	610	620
C6H5C1	0.83	0.452	0.356	0.02
C6H6	0.05	0.314	0.362	0.267
CPD	/	/	/	0.028
CH4	*	0.0145	0.0325	0.44
C2H2	*	0.0027	/	0.002
C2H4	*	0.010	0.0024	0.017
C2H6	*	0.022	0.034	0.06
CO	*	0.0151	0.025	0.033
Soot	0.12	0.170	0.188	0.133

/ : trace amount, & : by difference
 * : No analysis, CPD: cyclopentadiene

TABLE (5.5) Normalized Concentration (C/Co) of C6H5Cl
 C6H5Cl + H2 + O2 in 16.0 mm ID REACTOR AT **1.0** SEC Rt
O2 / H2 : 5%

TEMP (C)	560	590	610
C6H5Cl	0.815	0.405	0.051
C6H6	0.049	0.331	0.239
CH4	*	0.0179	0.398
C2H2	*	0.0026	0.0003
C2H4	*	0.011	0.0022
C2H6	*	0.019	0.0412
CO	*	0.019	0.0265
Soot	0.136	0.195	0.242

/ : trace amount, & : by difference

* : No analysis

TABLE (5.6) Normalized Concentration (C/Co) of C6H5Cl
 726NC1 + H2 + O2 16.0 mm ID REACTOR AT **2.0** SEC Rt

TEMP (C)	560	590	610	620	640
C6H5Cl	0.841	0.50	0.291	0.2441	0.09
C6H6	0.096	0.381	0.475	0.488	0.483
CH4	*	0.022	0.023	0.05	0.073
C2H2	*	/	/	/	/
C2H4	*	0.009	0.0002	0.008	0.007
C2H6	*	0.0525	0.0221	0.0712	0.07
CO	*	0.0054	0.009	0.009	0.011
Soot	0.063	0.03	0.18	0.13	0.27

/ : trace amount, & : by difference

* : No analysis

TABLE (5.7) Normalized Concentration (C/Co) of C₆H₅Cl
 C₆H₅Cl + H₂ + O₂ in 16.0 mm ID REACTOR AT 2.0 SEC Rt
 O₂ / H₂ : 2%

TEMP (C)	560	590	610	620	640
C ₆ H ₅ Cl	0.821	0.372	0.246	0.116	0.028
C ₆ H ₆	0.106	0.392	0.423	0.401	0.509
CPD	/	/	/	/	0.032
CH ₄	*	0.0272	0.026	0.08	0.132
C ₂ H ₂	*	0.0012	/	0.001	/
C ₂ H ₄	*	0.006	0.003	0.025	0.0083
C ₂ H ₆	*	0.0242	0.023	0.068	0.088
CO	*	0.010	0.012	0.017	0.022
Soot	0.073	0.168	0.292	0.29	0.180

/ : trace amount, & :]3y difference
 * : No analysis, CPD: cyclopentadiene

TABLE (5.8) Normalized Concentration (C/Co) of C₆H₅Cl
 C₆H₅Cl + H₂ + O₂ in 16.0 mm ID REACTOR AT 2.0 SEC Rt
 O₂ / H₂ : 3%

TEMP (C)	560	590	610	620	640
C ₆ H ₅ Cl	0.80	0.303	0.16	0.08	0.0
C ₆ H ₆	0.11	0.42	0.36	0.42	0.432
CPD	/	/	/	/	0.03
CH ₄	*	0.033	0.035	0.124	0.237
C ₂ H ₂	*	0.003	0.0004	0.001	/
C ₂ H ₄	*	0.008	0.0033	0.017	0.0078
C ₂ H ₆	*	0.032	0.023	0.091	0.0901
CO	*	0.016	0.019	0.0284	0.031
Soot	0.09	0.168	0.292	0.243	0.172

/ : trace amount, & : by difference
 * : No analysis, CPD: cyclopentadiene

TABLE (5.9) Normalized Concentration (C/Co) of C6H5Cl
 C6H5Cl + H2 + O2 in 16.0 mm ID REACTOR AT 2.0 SEC Rt
 O2 / H2 : 4%

TEMP (C)	560	590	610	620
C6H5Cl	0.751	0.269	0.132	0.01
C6H6	0.118	0.461	0.46	0.35
CPD	/	/	/	0.039
CH4	*	0.04	0.05	0.31
C2H2	*	0.007	0.0004	0.004
C2H4	*	0.011	0.0035	0.04
C2H6	*	0.075	0.027	0.074
CO	*	0.02	0.033	0.035
<hr/>				
Soot	0.131	0.170	0.295	0.141

/ : trace amount, & : by difference
 * : No analysis, CPD: cyclopentadiene

TABLE (5.10) Normalized Concentration (C/Co) of C6H5Cl
 C6H5Cl + H2 + O2 in 16.0 mm ID REACTOR AT 2.0 SEC Rt
 O2 / H2 : 5%

TEMP (C)	560	590	610
C6H5Cl	0.716	0.254	0.0033
C6H6	0.12	0.455	0.32
CH4	*	0.042	0.51
C2H2	*	0.0082	0.0009
C2H4	*	0.0109	0.004
C2H6	*	0.03	0.0263
CO	*	0.024	0.034
Soot	0.164	0.176	0.102

/ : trace amount, & : by difference
 * : No analysis

**TABLE (5.11) Normalized Concentration (C/Co) of C6H5Cl
C6H5Cl + H2 + O2 in 10.5 mm ID REACTOR AT 1.0 SEC Rt
O2 / H2 : 1%**

TEMP (C)	580	590	600	620	640
C6H5Cl	0.90	0.82	0.73	0.70	0.32
C6H6	0.04	0.06	0.10	0.18	0.30
&Soot	0.06	0.12	0.17	0.12	0.38
HCl.	0.01	0.05	0.15	0.20	0.43
*Loss Cl	0.09	0.13	0.12	0.1	0.25

: by difference(No examined light hydrocarbons)

* : 1 - (C6H5Cl + HCl)

**TABLE (5.12) Normalized Concentration (C/Co) of C6H5Cl
C6H5Cl + H2 + O2 in 10.5 mm ID REACTOR. AT 1.0 SEC Rt
O2 / H2 : 2%**

TEMP (C)	580	590	600	610	620	630	640	650
C6H5Cl	0.82	0.74	0.68	0.57	0.43	0.29	0.184	0.01
C6H6	0.06	0.077	0.10	0.161	0.26	0.31	0.32	0.38
&Soot	0.12	0.18	0.22	0.269	0.31	0.40	0.496	0.61
HCl	0.02	0.07	0.20	0.32	0.50	0.62	0.68	0.72
*Loss Cl	0.16	0.19	0.12	0.11	0.07	0.09	0.136	0.27

: by difference(No examined light hydrocarbons)

* : 1 - (C6H5Cl + HCl)

TABLE (5.13) Normalized Concentration (C/Co) of C6H5Cl
 C6H5Cl + H2 + O2 in 10.5 mm ID REACTOR AT 1.0 SEC Rt
 O2 / H2 : 4%

TEMP (C)	580	590	600	620	630	640
C6H5Cl	0.78	0.71	0.60	0.45	0.23	0.12
C6H6	0.065	0.092	0.201	0.30	0.32	0.41
Soot	0.155	0.198	0.199	0.25	0.45	0.47
HCl	0.05	0.11	0.26	0.42	0.59	0.73
* Loss Cl	0.17	0.18	0.14	0.13	0.18	0.15

: by difference(No examined light hydrocarbons)

* : 1 - (C6H5Cl + HCl)

TABLE (5.14) Normalized Concentration (C/Co) of C6H5Cl
 C6H5Cl + H2 + O2 in 4.0 mm ID REACTOR, Rt: 0.05 - 0.4 SEC.
 O2 / 1E2 : 1%
 TEMPERATURE : 640 °C

Rt (SEC)	0.05	0.1	0.15	0.2	0.3	0.4
C6H5Cl	0.96	0.74	0.59	0.472	0.32	0.257
C6H6	0.0093	0.117	0.234	0.279	0.373	0.394
CH4	0.0004	0.004	0.0134	0.0257	0.04	0.066
C2H2	/	0.0016	0.0012	/	0.0023	0.003
C2H4	/	0.004	0.0064	0.0085	0.01	0.013
C2H6	0.026	0.002	0.009	0.019	0.029	0.044
CO	/	0.0015	0.003	0.008	0.009	/
Soot	0.004	0.126	0.142	0.186	0.216	0.223

/ : trace amount, & : by difference

* : No analysis

TABLE (5.15) Normalized Concentration (C/Co) of C6H5C1
 C6H5C1 + H2 + O2 in 4.0 mm ID REACTOR, Rt: 0.05 - 0.3 SEC.
 O2 / 112 : 2%
 TEMPERATURE : 640°C

Rt (SEC)	0.05	0.08	0.1	0.15	0.2	0.3
C6H5C1	0.86	0.75	0.61	0.52	0.43	0.27
C6/16	0.007	0.08	0.132	0.23	0.31	0.39
CH4,	*	0.025	0.0065	0.017	0.03	0.055
C2H2	*	0.004	0.002	0.002	/	/
C2H4	*	0.005	0.0047	0.0078	0.094	0.012
C2H6		0.001	0.011	0.012	0.021	0.04
CO	/	/	0.0025	0.0036	0.006	0.01
Soot	0.132	0.148	0.231	0.21	0.192	0.23

/ : trace amount, & : by difference
 * : No analysis

TABLE (5.16) Normalized Concentration (C/Co) of C6H5C1
 :6H5C1 + H2 + O2 in 4.0 mm ID REACTOR, Rt: 0.05 - 0.4 SEC.
 /2 / H2
 TEMPERATURE : 650°C

Rt (SEC)	0.05	0.08	0.1	0.15	0.2	0.3	0.4
C6H5C1	0.94	0.81	0.645	0.45	0.36	0.233	0.17
C6H6	0.003	0.075	0.171	0.3	0.376	0.433	0.452
CH4	*	*	0.01	0.026	0.041	0.076	0.112
C2H2	*	*	/	0.013	0.002	0.005	0.008
C2H4	*	*	0.016	0.018	0.012	0.015	0.013
C2H6	*	*	0.017	0.036	0.031	0.051	0.058
CO	*	*	0.0015	0.004	0.006	0.085	0.017
Soot	0.057	0.115	0.14	0.152	0.17	0.18	0.176

/ : trace amount, & : by difference
 * : No analysis

TABLE(5.17) Normalized Concentration (C/Co) of C6H5Cl
 C6H5Cl + H2 + O2 in 4.0 mm ID REACTOR, Rt: 0.05 - 0.4 SEC.
 O2 / H2 : 2%
 TEMPERATURE : 650 °C

Rt (SEC)	0.05	0.08	0.1	0.15	0.2	0.3	0.4
C6H5Cl	0.899	0.76	0.54	0.39	0.32	0.20	0.16
C6H6	0.04	0.133	0.196	0.312	0.385	0.443	0.445
CH4	*	*	0.014	0.054	0.047	0.091	0.089
C2H2	*	*	0.02	0.022	0.004	0.003	0.003
C2H4	*	*	0.013	0.023	0.014	0.023	0.014
C2H6	*	*	0.014	0.043	0.034	0.066	0.053
CO	*	*	0.0016	0.005	0.007	0.01	0.02
Soot	0.061	0.107	0.219	0.144	0.187	0.164	0.22

/ : trace amount, & : by difference
 * : No analysis

TABLE(5.18) Normalized Concentration (C/Co) of C6H5Cl
 C6H5Cl + H2 + O2 in 4.0 mm ID REACTOR, Rt: 0.05 - 0.4 SEC.
 O2 / H2 : 3%
 TEMPERATURE : 650 °C

Rt (SEC)	0.05	0.08	0.1	0.15	0.2	0.3	0.4
C6H5Cl	0.9	0.73	0.51	0.36	0.28	0.23	0.143
C6H6	0.032	0.137	0.22	0.335	0.395	0.43	0.46
CH4	*	0.009	0.022	0.042	0.058	0.091	0.103
C2H2	*	0.007	0.009	0.023	0.003	0.021	0.008
C2H4	*	0.011	0.015	0.025	0.027	0.026	0.017
C2H6	*	0.006	0.018	0.03	0.064	0.08	0.081
CO	*	0.003	0.005	0.01	0.012	0.013	0.022
Soot	0.068	0.097	0.2	0.17	0.13	0.11	0.167

/ : trace amount, & : by difference
 * : No analysis

TABLE (5.19) Normalized Concentration (C/Co) of C6H5Cl
 C6H5Cl + H2 + O2 in 4.0 mm ID REACTOR, Rt: 0.05 - 0.4 SEC.
 O2 / H2 : 4%
 TEMPERATURE : 650°C

Rt (SEC)	0.05	0.08	0.1	0.15	0.2	0.3	0.4
C6H5Cl	0.87	0.67	0.47	0.31	0.21	0.16	0.14
C6H6	0.025	0.154	0.23	0.33	0.38	0.44	0.439
CH4,	*	*	0.027	0.053	0.099	0.101	0.084
C2H2	*	*	0.009	0.022	0.024	0.004	0.019
C2H4	*	*	0.017	0.028	0.031	0.018	0.028
C2H6	*	*	0.023	0.057	0.077	0.054	0.074
CO	*	*	0.0066	0.012	0.017	0.018	
Soot	0.105	0.17	0.22	0.254	0.16	0.204	0.216

/ : trace amount, & : by difference

* : No analysis

TABLE (5.20) Normalized Concentration (C/Co) of C6H5Cl
 C6H5Cl + H2 + O2 in 4.0 mm ID REACTOR, Rt: 0.05 - 0.4 SEC.
 O2 / H2 : 5%
 TEMPERATURE : 650°C

Rt (SEC)	0.05	0.08	0.1	0.15	0.2	0.3	0.4
C6H5Cl	0.74	0.58	0.46	0.28	0.22	0.14	0.1
C6H6	0.02	0.156	0.24	0.358	0.407	0.415	0.422
CH4	*	*	0.032	0.063	0.086	0.107	0.121
C2H2	*	*	0.036	0.004	0.032	0.005	0.005
C2H4	*	*	0.027	0.022	0.034	0.022	0.017
C2H6	*	*	0.049	0.033	0.043	0.047	0.046
CO	*	*	0.008	0.016	0.022	0.025	0.026
Soot	0.24	0.264	0.146	0.223	0.16	0.24	0.26

/ : trace amount, & : by difference

* : No analysis

second residence time, and only 3% of oxygen. Figures 5.42 through 5.44 show the benzene product distribution curve versus time in 16 mm ID reactor for temperature from 560 °C to 640 °C. The benzene increases with both residence time and temperature. Figure 5.45 also shows benzene production with temperature from 600 °C to 650 °C in the 10.5 mm ID reactor. Clearly, the production of benzene is faster in the 16 mm ID reactor.

Among the light hydrocarbons found, methane is present in the highest concentration - Methane levels also increased with residence time, temperature, and oxygen ratio. The amount of CH₄ is significantly affected by both the oxygen ratio and reaction time. Figure 5.46 illustrates CH₄ at several temperatures 5% of oxygen in 16 mm ID reactor for 2 second reaction times. Figure 5.47 also demonstrates the formation of light hydrocarbon at different oxygen ratio (from 1% to 4%) in 16 mm ID reactor. With 5%, the main light hydrocarbon is CH₄ which has a maximum value about 50% the initial chlorobenzene. This illustrates that some of the benzene ring is actually converted to smaller hydrocarbons, especially methane. In our system, we see significant amounts of CH₄, as does Baldwin, Scott, and Walker^{<41>}. This is also in good agreement with Louw, Dijks, and Mulder study^{<5>}. The following reaction schemes describe plausible mechanisms for the formation of methane, CO, and

**BENZENE PRODUCT OF CLBZ + H₂ + O₂, 1 ATM
L SIZE (D ■ 16 mm), 1% ,DIFF. TEMP.**

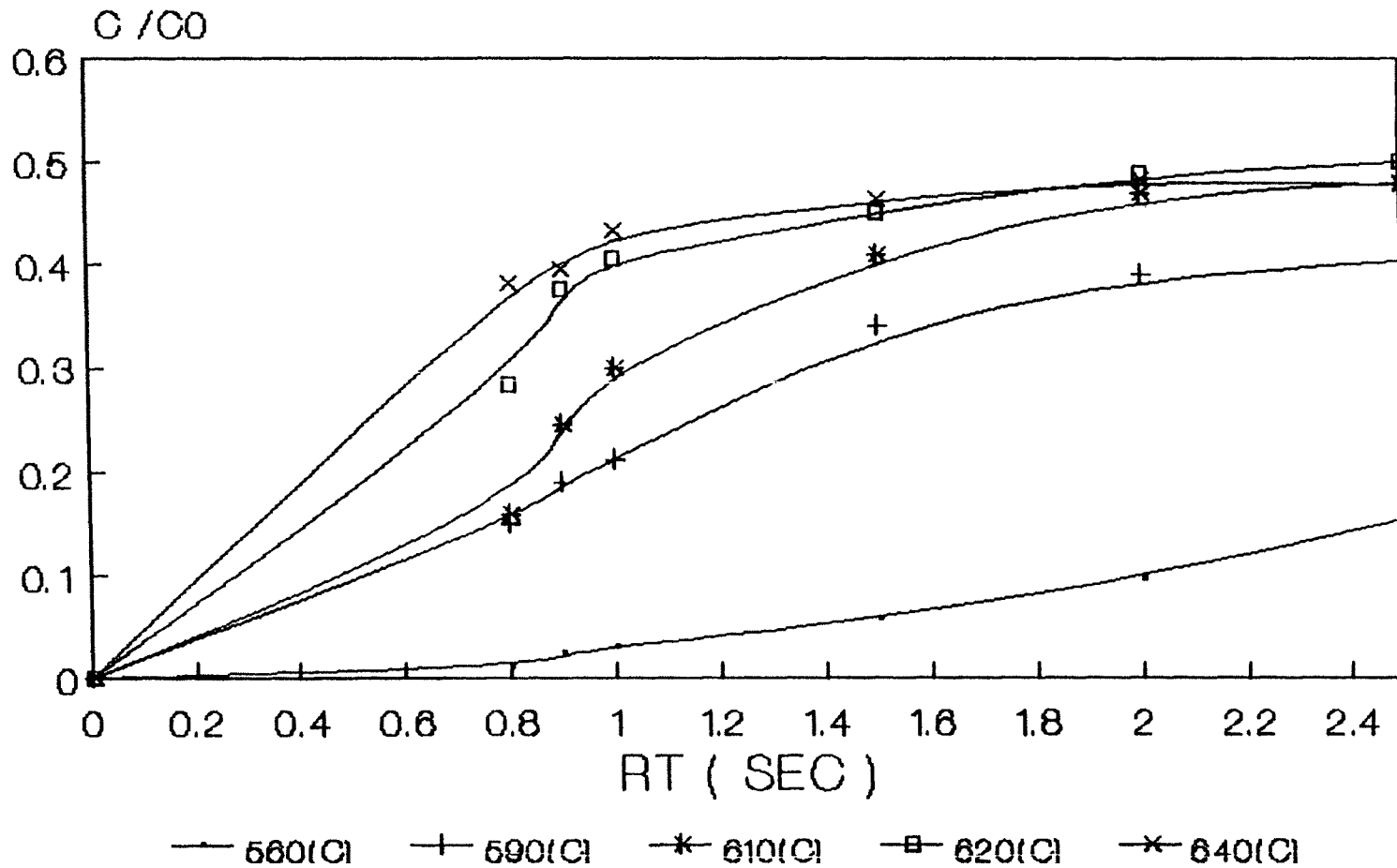


Figure 5.42

BENZENE PRODUCT O₂/H₂: 2%,
L SIZE (D = 16 mm), RIFF. TEMP.

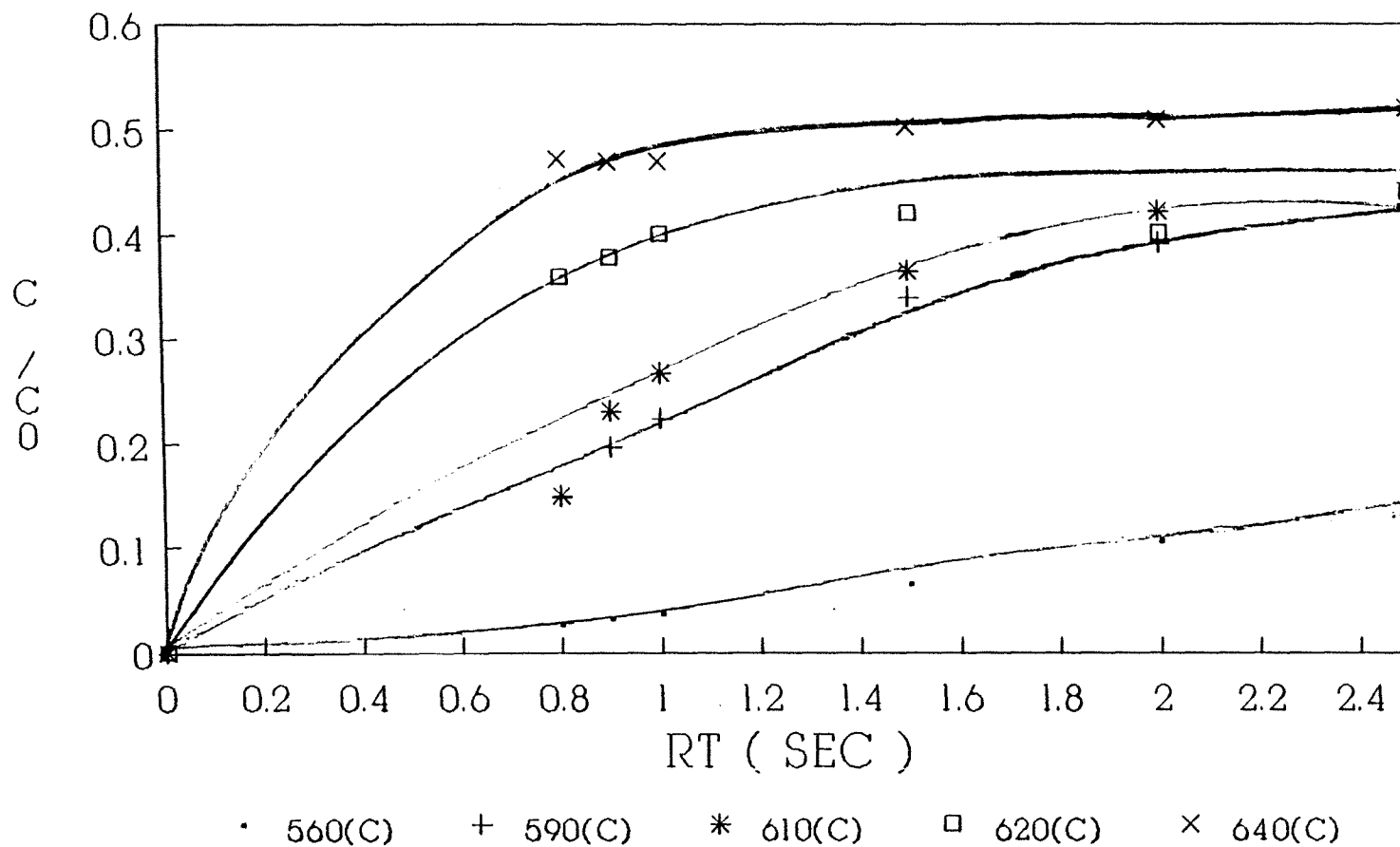


Figure 5.43

BENZENE PRODUCT ,02/H2: 3%,
L SIZE (D LI 16 mm), DIFF. TEMP.

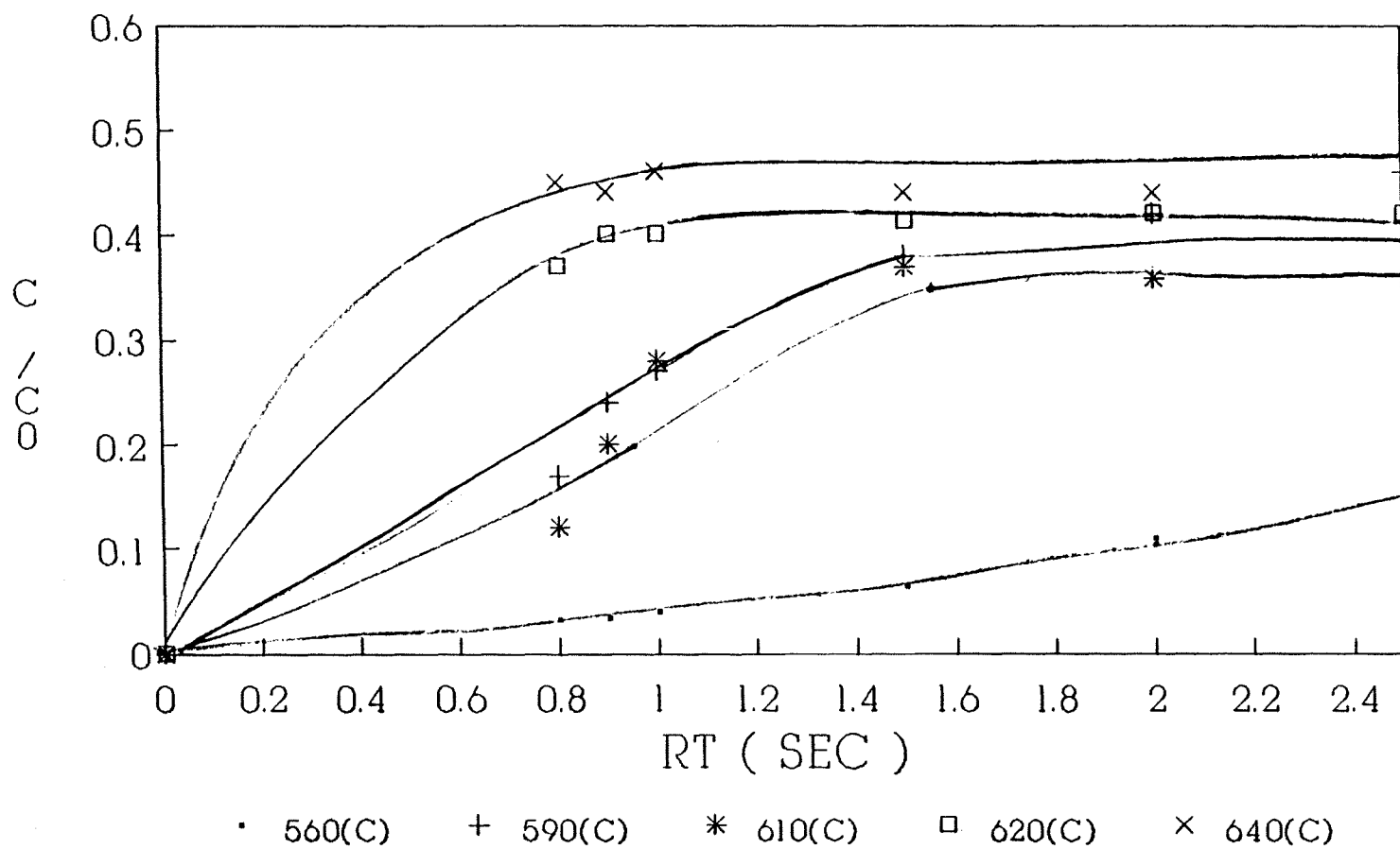


Figure 5.44

**BENZENE PRODUCT DISTR., O₂/H₂: 2%
M SIZE (ID ■ 10.5 mm), RIFF. TEMP.**

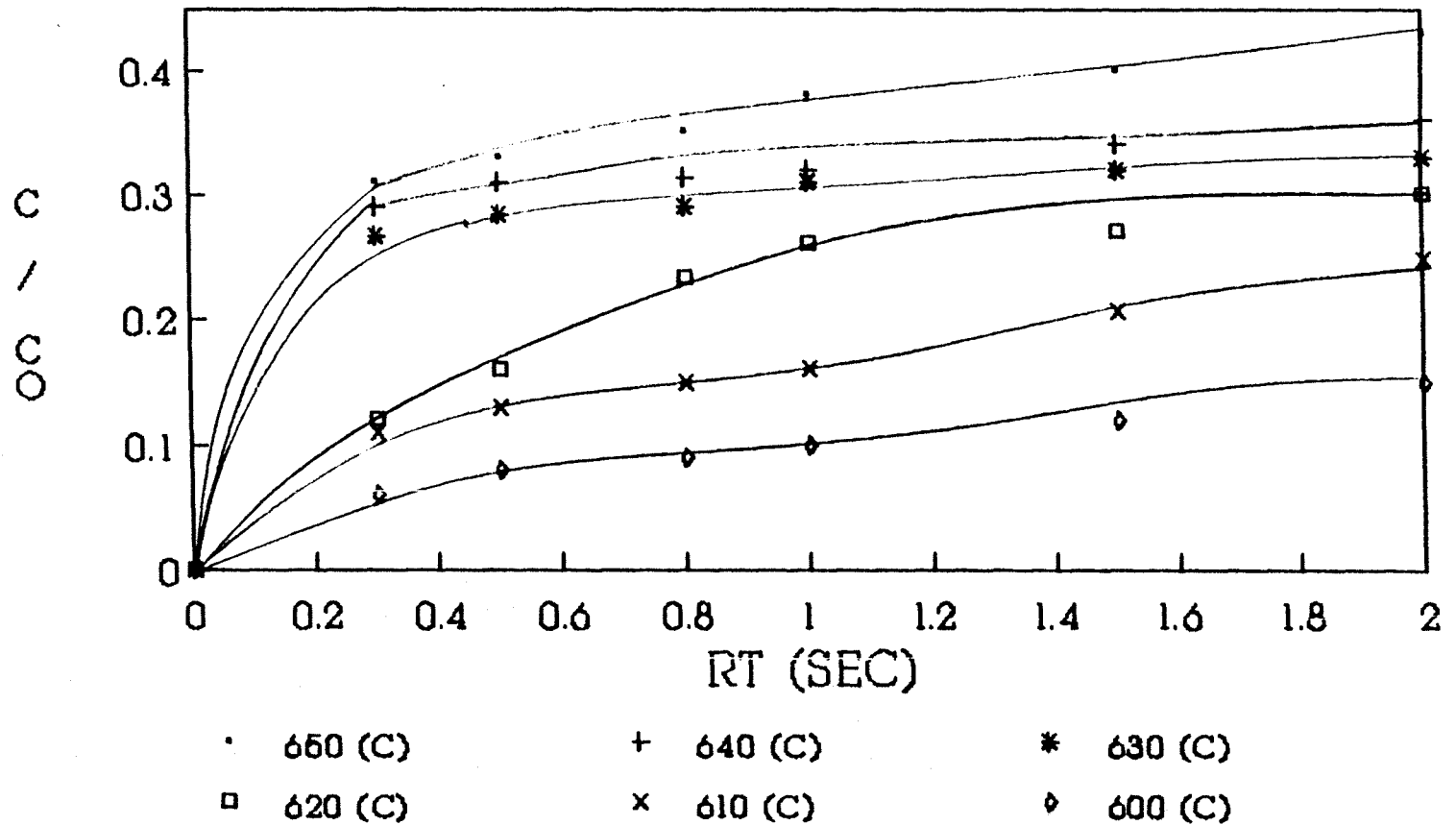


Figure 5.45

**REACTION OF CLBZ + H₂ + O₂, 1 ATM
 RT = 2 (SEC), O₂/H₂: 5% , ID 7-16 mm**

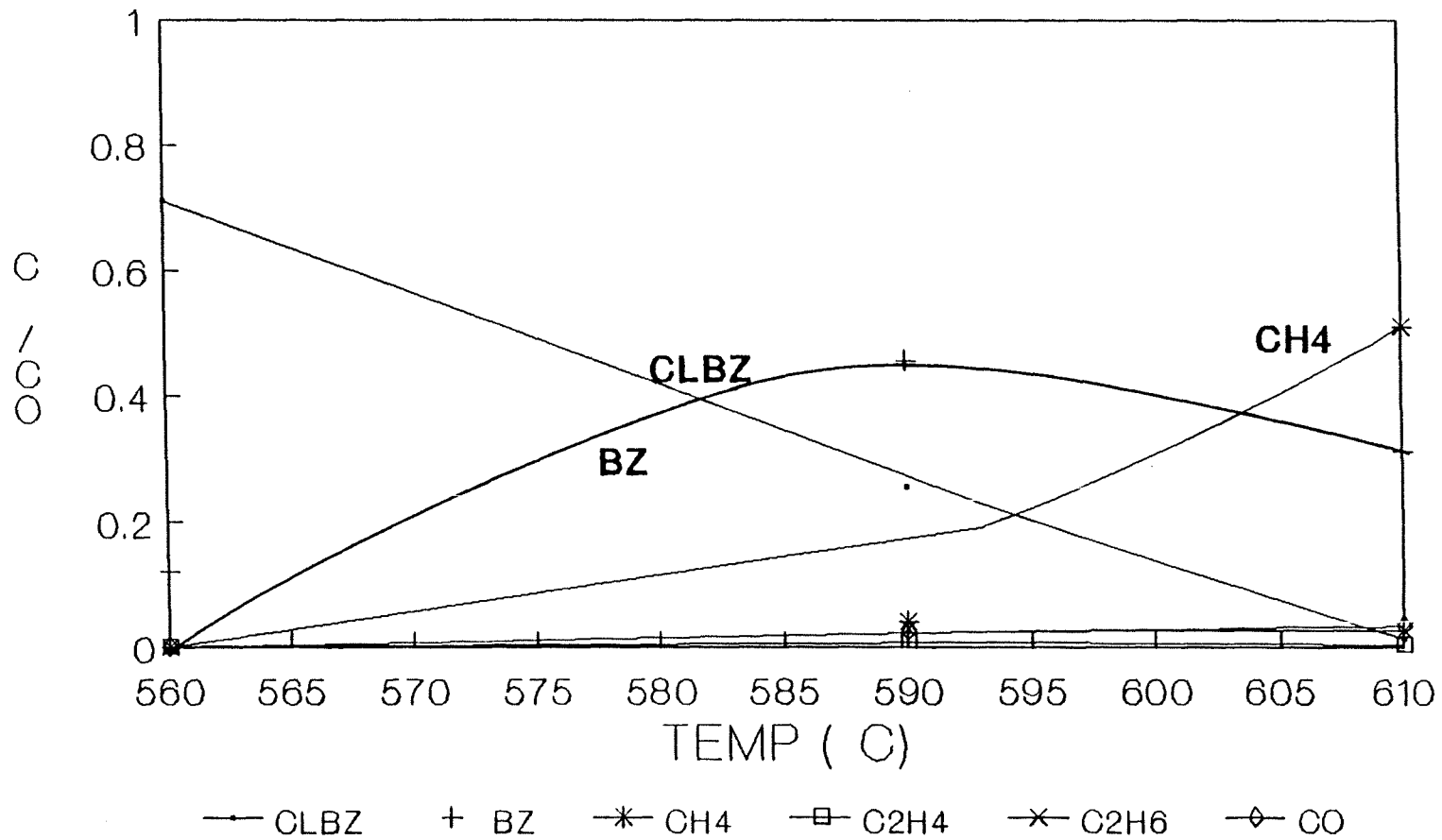
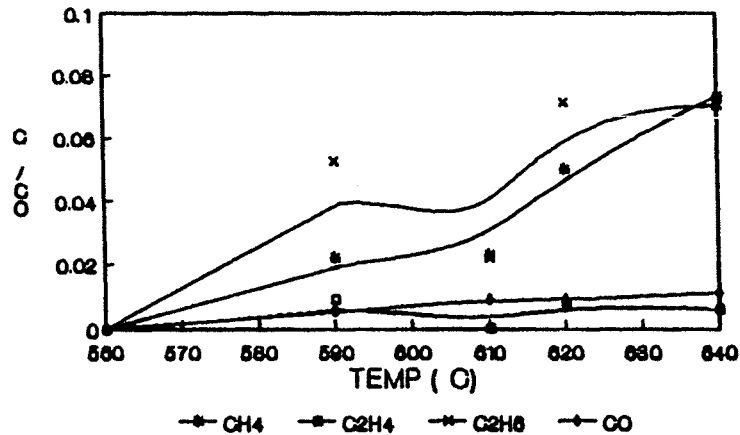
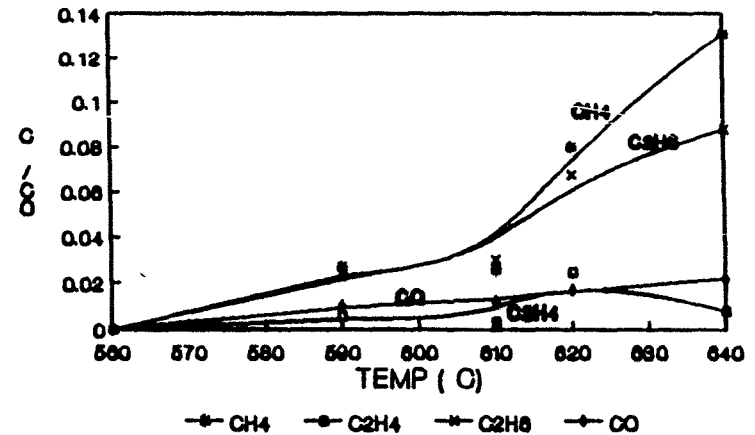


Figure 5:46

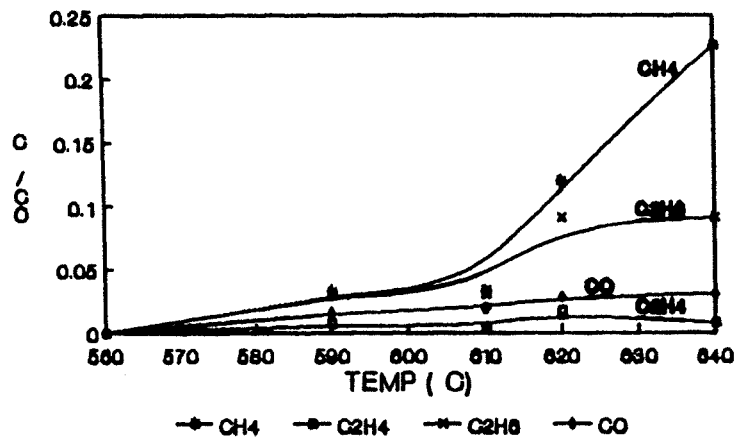
CLEM + H2 + O2 AT RT•2 (SEC), O2 / H2: 1%
LIGHT HYDROCARBON , L SIZE (ID • 16 mm)



CLBZ * H2 * O2 AT RT•2 (\$EC), O2 / H2 : 2%
LIGHT HYDROCARBON , L WE (ID • 16 min)



CI-BZ + H2 + O2 AT RT■2 (8C-C), O2 / H2 : 11%
LIGHT HYDROCARBON , L SIZE (ID • 16 min)



CLBZ * H2 + O2 AT RT•2 (13EC), O2 / H2 : 414
LIGHT HYDROCARBON , L 81ZE (ID • IQ min)

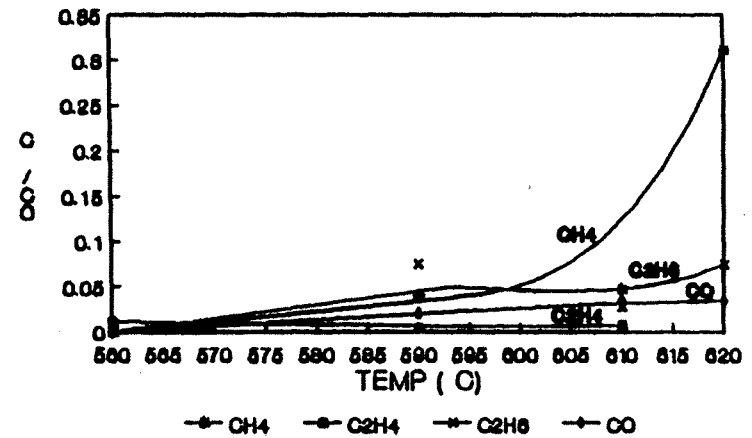
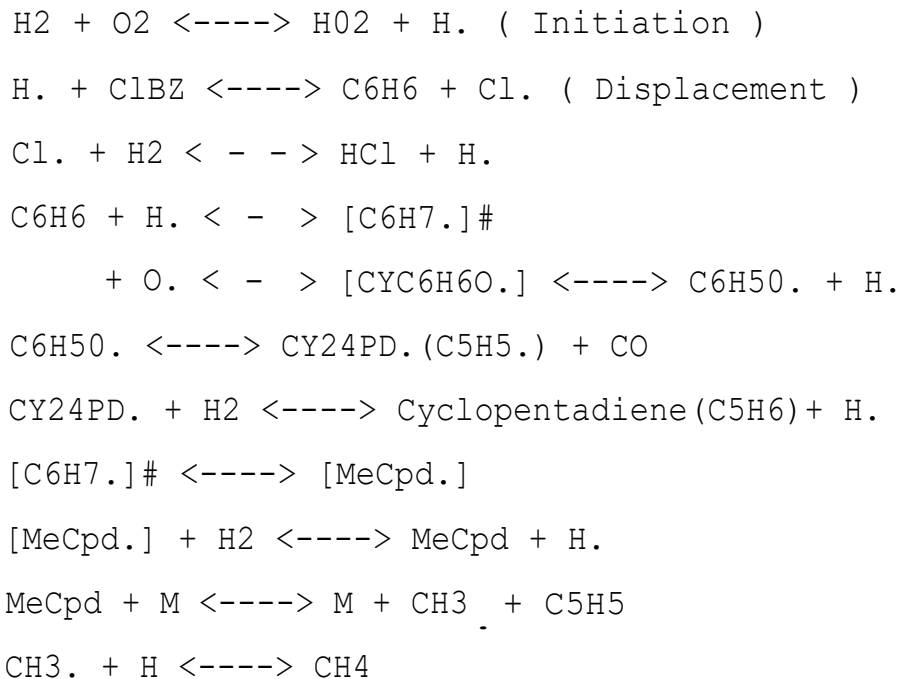


Figure 5.47

cyclopentadiene:



The conversion of benzene to CO or CH₃· + Cyclopentadiene radical is initiated by attack of hydrogen and oxygen radicals respectively on chlorobenzene on benzene. When the oxygen increases, the products of cyclopentadiene and CO also increase providing evidence that the above reaction routes are reasonable.

The C₂H₆ product is second highest light concentration hydrocarbon produced and is observed in the range of 1% to 10%, depending on the amount of oxygen. Figures 5.48 through 5.54 show several 1 second and 2 second residence time product distributions in the 16 mm ID reactor. The C₂H₄ plus C₂H₂ observed are small and comprise less than 2%

**REACTION OF CLBZ + H₂ + O₂, 1 ATM
 RT ra 1(SEC), O₂/H₂ : 1% , ID r= 16 mm**

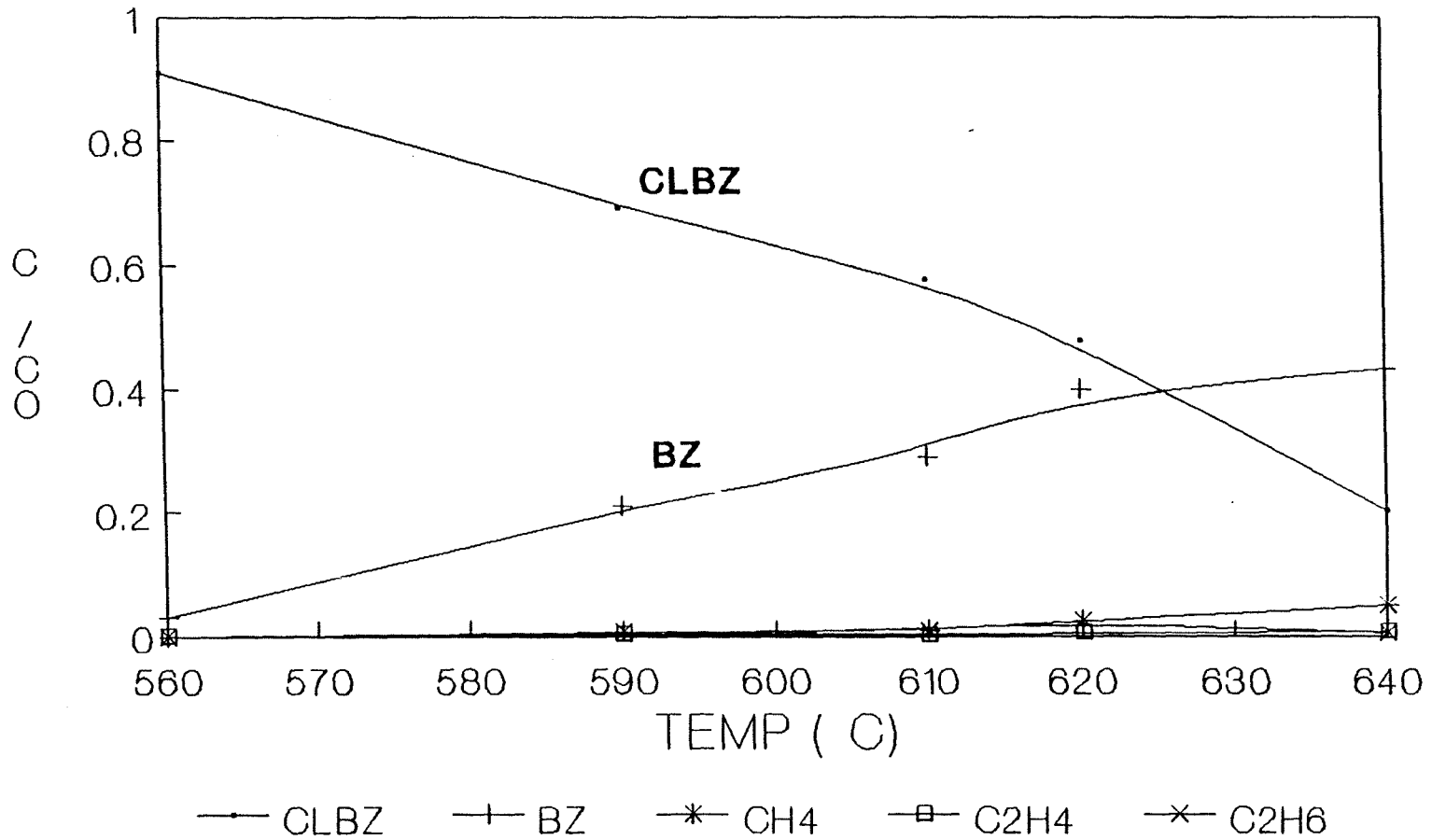


Figure 5.48

**REACTION OF CLBZ + H₂ + O₂ , 1 ATM
 RT 1 (SEC) , O₂ / H₂ : 2% , ID ra 16 mm**

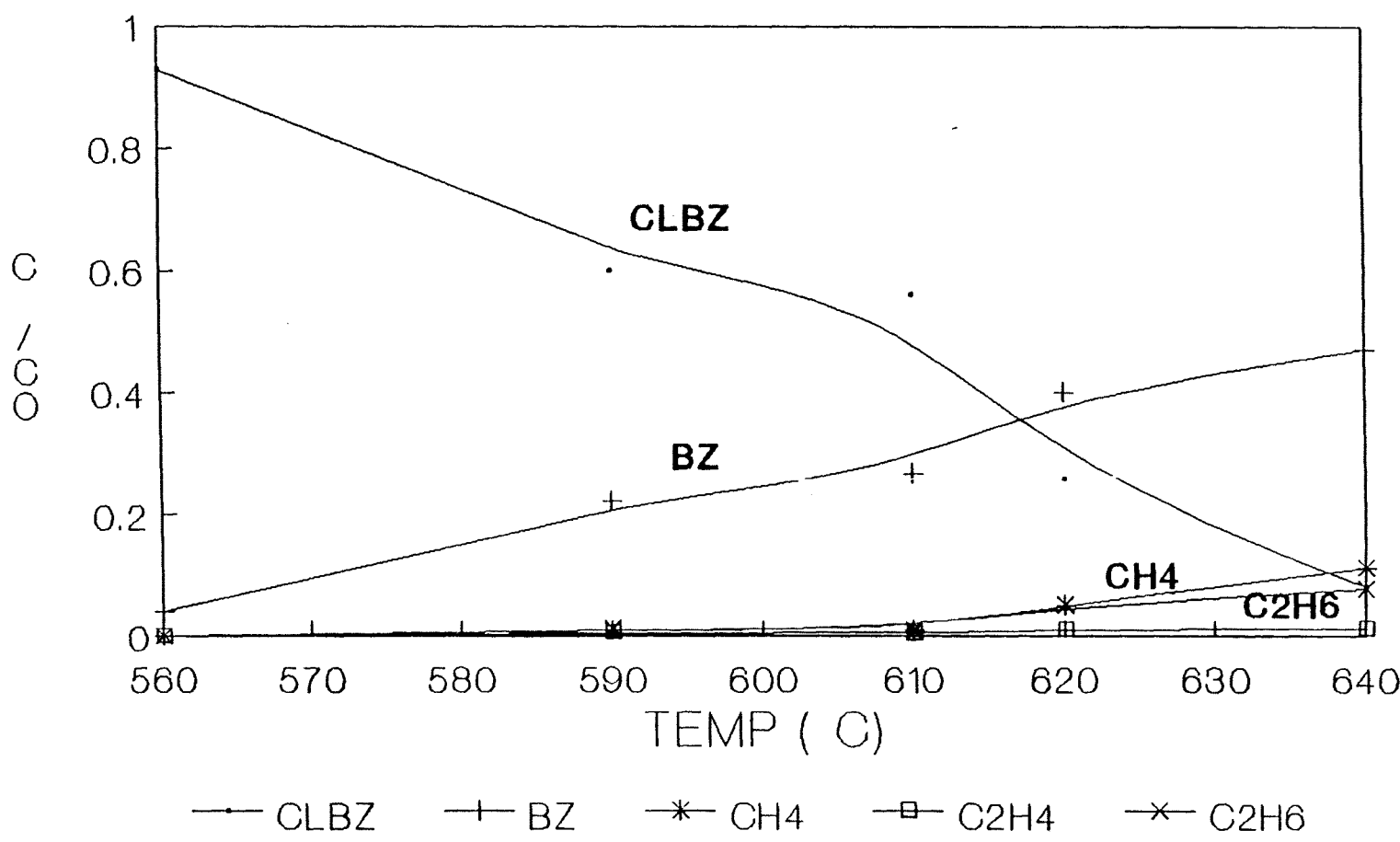


Figure 5.49

**REACTION OF CLBZ + H₂ + O₂ , 1 ATM
 RT = 1(SEC) , O₂/H₂: 3% .7. 16 mm**

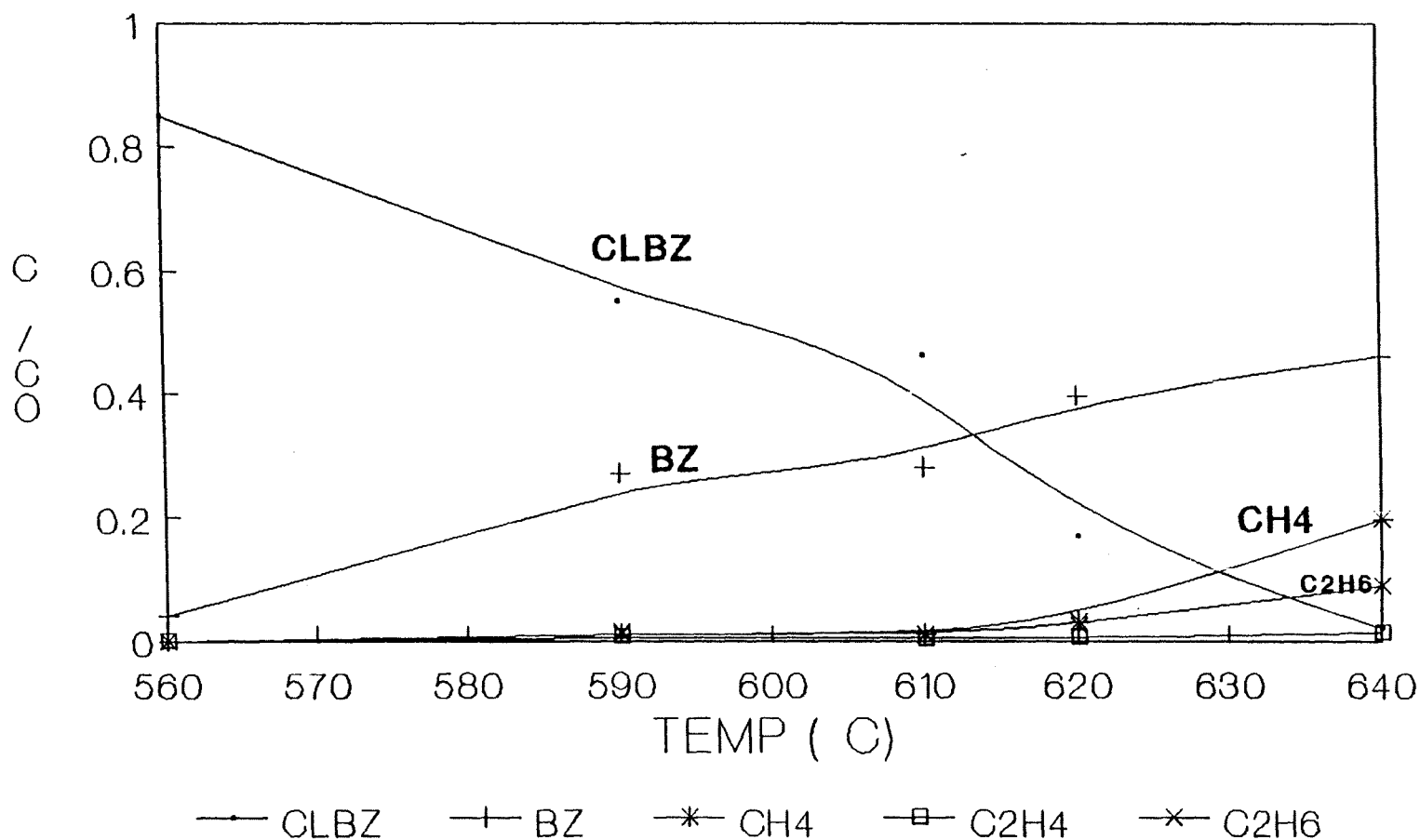


Figure 5, 50 ,

**REACTION OF CLBZ + H₂ + O₂ , 1ATM
 RT *a* 2 (SEC) , O₂/H₂: 1% , ID 7416 mm**

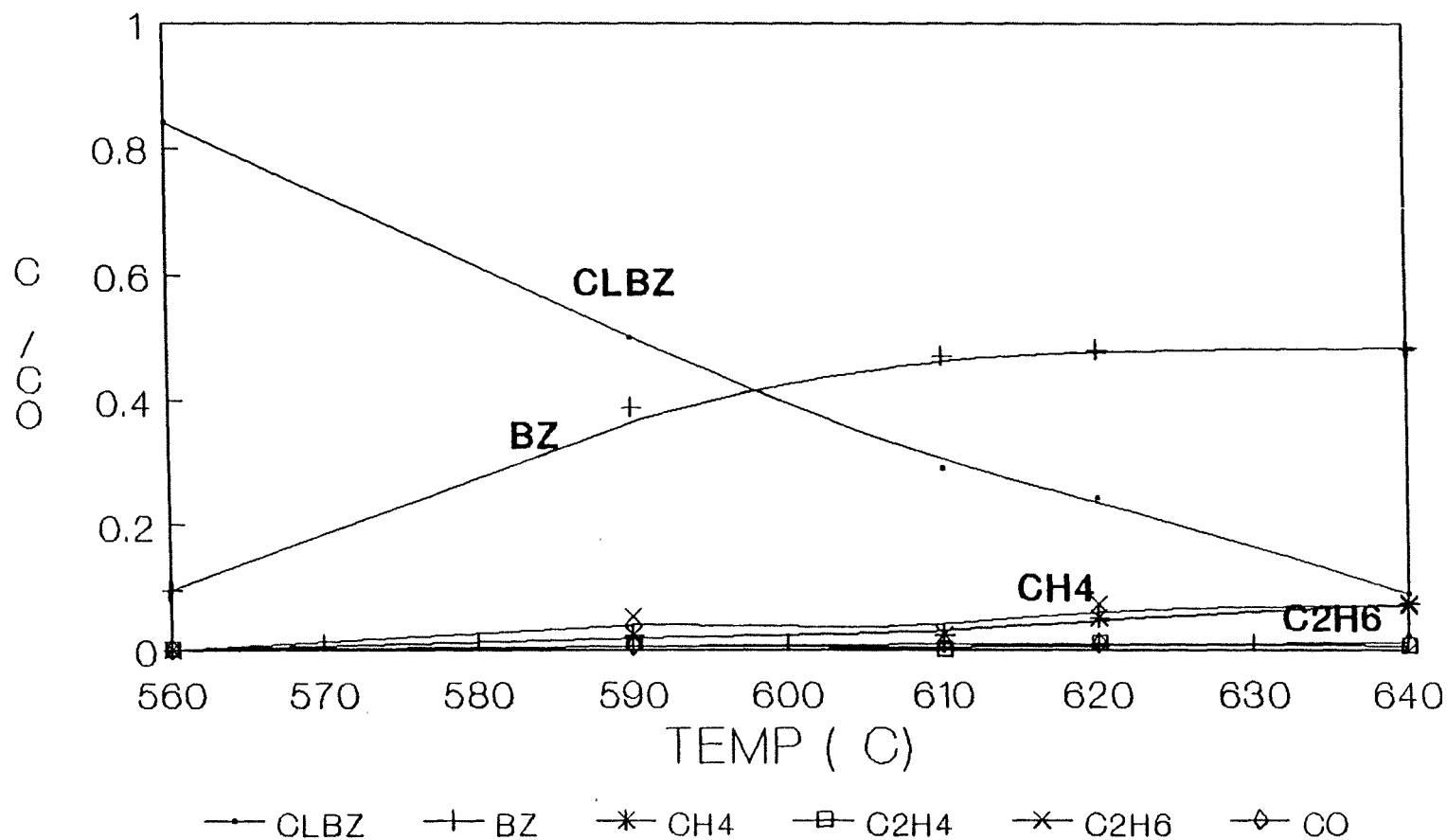


Figure 5.51

**REACTION OF CLBZ + H₂ + O₂ , 1 ATM
 RT = 2 (SEC) , O₂/H₂: 2% , ID if. 16 mm**

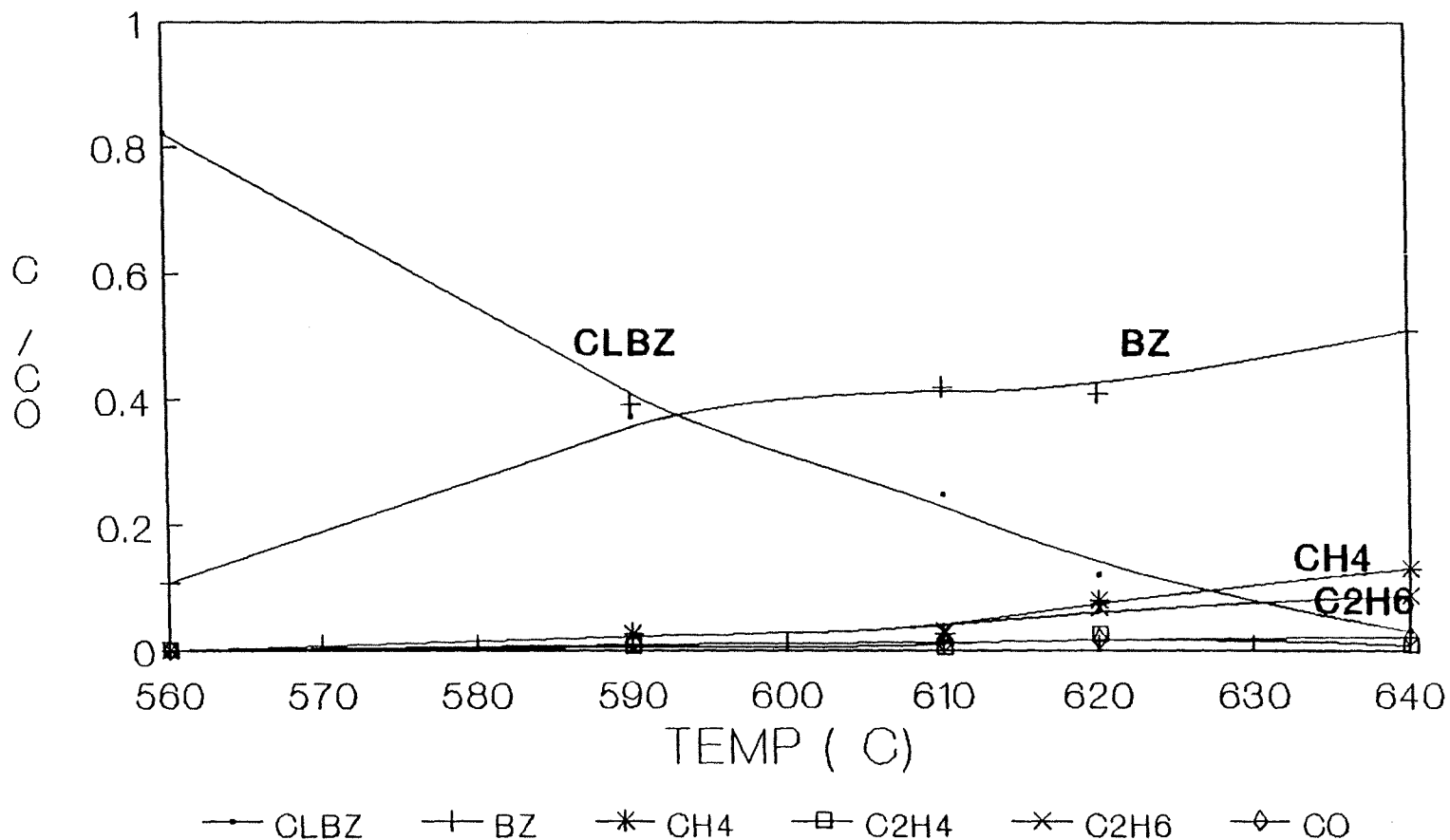


Figure 5.52

**REACTION OF CLBZ + H₂ + O₂, 1 ATM
 RT ra 2 (SEC), O₂/H₂: 3% , ID = 16 mm**

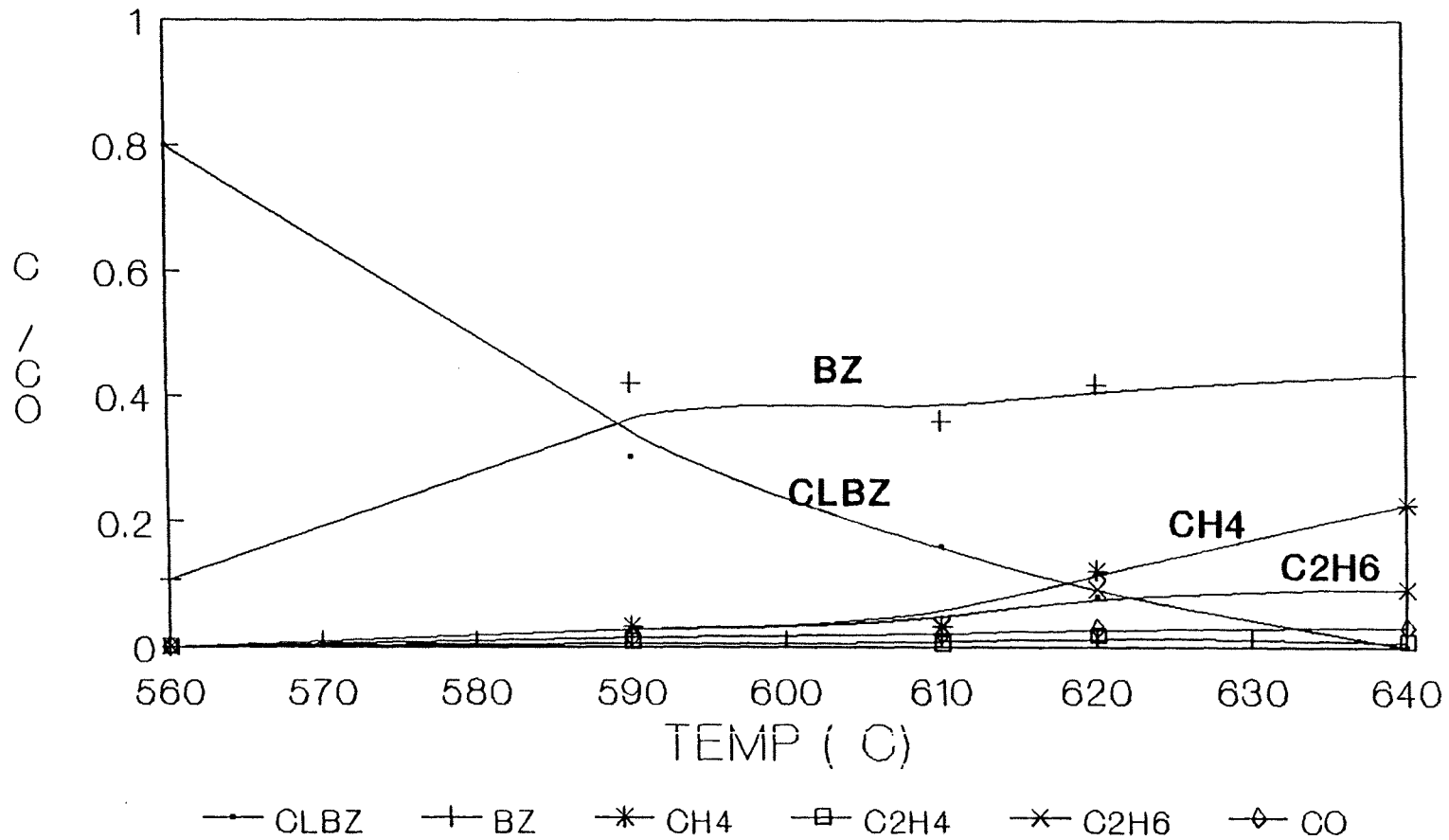


Figure 5.53

**REACTION OF CLBZ + H₂ + O₂ , 1 ATM
 RT = 2 (SEC) , O₂/H₂: 4% , ID = 16 mm**

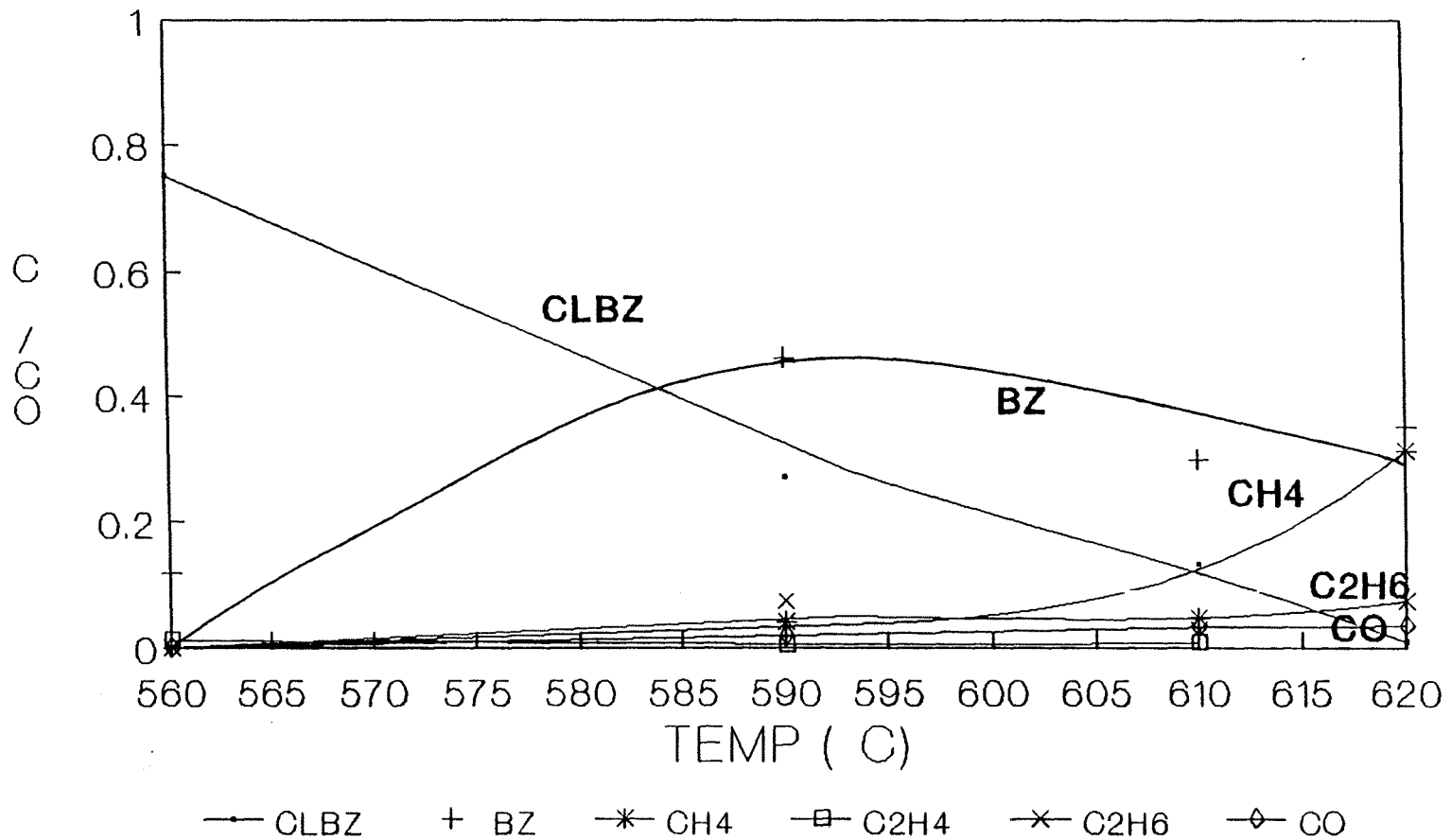


Figure 5.54

the initial C_6H_5Cl concentration. The products toluene and cyclopentadiene were detected by GC analysis using the capillary column. The concentration of toluene ($C_6H_5CH_3$) and cyclopentadiene (C_5H_6) rises from zero to an apparent steady state value of 2% to 3% the initial C_6H_5Cl concentration.

The products CO and CO₂ were examined with the carbosphere column and TCD analysis. The CO concentration was observed between 1% and 4%. The concentration of CO₂ was always very low (less than 1%), because there is little OH + CO reaction at these relatively low temperatures.

The HCl produced per mole of chlorobenzene is shown in Figures 5.20 through 5.22 as a function of temperature for reaction in the 10.5 mm ID reactor at a residence time of 1 second. The yield of HCl rises steadily as temperature is increased. The maximum yield is about 75% the initial C_6H_5Cl and occurs at a temperature of 630 °C. The uncertainties of analysis were due to several factors such as low chlorobenzene concentration, corrosion of metal connection tubing by HCl etc.

The tendency of aromatics to form solid carbon was studied. Tables 5.1 through 5.20 summarize the carbon material balance. Soot formation is believed to occur as the result of ring fusing reactions^{<21'9>}, with polycyclic

aromatic hydrocarbons and polyphenyls the expected products

C. Effect of the Amount of Oxygen

Several studies have previously been reported on the pyrolysis of chlorobenzene in different types of reactors, but they investigated the reaction temperature ranges which are all above 900°C (1173K) and did not involve O_2 reactions.

As shown in Figures 5.55 through 5.60, there are very significant effects by the presence of oxygen on the decomposition of $\text{C}_6\text{H}_5\text{Cl}$ in our experiments. The oxygen ratio is an important factor on the formation of CH_4 . Figures 5.61 and 5.62, show that both CH_4 and C_2H_6 increase as oxygen increases. And figures 5.63 and 5.64 show benzene increases as the oxygen ratio increases. This is through the reaction step from $\text{H} + \text{C}_6\text{H}_5\text{Cl}$ to benzene + Cl where H atom is from $\text{H}_2 + \text{O}_2$ to $\text{HO}_2 + \text{H}$.

Lower concentration of oxygen results in slower decay of $\text{C}_6\text{H}_5\text{Cl}$. A faster decay of chlorobenzene occurs at lower temperature when more oxygen is in the mixtures. Higher ratios of O_2 to H_2 allow lower the temperatures for the formation of CO and CO_2 . As temperature and O_2 concentration increase, the concentration of CO and CO_2 also increase.

DECAY CURVE OF CLBZ + H2 + O2
660(C) ,ID= 4 mm O2/H2 :1%-5%

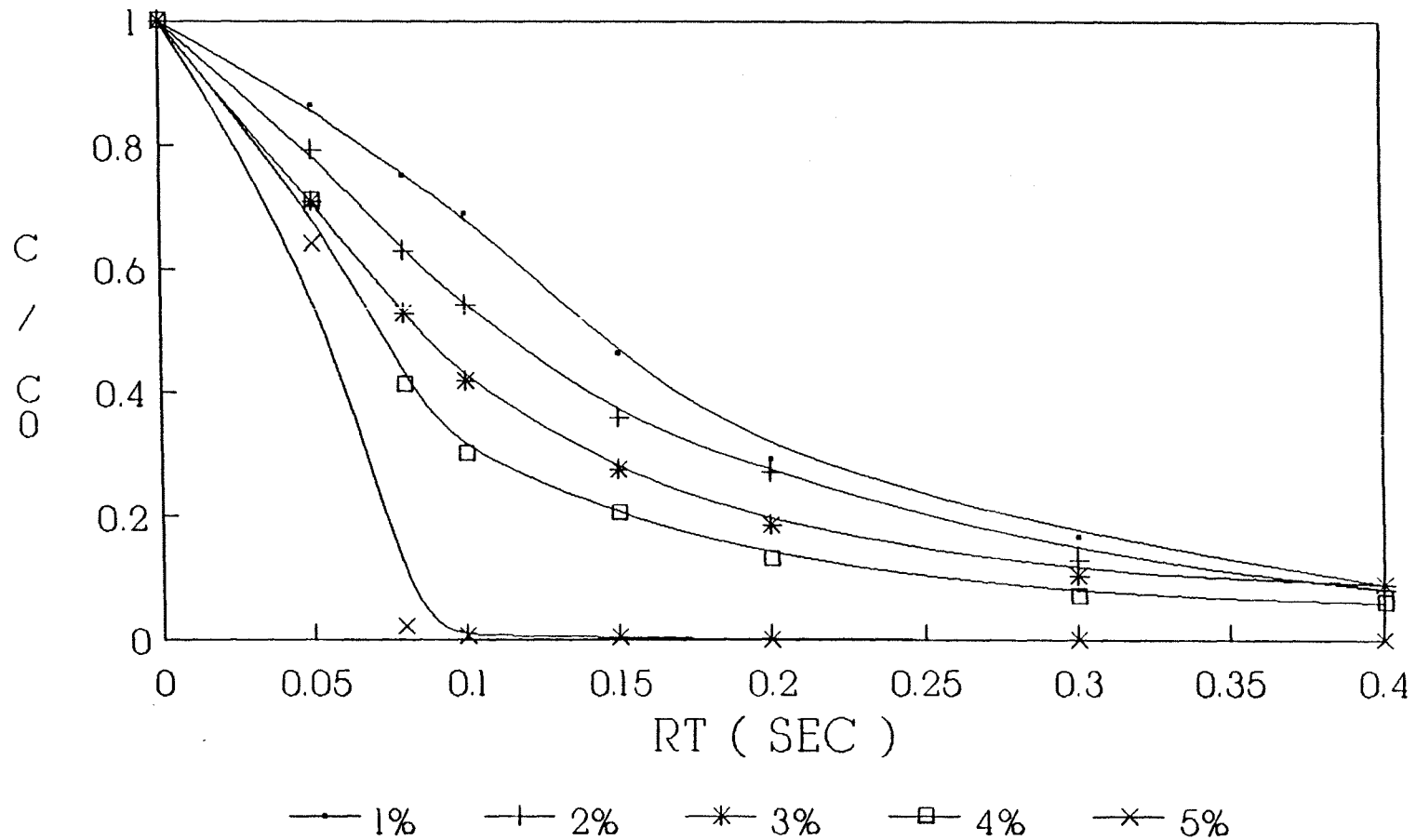


Figure 5.55

DECAY CURVE OF CLBZ + H2 + O2
650(C) , D= 4 mm , O2/H2 :1%-5%

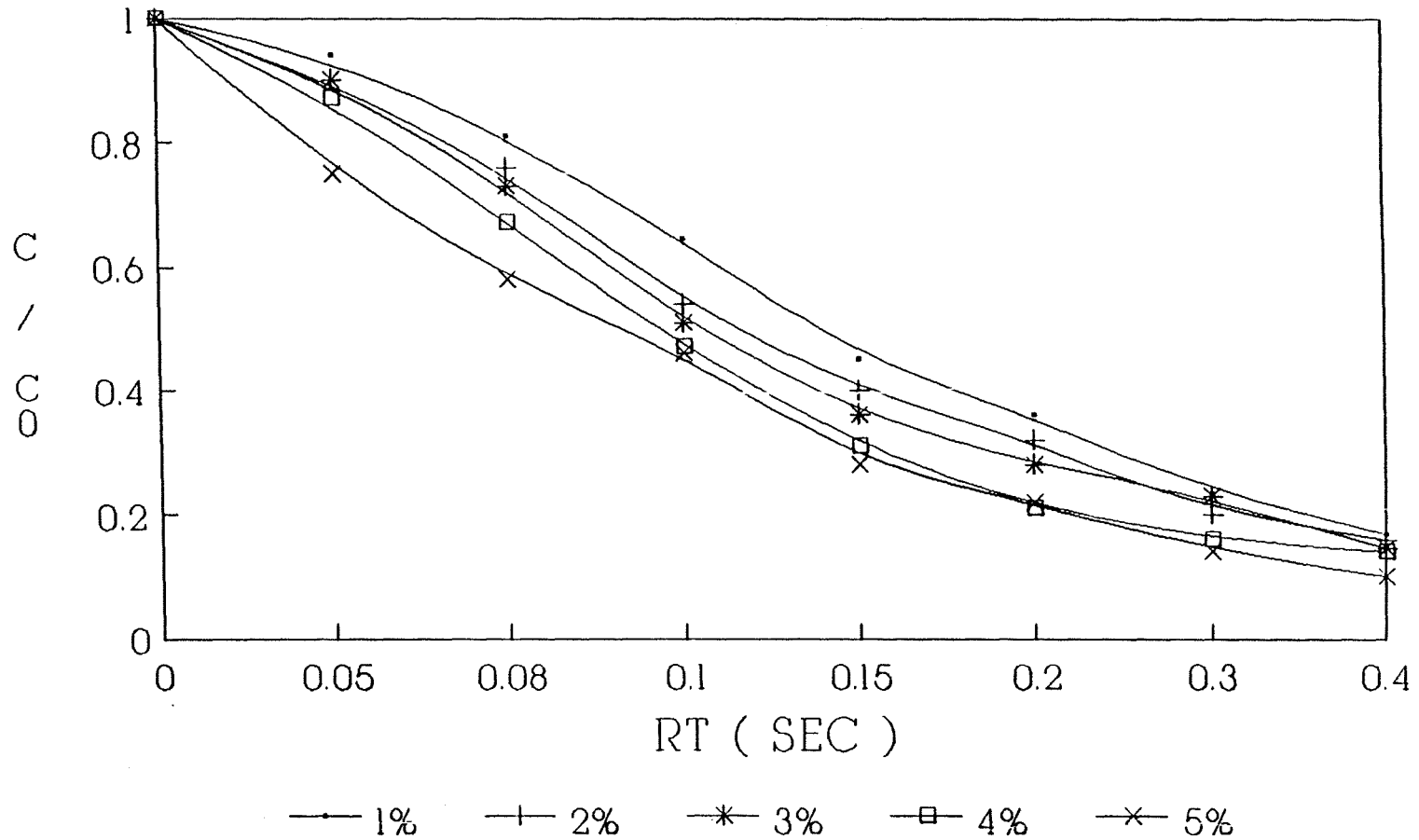


Figure 5.56

DECAY CURVE OF CLBZ + H₂ + O₂ 590(C) Dr; 16 MM O₂/H₂ :1%- 5%

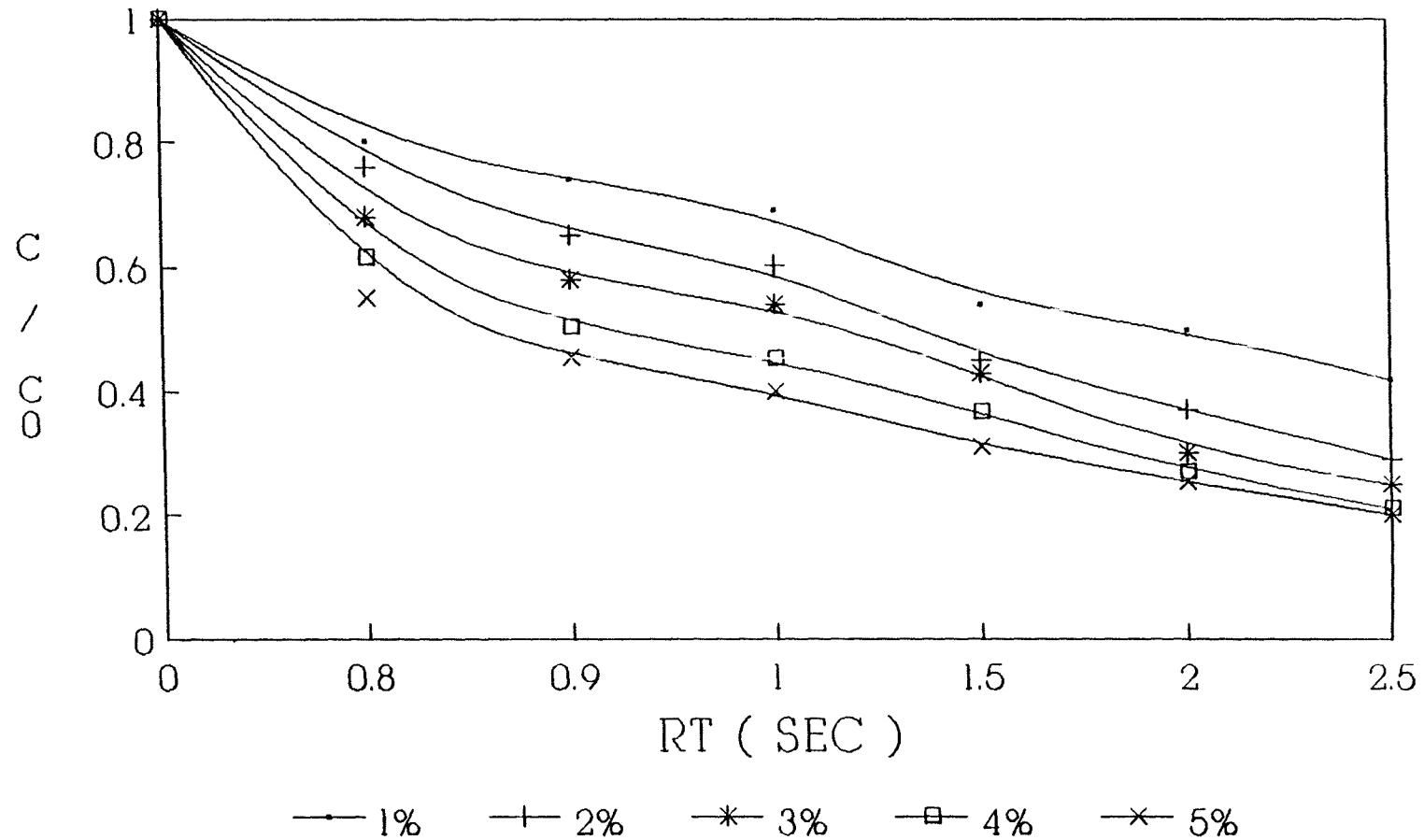


Figure 5.57

DECAY CURVE OF CLBZ + H2 + O2
610(C), ID=16 this O2/H2 :1%-5%

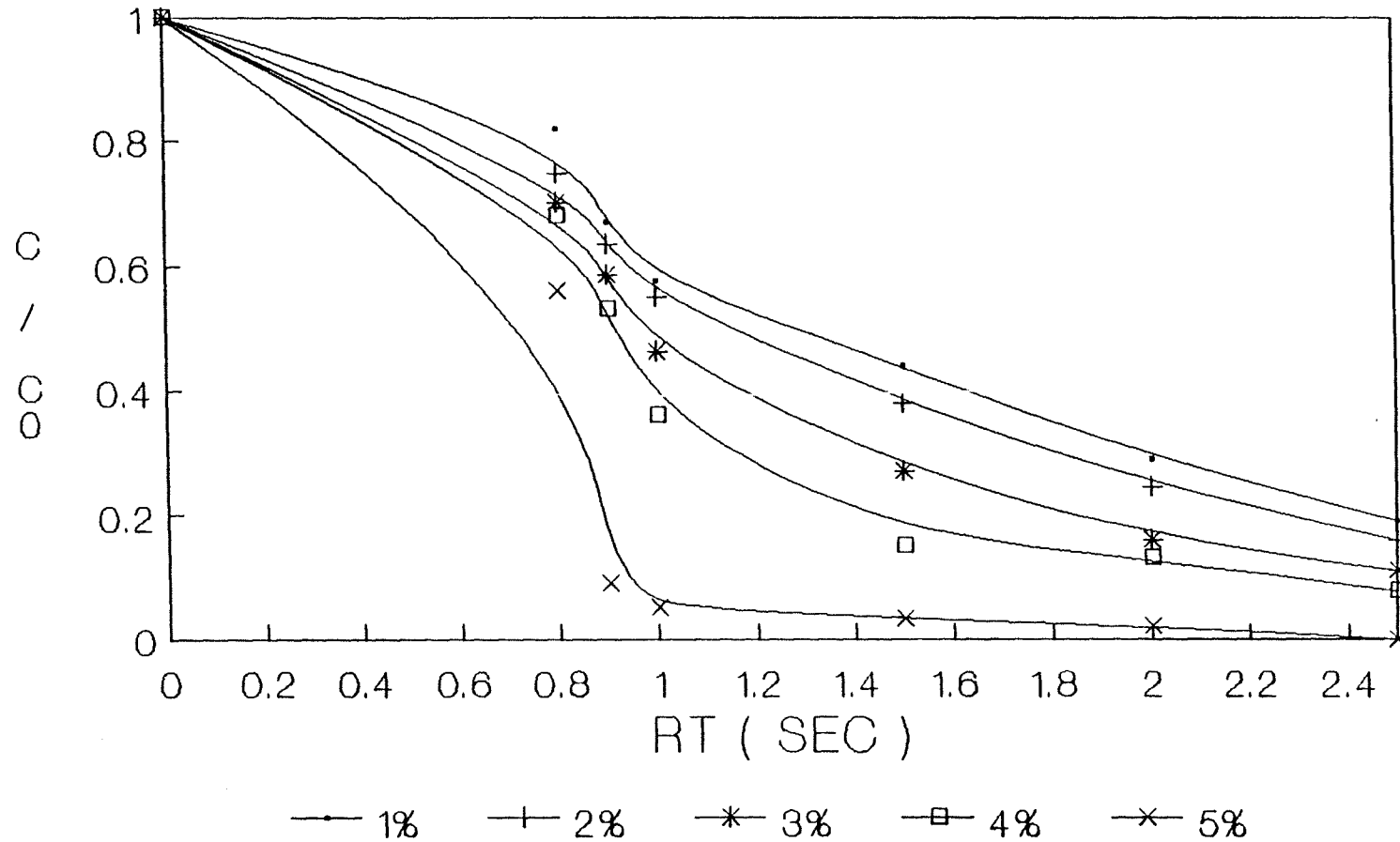


Figure 5.58

DECAY CURVE OF CLBZ + H2 + O2
620(C) , ID r= 16 mm , O2/H2 :1°/0-4%

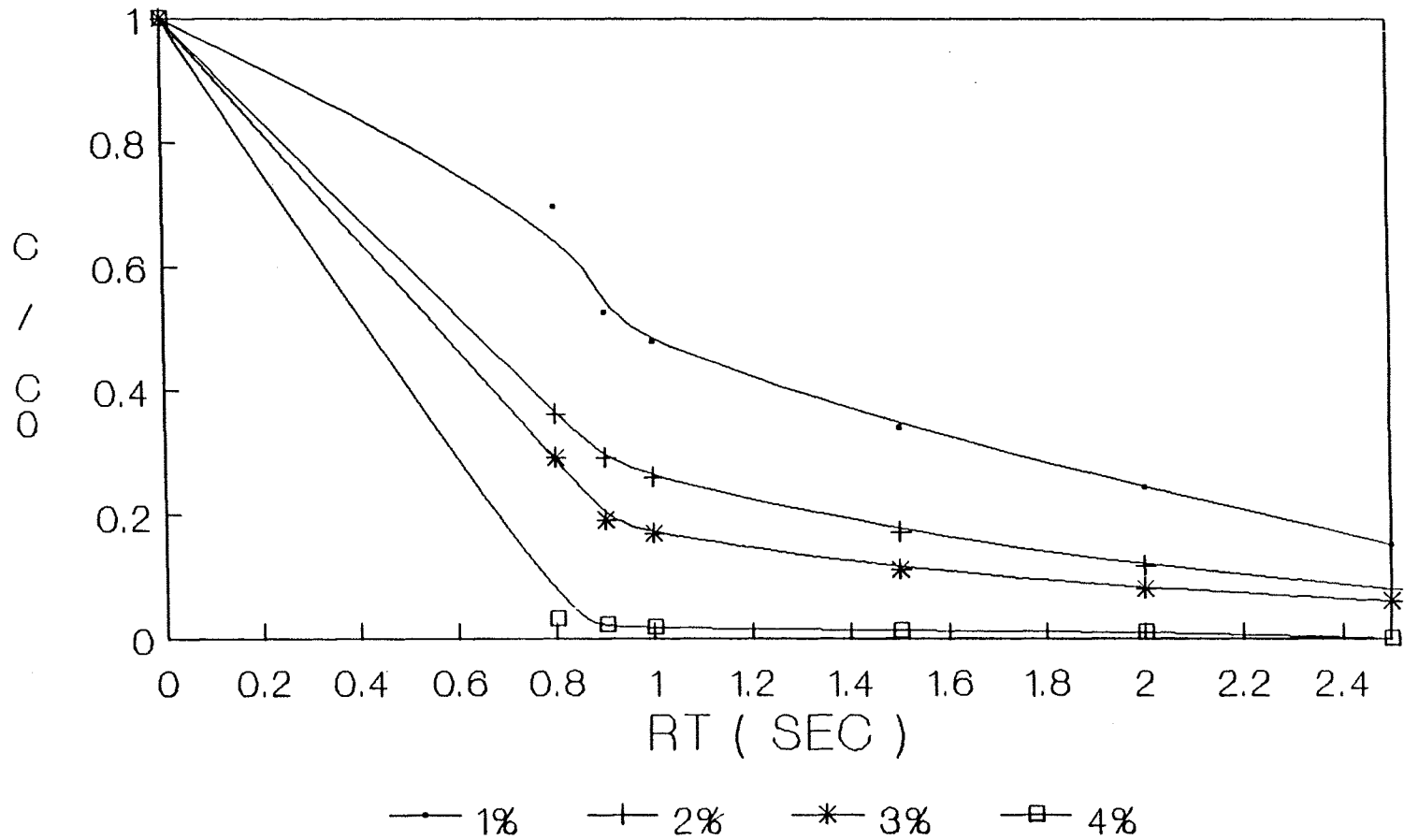


Figure 5:59,

DECAY CURVE OF CLBZ + H2 + O2 640(C), ID= 16 mm , O2/H2 :1%-3%

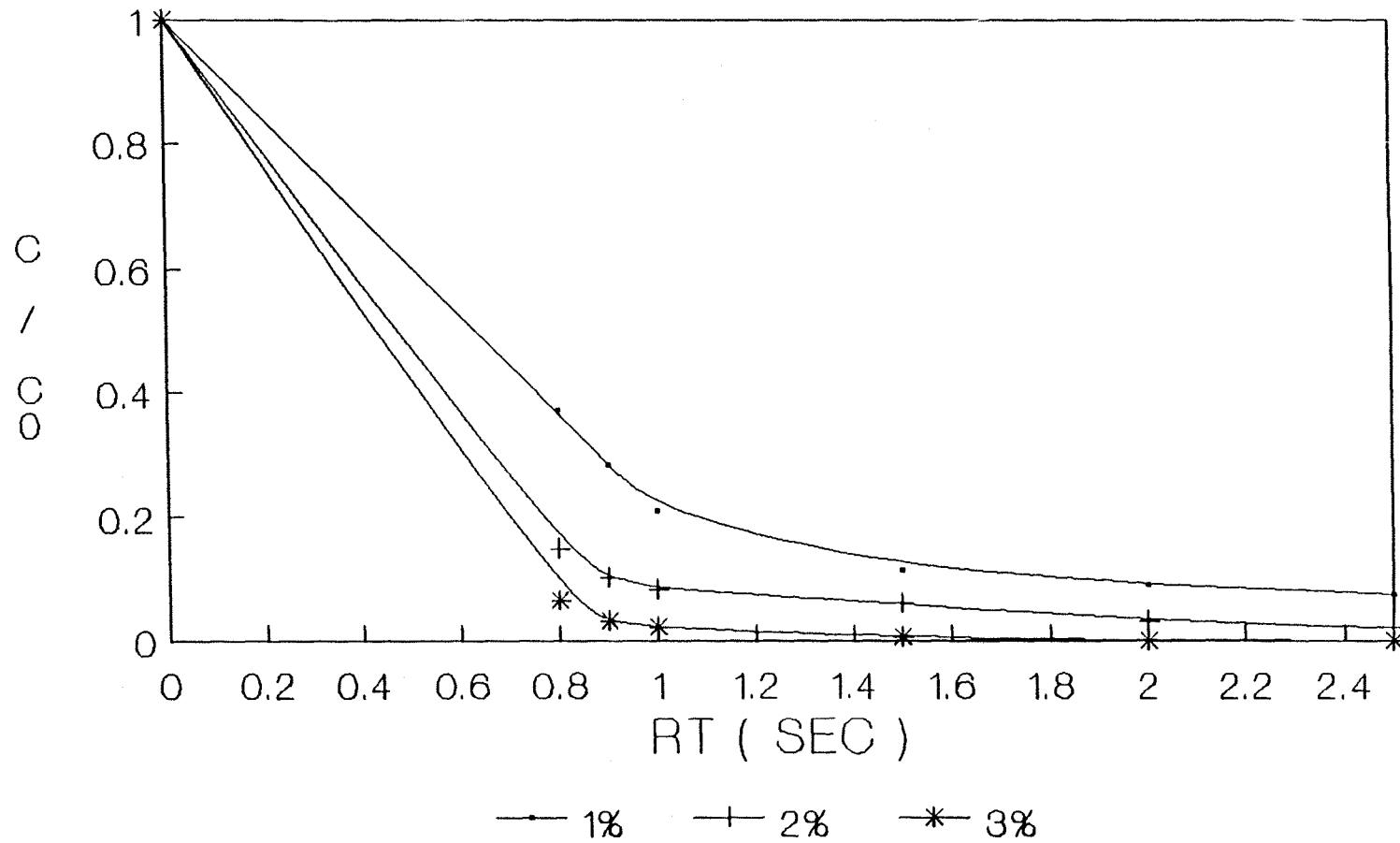
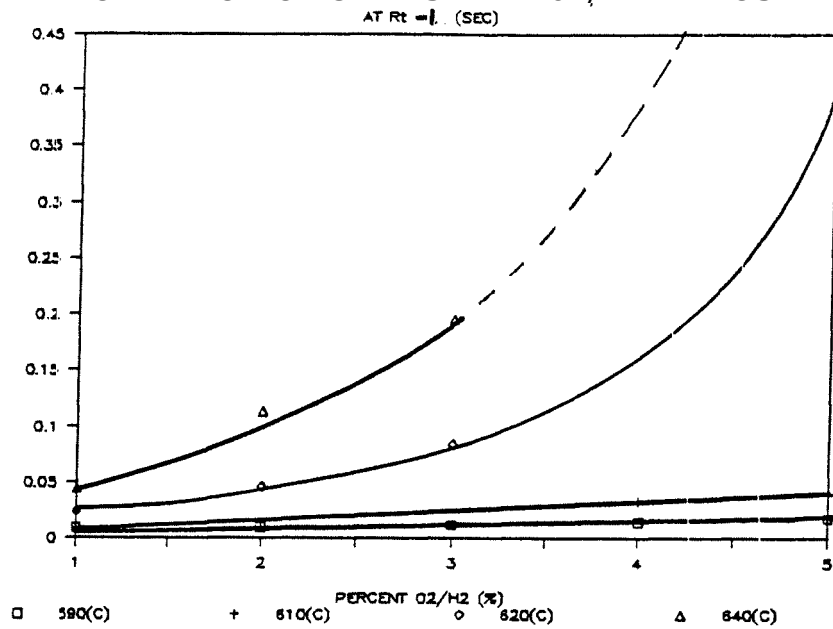


Figure 5.60

FORMATION OF CH₄ VS DIFF. O₂/H₂ RATIOS



FORMATION OF CH₄ VS DIFF. O₂/H₂ RATIOS

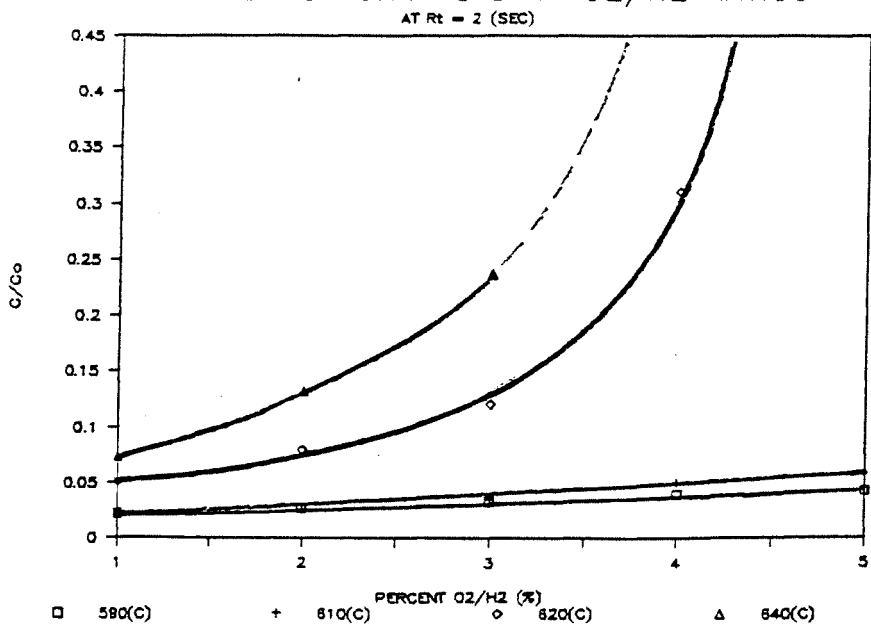
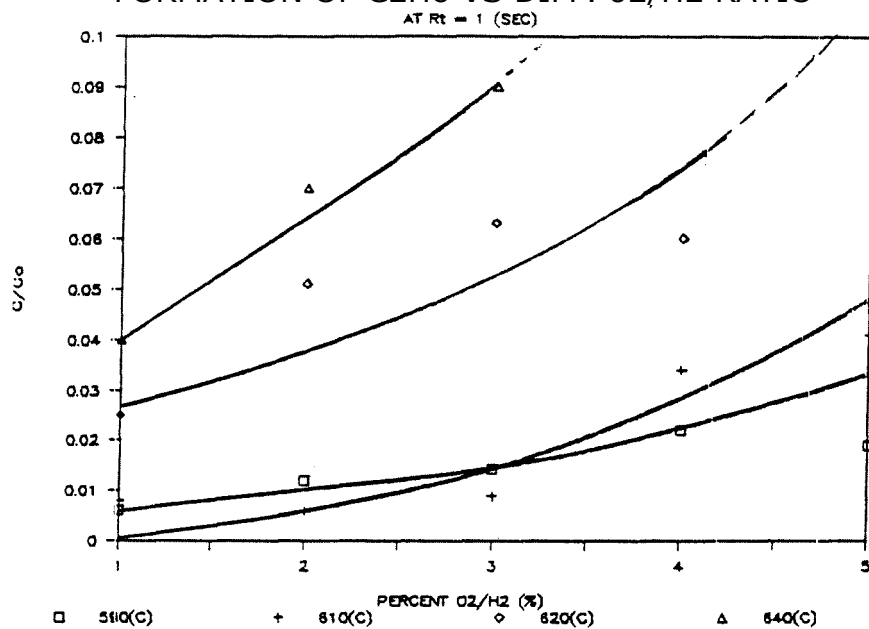


Figure 5.61

FORMATION OF C₂H₆ VS DIFF. O₂/H₂ RATIO



FORMATION OF C₂H₆ VS DIFF. O₂/H₂ RATIO

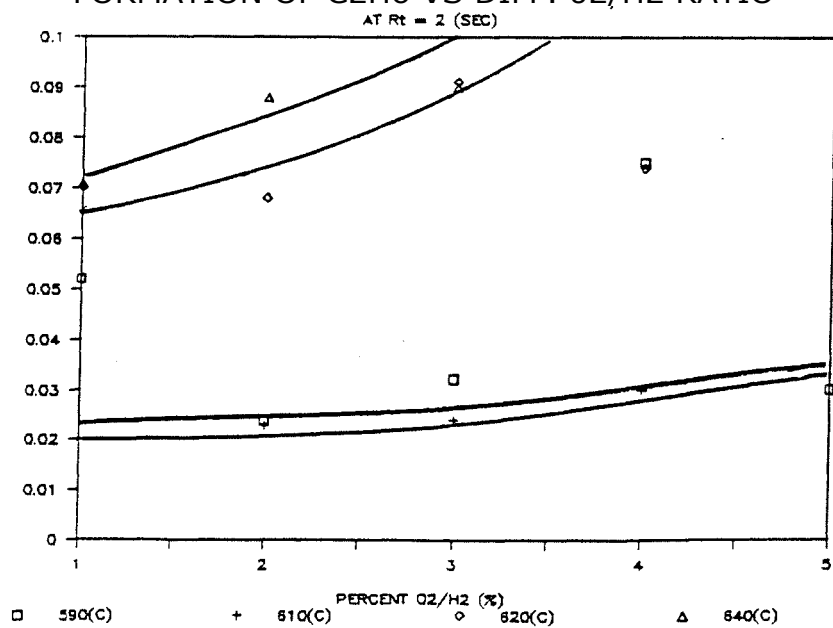


Figure 5.62

**BENZENE PRODUCT, M SIZE (ID ■ 10.5 mm)
TEMP - 625 (C), DIFF. O2/H2 RATIOS**

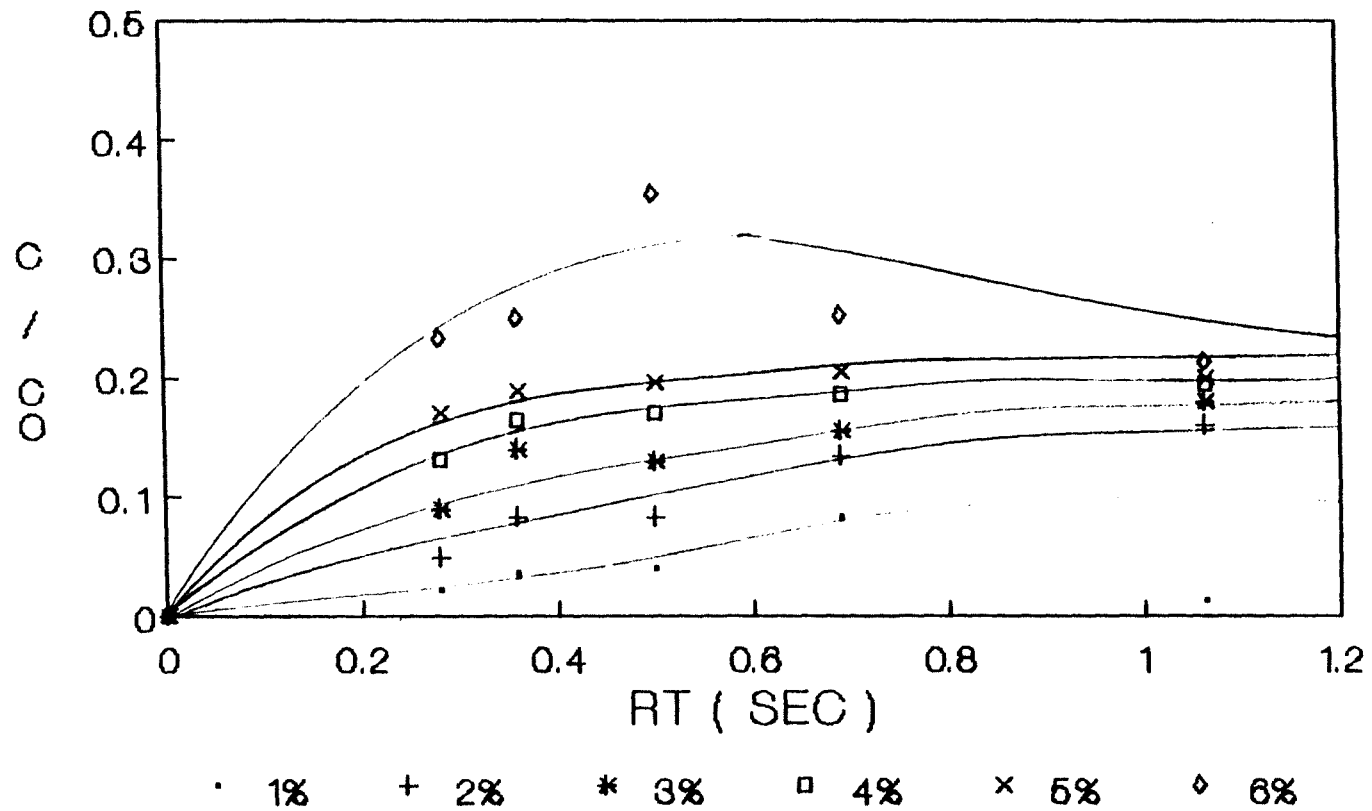


Figure 5.63

BENZENE PRODUCT; M SIZE OD= 10.5 mm)
TEMP ^{al} 615 (C), DIFF. O₂/H₂ RATIOS

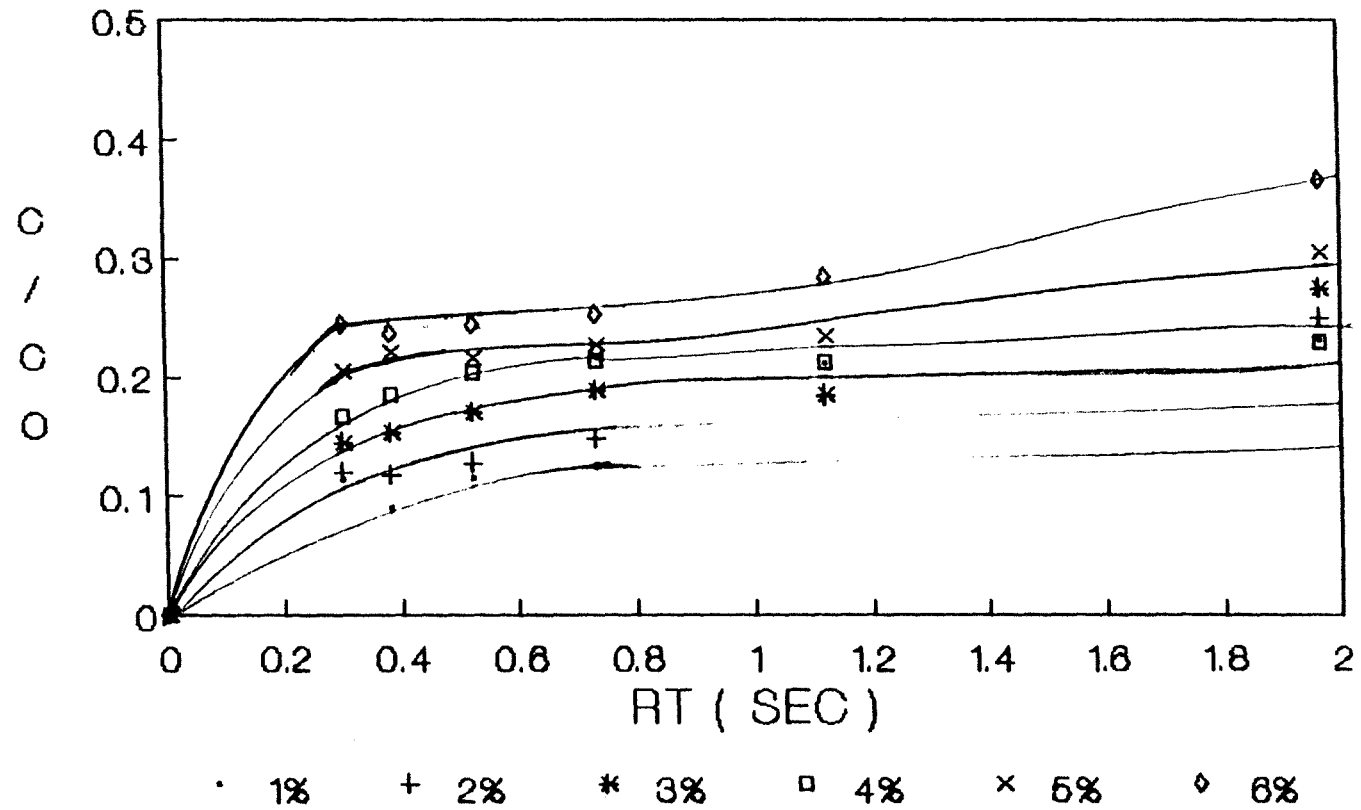


Figure 5.64

D. Comparison of Chlorobenzene Reaction of Previous Studies

Earlier studies by Cullis and Manton^{<11>} on pyrolysis of chlorobenzene in atmosphere of 770 and 850 °C indicated that aromatic ring rupture did not occur significantly in experiments below 800 °C.

Ritter studied the reaction of dilute mixture of chlorobenzene in hydrogen and helium atmospheres. It worth comparing two studies which are the decomposition of chlorobenzene in excess hydrogen with oxygen (this work) and without oxygen (Ritter). The major products observed for pyrolysis in excess hydrogen were benzene, HCl, and C(s), where the reaction temperatures range from 800 - 1000 °C. In this study, we found that the major products were also benzene, and HCl but we also observed very significant CH₄ (up to 50%) and C₂H₆. The minor products observed were toluene, cyclopentadiene, C₂H₂, C₂H₄, CO₂ and CO. Additional trace products were dichlorobenzene, naphthalene, chlorobiphenyl, and several PAH's^{<9>}. Relatively higher levels of CH₄ are also observed in the study of benzene oxidation by Baldwin, Scott, and Walker^{<41>}.

We found that the products of formation were different in the two studies. The input oxygen with H₂ present is a

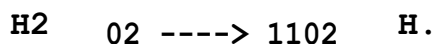
key factor the oxidation of chlorobenzene.

E. Kinetic Model and Calculations

Energized Complex/QRRK theory as presented by Westmoreland and Dean^{<23122s>} used for modeling of radical addition and combination reactions. This calculation has been modified by Ritter and Bozzelli^{<23>} to use gamma function. The **QRRK** computer code was used to determine the temperature and pressure energy dependent rate constants for all channels. The program incorporates **QRRK** theory to calculate rate constants as function of temperature and pressure. It is important in determination of the mechanism and choice of the paths (accurate product prediction from the activated complex).

A **QRRK** analysis of the chemically activated system, using generic estimates or literature values for high pressure rate constants and species thermodynamic properties for the enthalpies of reaction, yields apparent rate constants at varied temperatures and pressures. The results from the calculations input rate parameters used in these calculations are summarized in APPENDIX [A] Tables 1 through 6. The calculations were performed for each of six pressures between 0.76 torr and 7600 torr and over a temperature range of 300 to 1700K.

The initiation reaction occurring is followed:



This reaction provides a very reactive H atom in our reaction system. Hydrogen atom addition to the Cl-Carbon in chlorobenzene (ipso position) forms an energized complex. The energized adduct dissociates to benzene + Cl, which is a low energy exit channel. This displacement reaction is believed to be a major pathway to the hydrodechlorination of chlorobenzene to form benzene and HCl. Figure 5.65 shows an energy level diagram for the displacement.



Hydrogen atom will add to benzene to form cyclohexadienyl radical (CHD.) as reported by E. Ritter^{<9>} and W. Tsang^{<23>}. This CHD. complex may unimolecularly isomerize through a bicyclo intermediate to a cyclopentadiene methyl radical (CpdMe.), which can undergo a hydrogen shift to a stabilized methyl cyclopentadienyl radical (MeCpd.) or beta scission to fulvene + H. The MeCpd. complex can then react with H₂ to form H. + MeCpd, the MeCpd can then decompose to cyclopentadiene radical (C₅H₅·) + CH₃. The C₅H₅· radical will react with H₂ to form stable cyclopentadiene. The cyclopentadiene product has been observed in our GC analysis. The third possible isomerization is ring opening

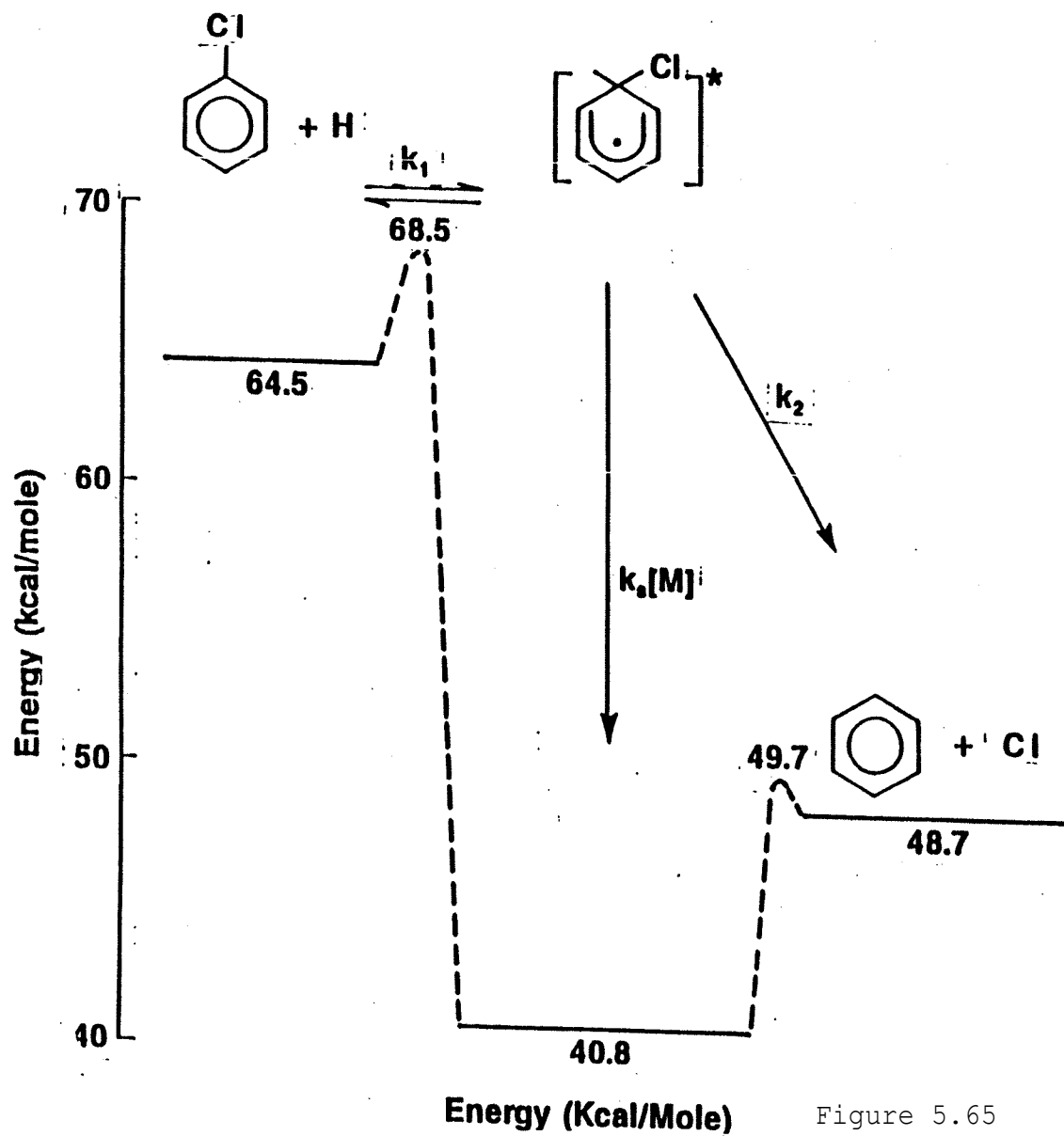
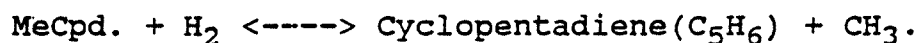
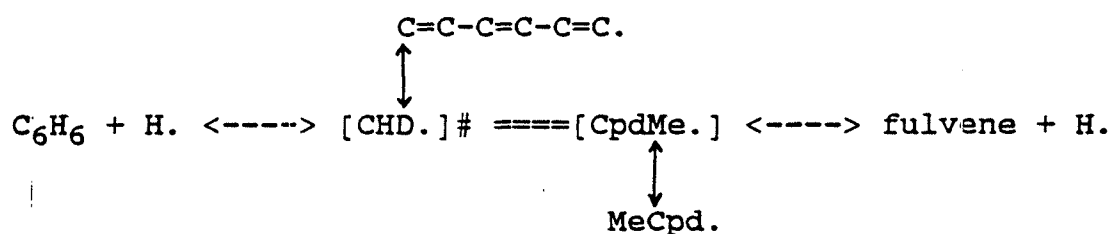


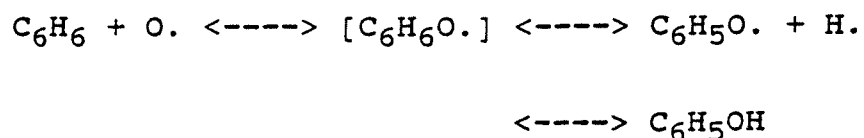
Figure 5.65

(Permitted by J. W. Bozzelli and Ritter⁹)

reaction to form linear C₆H₇. This channel is not very significant except temperature near 1500K, because of its very high endothermicity. Figures 5.66 and 5.67 show on energy level diagram for the reactions below.



The oxidation of aromatic compounds (Methyl Phenyl Ether) was studied by C. Y. Lin and M. C. Lin^{<25>}. They had indicated that oxidation of benzene generated C₆H₅OH which is the most important early stage oxidation product. In view of its known weak O-H bond, the C₆H₅OH generated in the early oxidation process is expected to readily produce C₆H₅O (phenoxy). Phenoxy radical is a very important intermediate compound in aromatic oxidation systems. The C₆H₅O. radical primarily undergoes the unimolecular decomposition reaction. The Dissociation analysis is shown in APPENDIX [A] Table 2. The evidence of CO product can explain the path way of phenoxy decomposition.



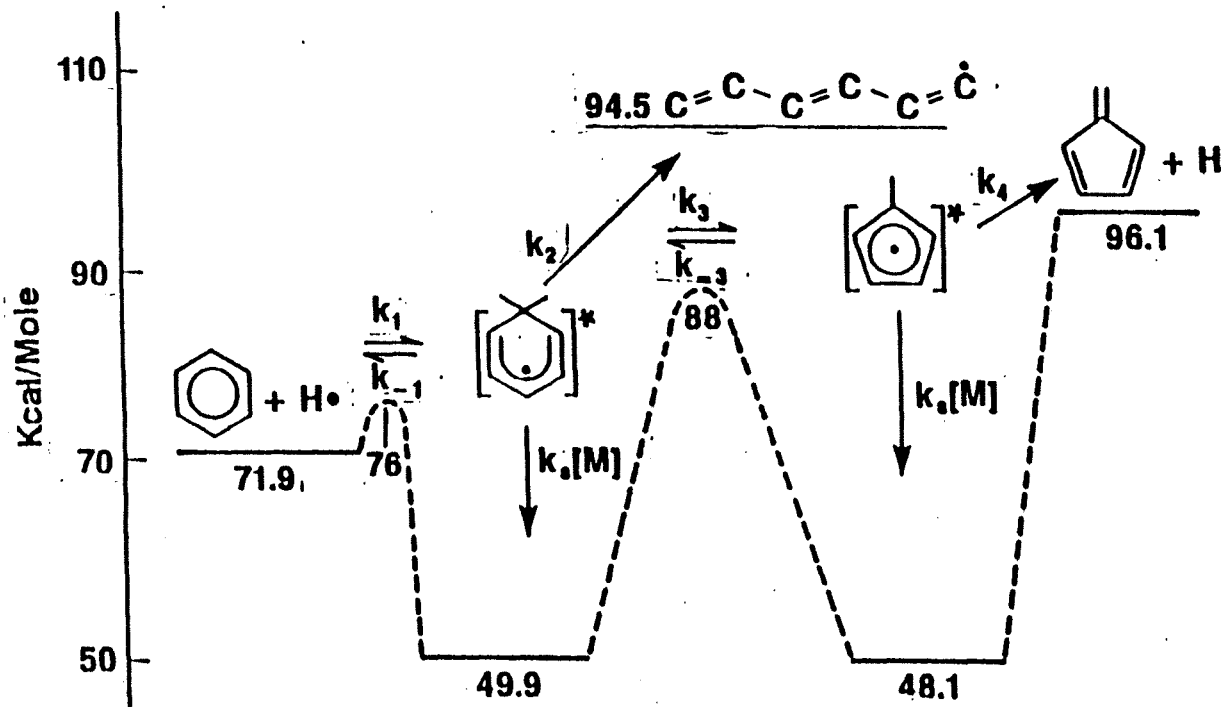


Figure 5.66

(Permitted by J. W. Bozzelli and Ritter⁹)

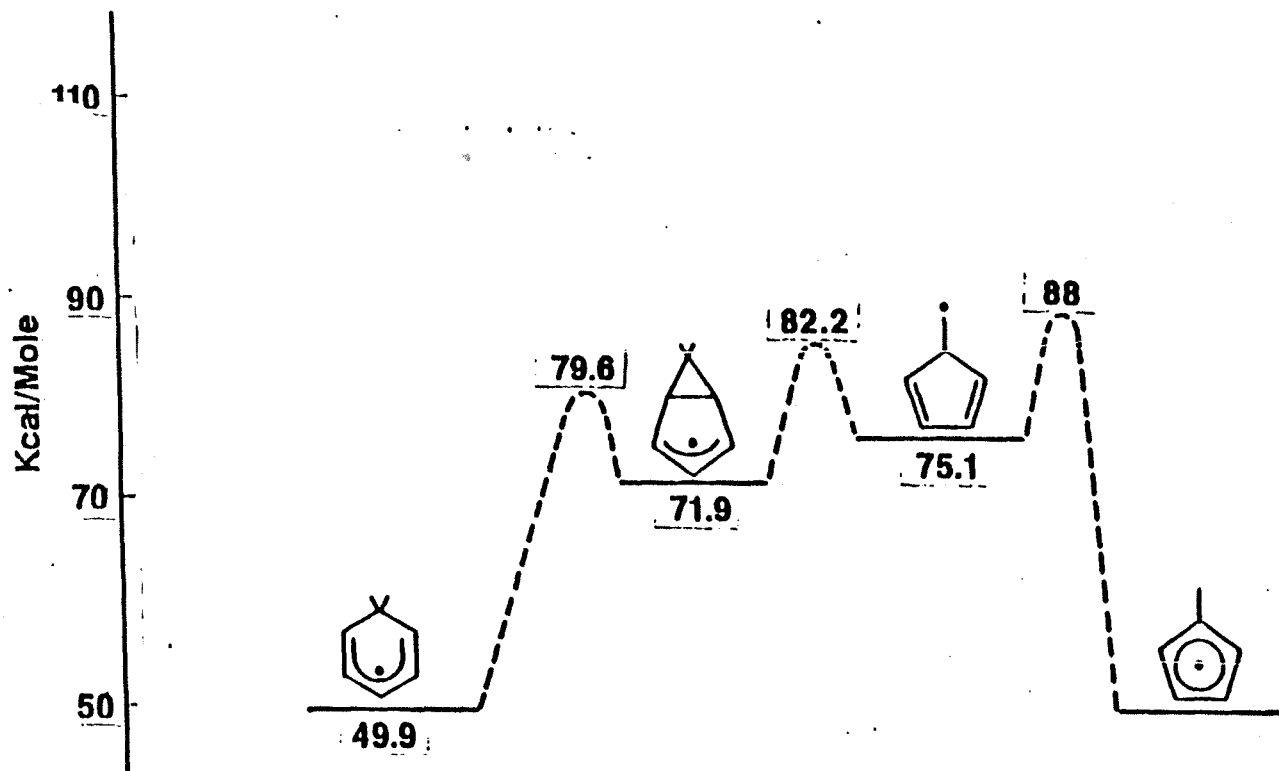
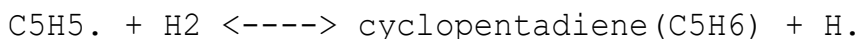
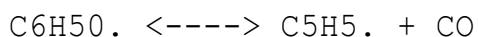
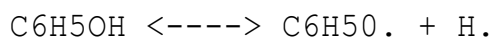
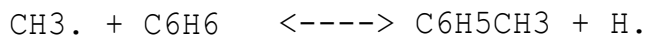


Figure 5.67

(Permitted by J. W. Bozzelli and Ritter⁹)



The toluene product may be formed by two possible reaction schemes. One, is CH₃ radical addition to chlorobenzene at ipso position to form toluene + Cl. Two, CH₃ addition to benzene to generate an activated complex MeCHD. Since the C-H bond in MeCHD. is stronger by about 10 Kcal than Cb-CH₃ bond, the methyl cyclohexadienyl radical will primarily dissociate back to CH₃. + C₆H₆ reactants in our system, but a small fraction (equilibrium concentration of toluene will be formed. The reaction of methyl radical with chlorobenzene was estimated to form toluene 10 times faster than for addition of methyl to benzene⁹. Figure 5.68 shows energy level diagram for the reactions below.



We have developed a detailed reaction mechanism for combustion of chlorobenzene using many the of reactions in the chlorobenzene pyrolysis study by E. Ritter as a starting point for the pyrolysis products. Elementary reaction rate parameters for abstraction reactions are based upon litera-

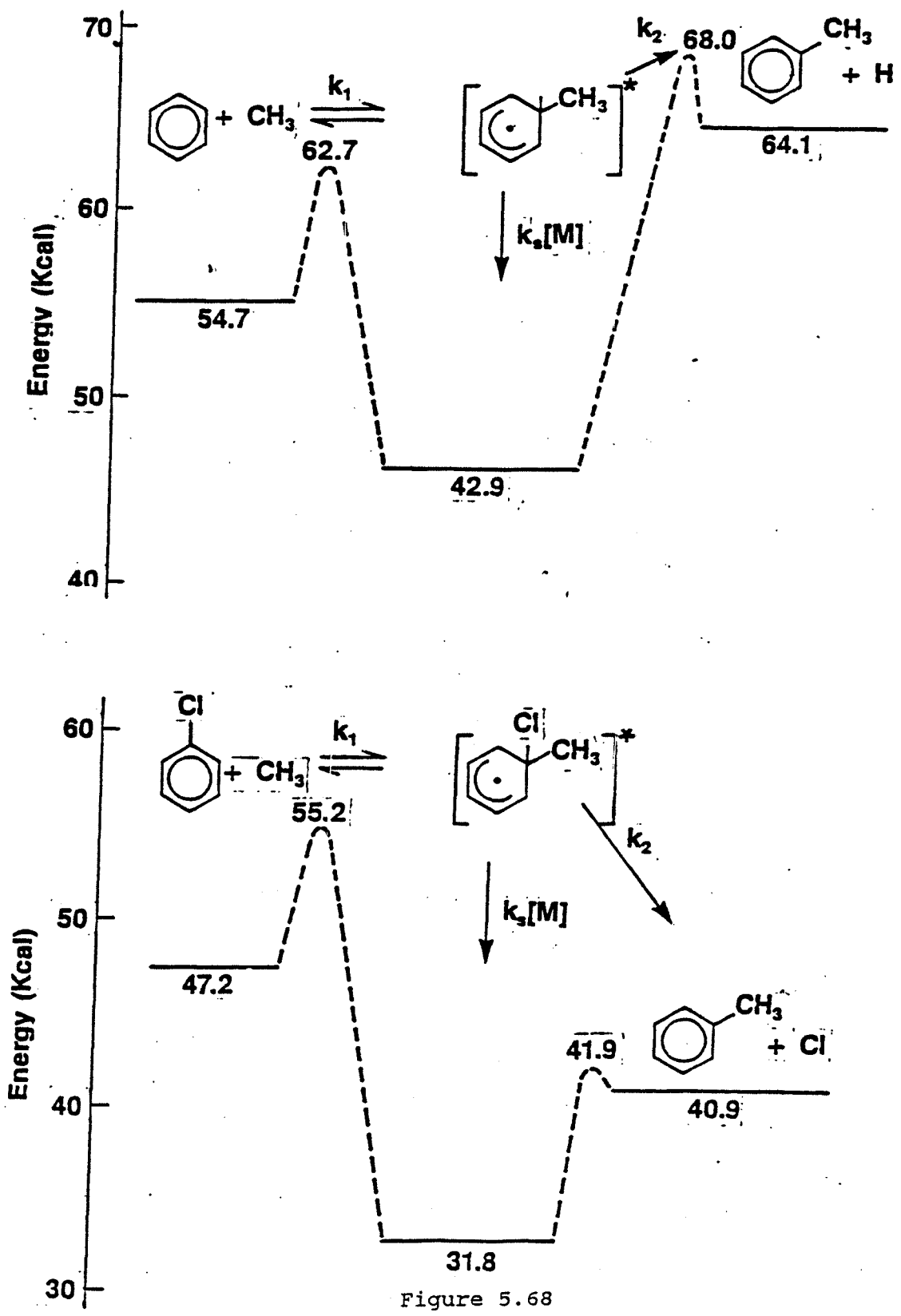


Figure 5.68

(Permitted by J. W. Bozzelli and Ritter⁹)

tune comparisons, thermodynamic estimation, and Transition State Theory methods of Benson²⁶. The QRRK calculations were used to estimate apparent rate parameters for addition, recombination, and elementary dissociation reactions.

Detailed reaction kinetic mechanism were developed to describe the systems of reactions studied. A mechanism composed of 84 elementary reactions, which appears in Table 5.21,, was found to fit experimental results.

Experimental data are compared with model predictions in Figures 5.69 for chlorobenzene decomposition at 620°C in different oxygen ratio sets. Figure 5.70 shows the experimental decay of chlorobenzene and the calculation data vs temperature for different oxygen ratios. As seen in Figure 5.71, predictions for decomposition of chlorobenzene between 560°C and 640°C (O₂/H₂: 1%) match experiment well. Figures 5.72 and 5.73 demonstrate the difference between experimental and calculated concentration of chlorobenzene and benzene products versus temperature at different oxygen ratio. Benzene is significantly over predicted by the calculation in cases of 1% and 2% oxygen ratios.

Figures 5.74 and 5.75 show the difference seen between calculated and experimental values for reagent and HCl vs temperature. Again HCl is over predicted for 1% and 2% oxygen ratio cases. At higher conversions, over-prediction

CLBZ +H2 +O2 ---)PRODUCT,AT 620(C)
 MODEL and EXPT, O2/H2 : 1% - 3%

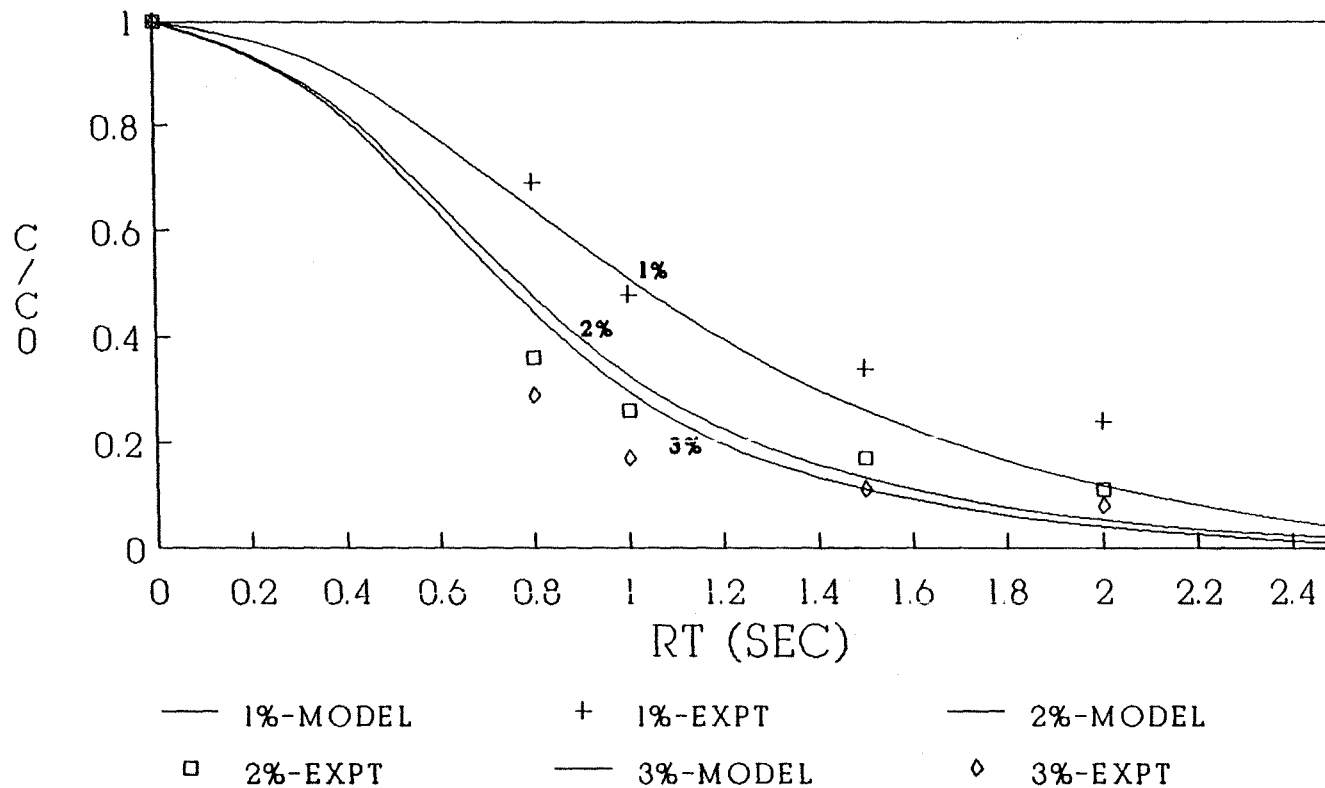


Figure 5.69

DECAY OF C6H5CL MODEL AND EXPT. VS TEMP

O2/H2 : 1% - 2%

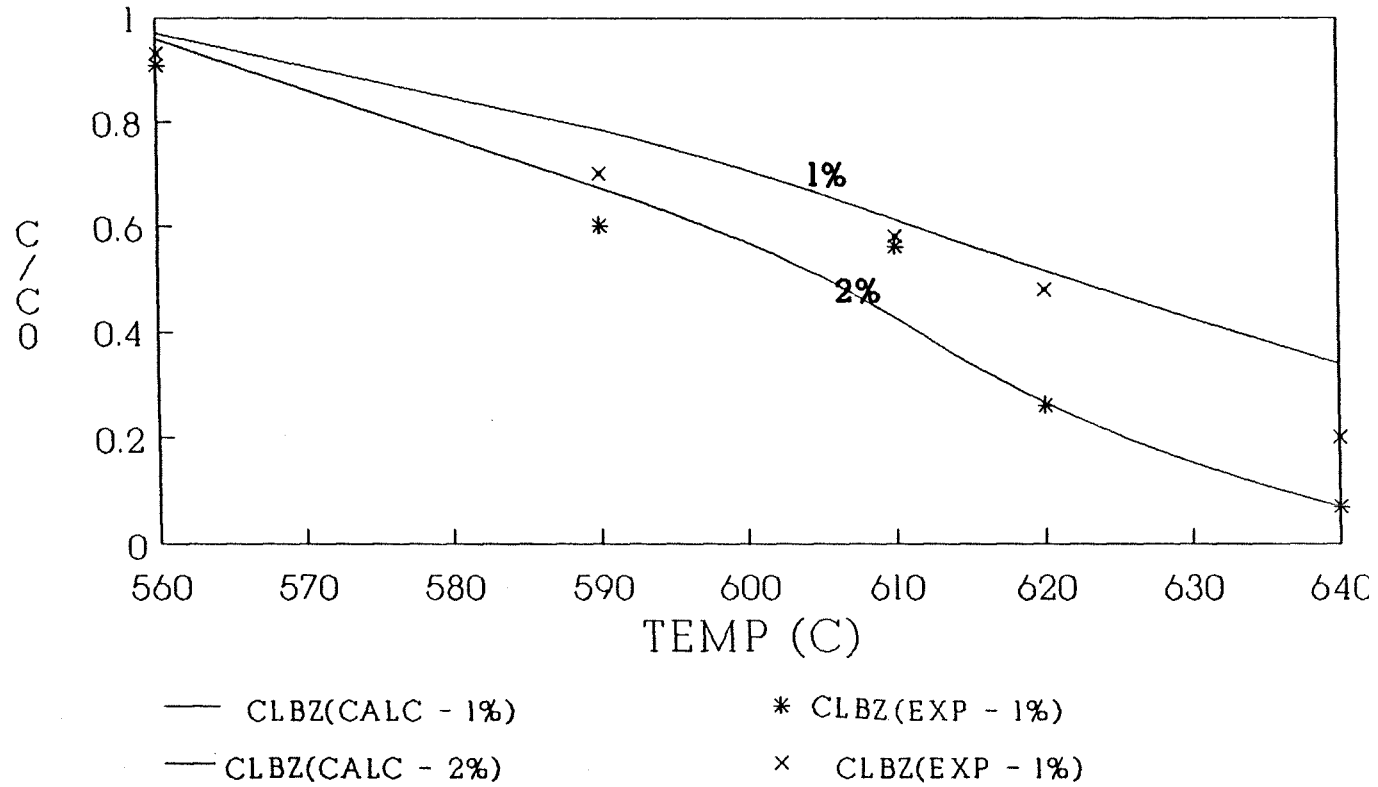
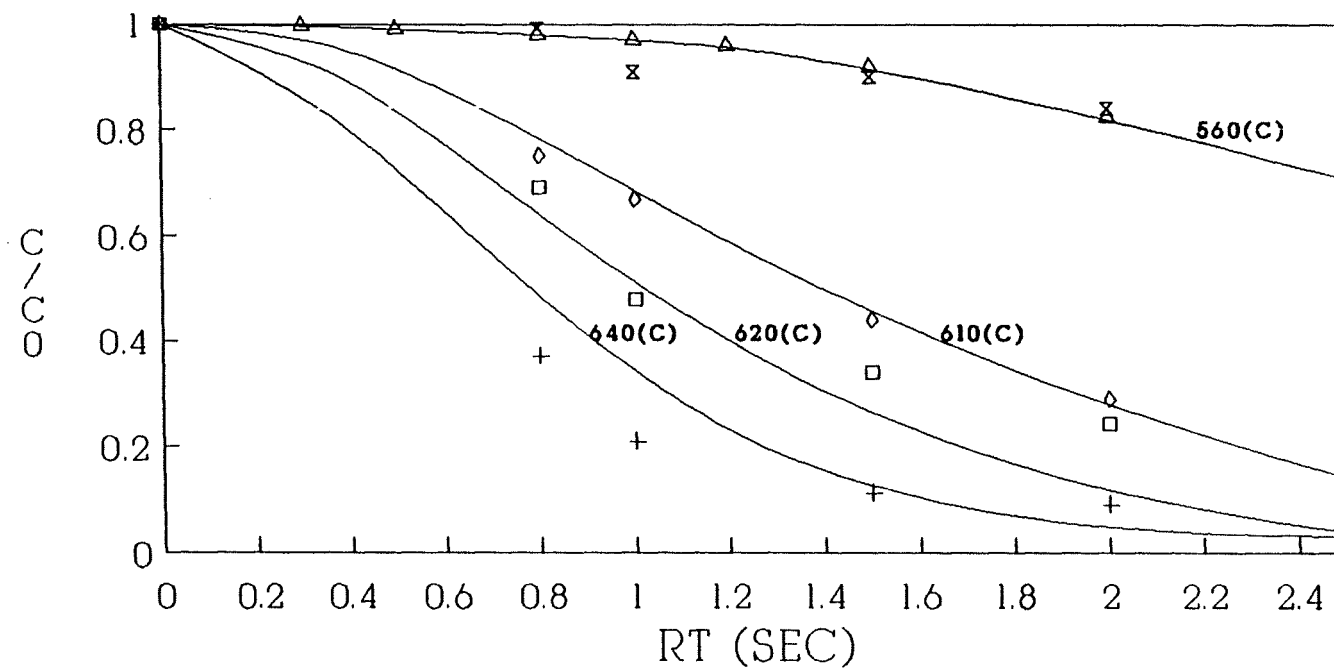


Figure 5.*0

CLBZ +H2 +O2 ---)PRODUCT, O2/H2: 1%
 MODEL and EXPT POINTS



— 640(C)Model + 640(C)Expt — 620(C)Model □ 620(C)Expt
 — 610(C)Model ◇ 610(C)Expt —△ 560(C)Model × 560(C)Expt

Figure 5.71

MODEL AND EXPT. PRODUCT DIST. VS TEMP
O₂/H₂:1%
RT = 1 (SEC),

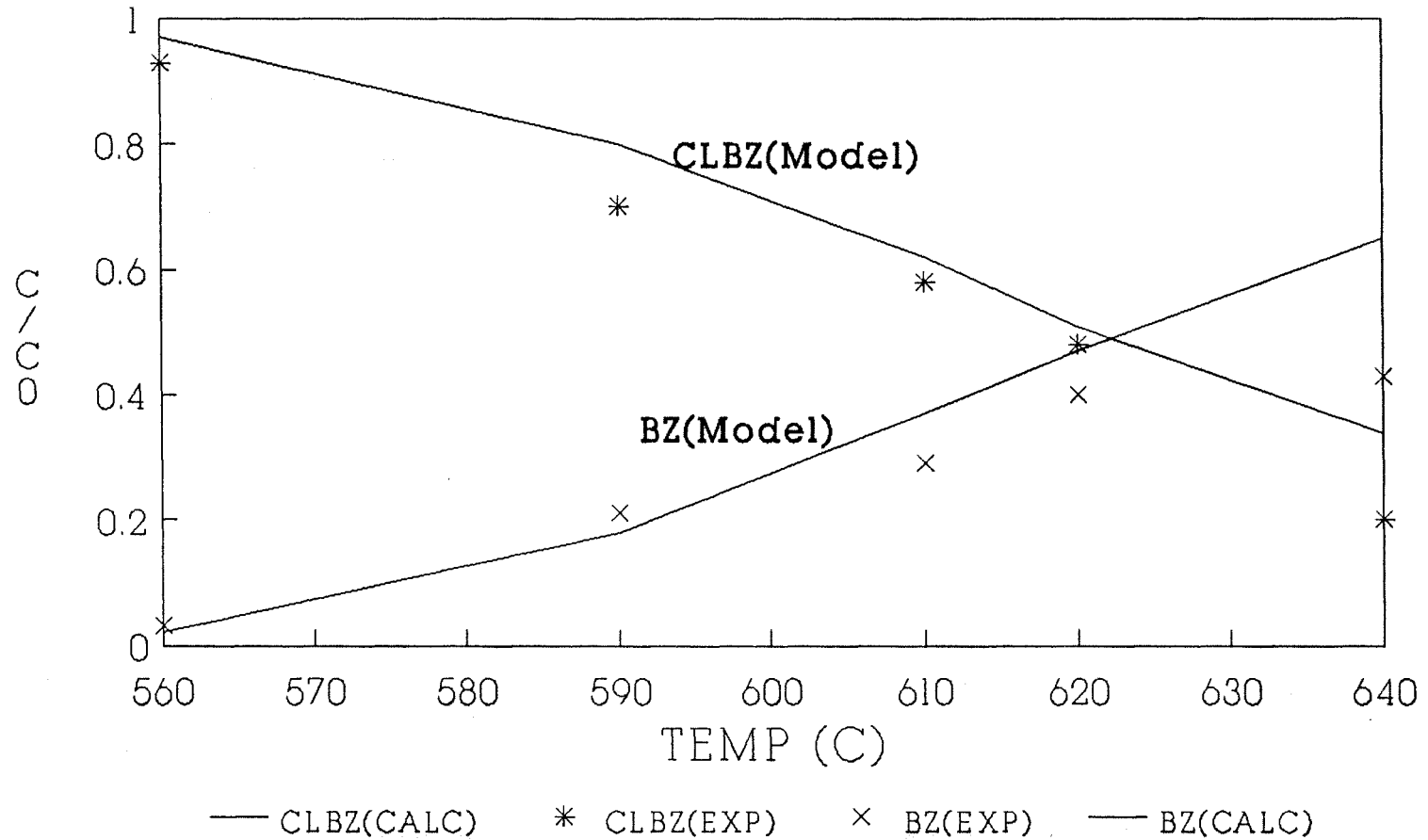


Figure 5.72

MODEL AND EXPT, PRODUCT DIST. VS TEMP
 O₂/H₂: 2%
 RT = 1 (SEC),

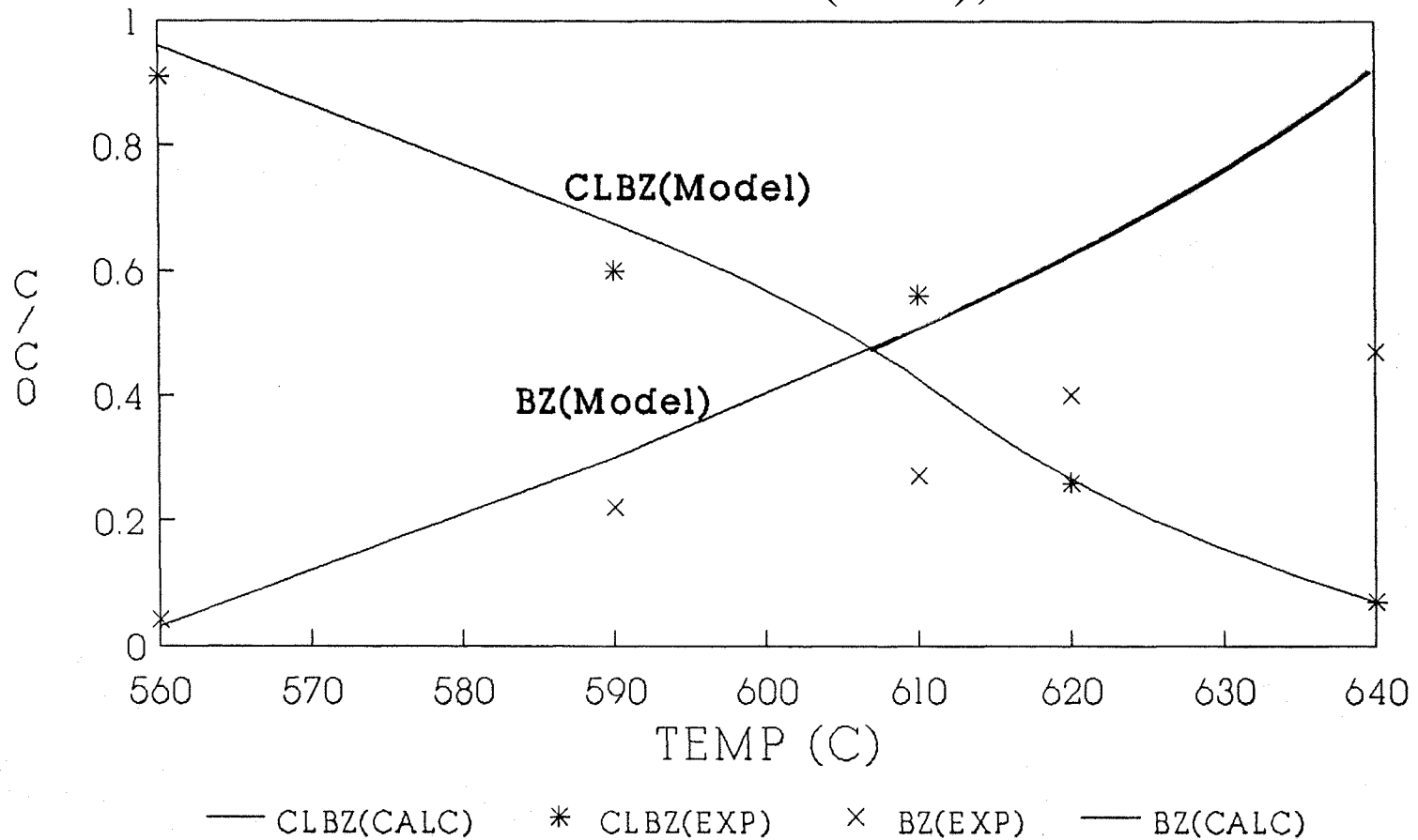
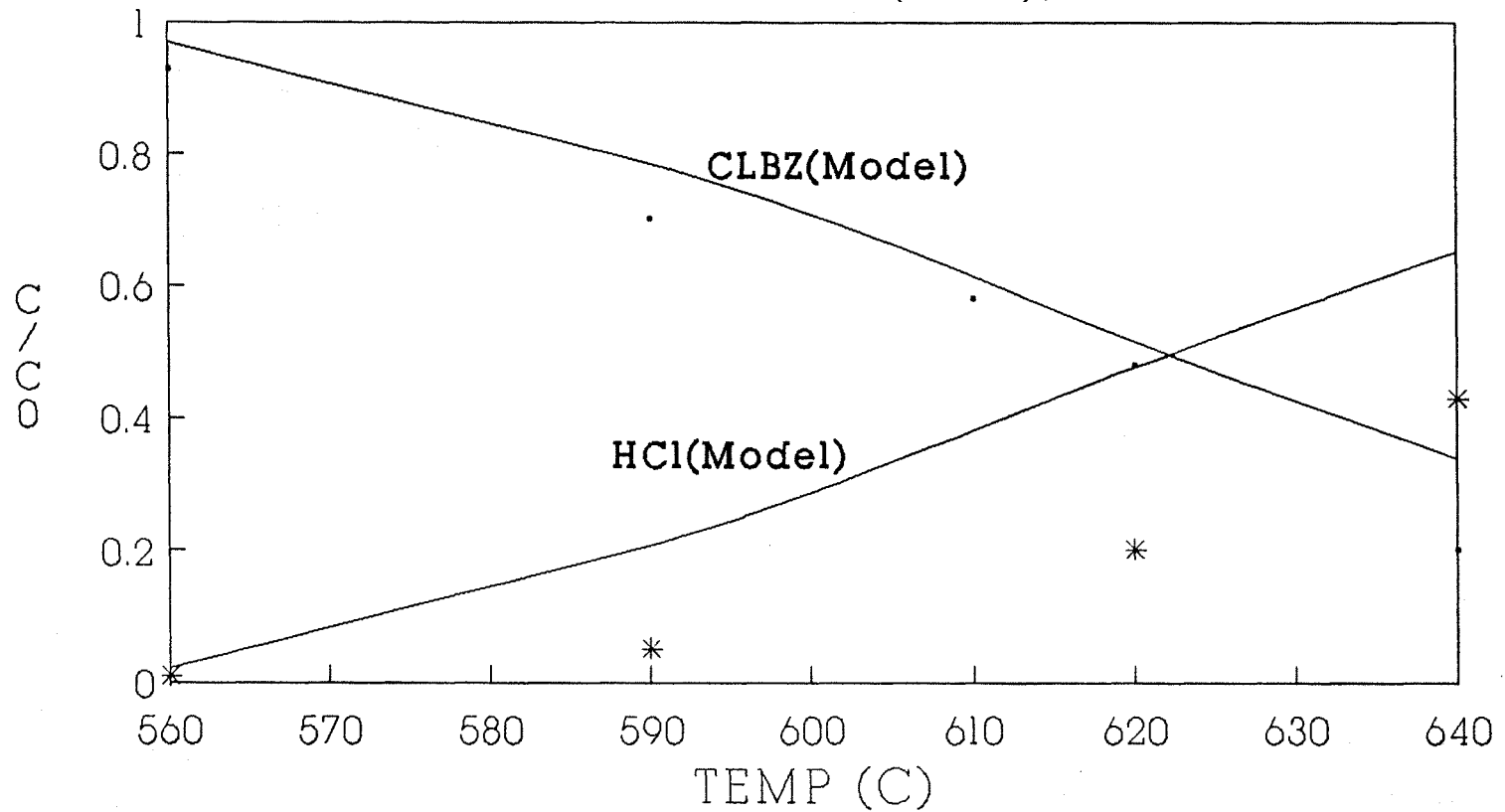


Figure 5.73'

MODEL AND EXPT. PRODUCT DIST. VS TEMP

O₂/H₂ : 1%

RT = 1 (SEC),



• CLBZ(EXP) — CLBZ(CALC) * HCl(EXP) — HCl(CALC)

Figure 5.74

MODEL AND EXPT. PRODUCT DIST. VS TEMP
 O₂/H₂ 2%
 PT = 1 (SEC).

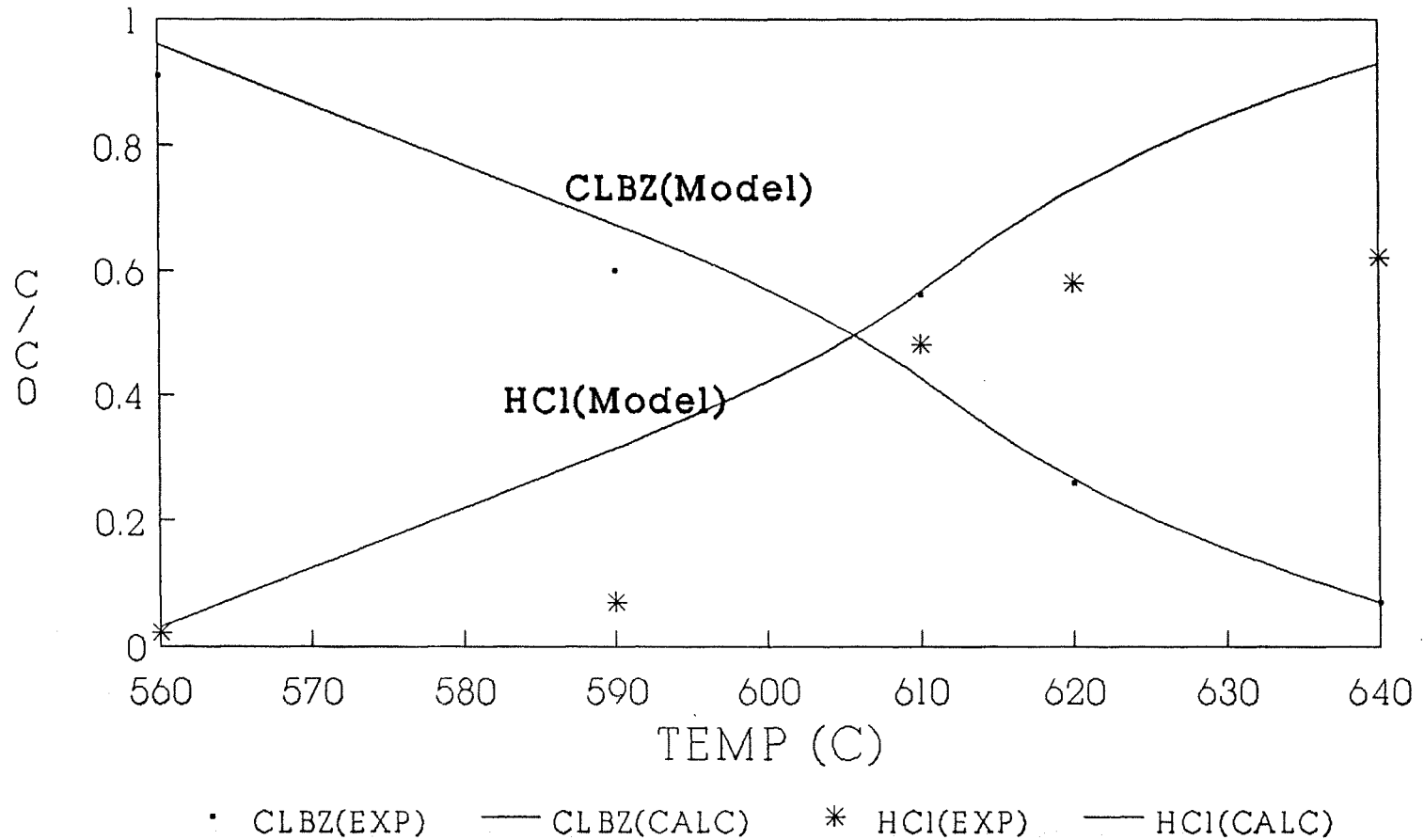


Figure 5.75

of benzene formation occurs because we does not totally account for the significant CH₄ formation in this mechanism. Some of the important reasons for this difference can be explained as following; First, the kinetic scheme does not include all possible products, specifically polyaromatic compounds and does not include paths to carbon (solid) production and second, the detailed mechanism only considers gaseous phase reaction; heterogeneous reaction effects are not included.

In order to find out the most influential reactions in our mechanism, a sensitivity analysis computer code SENS was utilized. SENS uses the CEEMKIN interpreter and an integrator code named Dassyll Dassac, which was also developed at Los Alomos by R. Kee's Group^{<27>}. As a representative example, the most influential reactions for the reaction products are given in Table 5.22 at 600°C(873K).

TABLE 5.21

REACTION MECHANISM OF C6H5C1 + O2 + 112

No.	REACTION	A	n	Ea(CAL/MOLE)	SOURCE
1.	C6H5C1 = CYC6H5 + C1	3.00E+15	0.0	96350.	[1]
2.	CYC6H6 = CYC6H5 + H	1.67E+16	0.0	111500.	[1]
3.	CYC6H6 + H = CYC6H7	4.87E+56	-12.73	26800.	[1]
4.	CYC6H7 = MECY24PD1	5.00E+12	0.0	38100.	[1]
5.	MECY24PD1+H2=MECY24PD+H	2.00E+13	0.0	46000.	[1]
6.	MECY24PD → CY13PD5 + CH3	1.00E+16	0.0	67500.	[1]
7.	MECY24PD1-H= CH3+CY13PD5	8.00E+13	0.0	0.	[1]
8.	CY13PD5 + H2 = CY13PD + H	2.50E+13	0.0	42000.	[1]
9.	CY13PD = CY13PD5 + H	6.00E+14	0.0	75100.	[1]
10.	C6H5C1 = C6H4C1 + H	1.30E+16	0.0	110500.	[1]
11.	C6H5C1 + H = CYC6H6 + C1	1.50E+13	0.0	7500.	[1]
12.	CH3 + H = CH4	8.09E+36	-7.19	9200.	[1]
13.	CH3 + H2 = CH4 + H	5.00E+12 6.60E+02	0.0 3.0	11000. 7776.	[1] [12]
14.	CH3 + C6H5C1 = C6H5CH3+C1	1.96E+14	-0.65	12000.	[1]
15.	CH3 + CYC6H6= C6H5CH3 + H	3.40E+26	-4.15	26400.	[1]
16.	C6H5C1 + H = C6H4C1 + H2	2.00E+13	0.0	18600.	[1]
17.	C6H5C1 + H = CYC6H5 + HC1	1.00E+13	0.0	11300.	[1]
18.	C1 + C6H5C1 = C6H4C1 + HC1	1.00E+13	0.0	12500.	[1]
19.	C1 + CYC6H6 = CYC6H5 + HC1	1.10E+13	0.0	12500.	[1]
20.	H + H + M = H2 + M	1.00E+18	0.0	0.	[1]
21.	H + C1 + M = HC1 + M	1.00E+17	0.0	0.	[1]

22.	$C12 = C1 + C1$	7.69E+08	0.0	55600.	[1]
23.	$C1 + H2 = HC1 + H$	4.80E+13	0.0	5000.	[1]
24.	$H + C12 = C1 + HC1$	7.94E+13	0.0	1200.	[1]
25.	$C6H5C1 + O = C6H4C1 + OH$	1.80E+13	0.0	10000.	[1]
26.	$C6i5C1 + OH = C6H4C1 + H2O$	1.44E+13	0.0	4490.	[1]
27.	$CYC6H6 + H = CYC6H5 + H2$	2.00E+13	0.0	18600.	[4, i]
		2.50E+13	0.0	16000.	[4, i]
		7.90E+13	0.0	9990.	[31]
		3.98E+14	0.0	8000.	[30]
28.	$CYC6H6 + O = CYC6H5. + OH$	3.60E+13	0.0	9900.	[5]
		3.20E+14	0.0	6000.	[31]
		3.16E+14	0.0	6000.	[30]
29.	$CYC6H6 + OH = CYC6H5 + H2O$	1.40E+13	0.0	4490.	[25]
		1.0E+14	0.0	6000.	[31]
		1.0E+13	0.0	6000.	[30]
		1.44E+13	0.0	4490.	[28]
30.	$C6H5C1 + O = CYC6H5O + C1$	*1.39E+13	0.0	4900.	[6]
31.	$C6H5C1 + OH = C6H5OH + C1$	*7.83E+12	0.0	4800.	[7]
32.	$CYC6H6 + O = C6H5OH$	*2.69E+13	0.0	4880.	[8]
33.	$CYC6H6 + O2 = CYC6H5.+HO2$	6.30E+13	0.0	10000.	[30]
34.	$CYC6H5O = BICYC6H5O$	*1.31E+22	-2.48	42100.	[9]
35.	$C6H5OH = CYC6H5O + H$	1.89E+15	0.0	85000.	[10]
36.	$CYC6H6 + OH = C6H5OH + H$	2.80E+26	-4.62	20290.	[11]
37.	$CYC6H6 + HO2 = CYC6H5.+H2O2$	1.00E11	0.0	18200.	[30]
38.	$C6H5OH + H = CYC6H5O + H2$	1.10E+14	0.0	12390.	[25]
		1.10E+14	0.0	12390.	[26]
		1.15E+14	0.0	12450.	[27]
		1.58E+10	0.0	6100.	[32]
39.	$C6H5OH + OH = CYC6H5O.+H2O$	6.00E+12	0.0	0.	[27]
40.	$CYC6H5.+O2 = CYC6H5O.+O.$	1.58E+12	0.0	0.	[29]

41.CYC6H5. =C4H3.+ C2H2	1.58E+15	0.0	82000.	[33]
	3.16E+17	0.0	86000.	[30]
42.C4H3. =C2H. + C2H2	3.16E+14	0.0	57200.	[16]
43.OH'+ H2 = H2O + H	1.00E+08	1.6	3300.	[12]
	1.10E+09	1.3	3646.	[20]
	1.17E+09	1.3	3626.	[21]
44.H + O2 = OH + O	1.10E+14	0.0	16176.	[12]
	1.86E+14	0.0	16790.	[19]
	4.50E+10	1.0	14805.	[20]
	5.13E+16	-0.816	16507.	[21]
	2.20E+14	0.0	16872.	[22]
45.O + H2 = SOH + H	1.80E+10	1.0	8929.	[12]
	1.82E+10	1.0	8900.	[19]
	1.80E+10	1.0	8900.	[20]
	1.80E+10	1.0	8826.	[21]
	1.50E+07	2.0	7680.	[22]
46.H + O2 + M = HO2 + M	2.90E+17	-0.72	0.	[14]
	2.10E+18	-1.0	0.	[21]
	2.00E+17	-0.8	0.	[22]
47.OH + HO2 = H2O + O2	2.00E+13	0.0	0.	[12]
	5.01E+13	0.0	1000.	[19]
	5.00E+13	0.0	1000.	[20]
	5.00E+13	0.0	1000.	[21]
	2.00E+13	0.0	0.	[22]
	7.50E+12	0.0	0.	[14]
48.H + HO2 = OH + OH	1.50E+14	0.0	1008.	[12]
	1.40E+14	0.0	1073.	[14]
	2.51E+14	0.0	1900.	[19]
	2.50E+14	0.0	1900.	[20]
	2.50E+14	0.0	1900.	[21]
	1.50E+14	0.0	1008.	[22]
49.O + HO2 = O2 + OH	2.00E+13	0.0	0.	[12]
	5.01E+13	0.0	1000.	[19]
	5.00E+13	0.0	1000.	[20]
	4.80E+13	0.0	1000.	[21]
	2.00E+13	0.0	0.	[22]
	1.40E+13	0.0	1073.	[14]
50.OH + OH = O + H2O	1.51E+09	1.14	0.	[12]
	6.00E+08	1.3	0.	[14]

	1.50E+09	1.1	0.	[13]
	3.16E+12	0.0	1100.	[19]
	2.14E+09	1.1	0.	[20]
	6.00E+08	1.3	0.	[21]
	1.50E+09	1.14	0.	[22]
51.H + OH + M = H2O + M	&2.20E+22	-2.0	0.	[20]
	7.50E+23	-2.6	0	[21]
	2.20E+22	-2.0	0.	[22]
	1.40E+23	-2.0	0.	[13]
52.H + O + M = OH + M	&6.20E+16	-0.6	0.	[13]
	1.00E+16	0.0	0.	[19]
53.H + HO2 = H2 + O2	1.25E+13	0.0	0.	[14]
	2.50E+13	0.0	720.	[13]
	&2.51E+13	0.0	0.	[19]
	2.50E+13	0.0	700.	[20]
	2.50E+13	0.0	700.	[21]
	2.50E+13	0.0	696.	[22]
54.O2+M = O+ O+M	&5.12E+15	0.0	11500.	[19]
	1.85E+11	0.5	95560.	[21]
55.H2O2+OH=H2O+HO2	&1.00E+13	0.0	1800.	[19]
	1.00E+13	0.0	1000.	[20]
	1.00E+13	0.0	1800.	[21]
56.HO2+HO2=O2+H2O2	&2.00E+12	0.0	0.	[20]
	2.00E+12	0.0	0.	[21]
	1.00E+13	0.0	1000.	[19]
57.H2O2+H=HO2+H2	&1.69E+12	0.0	3750.	[19]
	1.60E+12	0.0	3800.	[20]
58.H2O2+M = OH+OH+M	&1.20E+17	0.0	45500.	[19]
	1.20E+17	0.0	45500.	[20]
	1.30E+17	0.0	45500.	[21]
59.O + HCl = OH +Cl	5.24E+12	0.0	6400.	[15]
60.OH + HCl = Cl + H2O	2.45E+12	0.0	1100.	[15]
61.OO + O + M = CO2 + M	&6.17E+13	0.0	3000.	[14]
	5.88E+15	0.0	4100.	[19]
	3.80E+24	-3.0	6170	[20]
	3.20E+13	0.0	-4200.	[21]
62.OO + OH = CO2 + H	&4.40E+06	1.5	-700.	[13]
	1.51E+07	1.3	-758.	[20]

	1.51E+07	1.3	-758.	[14]
	1.28E+07	1.3	-770.	[19]
	1.51E+07	1.3	-758.	[21]
	4.40E+06	1.5	-744.	[22]
63.OO + O2 = CO2 + O	2.50E+13	0.0	48000.	[12]
	1.60E+13	0.0	41000.	[14]
	6.90E+07	1.0	34810.	[20]
	1.60E+13	0.0	41000.	[21]
64.OO + HO2 = CO2 + OH	1.50E+14	0.0	23688.	[12]
	5.80E+13	0.0	22934.	[14]
	1.51E+14	0.0	23650.	[19]
	1.00E+11	0.0	10000.	(20]
65.C2H6 = CH3 + CH3	5.71E-03	0.0	0.	[23]
66.CH4 + O =CH3 + OH	1.20E+07	2.1	7656.	[12]
67.C2H6 + H = C2H5 + H2	5.40E+02	3.5	5200.	[23]
	5.40E+02	3.5	5232.	[12]
	1.32E+14	0.0	9370.	[20]
	5.37E+02	3.5	5200.	[19]
	5.40E+02	3.5	5232	(22]
68.C2H6+O=C2H5+OH	3.00E+07	2.0	5136.	[22]
	2.51E+13	0.0	6360.	[19]
	1.82E+13	0.0	6100.	[20]
69.CH4+Cl =CH3 + HCl	5.14E+13	0.0	3800.	[15]
70.C2H5 = C2H4 + H	5.01E+13	0.0	40900.	[16]
71.C2H5+O2=C2H4+HO2	1.99E+10	0.0	0.	[18]
	1.00E+12	0.0	5000.	[19]
	1.51E+12	0.0	4860.	[20]
	2.00E+12	0.0	5016.	[22]
72.C2H4 +H =C2H3 + H2	1.50E+14	0.0	10200.	[12]
	1.50E+14	0.0	10248	[22]
	1.51E+07	2.0	6000.	[19]
73.C2H4+OH = C2H3 +H2O	7.00E+13	0.0	3024.	[22]
	4.78E+13	0.0	1230.	[19]
74.C2H4 + M= C2H2 + H2+M	2.60E+17	0.0	79680.	[12]
	9.33E+16	0.0	77200.	[19]
	2.95E+17	0.0	79280.	[20]

75.CH +CH3=C2H5+H	8.00E+13	0.0	26640.	[22]
	8.00E+14	0.0	26626.	[20]
76.C2H3 + O2 = C2H2 + HO2	1.00E+12	0.0	0.	[12]
	1.00E+12	0.0	0.	[22]
	1.00E+12	0.0	10000.	[19]
	1.58E+13	0.0	10000.	[21]
77.CY13PD+CH3=CH4+CY13PD5.	3.11E+11	0.0	5500.	[23]
78.CYPENE4.=CY13PD+H	1.02E+58	-13.06	60155.	[23]
79.CYPENE4.=C*CCC*C.	1.52E+58	-13.06	60616.	[23]
80.C*CC. +C2H2=C*CCC*C.	8.38E+30	-6.24	12824.	[23]
81.C*CC.+C2H2=CYPENE4.	3.42E+52	-12.19	27978.	[23]
82.C*CC+CH3=C*CC.+CH4	3.80E+11	0.0	9000.	[23]
83.C*CC. +C2H2= CY13PD+H	2.95E+32	-5.82	25733.	[23]
84.CH3 + C2H5 =CH4+C2H4	5.50E+11	0.0	0.	[23]
85.BICYC6H5O. = CYC5H4CHO.	2.86E+26	-4.12	28940.	[9]
86.CYC5H4CHO. = CY13PD5 + CO	3.87E+17	-2.54	2020.	[9]

REFERENCE :

1. Ritter, E., Ph.D. Disseration, NJIT (1986).
2. A factor is estimated about 3.60E+13. (ref:M. Frenklach, W. C. Gardiner, Combust. Sci. and Tech., 1986, Vol. 50, pp. 79-115).
Ea=del H * 0.2926 + 6.524 (Evan - Polanyi Plot O.+RH-7->R.+OH.:
del H =11.93, Ea = 11.93*0.2926 + 6.524 = 10.0 (kcal/mole).
3. A factor is estimated about 1.44E+13. Ea=4.49 (kcal/mole).
(ref: S. Madronich and W. Felder, J. Phys. Chem., 1985, Vol. 89, No. 16, pp. 3556-3561,1985).
4. (i).from Ritter thesis.

- (ii). $A = 2.50E+13$, $E_a = 16$ (kcal/mole).
(ref: J. H. Kiefer, L. J. Mizerka, M. R. Patel, and H.C. Wei, J. Phys. Chem., 1985, Vol. 89, No. 10, pp. 2013-2019).
5. A factor is estimated about $1.80E+13$.
(ref: M. Frenklach, W. C. Gardiner, Combust. Sci. and Tech., 1986, Vol. 50, pp. 79-115).
 $E_a = \Delta H * 0.2926 + 6.524$ (Evan - Polanyi Plot $O.+RH--->R.+OH.$)
 $\Delta H = 11.54$, $E_a = 11.93 * 0.2926 + 6.524 = 9.9$ (kcal/mole).
6. Chemact 3.
7. Chemact 2.
8. Chemact 1.
9. Dissoc 2.
10. Dissoc 1.
11. Chemact 4.
12. Warnatz, J., Combustion Chemistry; Gardiner, W. C., Jr., Ed.; Springer-Verlag: New York, 1984.
13. M. Frenklach, W. C. Gardiner, Combust. Sci. and Tech., 1986, Vol. 50, pp. 79-115.
14. J. A. Miller, M. C. Branch, W. J. Mclean, D. W. Chandler, M. D. Smoke, and R. J. Kee, Paper NO. 6, Twentieth Symposium (international) on Combustion (1984)
15. Kerr, J. A. and Moss, S. J., "Handbook of Bimolecular and Termolecular Gas Reaction, Vol. I & II", CRC Press Inc., 1981.
16. Dean, A. M., J. Phys. Chem., Vol. 89, No. 21, 4600, 1985.
17. Wu, Y. P., M. Sci. Thesis, NJIT (1989)

18. Work by Dr. Bozzelli and Yu, H. C. (CC. + 02 --- >Product).
19. Westbrook, C.K., Nineteenth Symposium (International) on Combustion/ The Combustion Institute, pp 153-166, 1982.
20. E., Levy, J. M., Taylor, B.R., Longwell, J. P., and Sarofim, A.F., Nineteenth Symposium (International) on Combustion / The Combustion Institute, pp 167-179, 1982.
21. Miller, J.M., Mitchell, R.E., Smooke, M.D., and Kee, R.J., Nineteenth Symposium (International) on Combustion / The Combustion Institute, pp 181-196, 1982.
22. Warnatz, J., Bockhorn, H., Moser, A., and Wenz, H. W., Nineteenth Symposium (International) on Combustion / The Combustion Institute, pp 197-209, 1982.
23. Dean, A. M., "**Detailed Kinetic Modeling of Autocatalysis in Methane Pyrolysis**", submitted to J. Phys. Chem., March 1989.
24. Lin, C. Y. and Lin, M.C., "**Thermal Decomposition of Methyl Phenyl Ether in Shock Waves: The Kinetics of Phenoxy Radical Reaction**", J. Phys. Chem., Vol. 90, No. 3, 1986.
25. He, Y. Z., Cui, J. P., Mallard, W. G., and Tsang, W., "**Rate Constants and Mechanism for the Reaction of Hydrogen Atom with Aniline**", J. Phys. Chem., Vol 92, pp 1510-1513, 1988.
26. Cui, J. P., He, Y. Z., and Tsang, W., "**Rate Constants for Hydrogen Atom attack on Some Chlorinated Benzene at High Temperatures**", J. Phys. Chem., Vol 93, pp 724-727, 1989.
27. He, Y. Z., Mallard, W. G., and Tsang, W., "**Kinetics of Hydrogen and Hydroxyl Radical attack on Phenol at High Temperatures**", J. Phys. Chem., Vol 92, pp 2196-2201, 1988.

28. Madronich, S. and Felder, W., **"Kinetics and Mechanism of the Reaction of OH with C₆H₆ over 790-1410K"**, J. Phys. Chem., Vol 89, pp 3556-3561, 1985.
29. Venkat, C., Brezinsky, K., and Glassman, I., **"High Temperature Oxidation of Aromatic Hydrocarbons"**, Nineteenth Symposium (International) on Combustion/ The Combustion Institute, pp 143-152, 1982.
30. Fujii, N. and Asaba, T., **"Shock Tube Study of the Reaction of Rich Mixture of Benzene and Oxygen"**, Fourteen Symposium (International) on Combustion/ The Combustion Institute, pp 433, 1973.
31. Hsu, D. S., Lin, C. Y., and Lin, M. C., **"CO Formation in Early Stage High Temperature Benzene Oxidation under Fuel Lean Conditions: Kinetics of the Initiation Reaction, C₆H₆ -->C₆H₅ -->H"**, Twentieth Symposium (International) on Combustion/ The Combustion Institute, pp 623-630, 1984.
32. Manion, J. A. and Lowu, R., **"Rates, Products, and Mechanism in the Gas-Phase Hydrogenlysis of Phenol Between 922 and 1175K"**, J. Phys. Chem., Vol 93, pp 3563-3574, 1989.
33. Kiefer, J. H., Mizerka, L. J., Patel, M. R., and Wei, H. C., **"A Shock Tube Investigation of Major Pathways in the High Temperature Pyrolysis of Benzene"**, J. Phys. Chem., Vol 89, pp 2013-2019, 1985.

* Pressure dependent : rate expression given for 760 torr.
Temperature ranges : 300 - 1700K.

DISSOC: apparent rate constant by DISSOCIATION computer code
analysis.

QRRK : apparent rate constant by QRRK computer code
analysis.

i Value selected

Tables 5.22! Sensitivity Analysis Summary

Temp. = 600 °C (873K), Rt = 1.0 (SEC)

Species	Reaction Number	
	Most Important $10^{-2} < S < 1$	Important $10^{-3} < S < 10^{-2}$
C6H5Cl	-I- 17,20,53,56 - 11,45,46,48,57,58	+ 27,29 - 40,43
C6H6,	+ 11,43,45,46,48,58 - 17,20,53,56	+ 40 - 4,7,27,29,44
HC1	+ 11,45,46,48,57,58 - 17,20,53,56	+ 40,43 - 7,27,29,44
CH ₄	+ 4,7,11,43,45,46,48,57,58 - 17,20,29,53,56	+ 16,30,40 - 8,9,26,27,31,38,44,47,55
C2H2	+ 4,7,9,11,30,31,38,40,45, 48,57,58 - 17,20,29,43,46,53,56	+ 16,39,44 - 10,26,27,47,55
C2H4	+ 4,7,9,11,30,31,38,40,45, 46,57,58,71,72,76,78,83 - 17,20,29,43,48,53,56,67,70	+ 16,39,44,74 - 8,10,13,26,27,47,55,73
C2H6	+ 4,7,9,11,30,31,38,40,45, 46,48,57,58,65,67,70,72, 76,78,83 - 13,17,20,27,29,56,71	+ 16,39,43,44,74 - 8,10,26,47,55,69
CO	+ 11,30,31,38,40,44,45,48, 57,58,78,81,83 - 17,43,46,53,56,72,76	+ 39 - 20,64

S: Sensitivity Coefficient; "+" S > 0, "-": S < 0.

VI. CONCLUSION

The decomposition of chlorobenzene in hydrogen bath gas and low concentrations of oxygen (1% - 5%) was carried out at 1 atmosphere pressure in tubular flow reactors of varied surface to volume ratio. Temperature ranged from 560 to 660 °C; and residence times studied were 0.03 to 2.5 seconds:.

Complete decay (99 %) for the chlorobenzene at 1 second residence time occurs at temperatures above 660 °C for all the O₂/H₂ ratio sets. The major products are benzene, CH₄, C₂H₆, HCl and carbon (solids). The minor products are toluene, cyclopentadiene, C₂H₂, C₂H₄, CO and CO₂. Naphthalene, chlorobiphenyl, and terphenyl of heavy molecular of products were not identified in our study. Oxygen fraction has a very significant effect on the decomposition of chlorobenzene; the oxidation of chlorobenzene occurred faster when more oxygen was added. The higher the ratio of O₂ to H₂, the lower temperature needed for reaction. A decrease in reactor tube surface to volume ratio (S/V) was observed to accelerate the decomposition process. The relative distribution of major products was, however, found to be insensitive to the S/V ratio of the reactor.

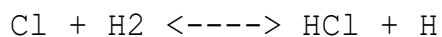
This study demonstrated that small amounts of oxygen (1% to 5%) provides a practical route of destruction of

chlorinated aromatics at lower temperatures. By this process, major products at temperature between 560°C) and 660°C were HCl and non-chlorinated hydrocarbons such as benzene, methane, ethylene and ethane plus up to 25% carbon(solids).

A detailed kinetic reaction mechanism was developed and used to model results obtained from the experiments. The reason for the higher conversion of C₆H₅Cl in O₂/H₂ at much lower temperature(550 - 650 °C) than observed in C₆H₅Cl plus H₂ only▶ is the reaction of H₂ + O₂ to H₂O₂ + H, to generate active hydrogen atoms which rapidly displace Cl atom on C₆H₅Cl to form benzene + Cl.



The Cl then undergoes chain reaction with H₂ generate HCl + H again. This process occurs rapidly producing a super equilibrium of H atom.



Significant concentration of CH₄ are observed and explained by an intramolecular isomerization reaction of the cyclohexadienyl (CHD.) intermediate(H + benzene adduct) to methylene cyclopentadiene. The CHD. radical is more stabilized at these relatively low temperatures, compared to the higher temperature of Ritter and Lowu, thus also increasing its equilibrium concentration and the reaction to Me.CPD.

VII. REFERENCES

- <1> Manion, J. A., Mulder, P. and Louw, R., Environ. Sci. Technol., Vol. 19, 280 (1985)
- <2> Sworn, E.M. and Ackerman, D.G., U.S. EPA-Report -6012-82-069, NTIS PB82-217498 (1982)
- <3> Karasek, F.W., Clement, R.E. and Viau, A.C., Vol 239, 239 (1982)
- <4> Shaub, W.M. and Tsang W., Environ. Sci. Technol., Vol 17, No. 12, 721 - 730 (1983)
- <5> Louw, R., Dijks, J. H. and Mulder, P., J. Chem. and Industry, Oct. 3, 759 (1983)
- <6> Graham, J.L., Hall, D.L. and Dellinger, B., Environ. Sci. Tech., 20, 703 (1986)
- <7> Rubey, W. A., Dellinger, B., Hall, D. L. and Mazerb, S. L., Chemosphere, 14, 1483 (1985)
- <8> Gochfeld, M., Gallo, M. and Kahn, P., New Jersey Medicine, Vol 85, 907 (1988)
- <9> Ritter, E.R., M. Sc. Thesis, NJIT (1986), J. Phys. Chem. accepted July 1989.
- <10> Cullis, C. and Priday, Proc. Roy. Soc. London A, 224, 308 (1954)
- <11> Cullis, C., Manton, Transcripts of the Faraday Soc., 54, 381 (1958)
- <12> Louw, R., Dijks, J. H. M. and Mulder, P., J. of Chemical Soc. Perkin Trans II, 40, 1635 (1973)

- <13> Yang, Y.D., Ph. D. Thesis, New Jersey Institute of Technology (1986)
- <14> Kaufman, F. ,Progress in Reaction Kinetics, Vol.VI, Pergamon Press, NY (1961), Chapter 1.
- <15> Hung, M., M. Sc. Thesis, NJIT (1986)
- <16> Zhu, L. J.,M. Sc. Thesis, NJIT (1988)
- <17> Levenspiel, O., Chemical Reaction Engineering, 2nd ed., John Wiley & Son Inc., NY (1962)
- <18> Chang, S. H. and Bozzelli, J. W., AICHE J.,Vol 33, No. 7, 1207 (1987)
- <19> Bird, R., Steward, W. amd Lightfoot, Transport Phenomena, (New York: John Wiley & Soc, 1960)
- <20> Dean, A. M., J. Phys. Chem., 89, 4600 (1985)
- <21> Frenklach, M., Ramachandra, M., Matula, A.,Symposium (Int.) on Combustion, 20, 871 (1984)
- <22> Westmoreland, P.R. and Dean, A.M., AIChE J., 32, 171 (1986)
- <23> Ritter, E, and Bozzelli, J.W. and Dean, A.M.'s paper Accepted in J. Phys. Chem. (1989)
- <24> Tsang, W., J. Phys. Chem., Vol 90, No. 6 (1986)
- <25> Lin, C. Y. and Lin, M. C., J. Phys. Chem., Vol 90, No.3, 425 (1986)
- <26> Benson, S.W., Thermochemical Kinetics, 2nd ed. Wiley, NY (1976)

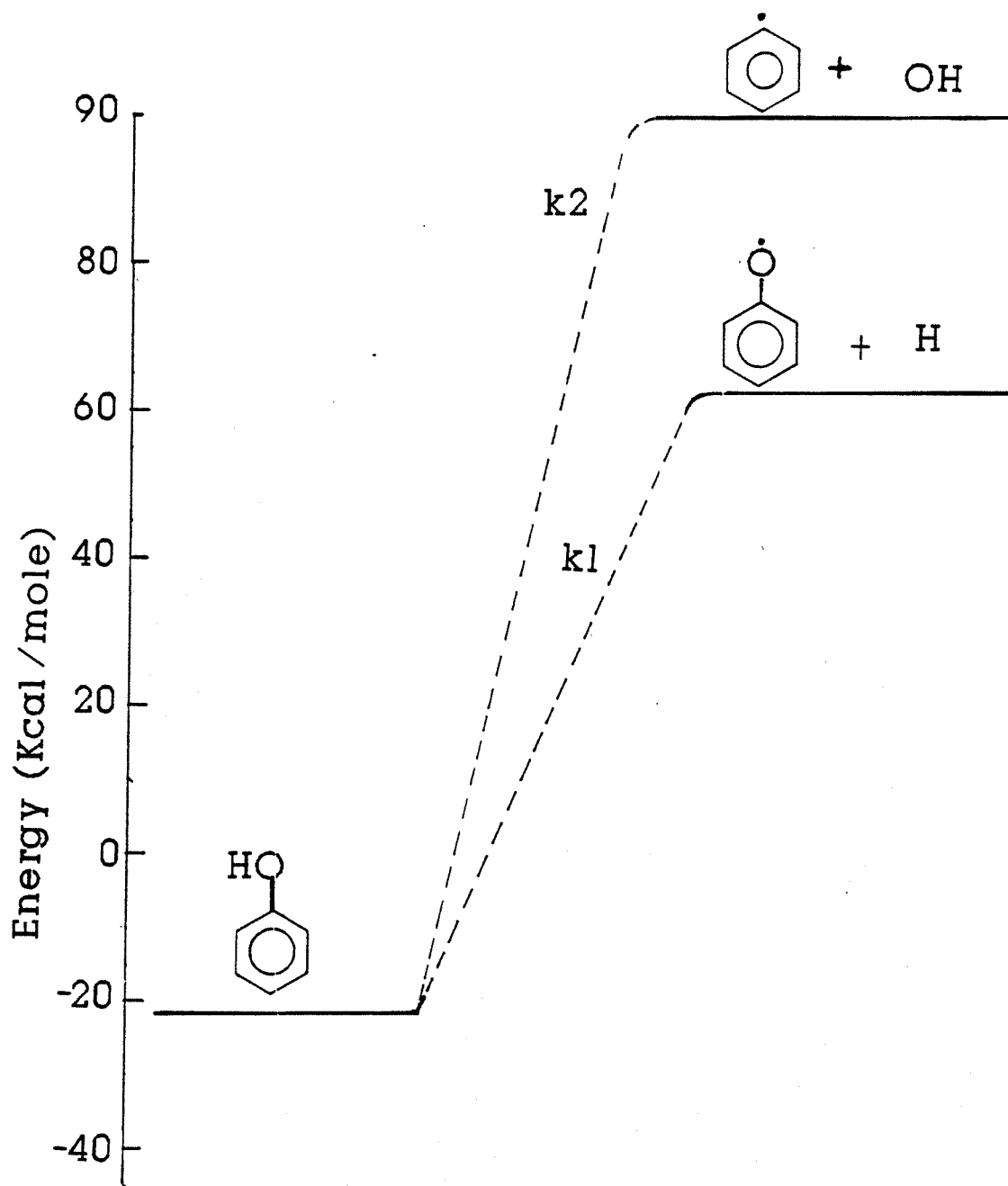
- <27> Kee, R.J., Miller, T.H. and Jefferson, T.H., CHEMKIN: A General-Purpose, Problem-Independent, Transportable, Fortran Chemical Kinetics Code Package, SANDIA (1980)
- <28> Harris, J. C., Anderson, P. C., Goodwin, B. E. and Rechsteiner, C. E., "Dioxin Emission from Combustion Sources: A Review of the Current State of Knowledge", Final Report to ASME, ASME, New York, NY (1980)
- <29> Esposito, M. P., Tiernan, T. O. and Dryden, F. E., U.S. Environ. Prot. Agency, 1980, EPA-600/2-80-197.
- <30> Gaudy, A. and Gaudy, E., Microbiology for Environmental Scientists and Engineers, McGraw - Hill (1980)
- <31> Mason, L. and Unget, S., U.S. EPA 600/2-79-198, NTIS 80-131964 (1979)
- <32> JANAF Thermochemical Tables issued as supplement No. 1, Vol. 14, J. Phys. Chem. Ref. Data (1985)
- <33> Ritter, E. and Bozzelli, J. W., "Thermochemical Estimation of Molecular and Radical", computer code submitted to J. Phys. Chem. Ref. Data for publication.
- <34> Chang, S.H., Doctoral Dissertation, New Jersey Institute of Technology (1985)
- <35> Hill, C.G., Chemical Engineering Kinetics & Reactor Design, John Wiley & Son Inc., (1977).
- <36> Reman, G.H., Chem. & Ind., 46 (1955)
- <37> Cremer, H.W. and Watkins, S.B., Chemical Engineering Practice, Vol. 8, Butterworth, London (1965)
- <38> Butt, J.B., Reaction kinetics and Reactor Design,

Prentice Hall (1980)

- <39> Poirier, R.V. and Carr, R.W., J. Phys. Chem., 74, 1593, (1971)
- <40> Kassel, L.S., "Studies in Homogeneous Gas Reactions II. Introduction of Quantum Theory," J. Phys. Chem., 32, 1065 (1928).
- <41> Baldwin, R. R., Scott, M., and Walker, R. W., Twenty-first Symposium (International) on Combustion/ The Combustion Institute, pp 991-1000 (1986)
- <42> Bozzelli, J. W., Ritter, E., and Patel, S., Combustion Institute Proceedings, Central States Meeting, May (1989)
- <43> Cui, J. P., He, Y. Z., and Tsang, W., J. Phys. Chem., Vol 93, pp 724-727 (1989)
- <44> Madronich, S. and Felder, W., J. Phys. Chem., Vol 89, pp 3556-3561 (1985)
- <45> Venkat, C., Brezinsky, K., and Glassman, I., Nineteenth Symposium (International) on Combustion/ The Combustion Institute, pp 143-152 (1982)

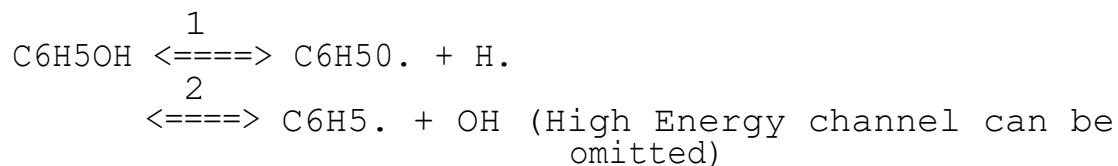
APPENDIX (A)

DISSOC & CHEMACT INPUT DAT
AND CALCULATION RESULTS



(Dissoc 1) DISSOCIATION INPUT DATA and CALCULATION RESULTS

Table 1 - a



k	A	Ea	source
1	9.89E+14	83.9	a
<v> = 1077.3 (cm-1)			b
Lennard-Jones Parameters :			c
sigma = 5.226 Å		e/k = 601.17 K	

a. A1 factor is calculated from as that for H. + C6H5O.
 ----> C6H5OH, which is A₁ factor 2.5E+14, from Y. Z. He,
 W.G. Mallard, and W. Tsang, "Kinetics of Hydrogen and Hydroxyl Radical Attack on Phenol at High Temperature",
 Journal Phys. Chem., Vol 92, pp 2196 - 2201, 1988.

Use. Therm Calculation Formula (1):

$$\ln (A_f / A_r) = \Delta S / R - (\Delta n) * (e/kT) \quad (1)$$

A1 = 9.89E+14. Ea1 = ΔH = 83.9 (kcal/mole).

b. < V > = 1077.3 (cm-1) Use Cpfite Program.

c. Sigma = Use Formula (2)

$$\text{Sigma} * (\text{Pc} / \text{Tc})^{1/3} = 2.3551 - 0.087 * \text{Omega} \quad (2)$$

e / k Use Formula (3)

$$e / k = (0.7915 + 0.1693 * \text{Omega}) * \text{Tc} \quad (3)$$

	Tc(K)	Pc (Atm)	Omega
<chem>C6H5OH</chem> =	694.2	60.5	0.44

$$\text{Sigma} = 5.226 \text{ (AO)} , e / k = 601.17 \text{ (:K)} .$$

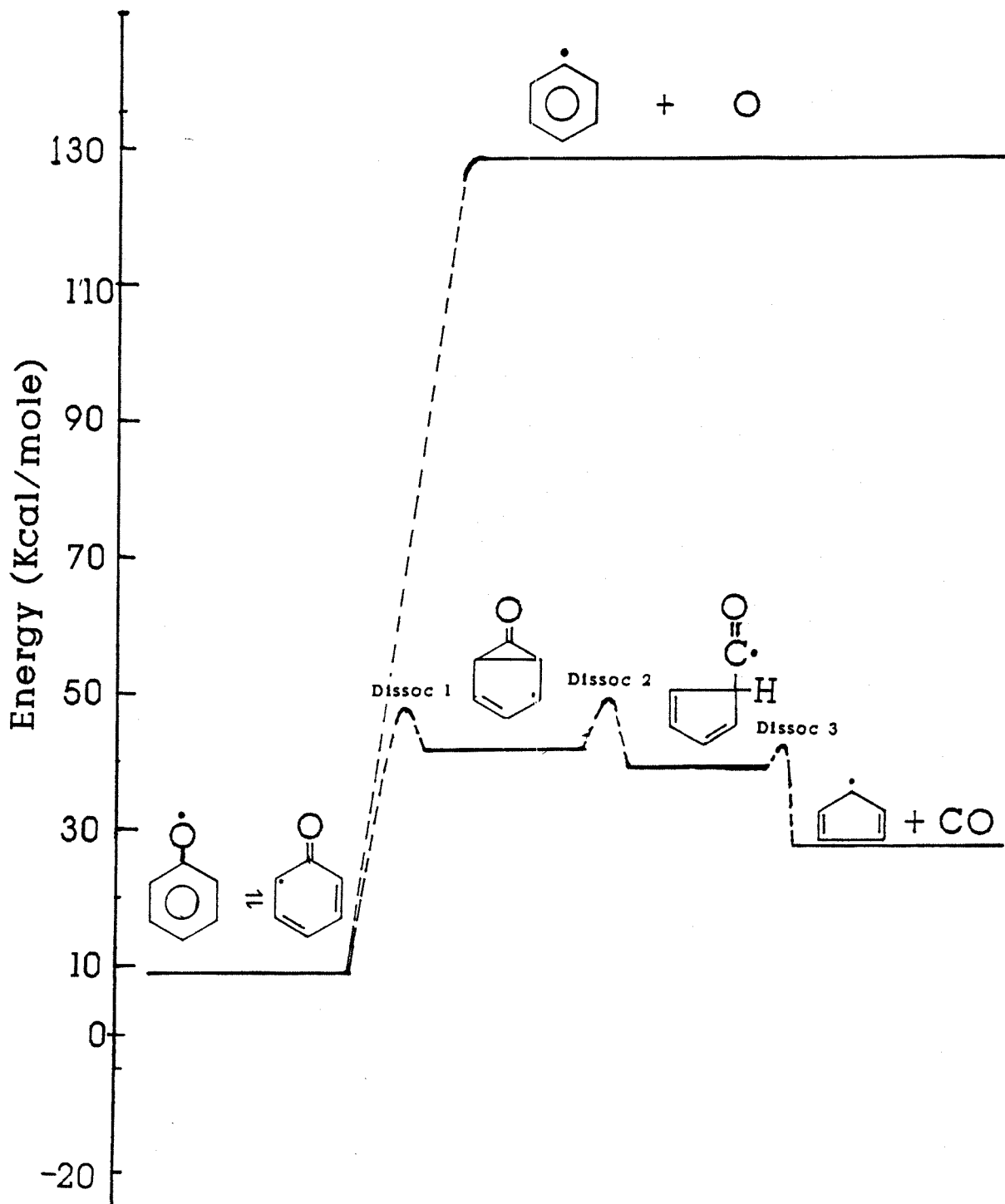
Critical property data taken from Reid, Prausnitz and Sherwood (The Properties and Gases and Liquids, 3rd ed.)

Table 1 - b

APPARENT REACTION RATE CONSTANTS PREDICTED
USING DISSOCIATION ANALYSIS

P (torr)	Reaction	A (cc/mol s)	N	Ea (Kcal/mol)
7.6	C6H5OH = C6H6O. + H.	1.88E+15	0.0	85.0
76.0		1.89E+15	0.0	85.0
760.0		1.89E+15	0.0	85.0
7600.0		1.89E+15	0.0	85.0

* Valid Temp from 300 - 1700K



(Dissoc 2) DISSOCIATION INPUT DATA and CALCULATION RESULTS

Table 2 - a

DISSOC 2.1] C6H5O. <===> BICYC6H5O.
[DISSOC 2.2] BICYC6H5O. <===> CYC5H4CHO.
<===> C6H5. + O
[DISSOC 2.3] CYC5H4CHO. <===> C5H5 + CO

[DISSOC 2.1]

¹
C6H5O. <===> BICYC6H5O.,

k	A	Ea	source
1	7.00E+13	38.1	a

<v> = 1290 (cm-1)

Lennard-Jones Parameters :

sigma = 5.62 Å e/k = 617.22 K

a.

A1 = 7.00E+13, which is taken from [CHD.] ---->[BICYC6H7],
E. Ritter and J. W. Bozzelli, J. Phys. Chem., accepted
1989.

Ea1 = 31.6 + 6.5 = 38.1 (kcal/mole).

The reaction of bicyclo ketone radical back to phenoxy
radical might be expected to have a slightly lower Ea
because of the deeper well of this channel than its

reaction to the cyclopentadiene carbonyl radical. Thus we reduce the E_a for this reaction to phenoxy by 1 kcal from that average shown by Dean of 7.5 to 6.5.

b. $\langle V' \rangle = 1290 \text{ (cm}^{-1} \text{)}$ Use Cffit Program.

c. Sigma = Use Formula (1)

$$\text{Sigma} * (\text{Pc} / \text{Tc})^{1/3} = 2.3551 - 0.087 * \text{Omega} \quad (1)$$

$e / I k = \text{Use Formula (2)}$

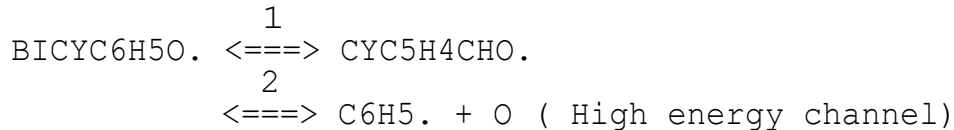
$$e / k = (0.7915 + 0.1693 * \text{Omega}) * \text{Tc} \quad (2)$$

CO5O.	$\frac{\text{Tc(K)}}{677}$	$\frac{\text{Pc(Atm)}}{46}$	$\frac{\text{Omega}}{0.71}$
-------	----------------------------	-----------------------------	-----------------------------

$$\text{Sigma} = 5.62 \text{ (AO)}, \quad e / k = 617.22 \text{ (K)}.$$

Thermodynamic critical property data taken from Reid, Prausnitz and Sherwood (The Properties and Gases and Liquids, 3rd ed.)

[DISSOC 2.2]



k	A	Ea	source
1	1.30E+13	23.6	a
2	3.10E+16	140.9	b

<v> = 1149 (cm-1)

Lennard-Jones Parameters :

sigma = 5.62 Å e/k = 617.22 K

a.

A1 = 1.30E+13, which is taken [BICYC6H7] ---->[Me.CPD], E. Ritter and J. W. Bozzelli, J. Phys. Chem., accepted 1989. Ea1 = 16.1 + 7.5 = 23.6 (kcal/mole), which is taken from Generic Beta scission (Ea) reaction of alkyl radical, Dean, A. M., J. Phys. Chem., Vol. 89, No. 21,1985, 4603.

b.

A2 = 3.10E+16, which is taken A_2 = 1.00E+14(H + C6H5. ----> C6H6), E. Ritter and J. W. Bozzelli, J. Phys. Chem., accepted 1989. A2 calculated from Thermo. Ea2 = del H = 140.9 (kcal/mole). Due to high energy barrier, this channel can be omitted.

c.

< v' > = 1149 (cm-1) Use Cpfit Program.

d.

Sigma = Use Formula (1)

$$\text{Sigma} * (\text{Pc} / \text{Tc})^{1/3} = 2.3551 - 0.087 * \text{Omega} \quad (1)$$

e / Ik = Use Formula (2)

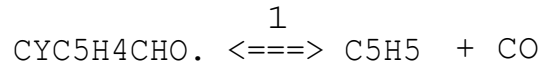
$$e / k = (0.7915 + 0.1693 * \text{Omega}) * \text{Tc} \quad (2)$$

$$\text{C050.} = \frac{\text{Tc(K)}}{677} \frac{\text{Pc(Atm)}}{46} \frac{\text{Omega}}{0.71}$$

Sigma = 5.62 (AO), e / k = 617.22 (K).

Reference: see [DISSOC 2.1) Source (c).

[DISSOC 2.3]



k	A	Ea	source
1	1.51E+13	2.5	a

$\langle v \rangle = 887 \text{ (cm}^{-1}\text{)}$

Lennarlf-Jones Parameters :

$\sigma = 25.62 \text{ \AA}$ $e/k = 617.22 \text{ K}$

a.

$A_1 = 1.51\text{E}+13$, $A_{-1} = 1011 \cdot 5' = 3.16\text{E}+11$, which is taken from the reaction of $\text{CH}_3 + \text{C}=\text{C}$, Dean, A. M., J. Phys. Chem., Vol. 89, No. 21, 1985, 4603. A1 Thermo Calculation.

$E_{a1} = 2.5 \text{ (kcal/mole)}$, which is taken from the reaction of $\text{CH}_3\text{CO} \rightarrow \text{CH}_3 + \text{CO}$, $E_a = 16.8 \text{ (kcal/mole)}$, Warnatz, J., Combustion Chemistry; Gardiner, W. C., Jr., Ed., Springer-Verlag: New York, 1984. $E_a] = 16.8 - \Delta H = 2.5$.

b.

$\langle v \rangle = 887 \text{ (cm}^{-1}\text{)}$ Use Cpfif Program.

c.

Sigma = Use Formula (1)
 $\text{Sigma} * (\text{Pc} / \text{Tc})^{1/3} = 2.3551 - 0.087 * \text{Omega} \quad (1)$

e / k = Use Formula (2)
 $e / k = (0.7915 + 0.1693 * \text{Omega}) * \text{Tc} \quad (2)$
 $\text{C6H5O} \quad =677 \quad \text{Tc(K)} \quad \text{Pc (Atm)} \quad \text{Omega} \quad 46 \quad 0.71$

$\text{Sigma} = 5.62 \text{ (\AA)}$, $e / k = 617.22 \text{ (K)}$.

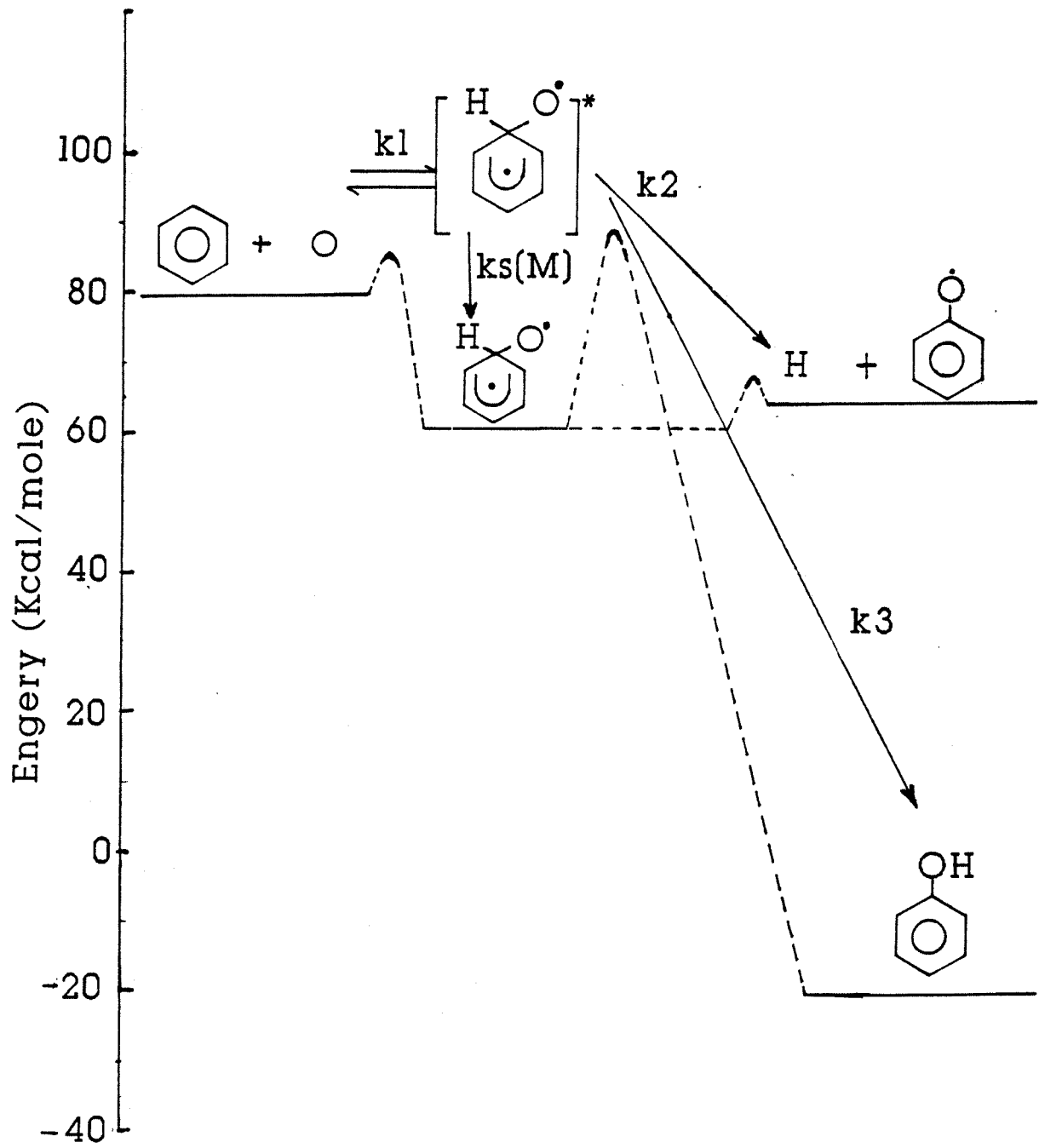
Reference: see [DISSOC 2.1] Source (c).

Table 2 - b

APPARENT REACTION RATE CONSTANTS PREDICTED
 USING DISSOCIATION ANALYSIS

P (torn)	Reaction	A (cc/mol s)	N	Ea (Kcal/mol)
7.6	C6H5O. = BICYC6H5O.	1.04E+35	-6.66	45.59
760.0	it	1.31E+22	-2.48	42.10
7.6	BICYC6H5O. = CYC5H4CHO.	8.36E+47	-11.2	34.35
760.0	"	2.86E+26	-4.12	28.94
7.6	CYC5H4CHO = C5H5. + CO	3.34E+15	-2.53	1.98
760.0	"	3.87E+17	-2.54	2.02

* Valid Temp from 300 - 1700K



1.58E+13 (cc/mol sec), $E_{a_i} = \Delta H + 4.9 = 25.41$
(kcal /mole).

b. A_2 is taken from E. Ritter and J. W. Bozzelli, Journal
Phys. Chem., accepted on 1989, (H + C6H5Cl ---->[C6H6Cl],
 $A_2 = 1.5 * 2.00E+13 = 3.00E+13$, thermo calculation $A_2 =$
 $1.23E+14$, $E_{a_2} = 5.0$, $E_{a2} = \Delta H + 5 = 7.76$ (kcal/mole).

c. A_3 is Transition State Theory, $\Delta S = 0$, $A_3 = 3.63E+13$.
 $E_{a3} = \Delta H + \text{Ring Strain} + E_a$ (Abstraction)
 $= 0 + 28 + 1 = 29$ (kcal /mole).
($T_{avg} = 750K$)

d. A_4 is taken from E. Ritter and J. W. Bozzelli., Journal
of Physical Chemistry, accepted 1989. $A_4 = 7.0E+13$, E_{a4}
 $= \Delta H + 2 = 21.3 + 2 = 23.3$ (kcal/mole).

e. $A_4 = 7.0E+13$, since $\Delta S = 0$
 $E_{a_4} = 2.0$ (kcal / mole).

f. ~~$A_5 = 2.0E+13$~~ is taken from Dean, A. M., Journal of
Physical Chemistry, Vol 89, No. 21 , 1985 ,4603.
 $E_{a5} = 7.0$ (kcal/ mole).

g- $\langle v \rangle = 77.3$ (cm⁻¹). Use Cpfit program.

h. L J Parameters : Sigma and e/k use Formula Calculation.
Critical property data taken from Reid, Prausnitz and
Sherwood (The Properties and Gases and Liquids, 3rd

ed.)

	Tc (k)	Pc (Atm)	Omega
C6H60 :	694.2	60.5	0.44

Sigma = 5.226 (Ao)

e / k = 601.17 (K)

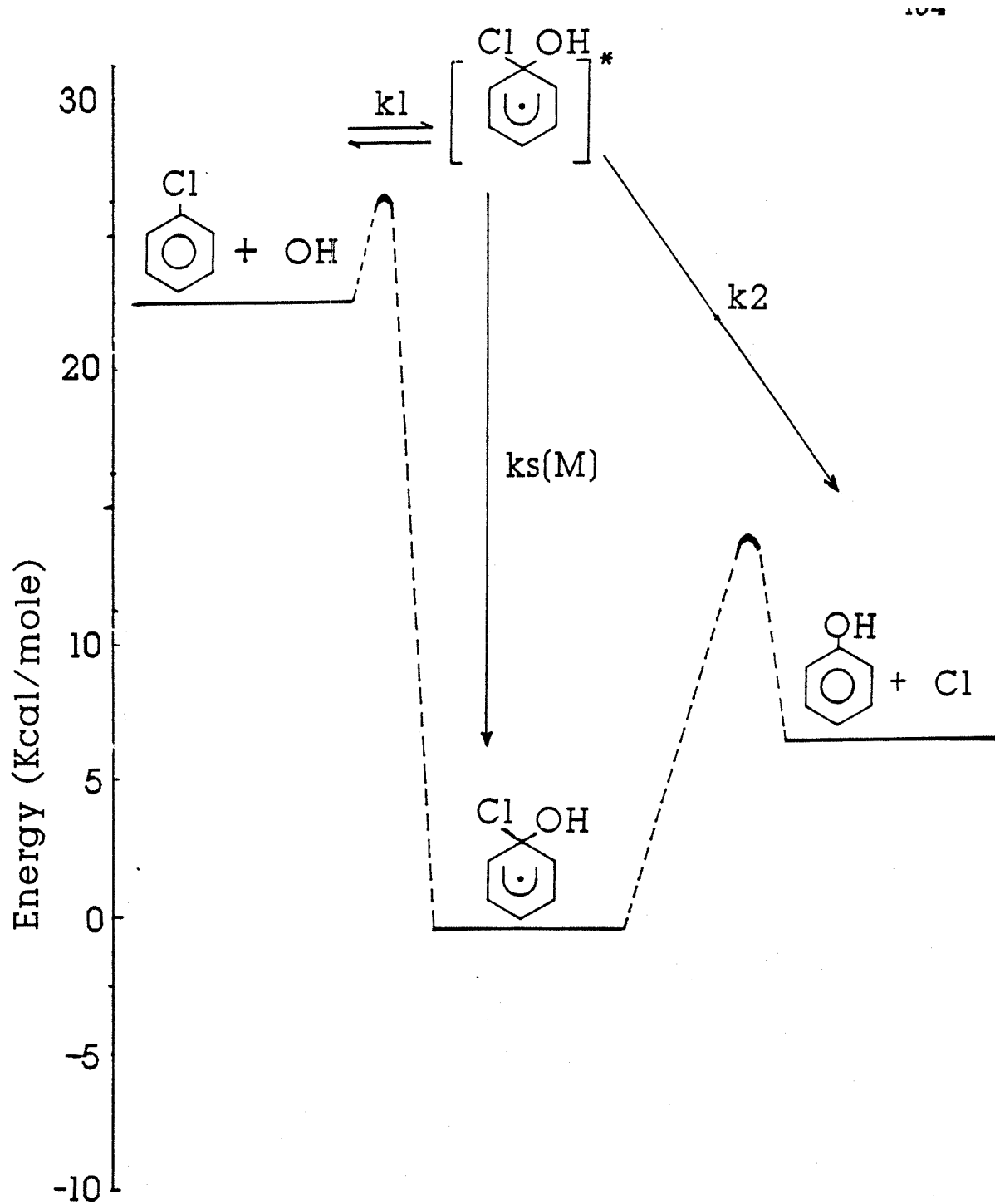
!

Table 3-b

APPARENT REACTION RATE CONSTANTS PREDICTED
 USING BIMOLECULAR QRRK ANALYSIS

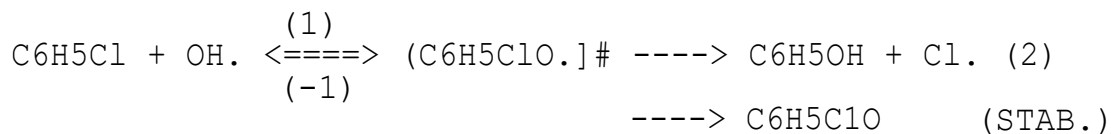
P (torr)	Reaction	A (cc/mol s)	N	Ea (Kcal/mol)
7.6	C6H6 + O. = C6H5O + H	3.01E+20	-4.02	6.38
760.0	u	3.11E+22	-4.03	6.39
7.6	C6H6 + O. = C6H5OH	2.77E+13	0.0	4.9
760.0	u	2.78E+13	0.0	4.91
7.6	C6H6 + O. = C6H6O (STAB)	5.36E+03	0.52	8.84
760.0	if	5.47E+05	0.52	8.85
7.6	C6H6 + O. = CHOCPD	5.61E+10	0.0	11.1
760.0	u	5.62E+10	0.0	11.1

* Valid from 300 - 1700K



(Chemact 2) GISOQRRK INPUT DATA and CALCULATION RESULTS

Table 4-a



k	A	Ea	source
1	7.20E+12	4.50	a
-1	5.28E+14	27.40	a
2	1.63E+14	14.29	b

$\langle v \rangle = 1011.24 \text{ (cm}^{-1}\text{)}$

Lennard-Jones Parameters :

$\sigma = 5.436 \text{ \AA}$ $e/k = 562.97 \text{ K}$

a.
A1 factor taken as 1/2 that for $\text{C6H6} + \cdot\text{OH} \text{ ---> Product}$, which is A1 factor $7.20\text{E}+12$, Tully, F. P., Ravishankara, A. R., M., Thompson, R. L., Shah, R. C., Kreutter, N. M., and Wine, P. H., "**Kinetics of the Reaction of Hydroxyl Radical with Benzene and Toluene**", J. Phys Chem., Vol 85, pp 2262-2269, 1981, $E_{a1}=4.5$

A_1 based upon (ΔS) for Therm Calculation with $A_1 = 5.28\text{E}+14 \text{ cc/mol sec}$, $E_{a_i} = \Delta H + 4.5 = 27.4 \text{ (kcal/mole)}$.

b.
A2 is taken from E. Ritter and J. W. Bozzelli, Journal

Phys. Chem., accepted on 1989 (Cl. + C6H6 ----> [Cl-CHD.])

A₂ = 2.0E+13, Thermo calculation, A₂ = 1.63E+14 (sec⁻¹).

E_{a2} = del H + (7 - 9) = 7.29 + 7 = 14.29 (kcal /mole).

c.

< VI > = 1011.24 (cm⁻¹). Use Cpfit program.

d.

•L J'Parameters : Sigma and e/k use Formula Calculation.

Critical property data taken from Reid, Prausnit2; and Sherwood (The Properties and Gases and Liquids, 3rd ed.)

$$\begin{aligned} \text{Sigma} &= (\text{sigma} [\text{phenol}] + \text{sigma} [\text{ClBZ}]) / 2 \\ &= (5.226 + 5.647) / 2 = 5.436 \text{ (A)} \end{aligned}$$

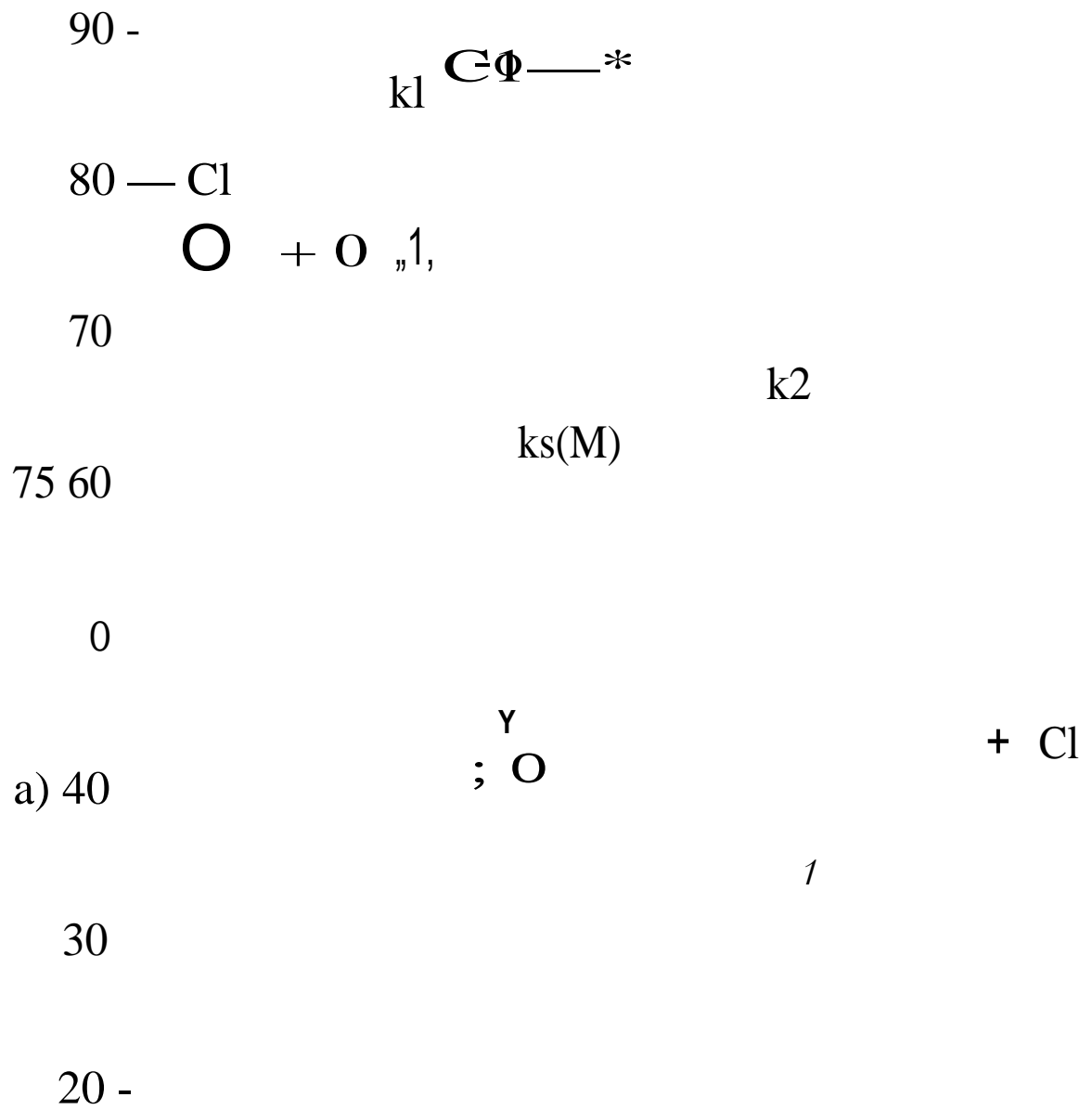
$$\begin{aligned} e / k &= \text{SQUARE}(e / k [\text{phenol}] * e / k [\text{ClBZ}]) \\ &= \text{SQUARE} (601.17 * 527.2) \\ &= 562.97 \text{ (K)} \end{aligned}$$

Table 4-b

APPARENT REACTION RATE CONSTANTS PREDICTED
 USING BIMOLECULAR QRRK ANALYSIS

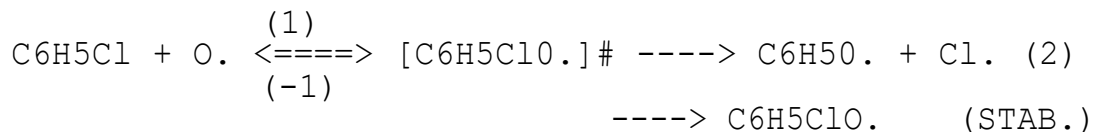
P (torr)	Reaction	A (cc/mol s)	N	Ea (Kcal/mol)
7.6	C6H5Cl + OH. = C6H5OH +Cl	6.74E+12	0.0	4.45
760.0	it	7.83E+12	0.0	4.80
7.6	C6H5Cl + OH. = C6H5CLO. (STAB)	2.97E+28	-6.43	7.09
760.0	it	2.14E+31	-6.67	7.74

*Valid Temp From 300 - 1700K.



(ChemAct 3) GISOQRRK INPUT DATA and CALCULATION RESULTS

Table 5-a



k	A	Ea	source
1	1.39E+13	4.9	a
-1	2.51E+14	43.44	a
2	3.83E+14	8.29	b

<v> = 816.58 (cm-1)

Lennard-Jones Parameters :

sigma = 5.331 Å e/k = 581.75 K

a.

A1 factor is taken as 1/2 that of C6H6 + O.---->Product, which is A1 factor 1/2 * 2.78E+13, Nicovich, J. M., Gump, C. A., and Ravishankara, J. Phys. Chem., Vol 86, pp1684-1690, 1982.

A1 = 1 / 2 * 2.78E+13 = 1.39E+13 (cm3 / mole - sec).

Ea1 = 4.9 (kcal / mole).

A_1 based upon (del S) for Thermo Calculation

LN (Af / Ar) = del S / R - (del n) * (ekT)

A_1 = 2.51E+14. Ea_1 = del H + 4.9 = 38.54 + 4.9 =43.44

b.

A2 is taken from E. Ritter and J. W. Bozzelli, Journal

Phys. Chem.", accepted on 1989. (Cl. + C6H6 ----> [Cl-CHD.])

A₂ = 2.0E+13 , Thermo calculation, A2 = 3.83E+14

Ea2 = del H + 1 = 8.29.

c. $\langle V \rangle = 816.54$ (cm⁻¹). **Use** Cpfit program.

d. L J Parameters : Sigma and e/k use Formula Calculation.
Thermodynamic critical property data taken from Reid,
Prausnitz and Sherwood (The Properties and Gases and Liquids
3rd ed.)

$$\begin{aligned}\text{Sigma} &= (\text{sigma} [\text{C6H6ClO.}] + \text{sigma} [\text{C6H60.}]) / 2 \\ &= (5.436 + 5.226) / 2 = 5.331 \text{ (A)}\end{aligned}$$

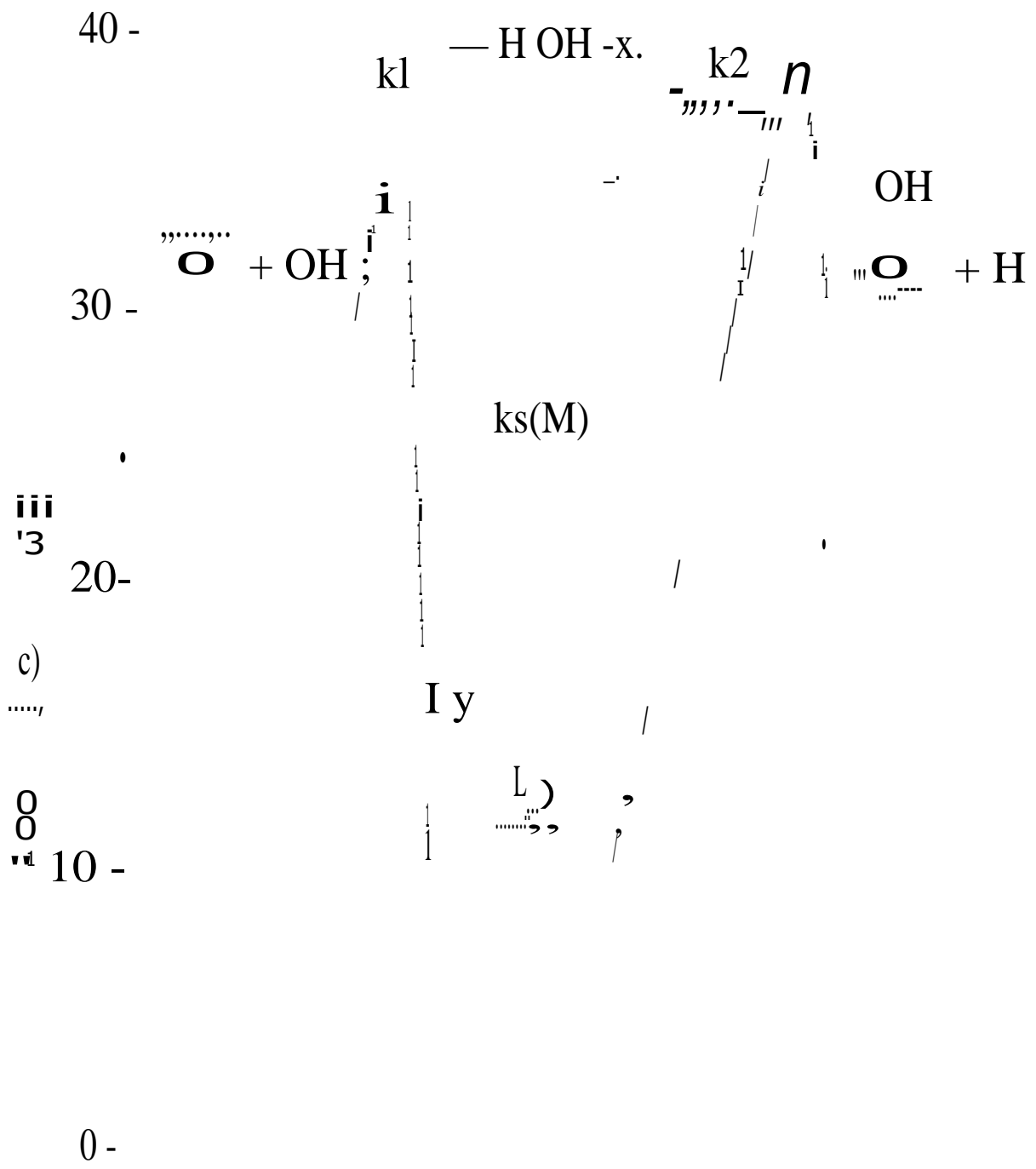
$$\begin{aligned}e / k &= \text{SQUARE}(e / k [\text{C6H6ClO.}] + e / k [\text{C6H60.}]) \\ &= \text{SQUARE} (562.97 + 601.17) \\ &= 581.75 \text{ (K)}\end{aligned}$$

Table 5 b

APPARENT REACTION RATE CONSTANTS PREDICTED
 USING BIMOLECULAR QRRK ANALYSIS

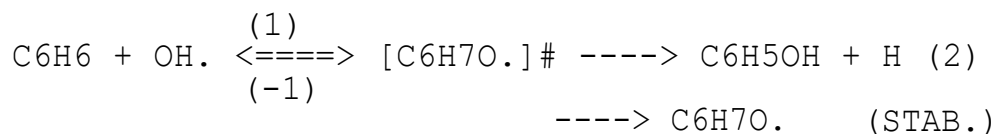
P (torn)	Reaction	A (cc/mol s)	N	Ea (Kcal/mol)
7.6	C6H5Cl + O. = C05O. + Cl.	1.39E+13	0.0	4.9
760.0	"	1.39E+13	0.0	4.9
7.6	C6H5Cl + O. = C6H5ClO.(STAB)	3.05E+17	-3.37	5.8
760.0	to	3.07E+19	-3.37	5.8

* Valid Temp Range from 300 - 1900 (K).



(ChemAct 4) GISOQRRK INPUT DATA and CALCULATION RESULTS

Table 6 - a



k	A	Ea	source
1	2.10E+13	4.58	a
-1	1.51E+14	23.42	a
2	5.01E+13	27.27	b

<v> = 1126.9 (cm-1)

Lennard-Jones Parameters :

sigma = 5.573 Å e/k = 576.51 K

a.

A1 factor is taken as that of C6H6 + OH., which is A factor 2.10E+13 , S. Madronich, W. **Felder**, "Kinetics and Mechanism of the Reaction of OH with C6H6 over 790-141010¹", Journal Physical Chemistry, 1985 , 89 , 3556- 3561.

A1 = 2.10E+13 (cm3 / mole - sec).

Ea1 = 4.58 (kcal / mole).

A_1 based upon (del S) for Thermo Calculation

LN (Af / A_r) = del S / R - (del n) * (ekT)

= 1.51E+14. Ea_i = del H + 2.5 = 18.84 + 4.58

= 23.42 (kcal / mole).

b.

A₂ is taken from H + C₆H₅OH → Product, He, Y. Z.,
Mallard, W. G., and Tsang, W., "Rate constants and Mechanism
for the Reaction of Hydrogen Atoms with Aniline", J. Phys.
Chem., Vol 92, pp 1510-1513, 1988.

A₂ = 2.20E+13, Ea₂ = 7.92 (kcal/mole)

Eat = del H + 7.92 = 27.27 (kcal / mole) .

A2 = 5.01E+13 (Thermo Calc.)

a.

< V > = 1126.9 (cm⁻¹). Use Cpfit program.

d.

L J Parameters : Sigma and e/k use Formula Calculation.
Thermodynamic critical property data taken from Reid,
Prausnitz and Sherwood (The Properties and Gases and
Liquids, 3rd ed.)

$$\begin{aligned}\text{Sigma} &= (\text{sigma} [\text{C}_6\text{H}_6\text{O.}] + \text{sigma} [\text{C}_6\text{H}_9\text{O.}]) / 2 \\ &= (5.226 + 5.92) / 2 = 5.573 \text{ (A)}\end{aligned}$$

$$\begin{aligned}e / k &= \text{SQUARE}(e / k [\text{C}_6\text{H}_6\text{O.}] * e / k [\text{C}_6\text{H}_9\text{O.}]) \\ &= \text{SQUARE} (601.17 * 552.88) \\ &= 576.88 \text{ (K)}\end{aligned}$$

Table 5 - b

APPARENT REACTION RATE CONSTANTS PREDICTED
 USING BIMOLECULAR QRRK ANALYSIS

P (torr)	Reaction	A (cc/mol s)	N	Ea (Kcal/mol)
7.6	C6H6 + OH. = C6H7O. (STAB)	7.33E+63	-16.67	20.04
760.0	II	1.11E+56	-13.48	21.87
7.6	C6H6 + OH. = C6H5OH + H.	1.47E+12	0.0	10.2
760.0	ft	4.17E+12	0.0	13.4

* Valid Temp Range from 300 - 1900K.

APPENDIX (B)

LIST OF THERMO DATA

SPECIES	HF(298)	s (298)	CP300	CP500	cp800	cp1000	cp1500	CP2000	COMMENTS	ELEMENTS
C(S)	0.00	21.83	2.06	3.50	4.73	5.16	5.65	5.89	J 3/61	C 1 O 0 0 0 0 0
C	171.29	37.76	5.00	4.97	4.97	4.97	4.97	5.01	J 3/61	C 1 O 0 0 0 0 0
c+	432.06	35.99	5.01	4.98	4.97	4.97	4.97	4.97	L12/66	C 1 E -1 0 0 0 0 0
C-	140.49	35.64	4.97	4.97	4.97	4.97	4.97	4.97	J 9/65	C 1 E 1 0 0 0 0
CH	142.00	43.72	6.97	7.03	7.41	7.77	8.74	9.36	J12/67	C 1 H 1 0 0 0 0
cat	388.80	31.79	6.97	7.02	7.36	7.65	8.24	8.62	J12/71	C 1 H 1 E -1 0 0 0
CH2	92.35	46.33	8.28	8.99	10.15	10.88	12.22	13.00	J1 ² /-2	C 1 H 2 0 0 0 0
C*CCC*C.	71.41	83.11	21.72	31.94	42.99	47.59	54.82	59.53		C 5 H 7 CL 0 0 0 0
CYPENE4.	54.33	62.51	17.24	29.39	39.19	43.00	49.11	53.20		C 5 H 7 CL 0 0 0 0
C*CC	4.91	63.89	15.26	22.67	30.51	34.32	40.48	43.87		C 3 H 6 CL 0 0 0 0
C*CC.	41.00	63.10	14.75	21.68	28.43	31.52	36.44	39.44		C 3 H 5 CL 0 0 0 0
C4H4	69.17	65.39	17.47	24.23	30.27	33.17	37.42	39.75		C 4 H 4 CL 0 0 0 0
C4H3	101.98	65.27	17.39	22.34	27.12	29.20	32.57	34.59		C 4 H 3 CL 0 0 0 0
ch3	34.82	46.38	9.26	10.81	12.90	14.09	16.26	17.56	J 6/69	C 1 H 3 O 0 0 0 0
ch4	-17.90	44.49	8.49	11.15	14.98	17.13	20.57	22.61	J 3/61	C 1 H 4 O 0 0 0 0
c2u2	54.19	48.00	10.60	13.03	15.29	16.30	18.34	19.57	J 3/61	C 2 H 2 O 0 0 0 0
C2H4	12.54	52.39	10.2 8	14.92	20.03	22.45	26.21	28.35	J 9/65	C 2 H 4 O 0 0 0 0
C2H6	-20.24	54.85	12.58	18.68	25.80	29.33	34.91	38.37	L 5/72	C 2 H 6 0 0 0 0 0
cyc6H10	-1.28	74.27	25.24	42.74	59.51	66.65	77.29	80.12		C 6 H 10 CL 0 0 0 0
cyc6H9	45.61	80.05	25.10	41.50	56.95	63.42	73.01	74.96		C 6 H 9 CL 0 0 0 0
MECY24PD1	48.10	75.50	23.11	36.37	49.85	55.84	64.70	68.39		C 6 H 7 CL 0 0 0 0
01c1c687	71.86	71.52	27.62	34.98	48.20	55.52	63.32	67.20		C 6 H 7 CL 0 0 0 0
sicyc6118	39.54	69.19	18.61	35.67	51.65	58.09	67.71	76.62		C 6 H 8 CL 0 0 0 0
H	52.11	27.39	4.97	4.97	4.97	4.97	4.97	4.97		C 0 H 1 CL 0 0 0 0
C2	200.24	47.64	10.30	8.91	8.50	8.62	8.93	12.03		C 2 H 0 CL 0 0 0 0
cyc6H5	81.37	69.20	18.79	30.52	41.70	46.37	53.18	56.21		C 6 H 5 CL 0 0 0 0
c1c6H6	19.82	64.34	19.55	33.07	48.14	54.77	62.27	67.35		C 6 H 6 CL 0 0 0 0
CYC6H7	49.86	72.01	20.79	35.11	48.74	54.33	62.34	67.34		C 6 H 6 CL 0 0 0 0
LINC6H7	93.05	84.80	27.27	40.09	50.85	55.00	62.12	65.00		C 6 H 7 CL 0 0 0 0
CHD14	26.16	70.80	22.63	37.47	52.04	58.27	67.47	72.45		C 6 H 7 O 0 0 0 0
chD	25.40	72.49	22.67	37.73	52.30	58.45	67.56	72.55		C 6 H 8 0 0 0 0
CY13PD5	54.30	62.40	17.24	29.40	39.46	43.13	49.10	53.20		C 5 H 5 CL 0 0 0 0
CY13PD	32.40	64.20	17.64	30.01	41.29	45.81	52.80	57.30		C 5 H 6 CL 0 0 0 0
mEcY24PD3	81.76	75.80	22.91	36.09	49.58	55.57	64.44	68.91		C 6 H 7 CL 0 0 0 0
MECY14PD4	79.66	75.40	22.95	36.09	49.58	55.57	64.44	68.91		C 6 H 7 CL 0 0 0 0
MECY14PD3	48.06	75.36	23.11	36.37	49.85	55.84	64.70	68.39		C 6 H 7 CL 0 0 0 0
MEcY24PD	28.30	73.00	23.03	36.74	51.51	58.23	67.83	73.50		C 6 H 8 CL 0 0 0 0
NAPTH	36.10	80.21	31.89	52.13	70.77	78.43	90.21	94.66		C 10 H 8 CL 0 0 0 0
C*CC*C	26.33	66.62	19.22	28.36	36.95	40.57	46.34	49.44		C 4 H 6 5 0 0 0 0
C*CC*C.	79.82	70.70	18.40	26.28	33.75	36.95	42.09	44.52		C 4 H 5 0 0 0 0 0
C*CC*CC*C	39.60	80.70	28.09	41.91	53.70	58.33	66.33	70.00		C 6 H 8 0 0 0 0 0
C#CC.*C	115.57	68.20	17.50	22.98	27.91	29.93	33.27	34.91		C 4 H 3 CL 0 0 0 0
cfcc*c.	126.27	69.60	17.50	22.98	27.91	29.93	33.27	34.91		C 4 H 3 CL 0 0 0 0
cfccfc.	112.30	59.86	17.19	21.77	25.33	26.55	28.72	30.16		C 4 H 2 CL 0 0 0 0
cfccfc.	192.20	62.72	14.98	18.59	21.50	22.53	24.21	25.44		C 4 H 1 CL 0 0 0 0
cfccilccfc	170.66	73.74	20.65	27.51	35.35	38.60	40.79	41.96		C 6 H 2 CL 0 0 0 0
ME.CY24PD	75.10	76.42	23.11	36.36	49.64	55.53	64.71	69.20		C 6 H 7 CL 0 0 0 0
c605c03	11.95	76.41	24.88	40.53	55.73	62.22	71.78	75.20		C 7 H 8 CL 0 0 0 0
CYC6H4	112.52	68.88	16.38	28.22	38.45	42.42	48.70	50.94		C 6 H 4 CL 0 0 0 0

H2	0.00	31.21	6.90	6.99	7.10	7.21	7.72	8.17	C	0 H	2 CL	0 0	0 G	
CL	28.90	39.47	5.20	5.40	5.35	5.30	5.20	3.14	C	0 ii	0 CL	1 0	0 G	
CL2	-0.01	53.29	8.10	8.59	8.91	8.99	9.10	9.16	C	0 H	0 CL	2 0	0 G	
C2H	131.98	49.55	8.92	10.21	11.55	12.18	13.31	14.10	C	2 H	1 CL	0 0	0 G	
C6H5CL	12.35	74.79	23.27	36.47	47.96	52.41	59.17	61.16	C	6 H	5 CL	1 0	0 G	
pHcLpHcL	28.72	112.76	44.07	66.94	86.58	93.99	104.92	108.68	C	12 H	8 CL	2 0	0 G	
PHCL2	6.32	82.09	27.35	39.70	50.37	54.36	59.96	61.67	C	6 H	4 CL	2 0	0 G	
C6H5C6H5	43.50	93.85	35.74	59.44	81.20	90.05	103.37	108.73	c	12 H	10 CL	0 0	0 G	
PHPHCL	35.82	105.39	39.90	63.17	83.88	92.03	104.14	108.25	C	12 H	9 CL	1 0	0 G	
HCL	-22.06	44.64	6.96	6.99	7.29	7.56	8.10	8.40	c	0 a	1 cL	1 0	0 G	
C6H4CL	74.34	77.78	22.92	34.33	45.16	49.86	57.75	61.39	C	6 H	4 CL	1 0	0 G	
LINC6H6	82.73	77.88	26.31	37.79	47.86	51.75	57.77	61.40	C	6 H	6 CL	0 0	0 G	
Litic6H5	136.55	80.70	25.50	36.41	45.21	48.39	53.56	55.10	C	6 H	5 CL	0 0	0 G	
CY13HD	25.40	72.90	22.44	37.70	52.35	58.47	67.44	72.28	C	6 H	8 CL	0 0	0 G	
PHPH	42.92	92.51	39.07	64.34	87.00	95.95	109.41	115.97	C	12 H	10 0	0 0	0 G	
PacYc6H4	104.47	98.02	38.20	62.11	83.59	92.10	104.91	110.93	C	12 H	9 0	0 0	0 G	
NAPTH	36.00	79.49	31.92	52.07	70.74	78.27	89.14	94.37	C	10 H	8 0	0 0	0 G	
NAPH.	97.55	83.62	31.05	49.85	67.33	74.42	84.64	89.35	C	10 H	7 0	0 0	0 G	
MECHD	18.46	80.61	27.63	46.24	63.43	70.55	81.91	87.65	C	7 H	10 0	0 0	0 G	
MEM	42.92	79.32	25.76	43.62	59.07	66.44	76.69	82.15	C	7 H	9 0	0 0	0 G	
ICLMECHD	7.32	86.91	31.29	50.08	66.57	73.09	83.70	88.77	C	7 H	9 CL	1 0	0 G	
ICLMECHD.	31.78	85.62	29.42	47.45	63.00	68.98	78.48	83.27	C	7 H	8 CL	1 0	0 G	
PHCHD	51.59	100.88	40.66	68.53	93.53	103.44	118.48	126.12	C	10 H	12 0	0 0	0 G	
PHCHD.	76.05	100.40	38.79	65.90	89.97	99.33	113.26	120.62	C	12 H	11 0	0 0	0 G	
CH	142.00	43.72	6.97	7.03	7.40	7.78	8.74	9.36	J12/67	C	1 H	1 0	0 0	0 G
HCL	-22.07	44.64	6.96	6.99	7.29	7.56	8.10	8.40	C	0 H	1 CL	1 0	0 G	
CL2	0.00	53.30	8.10	8.59	8.91	8.99	9.10	9.16	CL	2 0	0 0	0 0	0 G	
CH2	92.35	46.32	8.28	8.99	10.15	10.88	17.22	11.00	J12/72	C	1 H	2 0	0 0	0 G
CH3	35.12	46.38	9.26	10.81	12.90	14.09	16.26	17.56	J 6/69	C	1 H	3 0	0 0	0 G
CH4	-17.90	44.48	8.51	11.10	15.00	17.20	20.61	22.61	J 3/61	C	1 H	4 00	0 00	0 G
C2H	132.00	49.58	8.88	10.22	11.54	12.16	13.32	14.11	C	2 H	1 CL	0 0	0 G	
c2112	54.19	48.01	10.60	13.08	15.31	16.29	18.31	19.57	J 3/61	C	2 H	2 00	0 00	0 G
c203	67.10	56.20	10.89	13.87	17.16	18.73	21.34	23.20	C	2 H	3 CL	0 0	0 G	
C2H4	12.54	52.39	10.28	14.91	20.03	22.45	26.21	28.35	J 9/65	c	2 H	4 00	0 00	0 G
c205	28.36	57.90	12.26	17.13	22.85	25.74	30.54	33.31	C	2 H	5 CL	0 0	0 G	
c2116	-20.24	54.85	12.58	18.68	25.80	29.33	34.91	38.37	L 5/72	C	2 H	6 0	0 0	0 G
C3H2	106.65	117.98	12.96	16.94	20.26	21.59	23.85	25.59	C	3 H	2 0	0 0	0 G	
c3113	77.26	89.99	14.05	18.28	22.39	24.24	27.23	28.88	C	3 H	3 0	0 0	0 G	
C*C*C	45.92	58.30	14.19	19.77	25.45	28.02	32.04	34.07	C	3 H	4 0	0 0	0 G	
C305	40.97	63.01	14.75	21.68	28.58	31.62	36.44	39.44	D12/77	C	3 u	5 0	0 0	0 G
c306	4.88	63.80	15.26	22.67	30.66	34.43	40.48	43.87	T12/81	c	3 H	6 0	0 0	0 G
C3H8	-24.82	64.51	17.63	27.01	37.11	41.83	49.27	53.43	C	3 H	8 0 0	0 0	0 G	
C3H7	23.99	69.07	16.85	25.39	34.09	38.05	44.58	48.61	C	3 H	7 CL	0 0	0 G	
cfcc	44.32	59.30	14.56	19.71	25.06	27.72	31.85	34.00	C	3 H	4 CL	0 0	0 G	
C3H3	83.33	56.99	14.06	18.27	22.33	24.19	27.21	28.85	C	3 H	3 CL	0 0	0 G	
CcCC	-30.15	74.12	23.31	35.36	48.23	54.21	63.68	69.66	C	4 H	10 CL	0 0	0 G	
CLO	24.20	54.10	7.50	8.21	8.69	8.81	9.00	9.10	C	0 H	0 CL	1 0	1 G	
O	59.55	38.47	5.23	5.08	5.01	5.01	4.98	4.98	C	0 H	0 CL	0 0	1 G	
O2	0.0	49.01	7.02	7.44	8.04	8.35	8.73	9.04	C	0 u	0 CL	0 0	2 G	
OH	9.49	43.88	7.16	7.05	7.15	7.33	7.87	8.27	C	0 H	1 CL	0 0	1 G	
O20	-57.80	45.10	8.02	8.41	9.24	9.85	11.23	12.20	C	0 H	2 CL	0 0	1 G	
002	3.50	54.73	8.37	9.48	10.78	11.43	12.47	13.23	C	0 H	1 CL	0 0	2 G	
0202	-32.53	55.66	10.42	12.35	14.30	15.21	16.85	17.88	C	0 H	2 CL	0 0	2 G	
co	-26.42	47.21	6.96	7.13	7.61	7.94	8.41	8.67	C	1 H	0 CL	0 0	1 G	
CHO	10.40	53.66	8.27	9.27	10.73	11.51	12.55	13.15	C	1 H	1 CL	0 0	1 G	
CO2	-94.05	51.07	8.90	10.65	12.30	12.97	13.93	14.45	C	1 H	0 CL	0 0	2 G	
ca20	-27.70	52.26	8.45	10.49	13.34	14.86	16.95	18.14	C	1 H	2 CL	0 0	1 G	
BICYc6H50	41.11	78.07	19.09	33.73	47.29	52.26	59.10	62.23	C	6 a	5 CL	0 0	1 G	
CYC5H4cHO	39.18	80.01	23.56	36.75	48.25	52.67	57.91	61.48	C	6 H	5 CL	0 0	1 G	
ETCYc6H60	80.14	78.92	20.74	37.58	51.63	56.83	63.54	67.23	C	6 H	6 CL	0 0	1 G	

cH30	3.90	53.25	9.01	12.22	16.28	18.38	21.56	23.13	C	1 H	3 CL	0 O	1 G
cH2co	-14.60	57.79	12.98	16.92	20.31	21.61	23.80	25.55	C	2 H	2 CL	0 O	1 G
c113011	-48.06	57.28	10.48	14.34	19.00	21.35	24.96	27.25	C	1 ft	4 CL	0 O	1 G
CH3CHO	-39.69	63.20	13.22	18.16	24.17	27.00	30.60	34.20	C	2 H	4 CL	0 O	1 G
CYC6H7CLO2	-8.05	96.14	34.92	52.52	66.76	72.20	80.24	84.37	c	6 H	7 CL	1 O	2 G
CYC6H6CLO2	16.41	96.62	33.05	49.89	63.20	68.09	75.02	78.88	C	6 H	6 CL	1 O	2 G
c1211120	16.16	110.00	46.17	75.30	100.28	109.82	124.20	131.91	C	12 H	12 CL	0 O	1 G
c12H110	40.62	110.48	44.30	72.67	96.72	105.71	118.98	126.42	C	12 H	11 CL	0 O	1 G
P11-0-PH	11.94	106.35	42.29	69.18	92.09	101.29	114.98	121.70	C	12 H	10 CL	0 O	1 G
C12H110CL	5.02	116.30	49.82	79.16	103.38	112.39	125.98	133.04	C	12 H	11 CL	1 O	1 G
c12H100cL	29.48	116.78	47.95	76.53	99.82	108.28	120.76	127.54	C	12 H	10 CL	1 O	1 G
cyc6H8o2	-58.04	84.52	29.22	47.18	62.41	68.11	74.62	80.83	C	6 H	8 CL	0 O	2 G
cyc6H702	-33.58	86.38	27.35	44.55	58.85	64.00	69.40	75.34	c	6 H	7 cL	0 O	2 G
c1c611602	-65.86	81.57	30.12	44.52	56.18	60.82	66.24	71.14	C	6 H	6 CL	0 O	2 G
cYc611502	-31.46	81.72	28.74	41.99	52.74	57.01	61.36	65.86	C	6 H	5 CL	0 O	2 G
cyc6H80	-14.01	81.66	26.47	42.56	57.26	62.93	70.96	76.32	C	6 H	8 CL	0 O	1 G
cYc6H70	10.45	82.14	24.60	39.93	53.70	58.82	65.74	70.82	C	6 H	7 CL	0 O	1 G
CYC6H7CLO	-25.15	87.96	30.12	46.42	60.36	65.50	72.74	77.44	C	6 H	7 CL	1 O	1 G
cYc6H6cLo	-0.69	88.44	28.25	43.79	56.80	61.39	67.52	71.95	C	6 H	6 CL	1 O	1 G
cYc6H5cLo	33.71	85.84	26.87	41.26	53.36	57.58	62.64	66.67	C	6 H	5 cL	1 O	1 G
c6850H	-23.03	75.43	24.90	38.64	50.62	55.49	62.16	66.36	C	6 H	6 CL	0 O	1 G
cyc6H50	9.50	74.21	23.52	36.11	47.18	51.68	57.28	61.08	C	6 H	5 CL	0 O	1 G
cYc5H5	54.30	62.40	17.24	29.4	39.46	43.13	49.10	53.21	C	5 H	5 CL	0 O	0 G
c1c61160	58.84	84.49	24.90	38.64	50.62	55.49	61.60	66.40	C	6 H	6 CL	0 O	1 G
cH0c1O	6.53	51.91	23.72	37.92	50.80	55.98	62.81	68.83	C	6 H	6 CL	0 O	1 G

APPENDIX (C)

REACTION MECHANISM OF



END

SPECIES

C6H5CL HCL CYC6H6 CH4 C6H5OH C2H4 C2H6 CO C2H2 Bicyc6H50
CYC6H5 CL H CYC6H7 MECY24PD1 MECY24PD CO2 CH30 CH2o CYC5H4CHO
CY13PD5 CH3 CY13PD C6H5C6H5 PHPHCL C6H4CL CYPENE4. BICYC6H60
CL2 H2 C6H5CH3 PHCLPHCL C2H5 OH O C2H3 C4H3 C2H C*CCC*C.
H02 O2 H2O 8202 CYC6H60 CHOCPD cYc6H50 CHO C*CC C*CC.,
END

REACTIONS

C6H5CL	CYC6H5 + CL	3.00E15	0.0	96350.
CYC6H6	- CYC6H5 + H	1.67E16	0.0	111500.
CYC6H6	+ H -CYC6H7	4.42E13	0.0	4450.
CYC6H7	MECY24PD1	5.00E12	0.0	38100.
mECY24pD1+H2=MECY24PD+H		2.00E13	0.0	46000.
MECY24PD	CY13PD5 + CH3	1.00E16	0.0	67500.
MECY24PD1+H	-CY13PD5+CH3	8.00E13	0.0	0.
CY13pD5+H2	CY13PD + H	2.50E13	0.0	42000.
CY13PD	CY13PD5 + H	6.00E14	0.0	75100.
C6H5CL	C6H4CL + H	1.30E16	0.0	110500.
C6H5CL	+ H - CYC6H6 + CL	1.50E13	0.0	7500.
CH3+ H	CH4	8.09E36	-7.19	9200.
CH3+H2	CH4 + H	5.00E12	0.0	11000.
CH3+c6H5CL	-C6H5CH3+CL	1.96E14	-0.65	12000.
CH3+CYC6H6	-C6H5CH3+H	3.40E26	-4.15	26400.
C6H5CL+H	-C6H4CL + H2	2.00E13	0.0	18600.
C6H5CL	+H-CYC6H5+HCL	1.00E13	0.0	11300.
CL+c6H5CL=C6H4CL+HCL		1.00E13	0.0	12500.
CL+cyc6H6	-CYC6H5+HCL	1.10E13	0.0	12500.
H+H+M	- H2 + M	1.00E18	0.0	0.
H+CL+M	=HCL+M	1.00E17	0.0	0.
CL2-CL+CL		7.69E08	0.0	55600.
CL +H2	- HCL + H	4.80E13	0.0	5000.
H +CL2	CL +HCL	7.94E13	0.0	1200.
C6H5CL	+ O-C6H4CL+OH	1.80E13	0.0	10000.
C6H5CL	+ou=c6H4CL +H2O	1.44E13	0.0	4490.
CYC6H6	+H-CYC6H5+H2	2.00E13	0.0	18600.
c106116+	0-CYC6115+0H	3.60E13	0.0	9900.
CYC6H6+0H-CYC6H5+1120		1.40E13	0.0	4490.
C6H5CL+0-CYC6H50+CL		1.39E13	0.0	4900.
C6H5CL+OH-C6H50n+CL		7.83E12	0.0	4800.
CYC6H6+0-C6H50H		2.70E13	0.0	4880.
CYC6H6	+02-CYC6H5+H02	1.60E12	0.0	10000.
CYC6H50-BICYC6H50		1.31E22	-2.48	42100.
C605011	CYC6H50 +0	1.89E15	0.0	85000.
cyc6n6+0H-c6H50H+H		2.80E26	-4.62	20290.
CYC6H6+002-CYC6H5+H202		1.00E11	0.0	18200.
C6H50H	+H-cyc6H50+H2	1.10E14	0.0	12390.
C6H50H+OH-cyc6H50+H20		6.00E12	0.0	0.
CYC6H5+02-CYC6H50+0		6.60E13	0.0	0.
CYC6H5	- C4H3 + C2H2	1.58E15	0.0	82000.
C4H3-	c211 +C2H2	3.16E14	0.0	57200.
00+H2	- H2O +H	1.10E09	1.3	3646.
H+02	- OH +0	1.10E14	0.0	16176.
0+H2	OH +H	1.82E10	1.0	8900.
H+02+0	002+0	2.90E17	-0.72	0.
OH + H02	- H2O +02	2.00E13	0.0	0.
H + H02	OH + on	1.50E14	0.0	1008.
0 + H02	- 02 +oil	2.00E13	0.0	0.

OH+OH - O +H2O	1.51E09	1.14	0.
H+OH+M - H2O + M	2.20E22	-2.0	0.
H+O+M -- OH +M	6.20E16	-0.6	0.
H+HO2 = H2 + O2	2.50E13	0.0	0.
O2 + M - O +O+M	5.12E15	0.0	11500.
H2O2 + OH - H2O +HO2	1.00E13	0.0	1800.
H02 + H02 ... O2+H2O2	2.00E12	0.0	0.
H2O2+H-HO2+H2	1.89E12	0.0	3700.
H2O2 + M - OH +OH+M	1.25E17	0.0	45000.
O+HCL - OH +CL	5.24E12	0.0	6400.
OH + HCL -CL+H2O	2.54E12	0.0	1100.
CO+ O+M =CO2 + M	6.17E13	0.0	3000.
CO +OH = CO2 + H	4.40E06	1.5	-700.
CO+O2 - CO2 + O	2.50E13	0.0	48000.
CO + HO2 -Oo2 + OH	1.50E14	0.0	23688.
C2H6 - CH3 +CH3	5.71E-3	0.0	0.
CH4 + O - CH3 + OH	1.20E07	2.1	7656.
C2H6+H - C2H5 +H2	5.40E02	3.5	5200.
C2H6 + O - C2H5 +OH	2.51E13	0.0	6360.
CH4 + CL ... CH3 +HCL	5.14E13	0.0	3800.
C2H5 - C2H4 + H	5.01E13	0.0	40900.
C2H5 + O2 - C2H4 + HO2	1.99E10	0.0	0.
C2H4 + H ..- C2H3 + H2	1.50E14	0.0	10200.
C2H4 + OH .C2H3 + H2O	7.00E13	0.0	3024.
C2H4 + M - C2H2 + H2 + M	2.70E17	0.0	79680.
CH3 +CH3 - C2H5 +H	8.00E13	0.0	26640.
C2H3 + O2 ...C2H2 +HO2	1.00E12	0.0	0.
CY13PD + CH3=CH4+CY13P05	3.11E11	0.0	5500.
CYPENE4. = CY13PD + H	3.88E13	0.0	36171.
CYPENE4. - C*CCC*C.	8.72E13	0.0	37379.
C*CC. + C2H2=C*CCC*C.	8.38E30	-6.24	12824.
C*CC. + C2H2 -CYPENE4.	1.82E11	0.0	6372.
C*CC+CH3 - C*CC. +CH4	3.80E11	0.0	9000.
C*CC.+ C2H2 - CY13PD+H	2.95E32	-5.82	25733.
CH3 +C2H5 = CH4 +C2H4	5.50E11	0.0	0.
BICYC6H50 = CYC5H4CHO	2.86E26	-4.12	28940.
CYC5H4CH0 =. CY13PD5+CO	3.87E17	-2.54	2020.
END			